

AD-A252 653



FOR PUBLIC DISTRIBUTION

DTIC  
ELECTE  
JUL 8 1992  
S C D

(2)

ONR Grant N00014-90-J-1014: Final Scientific Report

**Title:** Coherent Radiative Control of Chemical Reactions

**Principal Investigator:** P. Brumer, Professor, Chemical Physics Theory Group, Department of Chemistry, University of Toronto, Toronto, Canada M5S 1A1  
(416-978-3569);

**Subcontractor:** M. Shapiro, Professor, Weizmann Institute of Science

**ONR Scientific Officer:** Dr. P. Reynolds

**Grant Period:** October 1989 - September 1992

**Submitted by:**

P. Brumer, Professor, Chemical Physics Theory Group, Dept. of Chemistry

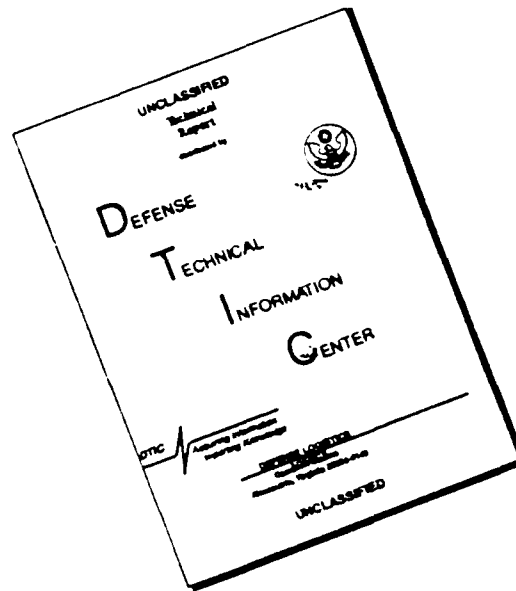
M. Shapiro, Professor, Chemical Physics Department

92-17533



92 7 06 054

# DISCLAIMER NOTICE



THIS DOCUMENT IS BEST QUALITY AVAILABLE. THE COPY FURNISHED TO DTIC CONTAINED A SIGNIFICANT NUMBER OF PAGES WHICH DO NOT REPRODUCE LEGIBLY.

Accession For		
NTIS	GRAD	<input checked="" type="checkbox"/>
DTIC	TAB	<input type="checkbox"/>
Unannounced		<input type="checkbox"/>
Publication		
Author/		
Availability Codes		
Available and/or		
Dist	Special	
A-1		

### Grant-Supported Publications

The following papers describe research supported under this grant. Papers numbered 1-12, as well as a sample conference proceedings review (number 18) are included with this report.

#### Publications:

##### A. Refereed Publications:

1. "Coherent Radiative Control of IBr Photodissociation via Simultaneous ( $\omega_1, \omega_3$ ) Excitation", C.K. Chan, P. Brumer and M. Shapiro, *J. Chem. Phys.* **94**, 2688 (1991).
2. "Interference Between Optical Transitions and Control of Relative Cross Sections", C.K. Chan, P. Brumer and M. Shapiro, *Phys. Rev Lett.* **62**, 3199 (1990).
3. "Two-Pulse Coherent Control of Electronic States in the Photodissociation of IBr: Theory and Proposed Experiment", I. Levy, M. Shapiro and P. Brumer, *J. Chem. Phys.* **93**, 2493 (1990).
4. "Quantum Beats Induced by Partially Coherent Laser Sources", X-P. Jiang and P. Brumer, *Chem. Phys. Letters* **180**, 222 (1991).
5. "Controlled Photon Induced Symmetry Breaking: Chiral Molecular Products From Achiral Precursors", M. Shapiro and P. Brumer, *J. Chem. Phys.* **95**, 8658 (1991).
6. "Laser Induced Unimolecular Isomerization: Theory and Model Applications", D. Gruner, P. Brumer and M. Shapiro, *J. Phys. Chem.* **96**, 281 (1992).

7. "Laser Control of Molecular Processes", P. Brumer and M. Shapiro, Annual Reviews of Physical Chemistry, **43**, xxx, (1992) (in press).
8. "Theory of Resonant Two-Photon Dissociation of  $\text{Na}_2$ ", Z. Chen, M. Shapiro and P. Brumer, J. Chem. Phys. (submitted).
9. "Coherent Radiative Control of Molecular Photodissociation via Resonant 2-Photon vs. 2-Photon Interference", Z. Chen, P. Brumer and M. Shapiro, Phys. Rev. Lett. (submitted).
10. "Three-Dimensional Quantum-Mechanical Computations of the Control of the  $\text{H}+\text{OD}\leftarrow\text{DOH}\rightarrow\text{D}+\text{OH}$  Reaction", M. Shapiro and P. Brumer, J. Chem. Phys. (submitted).
11. "Multiproduct Coherent Control of  $\text{Na}_2$  Photodissociation via 2-Photon vs. 2-Photon Interference", Z. Chen and P. Brumer and M. Shapiro, J. Chem. Phys. (to be submitted).
12. "Total  $N$ -Channel Control in the Weak Field Domain", M. Shapiro and P. Brumer, J. Chem. Phys. (submitted)

*B. Manuscripts in Preparation:*

13. "Partially Coherent Laser Pulses in Coherent Control of Chemical Reaction", X.P. Jiang, M. Shapiro and P. Brumer.
14. "Initial Value Representation for Polyatomic Photofragmentation", G. Campolieti, M. Shapiro and P. Brumer.

15. "SEP Preparation in  $\text{Na}_2$  Photodissociation and Control", J. Dods, P. Brumer and M. Shapiro.
16. "Asymmetric Synthesis via Coherent Radiative Control of Molecular Photodissociation", M. Shapiro and P. Brumer.
17. "Control of Photochemistry", P. Brumer and M. Shapiro, to appear in "Molecules in Laser Fields", ed. A. Bandrauk, (Marcel Dekker, N.Y.).

*C. Conference Proceedings*

18. "Coherence in the Control of Molecular Processes", P. Brumer and M. Shapiro, in "Coherence Phenomena in Atoms and Molecules in Laser Fields", ed. A.D. Bandrauk (in press).
19. "Quantum Interference and the Control of Molecular Processes", P. Brumer and M. Shapiro, in "Mode Selective Chemistry", pgs. 323-331, ed. J. Jortner et al, (Kluwer, Netherlands, 1991).
20. "Coherent Effects in Laser Chemistry", M. Shapiro and P. Brumer, in "Optical Methods for Time and State Resolved Chemistry", ed. C. Ng, SPIE Proceedings, Jan. 1992 (in press).

*D. Publications previously reported (Final Report - 1989) as submitted, now published*

21. "Coherent Radiative Control of Unimolecular Reactions: Selective Bond Breaking with Picosecond Pulses", T. Seideman, M. Shapiro and P. Brumer, J. Chem. Phys. **90**, 7132 (1989).

22. "Coherent Radiative Control of Bimolecular Reactions", J. Krause, M. Shapiro and P. Brumer, *J. Chem. Phys.* **92**, 1126 (1990).
23. "Coherence Chemistry: Controlling Chemical Reactions With Lasers", P. Brumer and M. Shapiro, *Accounts Chem. Res.* **22**, 407 (1989).
24. "Mode Selective Control of Reactions by Rapid or Shaped Laser Pulses: An Emperor Without Clothes ", P. Brumer and M. Shapiro, *Chemical Physics*, **139**, 221 (1989).
25. "Creation and Dynamics of Molecular States Prepared with Coherent and Partially Coherent Pulsed Light", X-P. Jiang and P. Brumer, *J. Chem. Phys.* **94**, 5833 (1991).

#### **Work In Progress**

26. "Coherent Radiative Control of Photodissociation on Surfaces", (with X-P. Jiang).
27. "Coherent Control in High Fields", (with Z. Chen).
28. " Natural Modes in HOD, HOT, etc.", (with X-P. Jiang).
29. "Semiclassical Propagation of Polyatomic Photofragmentation", (with J. Campolieti).
30. "Quantum Calculations of Above Threshold Ionization", (with R. Blank).
31. "Quantum Computations of Polyatomic Photofragmentation", (with A. Abrashkevitch).

## Research Accomplishments

We continue research on our method of coherent radiative control of chemical reactions, extending the general theory and theoretically designing laboratory scenarios for displaying control. We have, during the course of this grant period, done several seminal pieces of research which both extend the theory and provide the basis for considerably greater advances in the near future. Particularly notable successes during this research period include:

- a) the successful demonstration of extensive control in IBr photodissociation using both a three photon + one photon scenario<sup>1,2</sup> as well as a pump-dump scenario<sup>3</sup>;
- b) the development of a theory of the interaction of molecules with a partially coherent laser source<sup>4</sup> and examination of the extent of control under these conditions<sup>13</sup>;
- c) controlled asymmetric synthesis: the demonstration that coherent control can be used to obtain chiral molecular products from achiral initial precursors<sup>5,16</sup>;
- d) the development of a cw laser scheme which allows for controlled cis-trans isomerization<sup>6</sup>;
- e) the first successful computation of control in a chemical reaction (here  $\text{H} + \text{OD} \rightarrow \text{DOH} \rightarrow \text{D} + \text{OH}$ ) which forms two chemically distinct product arrangements<sup>10</sup>;
- f) the development of a resonant 2-photon plus 2-photon scheme which allows for the control of chemical reactions in a thermal environment and eliminates other uncontrolled contributions<sup>8,9</sup>. Successful demonstration of control over two and three<sup>11</sup> product channels in the dissociation of  $\text{Na}_2$ ;

- g) the development of a semiclassical method for computing photodissociation in multiparticle systems<sup>14</sup> and successful tests on a simple photodissociation model; and
- h) the determination of conditions under which total control can be achieved in the N-level problem<sup>12</sup> under weak field conditions.

In addition, work has begun on a number of new coherent control problems which serve as the basis for our proposal for continued funding.

This report provides a very brief sketch of results obtained; the accompanying preprints and reprints should be consulted for further details. We also note, later below, the appearance of several experiments which have verified the essential principle of coherent control in the one product channel case. Further experimental work, motivated by theoretical developments, are in progress at various institutions.

*A. Simultaneous  $\omega_3, 3\omega_1$  Excitation:*

We have previously shown that photodissociation of single bound state by excitation with frequencies  $\omega_3$  and  $3\omega_1$ , where  $3\hbar\omega_1 = \hbar\omega_3$ , affords a method of doing control [M. Shapiro, J.W. Hepburn and P. Brumer, Chem. Phys. Lett. **149**, 451 (1988)]. Theoretically, control arises through the quantum interference induced between two optical routes controlled by different transition operators, i.e. the one photon  $\mu$  and three photon  $T$  operators. Here  $T$  is defined as

$$T = (\hat{\epsilon}_1 \cdot \mu)_{e,g} (E_i - H_g + 2\hbar\omega)^{-1} (\hat{\epsilon}_1 \cdot \mu)_{g,e} (E_i - H_e + \hbar\omega)^{-1} (\hat{\epsilon}_1 \cdot \mu)_{e,g},$$

where  $H_g, H_e$  are the ground and excited state Hamiltonians,  $\hat{\epsilon}_1$  is the unit vector in the direction of the electric field and  $E_i$  is the energy of the initial bound state  $|\phi_i\rangle$ . In this

instance the probability  $P(E, q)$  of observing a product at energy  $E$  and in arrangement channel  $q$  is given by:

$$P(E, q) = \left(\frac{\pi}{\hbar}\right)^2 \left[ \varepsilon_3^2 \sum_n |\langle \psi^- | (\hat{\varepsilon}_3 \cdot \underline{\mu})_{e,g} | \phi_i \rangle|^2 + \varepsilon_1^6 \sum_n |\langle \psi^- | T | \phi_i \rangle|^2 - 2\varepsilon_3\varepsilon_1^3 \cos(\theta_3 - 3\theta_1 + \delta_{13}^{(q)}) |F_{13}^{(q)}| \right]$$

with the amplitude  $F_{13}^{(q)}$  and phase  $\delta_{13}^{(q)}$  defined by:

$$|F_{13}^{(q)}| e^{i\delta_{13}^{(q)}} = \sum_n \langle \phi_i | T | \psi(E, n, q)^- \rangle \langle \psi(E, n, q)^- | (\hat{\varepsilon}_3 \cdot \underline{\mu})_{e,g} | \phi_i \rangle$$

The first and second terms in  $P(E, q)$  give one photon and three photon dissociation probabilities with fields of intensities  $\varepsilon_3^2$  and  $\varepsilon_1^2$  whereas the third term arises from the quantum interference between these two processes. The latter term affords experimental control over  $P(E, q)$ . Specifically, by experimentally manipulating the laser electric field amplitudes  $\varepsilon_1, \varepsilon_3$  and relative phase of the lasers  $\theta_3 - 3\theta_1$ , one directly alters  $P(E, q)$ .

To ascertain the extent of possible control in *realistic* systems we computationally examined<sup>1,2</sup> coherent radiative control in the photodissociation of IBr, which produces I + Br and I + Br\*, using high quality potential surfaces and fully quantum mechanical photodissociation methods. Results showed that an extremely wide range of control (25% to 95%) could be achieved by varying the relative laser phase and intensity over a modest range. Such control was also maintained for high  $J$  states ( $J = 42$ ), despite the required extensive averaging over 85  $M_j$  states. In this regard, also of interest, was the observation that the dependence on control parameters (relative laser phase and amplitude) is relatively independent of the  $J$  values.

The fundamental principle of coherent control, as manifest in this 1 + 3 photon scenario, has now been demonstrated experimentally [C. Chen, Y-Y. Yin, and D.S. Elliott,

Phys. Rev. Lett., **64**, 507 (1990); S.M. Park, S-P. Lu, and R.J. Gordon, J. Chem. Phys. **94**, 8622 (1991); B.A. Baranova, A.M. Chudinov and B. Ya Zel'dovitch, Opt. Comm., **79**, 116 (1990)]. Extensions to include more than one product channel are being planned by a number of experimental groups.

*B. Pump-Dump Control in IBr Photodissociation:*

Whereas the 1+3 photon scenario described above relies upon the interference at a fixed energy induced by two different CW fields, an alternative approach [M. Shapiro and P. Brumer, J. Chem. Phys. **90**, 7132 (1989)] utilizes a pulsed laser to prepare a superposition of two or more bound states and a subsequent dump laser to carry the system to dissociation. Interference is induced in this scenario by the multitude of frequencies within the second pulse which carry each member of the superposition to the same range of continuum energies  $E$ .

In the general case the initial excitation pulse  $\bar{\epsilon}_x(t)$ , creates a linear superposition state in the excited state and the temporally separated dump pulse  $\bar{\epsilon}_d(t)$  brings the system to the regime where products are energetically accessible. The state prepared after the  $\bar{\epsilon}_x(t)$  is given in first order perturbation theory by:

$$|\phi(t)\rangle = |E_g\rangle e^{-iE_g t/\hbar} + \sum_j c_j |E_j\rangle e^{-iE_j t/\hbar}$$

with

$$c_j = (\sqrt{2\pi}/i\hbar) \langle E_j | \mu | E_g \rangle \epsilon_x(\omega_{jg}) = d_j \epsilon_x(\omega_{jg})$$

where  $\omega_{jg} = (E_j - E_g)/\hbar$ , the excitation frequency to level  $|E_j\rangle$  from the ground state  $|E_g\rangle$  and where  $d_j$  is defined by the second equality. Note that  $\epsilon_x(\omega)$  or  $\epsilon_d(\omega)$  denote the Fourier transform of the respective laser pulse.

Subsequently, the system is subjected to a  $\bar{\epsilon}_d(t)$  and perturbation theory, plus the rotating wave approximation, gives the probability  $P(E, q)$  of forming product in arrangement channel  $q$  at energy  $E$  as

$$P(E, q) = (2\pi/\hbar^2) \sum_n \left| \sum_j c_j \langle E, n, q^- | \mu | E_j \rangle \epsilon_d(\omega_{EE_j}) \right|^2$$

where  $\omega_{EE_j} = (E - E_j)/\hbar$  and  $c_j$  is given above.

Expanding the square gives the canonical form:

$$\begin{aligned} P(E, q) &= (2\pi/\hbar^2) \sum_{ij} c_i c_j^* \epsilon_d(\omega_{EE_i}) \epsilon_d^*(\omega_{EE_j}) \mu_{i,j}^{(q)}(E) \\ &= (2\pi/\hbar^2) \sum_{ij} d_i d_j^* \epsilon_x(\omega_{ig}) \epsilon_x^*(\omega_{jg}) \epsilon_d(\omega_{EE_i}) \epsilon_d^*(\omega_{EE_j}) \mu_{i,j}^{(q)}(E) \end{aligned}$$

Here  $\mu_{i,j}^{(q)}(E) = \langle E, n, q^- | \mu | E_i \rangle \langle E_j | \mu | E, n, q^- \rangle$ . An examination<sup>21</sup> of the expression for  $P(E, q)$  shows that the laboratory control parameters are the time delay  $\Delta t$  between the pulses and the coefficients  $c_i$  of the initially created superposition, controlled via properties of the initial excitation pulse.

Essentially this approach, in which a few states are excited by  $\bar{\epsilon}_x(t)$ , emphasizes quantum, rather than classical, characteristics, and encodes coherence in a minimum of states, allowing for the use of pulses in the convenient picosecond and even (for polyatomics) nanosecond range.

We have recently<sup>3</sup> utilized this technique to control Br vs Br\* production in the photodissociation of IBr. Specifically, the coupling of the electronic and nuclear angular momenta in the  $^1\Sigma^+$  and  $^3\Pi_1$  electronic states results in closely spaced ( $1 \text{ cm}^{-1}$ ) bound state levels. Pumping from the ground electronic state to form a superposition of a pair of these states, and subsequently pumping to the continuum above the Br\* threshold allowed

for control over Br vs Br\* yield. Indeed, by varying the time delay between pulses and the central frequency of the excitation pulse we were able to obtain yields ranging from 4% Br\* to 96% Br\*, i.e. almost total product control. Since pulse durations and delays were computed to be in the 10 picosecond region this appears to be an experiment which can readily be carried out with current technology.

*C. Partially Coherent Sources:*

Phase coherence, of both the laser and the molecule, are central to the success of our interference based control approach. That is, the quantum interference necessary for control relies upon a combination of the known molecular phases and the known laser electromagnetic field phases. However, real systems often display partial, rather than full coherence properties, i.e. the state of the molecule or laser is described by a density matrix rather than a wavefunction. This being the case, it is important to analyze the extent to which control survives the introduction of both molecular and laser phase incoherence. [Alternatively one may design schemes which bypass the phase incoherence effects-see M. Shapiro and P. Brumer, J. Chem. Phys. **90**, 6179 (1989) and the technique in Section G below.] Having previously provided a method for analyzing the effects of dephasing collisions on control [M. Shapiro and P. Brumer, J. Chem. Phys. **90**, 6179 (1989)] we have now examined<sup>13</sup> the effect of laser incoherence on the pump-dump control scenario. The approach follows directly from the pump-dump treatment above, in conjunction with a phase diffusion model [X-P. Jiang and P. Brumer, J. Chem. Phys. **94**, 5833-5843 (1991)] of the pulsed laser. Under conditions where the laser is partially coherent the expression

for  $P(E, q)$  becomes

$$P(E, q) = (2\pi/\hbar^2) \sum_{ij} d_i d_j^* \langle \epsilon_x(\omega_{ig}) \epsilon_x^*(\omega_{jg}) \rangle \langle \epsilon_d(\omega_{EE_i}) \epsilon_d^*(\omega_{EE_j}) \rangle \mu_{i,j}^{(q)}(E),$$

with the frequency-frequency correlation functions for the assumed Gaussian excitation pulse given by

$$\langle \epsilon_x(\omega_2) \epsilon_x^*(\omega_1) \rangle = \frac{\epsilon_{x0}^2 \tau_x T_x}{8} e^{i(\omega_2 - \omega_1)t_x} e^{-\tau_x^2(\omega_2 - \omega_1)^2/8} e^{-T_x^2(\omega_2 + \omega_1 - 2\omega_x)^2/8},$$

where

$$T_x = \tau_x \tau_{xc} / (\tau_x^2 + \tau_{xc}^2)^{1/2}.$$

A similar expression applies to the dump pulse. Here  $\tau_x$  is the duration of the excitation pulse, with center at time  $t_x$  and intensity  $\epsilon_{x0}^2$  and  $\tau_{xc}$  is the correlation decay time of the excitation pulse. Integrating over energy to collect all product produced by the pulse produces  $P(q)$ . The structure of  $P(q)$  now shows exponential decay of both the direct ( $i = j$ ) photodissociation probabilities as well as of the interference term between paths ( $i \neq j$ ), with the decay rate determined by the incoherence of the pump and dump pulses. However, a generalized Parseval Equality which we have obtained<sup>13</sup>, valid under well defined conditions, shows that the coherence characteristics of the latter are far less significant than those of the former.

Computational studies<sup>13</sup> on the decay of a model  $\text{DH}_2$  system, where the excitation pulse produced superpositions of pairs of states as well as large numbers of states, indicated that control could be maintained for pump pulses whose coherence was better than  $\tau_c/\tau \leq 2$  to 3, a range which precludes control with typical nanosecond laser pulses but allows control for typical picosecond incoherences. Computational results also made clear that

the degree to which control can be maintained in the presence of partial pulsed laser coherence is a strong function of the molecular transition matrix elements, suggesting that examination of specific systems of interest using the derived formalism is a worthwhile endeavor.

*D. Controlled Photon Induced Symmetry Breaking; Asymmetric Synthesis:*

Asymmetric synthesis has served as a goal for chemists since the time of Louis Pasteur. The goal of asymmetric synthesis is to produce a specific molecular enantiomer, as distinct from its mirror image (e.g., to produce the dextro, rather than levo, form of a molecule). As a consequence of intense research interest a number of schemes have been proposed; all require the use of some chiral precursor, such as a chiral catalyst or chiral reactant.

A number of efforts have been made to utilize photoexcitation to perform asymmetric synthesis but these tended to rely upon very small high order perturbation terms in the molecular Hamiltonian. Recently<sup>5</sup> we have shown that it is possible to selectively enhance the yield of a desired enantiomer by using coherent control applied to the photodissociation of meso-type molecules, i.e.  $ABA'$  where  $A$  and  $A'$  are enantiomers. Here  $ABA'$  dissociates as:



In essence we utilize a pump-dump scenario in which the pump prepares a linear superposition of a pair of selected bound states, followed by a dump pulse. Such a scheme, we showed, allowed for selective production of one enantiomer (e.g.  $A$ ) over another ( $A'$ ). This remarkable result uses linearly polarized light and requires only that the final products be separated in a weak magnetic field so that control can be achieved by taking

advantage of the (previously unrecognized) difference in total cross section for producing  $A+BA'$  in an specific  $M_j$  state and  $AB + A'$  in the same  $M_j$  state. Numerical results on a model system confirmed these predictions. Work is planned on methods of removing the requirement for a weak magnetic field through a focus on the differential cross section and on the possibility of doing chemistry on surfaces where the selection rules differ.

*E. Control of Cis-Trans Isomerization:*

The underlying principles of quantum scattering theory make clear that the essence of control lies in the character of the stationary eigenstates of the Hamiltonian. As such it deemphasizes ideas such as rapid time dependence competing with time scales of nuclear motion<sup>24</sup> or the explicit role of pulse time scales in the control of reactions. To make clear the extent to which control may rely solely upon stationary properties, and to consider the important case of control of cis-trans isomerization, we proposed a control approach based on differences in cis-trans stationary eigenfunctions<sup>6</sup>. Specifically, a nanosecond laser is used to excite a molecule from the cis (or trans) configuration to the excited electronic state. A second laser is then used to deexcite the system to an eigenstate of the trans (or cis) Hamiltonian. Since the energy eigenvalues of the cis and trans configuration differ, selective product yields are possible. Conditions on the molecule and laser under which such a scenario would be effective were determined and successful control was displayed using a model of Stilbene isomerization.

*F. Control over Chemically Distinct Products; The Photodissociation of HOD:*

The ability to control chemical reactions is of vital interest to the chemistry community, where product channels differ by atomic arrangement: e.g. product  $AB + C$  as distinct

from product AC + B in the decomposition of ABC. Current quantum mechanical methods for treating photodissociation are, as yet, incapable of handling such cases. For this reason we have suggested, as part of our proposed research, continuing studies into quantum and semiclassical methods for photodissociation.

Despite this state of affairs, the particular system



is amenable to computation at energies where the two channels may be realistically treated as decoupled [M. Shapiro in "Mechanisms for Isotopic Enrichment in Photodissociation Reactions", ACS Symposium Series, ACS Books (1991)]. The system is also of great interest because control over HOD decay presents a particularly serious challenge to control schemes since the two product channels differ only in mass factors, with the potential surface in both channels being identical.

We have carried out a detailed computational study of control over HOD photodissociation<sup>10</sup> using the pump-dump scenario. The initial excitation was assumed to prepare superpositions of a pair of bend and stretch modes in the ground electronic state and the subsequent dump lifted the system to the excited electronic B state. Results indicated that there was substantial control associated with variations of the frequency of the pump pulse and somewhat less control associated with variations in the time delay between pulses. The origin of the former was clearly in the natural preference of the two individual pumped states to photodissociate to HO + D and DO + H, respectively. The latter, an indication of true quantum interference based coherent control, showed variations in the yield over a range of 10%. Although this yield is not substantial it is impressive for a case

such as HOD where product channel differences are slight and bodes well for the future of control in systems with distinct chemical arrangements characterizing different product channels.

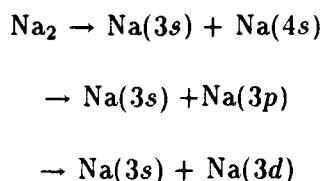
*G. Control in Thermal Environments; 2-Photon + 2-Photon Interference:*

Coherent control is based upon quantum interference. As noted above, to maximize such control both molecule and laser field should ideally be in a pure state since molecular and optical phases both play a crucial role. Incoherence effects leading to a mixed initial matter-photon state, such as partial laser coherence or an initially mixed molecular state, degrade control. As a consequence, all but one [M. Shapiro and P. Brumer, *J. Chem. Phys.* **90**, 6179 (1989)] of our previous coherent control scenarios were limited to isolated molecules in a pure state, e.g. molecular beam systems. In a recent study<sup>9,11</sup> we showed that it is possible to maintain control in a molecular system in thermal equilibrium by interfering two distinct resonant two-photon routes to photodissociation. In particular, the resonant character of the excitations insure that only a selected state out of the molecular thermal distribution participates in the photodissociation. Hence coherence is re-established by the excitation and maintained throughout the process.

The proposed control scenario also provides a method of overcoming loss of control due to the to phase jitter in the laser source. That is, consider the two two-photon routes, the first consisting of excitation with  $2\omega$  and the second of excitation with  $\omega_- + \omega_+ \equiv (\omega - \delta) + (\omega + \delta)$ . If, we assume that both  $\omega_-$  and  $\omega_+$  are produced by passing  $2\omega$  through a nonlinear crystal, then the phase difference between the two excitation routes is a constant, independent of jitter in the initial frequency  $\omega$  laser. Thus, effects due to phase incoherence

in the source are minimized. In addition, we have also shown that this approach allows the reduction of contributions from uncontrolled ancillary photodissociation routes (such as  $\omega + \omega_+$ , etc.), substantially increasing control.

Computational results on the multiproduct photodissociation of  $\text{Na}_2$ :



show a wide range of control over the two possible products at lower energy and the three products at energies above the  $\text{Na}(3s) + \text{Na}(3d)$  threshold. To compute these results required the development<sup>8</sup>, and computational implementation, of a theory of resonant two photon dissociation.

These results, we believe, constitute a major advance, providing a scenario eliminating three major incoherence effects and defining a method for controlling molecular reactions in natural environments.

#### *H. Semiclassical Propagation for Photodissociation:*

Since quantum mechanics will, in the foreseeable future, be limited to small molecules, we began to examine possible classical and semiclassical methods for treating laser controlled photodissociation.

Classical and semiclassical methods have been highly successful in providing both qualitative and quantitative results on unimolecular and bimolecular heavy particle reactions. Our interest is in light-induced reactions and simple classical trajectory methods have also been applied in such cases, e.g. to compute photodissociation cross sections. How-

ever, the methods which have been developed are not directly applicable to control since simple photodissociation calculations only require the computation of *probabilities* such as  $P(E, n, q) = | \langle E_i | \mu | E, n, q^- \rangle |^2$ . Here  $P(E, n, q)$  is the probability of forming a final state at energy  $E$  in an arrangement channel labeled  $q$  with quantum numbers  $n$ . Here the ket  $|E_i\rangle$  is an initial bound state at energy  $E_i$  from which photodissociation occurs. By contrast with such calculations, coherent control of chemical reactions requires both the magnitude and phases of *complex* matrix element products such as  $\langle E_i | \mu | E, n, q^- \rangle \langle E, n, q^- | \mu | E_j \rangle$ . We have begun to develop semiclassical methods to compute these types of quantities.

The essential difficulty in computing photodissociation amplitudes semiclassically arises from the "trajectory root search" problem in classical S-matrix theory, i.e. the requirement to locate classical trajectories which are defined by boundary values at both initial and final times. Such a requirement leads, for polyatomics, to multidimensional root searches in a virtually intractable two point boundary value problem. This deficiency was recognized early on by W.H. Miller but one solution, the so-called Initial Value Representation, in which required trajectories were specified by initial values, led to highly oscillatory integrands, and hence an equally intractable approach.

Motivated by the need for an efficient semiclassical method for photodissociation amplitudes we recently recently reexamined the initial value problem for inelastic scattering [G. Campolieti and P. Brumer, J. Chem. Phys. **96**, 5969 (1992)]. Specifically, we obtained both a useful formal initial value representation for inelastic and reactive scattering as well as an efficient numerical method for handling the oscillatory integrands which arise in this approach. These results motivated further consideration of the initial value representation

for photodissociation computations and hence for control over chemical reactions.

Thus far we have obtained an initial value representation for the required amplitudes, as described below, and tested the method on a model uncoupled photodissociation problem. Further work on this method is part of our current proposal for continued support.

The essence of our proposed approach is readily summarized. Consider photodissociation to a single product arrangement channel, allowing us to suppress the  $q$  channel label. The required photodissociation scattering amplitude may be written in terms of the Moller Wave Operator  $\Omega^{(-)}$  as:

$$\langle \psi^{(-)}(E, n) | \mu \cdot \epsilon | \psi_b \rangle = \langle E, n | \Omega^{(-)\dagger}(\mu \cdot \epsilon) | \psi_b \rangle. \quad (1)$$

Our asymptotic equivalence approach [G. Campolieti and P. Brumer, J. Chem. Phys. **96**, 5969 (1992) and Ref. 14] provides a means of obtaining an initial value representation for the Moller Wave operator, for an  $N$  degree of freedom system, resulting in the form<sup>14</sup>

$$\begin{aligned} \langle p'_2 | \Omega^{(-)\dagger} | p'_1 \rangle = & (-2\pi i\hbar)^{-3N/2} \int dq_1 dp_1 \left[ \det \left( \frac{\partial \tilde{q}}{\partial q_1}(q_1, p_1, T) \right) \right]^{1/2} \\ & \exp \left\{ \frac{i}{\hbar} (\Phi(T) + \tilde{q}(T)[p(T) - p'_2] - q_1[p_1 - p'_1]) \right\} \end{aligned} \quad (2)$$

Here  $q, p$  are  $3N$  canonical coordinates and momenta,  $T$  is a time after dissociation is over and  $\tilde{q} = q - \frac{p}{m}t$  and the classical action  $\Phi(T)$  is given by

$$\Phi(T) = \int_0^T \left[ q(t') - \frac{t}{m} p(t') \right] \dot{p}(t') + V^s(q(t'), p(t')) dt'. \quad (3)$$

The quantities  $q(t'), p(t')$  are obtained from trajectory dynamics with initial conditions  $q_1, p_1$  and  $V^s$  is the scattering interaction, i.e. the full Hamiltonian  $H$  minus the asymptotic channel Hamiltonian  $H_0$ . Note that Eq. (2) implies an integration over all trajectories with initial conditions  $p_1, q_1$ . Unlike the classical S-matrix approach,  $p'_2$  is a parameter and not final trajectory (target) conditions.

Inserting the integral representation for the propagator into Eq.(2) gives the convenient expression [with  $\tilde{q}(T) \equiv \tilde{q}(q_1, p_1, T)$ ]

$$\begin{aligned} \langle \psi^{(-)}(p'_2) | (\mu \cdot \epsilon) | \psi_b(N'_1) \rangle &= (2\pi\hbar)^{-N} \int dq_1 \int dp_1 \left[ \det \left( \frac{\partial q(T)}{\partial q_1} \right) \right]^{1/2} (\mu(q_1) \cdot \epsilon) \psi_b^{N'_1}(q_1) \\ &\times \exp \left\{ \frac{i}{\hbar} (\Phi(T) + q(T) \cdot [p(T) - p'_2] - q_1 \cdot p_1) \right\} \end{aligned} \quad (4)$$

Note the simplicity of the expression insofar as one initiates trajectories in phase space and propagates them to dissociation, carrying the appropriate semiclassical phase. The interference between them is automatically taken care of in the integration and there is no need to do any root searches.

Preliminary tests of this method have been performed on a model system consisting of IBr dissociation on uncoupled diabatic potential energy curves. The results *obtained with a single classical trajectory per E* were found to be highly accurate and further work on this method is contained in our proposal.

### *I. Complete N-Level Control:*

Attempts to maximize the yield of a particular channel have utilized optimal control theory techniques to find laser pulse shapes which optimize the desired yield<sup>7</sup>. The resultant pulses are highly structured and the problem computationally complex insofar as the high fields considered result in a complicated nonlinear optimization problem.

Recently<sup>12</sup> we examined the case of yield optimization in the weak laser pump-dump scenario and have determined conditions under which complete control over populations is possible. Specifically, we have considered the case where the pump prepares a superposition of N bound state levels which are then photodissociated by the dump pulse. The result, an extension of our theorem for complete control with N=2 [P. Brumer and M.

Shapiro, Chem. Phys. Lett. **126**, 541 (1986)], shows that *complete control* is possible when (a) the continuum absorption spectrum is composed of a series of sufficiently-narrow resonances, and b) that the photodissociation process is a non-factorizable one, i.e., it cannot be broken up to an excitation process (of a "bright" state) and a dissociation process (to a set of "dark" states).

This important prediction motivates further studies on the linear optimization scheme which paper are included in our proposal for future research.

#### **Additional Work in Progress**

In addition, two other major studies have been initiated, one on coherent control on surfaces<sup>26</sup> and the other on control in high fields<sup>27</sup>. Both form major components of the research which we propose in our request for renewal of this grant. They are therefore discussed there in detail.

# Coherent radiative control of IBr photodissociation via simultaneous ( $\omega_1, \omega_3$ ) excitation

C. K. Chan and P. Brumer

Chemical Physics Theory Group, Department of Chemistry, University of Toronto,  
Toronto, Canada M5S 1A1

M. Shapiro

Department of Chemical Physics, The Weizmann Institute of Science, Rehovot, Israel 76100

(Received 11 April 1990; accepted 7 November 1990)

We show that simultaneous one- and three-photon photodissociation of IBr can be used to control the relative product yield of ground and excited state Br atoms. The control attained is substantial insofar as it is possible to vary the Br\* yield over the range of 25%–95%, even for a high  $J$  case which involves extensive averaging over  $M_J$  states.

## I. INTRODUCTION

Controlling the yield of molecular reaction using lasers has been a longstanding goal in chemical dynamics. Early laser-based attempts at control relied either on the frequency resolution of lasers to locate a frequency which maximizes the yield, or on the use of high power lasers to alter the dynamics. Both methods suffer from severe drawbacks; the former depends on the chance existence of a favorable branching ratio and the latter requires extremely high powers which make it impractical. In addition, both of these methods are passive in the sense that the yield is primarily determined by molecular properties and cannot be controlled by experimental design.

Recently, we proposed a theoretical approach for *actively* controlling the yield using low power lasers<sup>1,2</sup> which is based upon the following general idea. Suppose that we invoke two simultaneous coherent paths  $a$  and  $b$  to get to the products. Under these circumstances the probability  $P$  of producing products is given by

$$P = |A_a|^2 + (A_a A_b^* + A_a^* A_b) + |A_b|^2. \quad (1)$$

Here  $A_i$  is the probability amplitude of obtaining products through path  $i$ , so that  $|A_a|^2$  and  $|A_b|^2$  are the probabilities for independently obtaining products from path  $a$  and path  $b$ . The second term, the cross term, can be positive or negative and arises from the quantum interference between the two paths. If both paths  $a$  and  $b$  lead to more than one product channel then the branching ratio  $R_{qq'}$  for channels  $q$  and  $q'$  is of the form

$$R_{qq'} = \frac{|A_a^{(q)}|^2 + (A_a^{(q)} A_b^{(q)*} + A_a^{(q)*} A_b^{(q)}) + |A_b^{(q)}|^2}{|A_a^{(q')}|^2 + (A_a^{(q')} A_b^{(q')*} + A_a^{(q')*} A_b^{(q')}) + |A_b^{(q')}|^2}. \quad (2)$$

Here,  $A_b^{(q)}$  is the probability amplitude for obtaining products in channel  $q$  from path  $a$  and other  $A$  quantities are similarly defined.

To have active control over the product distribution means that one can experimentally manipulate the magnitude of the numerator or the denominator in Eq. (2). Thus, if one can design an experimental scenario such that by varying laboratory parameters one varies the sign and magnitude

of the cross term, then one gets control over product distributions and product yields. We term this overall approach, which relies upon coherence and the use of interference between a minimum of two paths, coherent radiative control.<sup>1,2</sup> Alternate methods, based upon time dependent wave packet approaches, have been developed by others.<sup>3</sup>

We first implemented these general principles in an example of one-photon dissociation of a superposition state.<sup>1(a)-1(c)</sup> Specifically, we suggested preparing and dissociating a superposition of two bound states. In this case, the dissociation from two components of the superposition state were the two required simultaneous independent paths and the cross term, essential to control, arose from the interference between them. Our computational results<sup>1</sup> showed that the cross term could be manipulated to give a vast range of possible control, by experimentally varying the combined phases and amplitude ratio due to the lasers used to prepare the superposition state and to dissociate the molecule. Experimental verification of this particular implementation of coherent control may be realizable through the use of nonlinear optical techniques.<sup>1(d)</sup>

Subsequently, we proposed a number of other experimental routes for achieving coherent control.<sup>1(d)-1(k),2</sup> A number of these involve dissociating a single eigenstate, rather than a superposition state. For example, in one case<sup>1(k)</sup> we obtained active control over differential cross sections with a single laser frequency of variable elliptical polarization. Here dissociating the molecule via the two orthonormal components of the polarization vector act as the two simultaneous coherent paths and the interference between them provides the cross term for control. Experimental control over the branching ratio is obtained by varying the phase difference and the degree of elliptical polarization of the incident light. Another scenario,<sup>2</sup> of particular interest to this paper, uses two lasers of frequency  $\omega_1$  and  $\omega_3 = 3\omega_1$  to simultaneously dissociate an initial eigenstate. The resulting one- and three-photon dissociation routes create the necessary interference for control. The product yields may be controlled by varying the relative phases and the amplitudes of the  $\omega_1$  and  $\omega_3$  lasers.

Recently, an experimental verification of this effect, using three- vs five-photon absorption in the ionization of Hg.

has been published.<sup>4</sup> In this experiment, control of only a single channel, i.e., the ionization process itself, has been demonstrated. In addition, the effect was also confirmed theoretically in the strong field limit.<sup>5</sup>

Previously,<sup>2</sup> we developed the general theory of control via one-plus-three photon dissociation but provided no computational study to assess the range of control afforded by this route. Here we apply this simultaneous  $(\omega_1, \omega_3)$  excitation method to control the dissociation<sup>6-8</sup> of IBr to either  $I(^2P_{3/2}) + Br(^2P_{3/2})$  or  $I(^2P_{1/2}) + Br(^2P_{1/2})$  and demonstrate extensive control over product yield. For example, photodissociation of IBr with  $\lambda < 526$  nm is known<sup>7,9,10</sup> to yield  $Br(^2P_{1/2})$  almost exclusively, i.e.  $(Br(^2P_{1/2})/Br(^2P_{3/2})) \approx 3-4$ . However, as demonstrated below, simultaneous  $(\omega_1, \omega_3)$  excitation allows us to easily reverse this trend to obtain predominantly  $Br(^2P_{3/2})$ .

This paper is organized as follows. In Sec. II, we summarize the implementation of coherent control via one-plus-three photon dissociation. Application is made to IBr dissociation in Sec. III and numerical results for yield control in IBr are presented in Sec. IV.

## II. ONE-PLUS-THREE PHOTON-INDUCED DISSOCIATION

We briefly summarize the one-plus-three photon implementation of coherent control.<sup>2</sup> Consider an isolated molecule  $A$  which dissociates, upon excitation to an excited electronic state at energy  $E$ , to several possible chemically distinct arrangement channels (e.g.,  $B + C, D + F$ ), labeled  $q = 1, 2, \dots$ . Let  $H_g$  and  $H_e$  be the nuclear Hamiltonians for the ground and excited states, respectively, and  $|E_i\rangle$  be the ground eigenstate, i.e.,  $H_g|E_i\rangle = E_i|E_i\rangle$ . (In the computational section below the notation  $|E_i\rangle$  is expanded to include the angular momentum quantum numbers. They are left out here for simplicity.) We define  $|E, n, q^-\rangle$  as the continuum eigenstates of  $H_e$  which satisfy incoming boundary conditions, i.e.  $|E, n, q^-\rangle$  goes asymptotically to the product state described by quantum number  $n$ , energy  $E$  and molecular arrangement  $q$ .

The molecule, initially in  $|E_i\rangle$ , is subjected to two electric fields given by

$$\begin{aligned} \epsilon(t) = & \epsilon_1 \cos(\omega_1 t + \mathbf{k}_1 \cdot \mathbf{R} + \theta_1) \\ & + \epsilon_3 \cos(\omega_3 t + \mathbf{k}_3 \cdot \mathbf{R} + \theta_3). \end{aligned} \quad (3)$$

Here  $\omega_3 = 3\omega_1$ ,  $\epsilon_l = \epsilon_l \hat{\epsilon}_l$ ,  $l = 1, 3$ ;  $\epsilon_l$  is the magnitude and  $\hat{\epsilon}_l$  is the polarization of the electric fields. The two fields are

chosen parallel, with  $\mathbf{k}_3 = 3\mathbf{k}_1$ . Excitation with the first and second electric field provide the two simultaneous paths to the dissociation products. As discussed in Sec. I, the probability  $P(E, q; E_i)$  of producing product with energy  $E$  in arrangement  $q$  from a state  $|E_i\rangle$  is given by the probabilities  $P_1(E, q; E_i)$  and  $P_3(E, q; E_i)$  due to the  $\omega_1$  and  $\omega_3$  excitation, plus the cross term  $P_{13}(E, q; E_i)$  due to the interference between the two excitations

$$\begin{aligned} P(E, q; E_i) \\ = P_3(E, q; E_i) + P_{13}(E, q; E_i) + P_1(E, q; E_i). \end{aligned} \quad (4)$$

[We adhere, throughout this paper, to the (initially confusing) nonlinear optics convention that the subscript 3 denotes the tripled photon and hence induces one-photon photodissociation. Similarly,  $P_1$  and  $\omega_1$  relate to the three-photon process.]

In the weak field limit,<sup>11,12</sup>  $P_3(E, q; E_i)$  is given by

$$P_3(E, q; E_i) = \left(\frac{\pi}{\hbar}\right)^2 \epsilon_3^2 \sum_n |\langle E, n, q^- | (\hat{\epsilon}_3 \cdot \boldsymbol{\mu})_{e,g} | E_i \rangle|^2. \quad (5)$$

Here  $\boldsymbol{\mu}$  is the electric dipole operator, and

$$(\hat{\epsilon}_3 \cdot \boldsymbol{\mu})_{e,g} = \langle e | \hat{\epsilon}_3 \cdot \boldsymbol{\mu} | g \rangle, \quad (6)$$

where  $|g\rangle$  and  $|e\rangle$  are the ground and excited electronic state wave functions, respectively. Assuming also that  $E_i + 2\hbar\omega_1$  is below the dissociation threshold, with dissociation occurring from the excited electronic state,  $P_1(E, q; E_i)$  is given in third order perturbation theory by<sup>2</sup>

$$P_1(E, q; E_i) = \left(\frac{\pi}{\hbar}\right)^2 \epsilon_1^2 \sum_n |\langle E, n, q^- | T | E_i \rangle|^2, \quad (7)$$

with

$$\begin{aligned} T = & (\hat{\epsilon}_1 \cdot \boldsymbol{\mu})_{e,g} (E_i - H_g + 2\hbar\omega_1)^{-1} \\ & \times (\hat{\epsilon}_1 \cdot \boldsymbol{\mu})_{g,e} (E_i - H_e + \hbar\omega_1)^{-1} (\hat{\epsilon}_1 \cdot \boldsymbol{\mu})_{e,g}. \end{aligned} \quad (8)$$

A similar derivation<sup>2</sup> gives the cross term in Eq. (4) as

$$\begin{aligned} P_{13}(E, q; E_i) \\ = -2 \left(\frac{\pi}{\hbar}\right)^2 \epsilon_3 \epsilon_1^2 \cos(\theta_3 - 3\theta_1 + \delta_{13}^{(q)}) |F_{13}^{(q)}| \end{aligned} \quad (9)$$

with the amplitude  $|F_{13}^{(q)}|$  and phase  $\delta_{13}^{(q)}$  defined by

$$\begin{aligned} |F_{13}^{(q)}| \exp(i\delta_{13}^{(q)}) \\ = \sum_n \langle E_i | T | E, n, q^- \rangle \langle E, n, q^- | (\hat{\epsilon}_3 \cdot \boldsymbol{\mu})_{e,g} | E_i \rangle. \end{aligned} \quad (10)$$

The branching ratio  $R_{qq'}$  for channels  $q$  and  $q'$ , can then be written as

$$R_{qq'} = \frac{P(E, q; E_i)}{P(E, q'; E_i)} = \frac{\epsilon_3^2 F_3^{(q)} - 2\epsilon_3 \epsilon_1^2 \cos(\theta_3 - 3\theta_1 + \delta_{13}^{(q)}) |F_{13}^{(q)}| + \epsilon_1^2 F_1^{(q)}}{\epsilon_3^2 F_3^{(q')} - 2\epsilon_3 \epsilon_1^2 \cos(\theta_3 - 3\theta_1 + \delta_{13}^{(q')}) |F_{13}^{(q')}| + \epsilon_1^2 F_1^{(q')}} \quad (11)$$

where

$$F_3^{(q)} = \left(\frac{\hbar}{\pi}\right)^2 \frac{P_3(E, q; E_i)}{\epsilon_3^2}, \quad F_1^{(q)} = \left(\frac{\hbar}{\pi}\right)^2 \frac{P_1(E, q; E_i)}{\epsilon_1^2}, \quad (12)$$

with  $F_3^{(q')}$  and  $F_1^{(q')}$  defined similarly. Next, we rewrite Eq. (11) in a more convenient form. We define a dimensionless parameter  $\bar{\epsilon}$ , and a parameter  $x$  as follows:

$$\epsilon_l = \bar{\epsilon}_l \epsilon_{0l}; \quad x = \bar{\epsilon}_1^2 / \bar{\epsilon}_3 \quad (13)$$

for  $l = 1, 3$ . The quantity  $\epsilon_0$  essentially carries the unit for the electric fields; variations of the magnitude of  $\epsilon_0$  can also be used to account for unknown transition dipole moments. Utilizing these parameters, Eq. (11) becomes

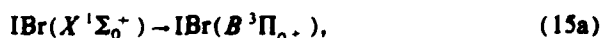
$$R_{qq} = \frac{F_3^{(q)} - 2x \cos(\theta_3 - 3\theta_1 + \delta_{13}^{(q)}) \epsilon_0^2 |F_{13}^{(q)}| + x^2 \epsilon_0^4 F_1^{(q)}}{F_3^{(q)} - 2x \cos(\theta_3 - 3\theta_1 + \delta_{13}^{(q)}) \epsilon_0^2 |F_{13}^{(q)}| + x^2 \epsilon_0^4 F_1^{(q)}} \quad (14)$$

Experimental control over  $R_{qq}$  is therefore obtained by varying the difference  $(\theta_3 - 3\theta_1)$  and the parameter  $x$ . The former is the phase difference between the  $\omega_3$  and the  $\omega_1$  laser fields and the latter, via Eq. (13), incorporates the ratio of the two lasers amplitudes. Since "tripling" is a common method for producing  $\omega_3$  from  $\omega_1$ , of fixed relative phase, the subsequent variation of the phase of one of these beams provides a straightforward method of altering  $\theta_3 - 3\theta_1$ .

### III. APPLICATION: PHOTODISSOCIATION OF IBr

In this section, we apply this scenario to control product yields in the photodissociation of IBr. In particular, we are interested in the energy regime where IBr dissociates to both  $I(^2P_{3/2}) + Br(^2P_{3/2})$  and  $I(^2P_{3/2}) + Br^*(^2P_{1/2})$ .

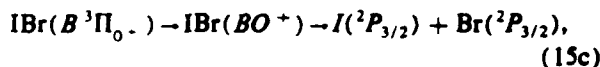
The IBr potential curves<sup>5</sup> used in the calculation are shown in Fig. 1. In accordance with the notation in the figure, the photodissociation process can be understood in terms of the following virtual steps:<sup>7</sup> (a) Photoexcitation,



followed by either (b) a "diabatic-like" dissociation,



yielding excited  $Br^*$  atom or (c) an "adiabatic-like" dissociation,



in which the molecule follows the adiabatic curve and dissociates to ground state atoms.

An appropriate IBr computation requires inclusion of the angular momentum component. Thus the  $|E_i\rangle$  of Sec. II are replaced by  $|E_i, J_i, M_i\rangle$ , the bound eigenstate of the ground potential surface. Here  $J_i$  is the angular momentum,  $M_i$  is its  $z$  projection and the ket is of energy  $E_i$ , whose value incorporates specification of the vibrational quantum number  $v$ . Where no confusion arises, we continue to use  $|E_i\rangle$  for simplicity.

The primary quantity required in the control calculation is the photodissociation amplitude  $\langle E, n, q^- | (\hat{e}_i \cdot \mu)_{e,g} | E_i, J_i, M_i \rangle$ ,  $\hat{e}_i = \hat{e}_1, \hat{e}_3$  where the quantum number  $n$  in the continuum state  $|E, n, q^- \rangle$  denotes the scattering angles  $\hat{k} = \phi_k, \theta_k$  and  $q = 1, 2$  labels either the  $Br(^2P_{3/2})$  or  $Br^*(^2P_{1/2})$  channel. In terms of this notation, the one-photon photodissociation amplitude is given by<sup>13</sup>

$$\begin{aligned} & \langle E, \hat{k}, q^- | (\hat{e}_i \cdot \mu)_{e,g} | E_i, J_i, M_i \rangle \\ &= \frac{(2mk)^{1/2}}{h} \sum_T (2J+1)^{1/2} \begin{pmatrix} J & 1 & J_i \\ -M_i & 0 & M_i \end{pmatrix} \\ & \times D_{0,M}^J(\phi_k, \theta_k, -\theta_k) t(E, J, q | E_i, J_i). \end{aligned} \quad (16)$$

Here  $m$  is the reduced mass of IBr,  $k$  is the relative momentum of the dissociated particles,  $D_{0,M}^J$  is the rotation matrix element,  $(\begin{smallmatrix} J_i & 1 & J \\ -M_i & 0 & M \end{smallmatrix})$  is the Wigner 3- $j$  symbol, and  $t(E, J, q | E_i, J_i)$  is the ( $M_i$  independent) reduced amplitude, containing the essential dynamics of the photodissociation process.<sup>13</sup> Equation (16) follows from the usual procedure of expanding  $\langle E, \hat{k}, q^- | \phi_k, \theta_k, r \rangle$ , where  $r$  is the I-Br distance, in partial waves labeled by angular momentum  $J$  and its  $z$  projection. The angular integration of the resulting expression follows from the Wigner-Eckart theorem and the  $r$  integration is incorporated in  $t(E, J, q | E_i, J_i)$ . We have calculated these  $t(E, J, q | E_i, J_i)$  exactly using Shapiro's artificial channel method<sup>8,13</sup> and the potential curves and coupling strength given by Child.<sup>6(a)</sup>

As shown below, the required  $P_3(E, q; E_i, J_i, M_i)$ ,  $P_{13}(E, q; E_i, J_i, M_i)$  and  $P_1(E, q; E_i, J_i, M_i)$  [Eq. (4)] are conveniently expressed in terms of the primary quantities  $\mu^{(q)}(E, J_i, M_i; E_i, J_i, M_i; E)$ , where

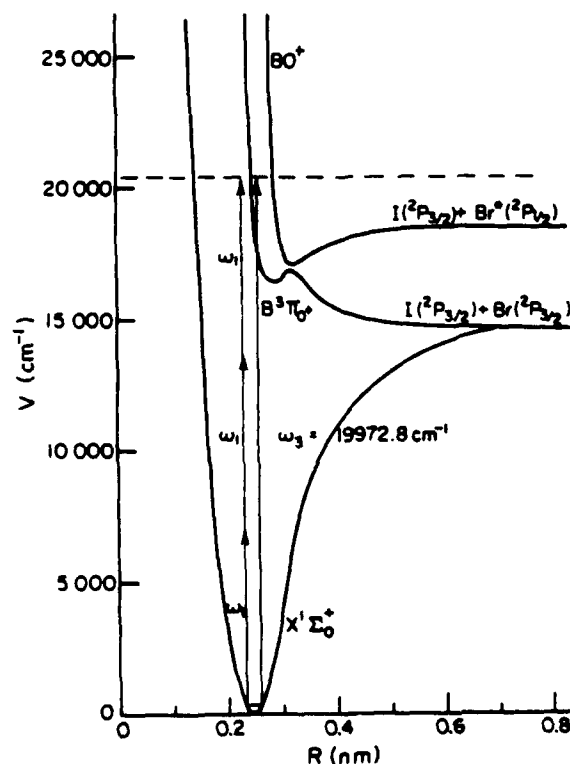


FIG. 1. IBr potential curves relevant in this one-plus-three photon induced dissociation.

$$\begin{aligned} & \mu^{(q)}(E, J, M; E, J, M; E) \\ &= \int d\hat{k} \langle E, J, M | (\hat{\epsilon}_i \cdot \boldsymbol{\mu})_{e,g} | E, \hat{k}, q^- \rangle \langle E, \hat{k}, q^- | (\hat{\epsilon}_i \cdot \boldsymbol{\mu})_{e,g} | E, J, M \rangle \\ &= \frac{8\pi m k}{h^2} \sum_{\mathcal{J}} \begin{pmatrix} J & 1 & J_i \\ -M & 0 & M_i \end{pmatrix} \begin{pmatrix} J & 1 & J_j \\ -M & 0 & M_j \end{pmatrix} \delta_{M, M_i} t^*(E, J, q | E, J) t(E, J, q | E, J). \end{aligned} \quad (17)$$

The integration over the scattering angles  $\hat{k}$  corresponds to the  $n$  summation in Eqs. (5) and (7), and the Kronecker delta  $\delta_{M, M_i}$  arises from the fact that the laser-molecule interaction does not depend on the azimuthal angle for the case of linearly polarized light. Note that the symmetry properties of the 3- $j$  symbols imply

$$\mu^{(q)}(E, J, M; E, J, M; E) = (-1)^{J_i - J} \mu^{(q)}(E, J, -M; E, J, -M; E), \quad (18)$$

an identity which will be used later below.

The probability  $P_3(E, q; E, J, M)$  is given, from the definition of  $\mu^{(q)}$  and from Eq. (5), by

$$P_3(E, q; E, J, M) = \left(\frac{\pi}{\hbar}\right)^2 \epsilon_3^2 \mu^{(q)}(E, J, M; E, J, M; E). \quad (19)$$

The terms  $P_{13}(E, q; E, J, M)$  and  $P_1(E, q; E, J, M)$  can also be written in terms of the  $\mu^{(q)}$ . To do so we express  $\langle E, n, q^- | T | E_i \rangle$  in Eq. (8) explicitly in terms of  $\langle E, n, q^- | (\hat{\epsilon}_i \cdot \boldsymbol{\mu})_{e,g} | E_i \rangle$  by inserting appropriate resolutions of the identity  $\langle E, n, q^- | T | E_i \rangle$

$$= \sum_j \sum_n \sum_q \int dE' \frac{\langle E, n, q^- | (\hat{\epsilon}_i \cdot \boldsymbol{\mu})_{e,g} | E_j \rangle \langle E_j | (\hat{\epsilon}_i \cdot \boldsymbol{\mu})_{e,g} | E', n', q'^- \rangle \langle E', n', q'^- | (\hat{\epsilon}_i \cdot \boldsymbol{\mu})_{e,g} | E_i \rangle}{(E_j - E_i - 2\hbar\omega_1)(E' - E_i - \hbar\omega_1)}. \quad (20)$$

Here, as noted above,  $|E_i\rangle$  denotes all of  $|E, J, M_i\rangle$  and the  $j$  summation indicates a sum over all bound states  $|E_j\rangle$  of the ground  $X^1\Sigma_0^+$  potential surface. All summations are complete except the latter, in which the continuum eigenstates of  $X^1\Sigma_0^-$  are neglected. Rather, only the larger bound state contribution is included. Indeed, of all the bound eigenstates of  $X^1\Sigma_0^+$ , the contribution to  $\langle E, n, q^- | T | E_i \rangle$  is dominated by those states with energy  $E_j$  satisfying the condition

$$E_j \approx E_i + 2\hbar\omega_1. \quad (21)$$

This near two-photon resonance condition is explicitly used in Sec. IV below to simplify the computation.

From Eq. (20) and the definition of  $\mu^{(q)}$ ,  $|F_{13}^{(q)}| \exp(i\delta_{13}^{(q)})$  in the cross term  $P_{13}(E, q; E, J, M)$ , is given by

$$|F_{13}^{(q)}| \exp(i\delta_{13}^{(q)}) = \sum_{E_j} \sum_{J_j} \sum_{q'} \int dE' \frac{\mu^{(q)}(E, J, M; E, J, M; E) \mu^{(q)*}(E, J, M; E, J, M; E')}{(E_j - E_i - 2\hbar\omega_1)(E' - E_i - \hbar\omega_1)}, \quad (22)$$

where the  $J_j$  and the  $E_j$  summation indicates a summation over all bound eigenstates of the  $X^1\Sigma_0^+$  state.

Similarly, using Eqs. (7) and (20), the probability for the three-photon process is given by

$$\begin{aligned} P_1(E, q; E, J, M) &= \sum_{E_j} \sum_{J_j} \sum_{q'} \int dE' \int d\bar{E} \\ &\times \frac{\mu^{(q)}(E, J, M; E, J, M; E) \mu^{(q)}(E, J, M; E, J, M; E') \mu^{(q)*}(E, J, M; E, J, M; \bar{E})}{(E_j - E_i - 2\hbar\omega_1)(E_i - E_j - 2\hbar\omega_1)(E' - E_i - \hbar\omega_1)(\bar{E} - E_i - \hbar\omega_1)}. \end{aligned} \quad (23)$$

Later below we describe a simple qualitative route for tabulating the terms which enter into this expression. Given these results the quantities  $F_{13}^{(q)}$  and  $F_1^{(q)}$  in the branching ratio ( $R_{qq}$ ) expression of Eq. (14) [and Eq. (11)] are then written easily in terms of  $\mu^{(q)}$  using Eqs. (12), (19), (22), and (23).

#### IV. RESULTS

In this section, we present numerical results which demonstrate the large range of possible control in IBr. Both  $M$ -polarized and the  $M$ -averaged calculations are described. In the former the isolated molecules are assumed to have the magnetic quantum number  $M$  which is selected prior to laser excitation; in the latter, no such selection is assumed.

In the  $M$ -polarized case the molecules are initially in a single  $|E, J, M_i\rangle$  state. Equation (18) then implies that

$$P_i(E, q; E, J, M_i) = P_i(E, q; E, J, -M_i),$$

$$P_i = P_1, P_3,$$

$$P_{13}(E, q; E, J, M_i) = P_{13}(E, q; E, J, -M_i), \quad (24)$$

where the probabilities for the one- and three-photon process  $P_i$  and the cross term  $P_{13}$  are those defined in Sec. III, but with the  $J, M_i$  dependence explicitly shown. As a consequence of Eq. (24), the branching ratio for the relative product yield is identical for the case of  $M_i$  and  $-M_i$ .

In the  $M$ -averaged case, the magnetic quantum numbers of the molecules to be excited assume all of the possible  $2J_i + 1$  values with equal probability, i.e., the  $M_i$  are random. In this case each  $M_i$  state is treated independently and the average  $P_i(E, q; E, J), i = 1, 3$  is then obtained by averaging over the  $2J_i + 1$  values of  $P_i(E, q; E, J, M_i)$ , i.e.,

$$\begin{aligned}
 P_i(E, q; E_i, J_i) &= \frac{1}{2J_i + 1} \sum_{M_i = -J_i}^{J_i} P_i(E, q; E_i, J_i, M_i) \\
 &= \frac{1}{2J_i + 1} \sum_{M_i = 0}^{J_i} (2 - \delta_{M_i, 0}) P_i(E, q; E_i, J_i, M_i). \quad (25)
 \end{aligned}$$

An analogous formula exists for the cross term  $P_{13}(E, q; E_i, J_i)$ . Finally, using the  $P_i(E, q; E_i, J_i)$  and  $P_{13}(E, q; E_i, J_i)$  the branching ratio expression can be easily written down for the  $M$ -averaged case.

Below we present results for vibrational state  $v = 0$ , with  $J_i = 0, 1$ , and 42. The range of initial  $J_i$  chosen reflects an effort to assess the dependence of control, for typical states populated thermally, on changes in  $J_i$ . The laser frequencies  $\omega_1, \omega_3$  inducing the photodissociation are shown qualitatively, along with the potentials, in Fig. 1. Quantitatively,  $\omega_1$  is chosen so that absorption of two photons to energy  $E_i + 2\hbar\omega_1$  leaves the system almost resonant with the (arbitrarily chosen) bound state with vibrational quantum number  $v = 77$ . Under these circumstances, the  $j$  sum in Eq. (20) includes only the bound states of the ground potential curve with quantum numbers  $(J_j, v = 77)$ , where  $J_j$  are the angular momentum values allowed by selection rules. Other bound states have contributions which are negligible and are omitted from the computation. A similar approximation is used in computing Eqs. (22) and (23). The energy values of some relevant  $(J_j, v = 77)$  bound states of  $X^1\Sigma_0^+$  are listed in Table I and are referred to later below. Also provided below are figures displaying the angular momentum values involved in the one-plus-three photon absorption. These diagrams provide important insights into control since selection rules dictate the values of the angular momenta of the continuum states created in the photoexcitation. These angular momentum values are relevant since only continuum states with the same  $J$  can contribute to interferences leading to control of integral cross sections.

(A)  $J_i = 0$ : Here  $|E_i, J_i, M_i\rangle = |E_i, 0, 0\rangle$  with the energy corresponding to the  $v = 0$  state. The angular momentum values associated with the one- and three-photon absorption routes are summarized in Fig. 2(a). In the figure, the solid horizontal line represents angular momentum states of the ground potential surface ( $X^1\Sigma_0^+$ ) and the dashed horizontal line represents those of the excited potential surfaces ( $B^3\Pi_{0+}$  and  $BO^+$ ). The succession of transitions follows from the usual dipole selection rules for linearly polarized light ( $\Delta J = \pm 1, \Delta M = 0$ ) for transitions between  $\Omega$  (total electronic angular momentum along the molecular axis) = 0 states. Note that of the two  $J$  states which arise from the three photon absorption, i.e.,  $J = 1$  and  $J = 3$ , only the  $J = 1$  contributes to the interference with the one photon route since only states with the same  $J$  quantum number have a nonzero interference term. Thus the  $J = 3$  term, included in the computation, contributes an uncontrollable term to the photodissociation.

Diagrams such as those shown in Fig. 2 also provide a qualitative means of tabulating the dipole matrix elements which enter as contributions in the expressions for  $P_1, P_3$ , and  $P_{13}$ . Consider, for example, contributions to  $P_1$  [Eq.

TABLE I. The energy values ( $E$ ) in a.u. of relevant  $(J, v = 77)$  bound states of  $X^1\Sigma_0^+$ .

$J_j$	$E$
0	-0.005 717 67
1	-0.005 717 39
2	-0.005 716 82
3	-0.005 715 98
40	-0.005 487 48
41	-0.005 476 00
42	-0.005 464 23
43	-0.005 452 19
44	-0.005 439 87

(23)] for the case of  $J_i = M_i = 0$ . The relevant diagram is then that shown on the right hand side of Fig. 2(a). Detailed consideration of Eq. (23) shows that the following diagrammatic method gives the appropriate dipole contributions to  $P_1$ . One starts at the bottom of the diagram (here  $J = 0$ ) and proceeds to a state at the top of the diagram, and then back

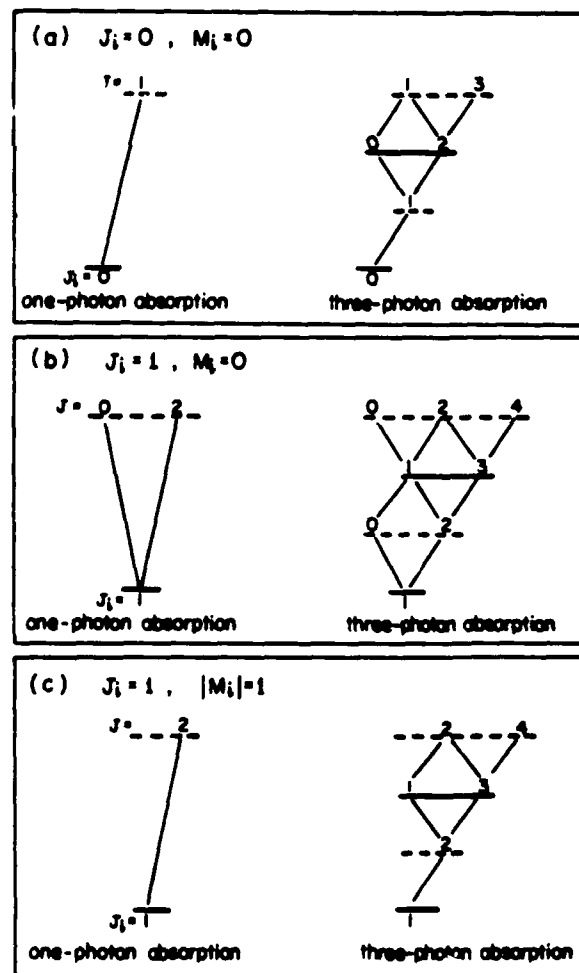


FIG. 2. Angular momentum levels available for one- and three-photon absorption from (a)  $J_i = 0$  and (b)  $J_i = 1$  state.

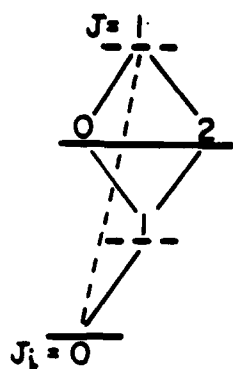


FIG. 3. Angular momentum levels (for the  $J = 0$  case) connected by both one- and three-photon routes to the continuum  $J$  state which is shared by both types of absorption. The diagram may be used to qualitatively identify terms which contribute to the  $(\omega_1, \omega_2)$  interference, as described in the text.

down to the initial state. Each pair of levels encountered in this route contributes one dipole matrix element to the product in Eq. (23). A sample case would be the route  $0 \rightarrow 1 \rightarrow 2 \rightarrow 1 \rightarrow 0 \rightarrow 1 \rightarrow 0$  which contributes a term of the form [where the value of the angular momentum is indicated and where the electronic states are distinguished as being unprimed (ground state) or primed (excited state)]:  $\langle 0|\mu|1' \rangle \langle 1'|\mu|2 \rangle \langle 2|\mu|1' \rangle \langle 1'|\mu|0 \rangle \langle 0|\mu|1' \rangle \langle 1'|\mu|0 \rangle$ . Equation (23) would include all terms, of which this is one, with products of six dipole transition operators which can arise from this figure in the manner prescribed. Similarly, contributions to  $P_3$  arise from the only diagram contributing to the left hand side of Fig. 2(a), i.e.  $|\langle 0|\mu|1' \rangle|^2$ . Finally, contributions to the interference term  $P_{13}$  can be obtained from Fig. 3, which results from superimposing the two angular momentum ladders in Fig. 2(a) for those continuum angular momentum states which contribute to the interference term. To obtain the contribu-

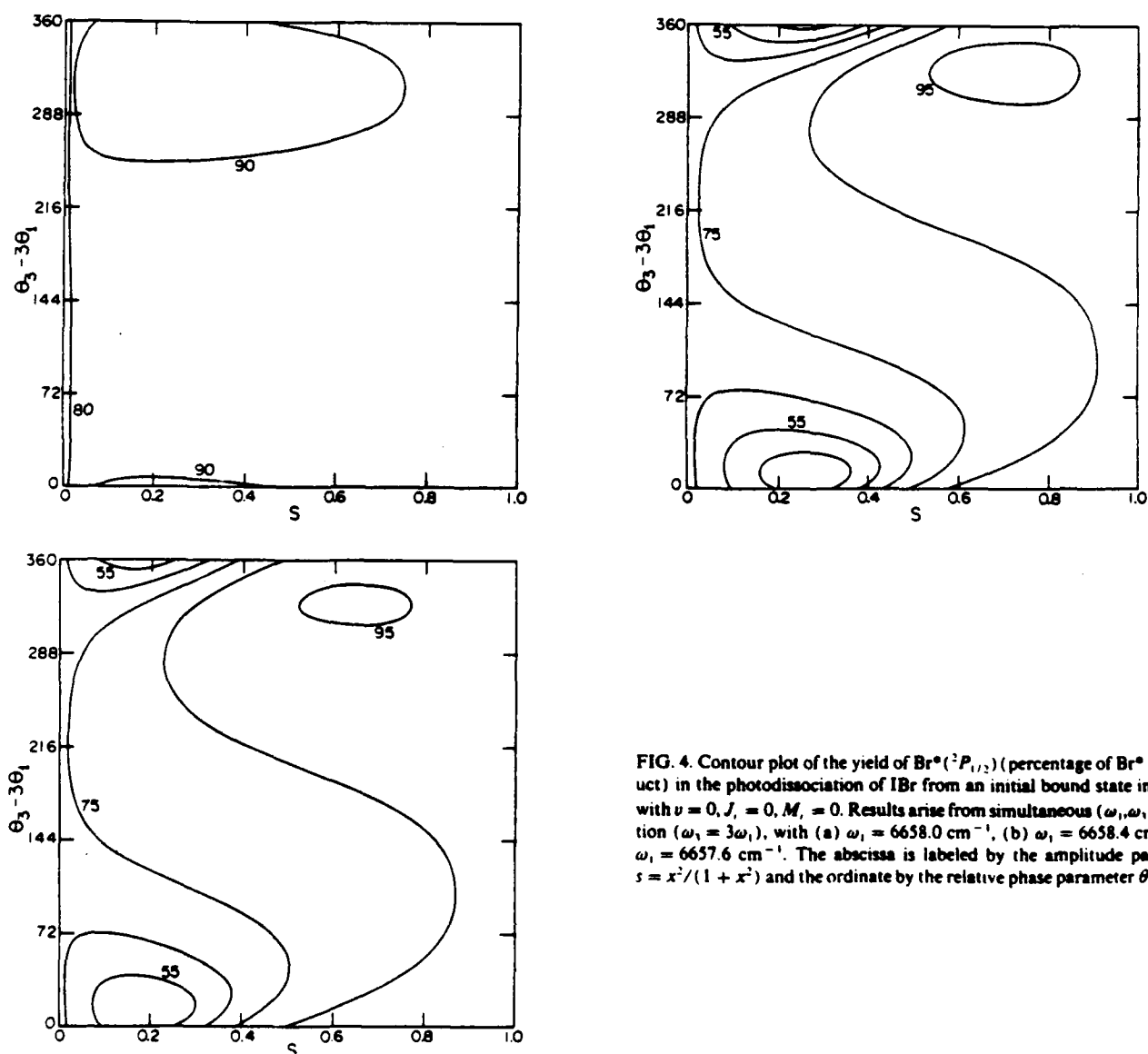


FIG. 4. Contour plot of the yield of  $\text{Br}^*(^2P_{1/2})$  (percentage of  $\text{Br}^*$  as product) in the photodissociation of IBr from an initial bound state in  $X^1\Sigma_g^+$  with  $v = 0, J = 0, M = 0$ . Results arise from simultaneous  $(\omega_1, \omega_2)$  excitation ( $\omega_2 = 3\omega_1$ ), with (a)  $\omega_1 = 6658.0 \text{ cm}^{-1}$ , (b)  $\omega_1 = 6658.4 \text{ cm}^{-1}$  (c)  $\omega_1 = 6657.6 \text{ cm}^{-1}$ . The abscissa is labeled by the amplitude parameter  $s = x^2/(1+x^2)$  and the ordinate by the relative phase parameter  $\theta_3 - 3\theta_1$ .

tions to  $P_{13}$ , one constructs all matrix element products which involve *four* dipole transitions in making a complete circuit from ground state  $J = 0$ , through the continuum level, and back down to the ground state.

Figure 4 displays the yield of  $\text{Br}^*(^2P_{1/2})$  (i.e., the ratio of the probability of  $\text{Br}^*$  to the sum of the probabilities to form  $\text{Br}$  plus  $\text{Br}^*$ ) for this  $\nu = 0, J_i = 0$  case. The figure axes are the amplitude parameter  $s = x^2/(1+x^2)$  and the phase parameter  $\theta_3 - 3\theta_1$  and Figs. 4(a)–4(c) show results for three different sets of  $(\omega_1, \omega_3)$  with  $\epsilon_0 = 1/2$  a.u. (where 1 a.u. =  $5.142 \times 10^9$  volt/cm). It is convenient, when discussing these figures, to introduce a parameter  $e = E_i + 2\hbar\omega_1$ . In Fig. 4(a),  $\omega_1 = 6658.0 \text{ cm}^{-1}$  ( $\omega_3 = 3\omega_1$ ) with the corresponding  $e = -0.00571700$  a.u. a value which is very close to the energy of the ( $J_i = 2, \nu = 77$ ) bound state [see Table I]. The contour plot shows little control, being very flat throughout, with a maximum of 91% and a minimum of 70%.  $\text{Br}^*(^2P_{1/2})$  is the dominant product throughout the full range of the laser parameters  $s$  and  $\theta_3 - 3\theta_1$ , qualitatively the same result as if using either the  $\omega_1$ , or the  $\omega_3$  excitation alone.

In Fig. 4(b),  $\omega_1 = 6658.4 \text{ cm}^{-1}$ , slightly larger than that of the previous case. As a consequence  $e = -0.00571400$  a.u., further off resonance with the ( $J_i = 0, \nu = 77$ ) and ( $J_i = 2, \nu = 77$ ) levels than in the previous case. This small change in  $\omega_1$  makes an enormous difference in control, with Fig. 4(b) showing a very wide range of control: The  $\text{Br}^*(^2P_{1/2})$  quantum yield changes from less than 47%, for  $s = 0.2, \theta_3 - 3\theta_1 = 20^\circ$ , to greater than 95% for  $s = 0.5$  and  $\theta_3 - 3\theta_1 = 300^\circ$ . Similar results attain for Fig. 4(c), where  $\omega_1 = 6657.6 \text{ cm}^{-1}$  and  $e = -0.00572100$  a.u., which is even further away from ( $J_i = 0, \nu = 77$ ). The yield control plot is essentially the same as in Fig. 4(b).

These results are consistent with the following interpretation, easily understood in terms of Fig. 2. The first of these cases, which gives weak control [Fig. 4(a)], uses a frequency which yields near-resonant absorption with the  $J_i = 2, \nu = 77$  level, a level which connects with both the  $J = 3$  and  $J = 1$  in the continuum. Since  $J = 3$  is uncontrolled (i.e., there is no corresponding  $J = 3$  term from the one photon absorption) pumping very close to  $J_i = 2, \nu = 77$  enhances production of continuum  $J = 3$ , undesirable for purposes of control. Tuning away from this level hence enhances control. Specifically, in both nonresonant cases, i.e., Figs. 4(b) and 4(c), the  $J = 0$  and  $J = 2$  routes in the three photon excitation are energy-denominator-weighted equally. By contrast, in the case of Fig. 4(a), the resonant energy denominator overweights the  $J = 2$  route by a factor of four, substantially reducing control.

(B)  $J_i = 1$ : In this case,  $M_i$  can be  $-1, 0$  or  $+1$  for the  $M$ -polarized case. The angular momentum channels involved in the calculation are summarized in Figs. 2(b) and 2(c). Figs. 5(a) and 5(b) display the yield of  $\text{Br}^*(^2P_{1/2})$  for the  $M$ -selected calculation with  $M_i = 0$  and  $M_i = +1$  or  $-1$ , respectively. Results are shown at  $\omega_1 = 6657.5 \text{ cm}^{-1}$  with  $e = -0.00572100$ . Both figures are essentially the same as that of Fig. 4(b)–4(c), and a wide range of control (here 25%–95% for  $M_i = 0$  and 45%–95% for  $M_i = 1$ ) is

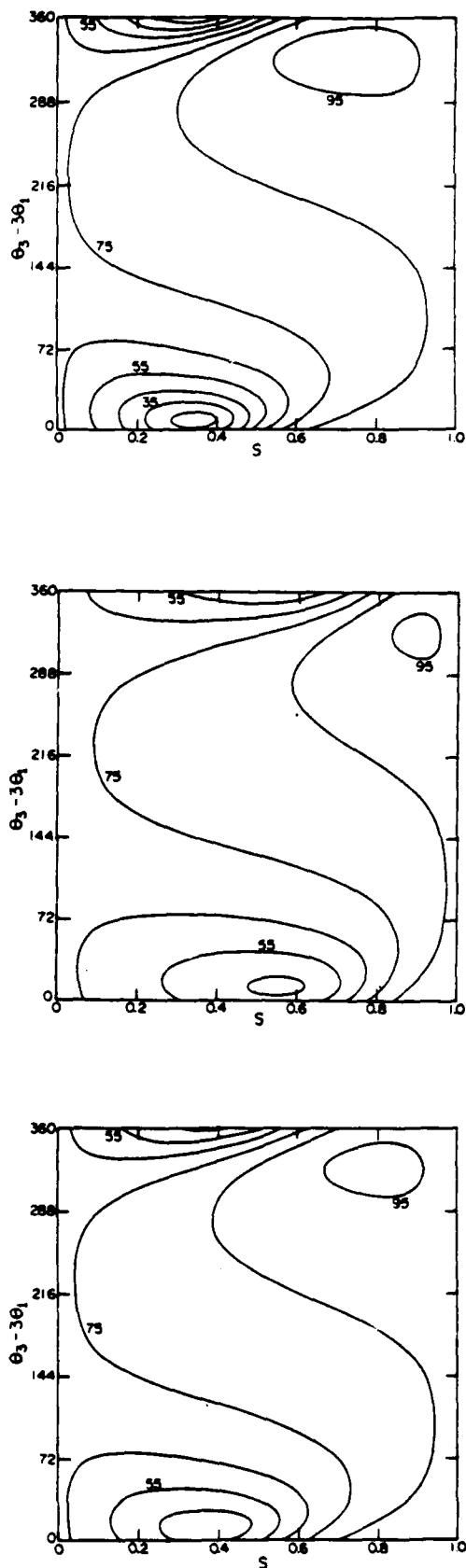


FIG. 5. As in Fig. 4 but for  $\nu = 0, J_i = 1, \omega_1 = 6657.5 \text{ cm}^{-1}$ . (a)  $M_i = 0$ . (b)  $M_i = 1$  and  $M_i = -1$  and (c)  $M$ -averaged. (a), (b), (c) denote upper, middle, and bottom panels, here and below.

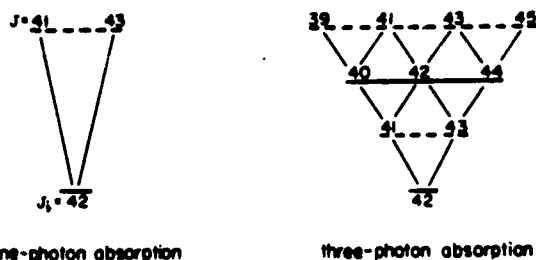
demonstrated. This control is maintained in Fig. 5(c), which displays the yield of  $\text{Br}^*(^2P_{1/2})$  for the  $M$ -averaged calculation.

(C)  $J_i = 42$ : Finally, we examine the case of  $J_i = 42$ , chosen because it is the most populated angular momentum state at room temperature. The results on  $J_i = 42$  control should therefore serve as a useful test of the effects of the extensive  $M$  averaging accompanying such temperatures. The angular momentum levels involved in the computation are summarized in Fig. 6 for the case of  $0 < |M_i| < 39$ . An analogous diagram can be drawn for  $40 < |M_i| < 42$ . For the cases shown,  $J = 41, 43$  lead to interference terms whereas the remaining  $J = 39, 45$  terms are uncontrolled.

Here we present result for  $\omega_1 = 6635.0 \text{ cm}^{-1}$  a frequency which gives two-photon excitation very close ( $e = -0.00546400 \text{ a.u.}$ ) to the  $J_i = 42, v = 77$  bound state [see Table I]. In accordance with Fig. 6, tuning close to this bound state substantially reduces contributions from the uncontrolled  $J = 39$  and  $J = 45$  continuum states.

Systematically examining contour plots of yields vs  $s$  and  $\theta_3 - 3\theta_1$  on a coarse  $s$  scale suggests that there is little control for most of the smaller  $|M_i|$  values. Control on this coarse  $s$  scale does appear, however, for larger  $|M_i|$ , an example of which is shown in Fig. 7(a) for  $|M_i| = 38$ . Similar results are seen for higher values of  $|M_i|$  with the maxima and minima of the yield shifted to larger values of  $s$ , similar to the trend seen in Figs. 5(a) and 5(b). These higher  $|M_i|$  values contribute little, however, to the overall averaged yield so that the average shows virtually no control over yield on a coarse  $s$  scale. However, examination of the yield vs  $s$  and  $\theta_3 - 3\theta_1$  on a finer  $s$  scale for both small  $M_i$  and for the overall  $M$  average, shows that extensive control exists and does survive  $M$  averaging. These results are shown in Fig. 7(b) where the yield varies over a range of 30–95% as  $s$  varies between 0 and 0.01.

We have little doubt that a further search of the  $\omega_1$  space will allow us to obtain similar control over a wider  $s$  range, making control experiments somewhat easier. This study is, however, unwarranted. Specifically, the actual range of  $s$  over which one sees control (although not the magnitude of the maximum and minimum yield) is affected by the size of the transition dipole moment. We have chosen here to incorporate this unknown value in the magnitude of  $\epsilon_0$ , so that varying  $\epsilon_0$  corresponds to changing this dipole. However,



one-photon absorption

three-photon absorption

FIG. 6. Angular momentum levels available for the one- and three-photon absorption from  $J_i = 42$  with  $0 < |M_i| < 39$ .

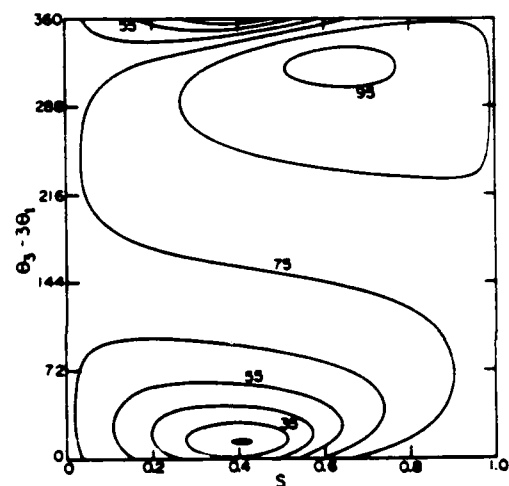
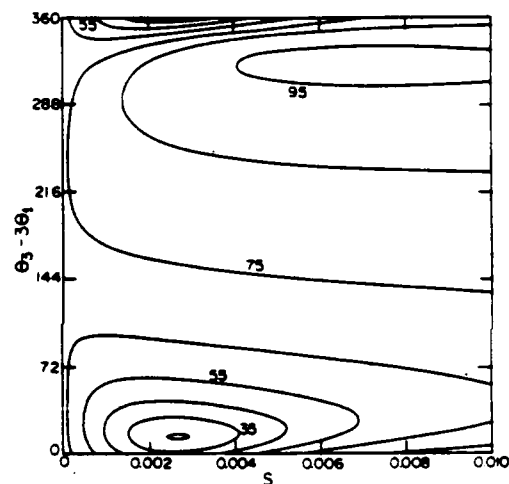
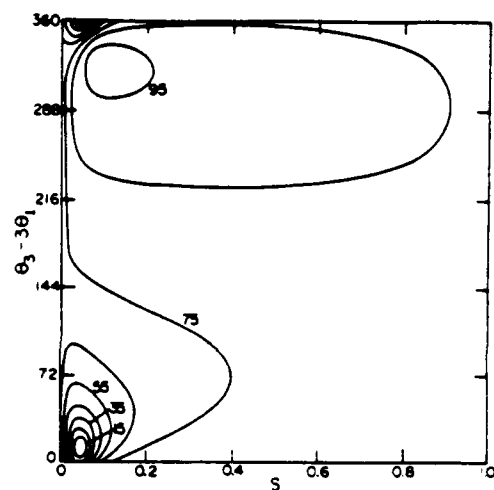


FIG. 7. As in Fig. 4 but for  $v = 0, J_i = 42, \omega_1 = 6635.0 \text{ cm}^{-1}$  (a)  $|M_i| = 38$ , (b)  $M$ -averaged (standard  $\epsilon_0 = 1/2 \text{ a.u.}$ ), note abscissa range (c)  $M$ -averaged ( $\epsilon_0 = 1/8 \text{ a.u.}$ ).

examining Eq. (14) shows that changing  $\epsilon_0$  also corresponds to changing  $x$  and hence to altering the scale of the  $s$  axis, albeit nonlinearly. In particular, reducing  $\epsilon_0$  has the effect of magnifying the small  $s$  regime of the yield plot. This is clearly shown in Fig. 7(c), where the  $M$ -averaged yield for the case shown in Fig. 7(b) is now shown with  $\epsilon_0 = 1/8$  a.u. Control is seen to be restored over a wide range of  $s$ .

## V. SUMMARY

We have shown that it is possible, in a relatively straightforward way, to use interference between one-photon and three-photon optical paths to control the relative yield of product in the photodissociation of IBr. Control was also shown to survive extensive averaging over  $M_j$  states and to allow a wide range of control over the product ratio.

## ACKNOWLEDGMENT

Support for this work has been provided by the U. S. Office of Naval Research under Contract No. N00014-87-J-1204.

<sup>1</sup>(a) P. Brumer and M. Shapiro, *Chem. Phys. Lett.* **126**, 541 (1986); (b) *Faraday Discuss. Chem. Soc.* **82**, 177 (1987); (c) M. Shapiro and P.

Brumer, *J. Chem. Phys.* **84**, 4103 (1986); (d) G. Kunzki, M. Shapiro, and P. Brumer, *Phys. Rev. B* **39**, 3435 (1989); (e) M. Shapiro and P. Brumer, *J. Chem. Phys.* **90**, 6179 (1989); (f) T. Seideman, M. Shapiro, and P. Brumer, *J. Chem. Phys.* **90**, 7132 (1989); (g) For an introductory discussion, see P. Brumer and M. Shapiro, *Accounts Chem. Res.* **22**, 407 (1989); (h) P. Brumer and M. Shapiro, *Chem. Phys.* **139**, 221 (1989); (i) I. Levy, M. Shapiro, and P. Brumer, *J. Chem. Phys.* **93**, 2493 (1990); (j) M. Shapiro and P. Brumer (to be published); (k) C. Asaro, P. Brumer, and M. Shapiro, *Phys. Rev. Lett.* **60**, 1634 (1988).

<sup>2</sup>M. Shapiro, J. W. Hepburn, and P. Brumer, *Chem. Phys. Lett.* **149**, 451 (1988).

<sup>3</sup>D. J. Tannor and S. A. Rice, *J. Chem. Phys.* **83**, 5013 (1985) For recent developments see S. H. Tersigni, P. Gaspard, and S. A. Rice, *J. Chem. Phys.* **93**, 1670 (1990), and references therein.

<sup>4</sup>C. Chen, Y. Y. Yin, and D. S. Elliott, *Phys. Rev. Lett.* **64**, 507 (1990)

<sup>5</sup>A. Szoke, K. C. Kulander, and J. N. Bardsley (to be published).

<sup>6</sup>For earlier studies of IBr photodissociation see (a) M. S. Child, *Mol. Phys.* **32**, 495 (1976); (b) M. S. Child and R. B. Bernstein, *J. Chem. Phys.* **59**, 5916 (1973); (c) A. D. Bandrauk, G. Turcotte, and R. Lefebvre, *J. Chem. Phys.* **76**, 225 (1982).

<sup>7</sup>H. Bony, M. Shapiro, and A. Yogeve, *Chem. Phys. Lett.* **107**, 603 (1984)

<sup>8</sup>M. Shapiro and H. Bony, *J. Chem. Phys.* **83**, 1588 (1985).

<sup>9</sup>R. J. Donovan and D. Husain, *Trans. Faraday Soc.* **62**, 2643 (1966); **64**, 2325 (1968).

<sup>10</sup>M. S. de Vries, N. J. A. van Veen and A. E. de Vries, *Chem. Phys. Lett.* **56**, 15 (1978); M. S. de Vries, N. J. A. van Veen, M. Hutchinson, and A. E. de Vries, *Chem. Phys.* **51**, 159 (1980).

<sup>11</sup>M. Shapiro and R. Bersohn, *Annu. Rev. Phys. Chem.* **33**, 409 (1982).

<sup>12</sup>P. Brumer and M. Shapiro, *Adv. Chem. Phys.* **60**, 371 (1985).

<sup>13</sup>M. Shapiro, *J. Phys. Chem.* **90**, 3644 (1986).

### Interference between Optical Transitions and Control of Relative Cross Sections

In a recent Letter, Chen, Yin, and Elliott<sup>1</sup> showed that the probability of ionization can be altered by varying the relative laser phase in the simultaneous five-photon and three-photon excitation of Hg. This result provides an important experimental demonstration of the utility of pure quantum interference in altering this process. It also provides the first laboratory demonstration of an experimental scenario<sup>2</sup> based upon a general principle for controlling atomic and molecular processes termed<sup>3</sup> coherent radiative control. Other experimental scenarios based upon the same interference principle include one-photon photodissociation of a superposition state<sup>3(a)-3(c)</sup> with applications to currents in semiconductors,<sup>3(d)</sup> pulse-pulse schemes for both unimolecular and bimolecular processes,<sup>3(f),3(i)</sup> and variable-elliptic-polarization control of differential cross sections.<sup>3(j)</sup> In all cases the theory suggests generalizations of the experiment of Chen, Yin, and Elliott<sup>1</sup> to systems with multiple product channels.

The purpose of this Comment is to computationally demonstrate that the molecular multiple-product-channel generalization of the experiment of Chen, Yin, and Elliott<sup>1</sup> affords the prospect of a vast range of experimental control over the ratio of total product cross sections (i.e., the relative yield of products). The computation presented below is based upon our previous<sup>3</sup> formal treatment and provides the first numerical evidence that interfering optical excitation paths allow for enormous control over total cross sections in photodissociation from stationary states.

Specifically, consider simultaneous one- and three-photon excitation ( $\omega_3 = 3\omega_1$ ) of IBr to produce  $I(^2P_{3/2}) + Br(^2P_{3/2})$  and  $I(^2P_{3/2}) + Br(^2P_{1/2})$ . Reliable potential surfaces and coupling strengths<sup>4</sup> were used in conjunction with the artificial channel method<sup>5</sup> to produce accurate one- and three-photon photodissociation amplitudes. These were then appropriately combined<sup>3</sup> to produce the overall dissociation probabilities. As an example consider photodissociation from the ground vibrational state of  $X^1\Sigma_0^+$  with rotational quantum number  $J=1$  using  $\omega_1 = 6657.5 \text{ cm}^{-1}$ ,  $\omega_3 = 3\omega_1$ . Excitation with either of the two frequencies, with electric-field amplitudes  $\bar{e}_1$  and  $\bar{e}_3$ , independently produces predominantly (> 70%)  $I + Br^*$ . The results of simultaneous photodissociation with both frequencies is shown as a contour plot of constant yield (i.e.,  $Br^*$  probability divided by  $Br^* + Br$  probability) in Fig. 1. Here the figure axes are labeled by the amplitude parameter  $s = x^2/(1+x^2)$ ,  $x = \bar{e}_1/\bar{e}_3$ , and the relative laser phase  $\theta_3 - 3\theta_1$ . The results demonstrate extensive control over product yield, the ratio varying from 45% to 95%.

Previous theoretical studies<sup>3</sup> have indicated that similar control can be exercised over chemically distinct arrangement channels and over rotational-vibrational distributions within a particular product channel.

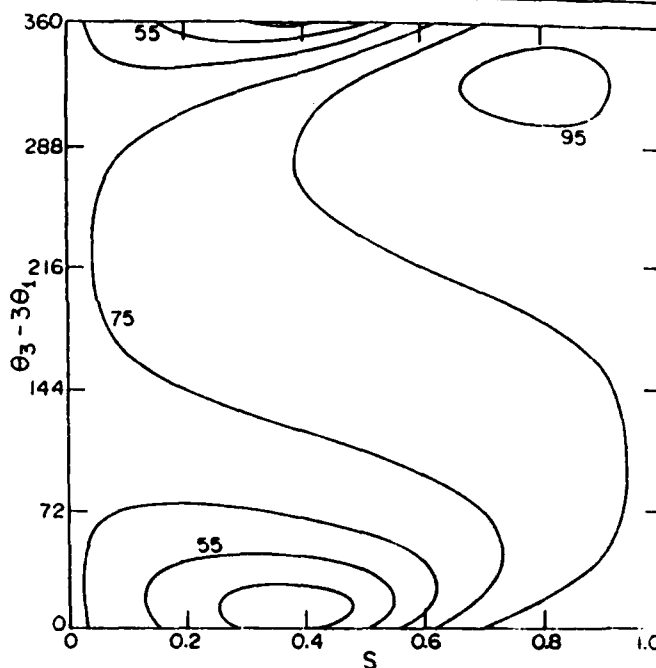


FIG. 1. Contours of constant  $Br^*$  vs relative laser amplitude and phase.

Support for this work has been provided by the U.S. Office of Naval Research under Contract No. N00014-87-J-1204.

C. K. Chan and P. Brumer  
Chemical Physics Theory Group  
Department of Chemistry  
University of Toronto  
Toronto, Canada M5S 1A1

M. Shapiro  
Department of Chemical Physics  
The Weizmann Institute of Science  
Rehovot, Israel 76100

Received 10 April 1990

PACS numbers: 32.80.Rm

<sup>1</sup>C. Chen, Y.-Y. Yin, and D. S. Elliott, Phys. Rev. Lett. 64, 507 (1990).

<sup>2</sup>M. Shapiro, J. W. Hepburn, and P. Brumer, Chem. Phys. Lett. 149, 451 (1988).

<sup>3</sup>(a) P. Brumer and M. Shapiro, Chem. Phys. Lett. 126, 541 (1986); (b) Faraday Discuss. Chem. Soc. 82, 177 (1987); (c) M. Shapiro and P. Brumer, J. Chem. Phys. 84, 4103 (1986); (d) G. Kurizki, M. Shapiro, and P. Brumer, Phys. Rev. B 39, 3435 (1989); (e) M. Shapiro and P. Brumer, J. Chem. Phys. 90, 6179 (1989); (f) T. Seideman, M. Shapiro, and P. Brumer, J. Chem. Phys. 90, 7132 (1989); J. Krause, M. Shapiro, and P. Brumer, J. Chem. Phys. 92, 1126-1131 (1990); (g) for an introductory discussion, see P. Brumer and M. Shapiro, Acc. Chem. Res. 22, 407 (1989); (h) Chem. Phys. 139, 221 (1989); (i) I. Levy, M. Shapiro, and P. Brumer (to be published); (j) C. Asaro, P. Brumer, and M. Shapiro, Phys. Rev. Lett. 60, 1634 (1988).

<sup>4</sup>M. S. Child, Mol. Phys. 32, 495 (1976).

<sup>5</sup>M. Shapiro and R. Bersohn, Annu. Rev. Phys. Chem. 33, 409 (1982).

# Two-pulse coherent control of electronic states in the photodissociation of IBr: Theory and proposed experiment

Izak Levy

Department of Chemical Physics, The Weizmann Institute of Science, Rehovot, 76100 Israel

Moshe Shapiro

Department of Chemistry, University of California, and Materials and Chemical Sciences Division, Lawrence Berkeley Laboratory, Berkeley, California 94720 and Department of Chemical Physics, The Weizmann Institute of Science, Rehovot, 76100 Israel

Paul Brumer

Chemical Physics Theory Group, Department of Chemistry, University of Toronto, Toronto M5S 1A1, Canada

(Received 27 February 1990; accepted 26 April 1990)

It is shown how the principles of coherent control can be applied to a *pulsed* experiment aimed at controlling curve-crossing processes. A realistic computational study (incorporating the ground, *A*, *B*, and *Y* electronic states of IBr) of control of atomic states produced in the photodissociation of IBr is presented. The suggested scheme, which consists of applying an excitation pulse followed by a dissociation pulse, is theoretically shown to yield essentially *total* control over the  $\text{Br}^*/\text{Br}$  atomic branching ratio. It is shown that the only external parameters that need to be varied are the central frequency of the excitation pulse and the time delay between the two pulses. A brief description of a proposed experiment is provided.

## I. INTRODUCTION

Considerable progress has been made in recent years in our understanding of how to resolve the long-standing objective of using lasers to control chemical reactions.<sup>1-4</sup> The emerging new field, termed coherent control of chemical reactions, has, however, consisted solely of theoretical studies. One of the reasons for this is that most of these studies have dealt with the *principles* of coherent control and were less concerned with real molecular systems. In this paper we wish to carry the theory one step further by presenting a detailed, realistic study of a coherent control process. This study will hopefully form a basis for an experimental demonstration of the predicted effect.

In order to demonstrate that coherent control principles can be extended to the pulsed laser domain, we recently derived a pump-dump scheme for controlling both unimolecular<sup>1,5</sup> and bimolecular<sup>6</sup> reactions. The scenario was computationally implemented for two model collinear systems, and was shown to be highly successful. For example, we were able to show<sup>5</sup> that the yield of the  $\text{D} + \text{H}_2$  product (with  $\text{DH} + \text{H}$  being the other product) can be altered over a range of 18% to 84% by varying external laser parameters, such as center frequency and time delay. Of particular importance was our demonstration that the implementation of these ideas can be carried out on a *picosecond* time scale, well within the grasp of most laser chemists.

Our previous pulsed work was, however, not aimed at exploring *real* systems: Our calculations were confined to the collinear domain and, in the unimolecular work,<sup>1,5</sup> we followed Tannor and Rice<sup>2</sup> in assuming a model of a hypothetical  $\text{DH}_2$  molecule.

In this paper we present a realistic study in which we examine electronic curve-crossing processes occurring during IBr dissociation. Our aim is to control the electronic states of atoms resulting from this photodissociation process. We have chosen IBr because its electronic structure is sufficiently well characterized to allow for accurate modeling of all aspects of a nonadiabatic photodissociation control experiment. Theoretical demonstrations of control in IBr, followed by a successful experiment of this type, will pave the way to controlling more "chemical" processes such as bond breaking in polyatomic molecules.

## II. CONTROL OVER THE PHOTODISSOCIATION OF IBr

IBr, when subjected to visible radiation, (e.g., at  $0.5 \mu$ ), dissociates to yield both Br and  $\text{Br}^*$  atoms<sup>7</sup> as



The "natural"  $\text{Br}/[\text{Br}^* + \text{Br}]$  yield is  $\approx 0.3$  at  $h\nu = 0.5 \mu$ . This ratio is not zero, although the molecule is formed initially on the *B* state, which correlates with  $\text{I} + \text{Br}^*$ . This, as illustrated in Fig. 1, is due to a curve-crossing process that diverts some of the molecules from the *B* state to the *Y* state, the latter giving rise to the  $\text{I} +$  ground state Br products.

We show below that it is possible to control the yield in this process, using two picosecond pulses in the following way. First, as illustrated in Fig. 1, an "excitation pulse"  $\epsilon_x(t)$  is used to simultaneously pump two excited bound states, resulting in the formation of a nonstationary *superposition* state,

$$|\chi\rangle = c_1|E_1\rangle + c_2|E_2\rangle. \quad (1)$$

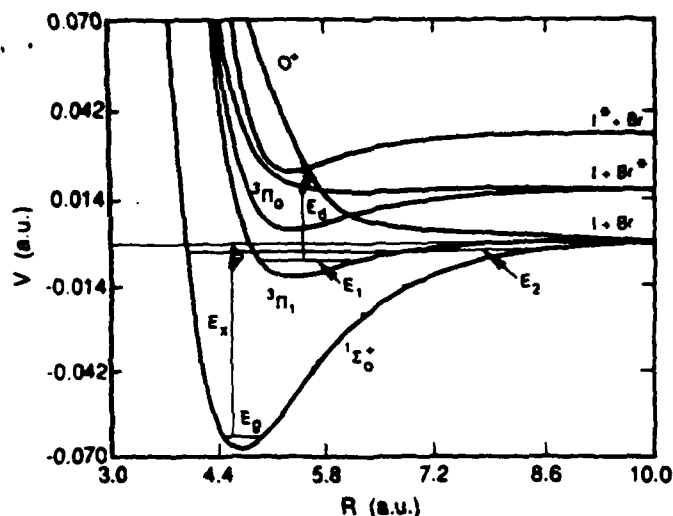


FIG. 1. Potential curves for IBr and the two-pulse excitation-dissociation scheme. The length of the arrows do not represent the actual frequencies used in the calculations.

The generation of  $|\chi\rangle$  is possible if  $E_1$  and  $E_2$  are within the excitation-laser bandwidth. (Since we have a picosecond laser in mind,  $E_1$  and  $E_2$  can be no more than a few  $\text{cm}^{-1}$  apart.) In the second step,  $|\chi\rangle$  is subjected, after some time delay  $\tau$ , to a second pulse  $\epsilon_d(t)$ , which dissociates the molecule by forcing a transition (see Fig. 1) to an energy above the dissociation limit.

Assuming for simplicity that each pulse, given as

$$\epsilon_a(t) = \int dE_p \epsilon_p(E_p) \cos[E_p/\hbar + \mathbf{k} \cdot \mathbf{R} + \phi(E_p)], \quad (2)$$

is Gaussian, we have that

$$\begin{aligned} \epsilon_a(E_p) &= \epsilon_a(E_a) \exp\{-4 \ln 2 [(E_p - E_a)/\Delta_a]^2\}; \\ a &= x, d, \end{aligned} \quad (3)$$

$$\begin{aligned} P(q, \mathbf{n}|E) &= \pi^2 \{ |c_1|^2 \epsilon_d^2(\omega_{E,1}) |\mu(q, \mathbf{n}, 1)|^2 + |c_2|^2 \epsilon_d^2(\omega_{E,2}) |\mu(q, \mathbf{n}, 2)|^2 \\ &+ 2 |c_1 c_2| \epsilon_d(\omega_{E,1}) \epsilon_d(\omega_{E,2}) |\mu(q, \mathbf{n}, 1)| |\mu(q, \mathbf{n}, 2)| \cos[\alpha(q, \mathbf{n}, 1) - \alpha(q, \mathbf{n}, 2) - \omega_0 \tau] \}, \end{aligned} \quad (8)$$

In deriving Eq. (8), it was assumed that the optical phases of different modes within  $\epsilon_d$  are the same, i.e., that  $\phi(\omega_{E,1}) = \phi(\omega_{E,2})$ . The same goes for  $\epsilon_x$ , an assumption justified for mode-locked pulses. Notice also that, because  $\mathbf{k}_{E,1} \cdot \mathbf{R}$  of Eq. (4b) is added to  $\mathbf{k}_{E,2} \cdot \mathbf{R}$  of Eq. (6), all  $\mathbf{R}$ -dependence disappears from Eq. (8), provided that  $\epsilon_x$  and  $\epsilon_d$  are co-propagating.

$P(q)$ , the total probability to populate arrangement  $q$ , is obtained from  $P(q, \mathbf{n}, E)$  by summing of  $\mathbf{n}$  and integrating over the frequencies of the dissociating pulse. An ana-

lytical result may be obtained<sup>18</sup> if one assumes that the  $\mu(q, \mathbf{n}, i)$  amplitudes do not vary appreciably over the energy range spanned by the dissociating pulse. This assumption, though justified for IBr,<sup>7</sup> was not made here because the computations are simple enough to be carried out exactly.

$$c_i = \pi \mu(i, g) \epsilon_x(i); \quad i = 1, 2, \quad (4a)$$

where  $\mu(i, g) \equiv \langle E_i | \mu | E_g \rangle$  ( $i = 1, 2$ ) is the transition dipole matrix element between the  $|E_g\rangle$  and  $|E_i\rangle$  states, and

$$\epsilon_x(i) \equiv \epsilon_x(\omega_{i,g}) \exp\{-i[\mathbf{k}_{i,g} \cdot \mathbf{R} + \phi(\omega_{i,g})]\}; \quad i = 1, 2. \quad (4b)$$

The wave vector  $\mathbf{k}_{i,g}$  is that associated with the  $\omega_{i,g}$   $[= (E_i - E_g)/\hbar]$  frequency absorbed from the excitation pulse at the end of the transition process.

The time evolution of  $|\chi\rangle$  to  $t = \tau$  causes each  $c_i$  coefficient to acquire an extra phase,

$$c_i(\tau) = c_i \exp(-iE_i \tau/\hbar); \quad i = 1, 2. \quad (5)$$

Assuming that at time  $\tau$  the excitation pulse is over, the probability of dissociating  $|\chi(\tau)\rangle$  to yield fragments of a given electronic state  $g$ , vib-rotational quantum numbers  $\mathbf{n}$ , at energy  $E$ , is given, in first-order perturbation theory, by

$$\begin{aligned} P(q, \mathbf{n}|E) &= \pi^2 |c_1(\tau) \epsilon_d(1) \mu(q, \mathbf{n}, 1) + c_2(\tau) \epsilon_d(2) \mu(q, \mathbf{n}, 2)|^2, \end{aligned} \quad (6a)$$

where  $\mu(q, \mathbf{n}, i) \equiv \langle E, \mathbf{n}, q^- | \mu | E_i, \mathbf{n}, q^- \rangle$ , and where  $|E, \mathbf{n}, q^- \rangle$  denotes a scattering state leading, as  $t \rightarrow \infty$ , to the desired  $[q, \mathbf{n}]$  product. In Eq. (6), in analogy to Eq. (4b),  $\epsilon_d$  is defined as

$$\epsilon_d(i) \equiv \epsilon_d(\omega_{E,i}) \exp\{-i[\mathbf{k}_{E,i} \cdot \mathbf{R} + \phi(\omega_{E,i})]\}; \quad i = 1, 2. \quad (6b)$$

In order to better analyze the interference inherent in the probability expression of Eq. (6), we separate out the phase factors from the molecular matrix elements. Writing

$$\mu(q, \mathbf{n}, i) \equiv |\mu(q, \mathbf{n}, i)| \exp[\alpha(q, \mathbf{n}, i)], \quad (7)$$

we can, using Eqs. (4b), (6b), expand Eq. (6) to obtain

varying the  $c_i$  coefficients (this can be most conveniently done by shifting the  $E_x$  pulse center), one can alter the yield of a desired product. Computations provided below show the extent of this yield control in the case of IBr.

### A. IBr level structure

The scenario proposed here relies on the existence of pairs of levels that are spaced no more than a few  $\text{cm}^{-1}$  apart and that are optically accessible from the ground state. As pointed out above, the required spacing between the two levels stems from our desire to use an excitation pulse that is close to transform limited. Since most available nanosecond lasers are far from this limit, this dictates the use of picosecond lasers, which in turn dictates the energy spacing of a few  $\text{cm}^{-1}$ . Another requirement of this particular formulation is that these adjacent pairs of levels should be isolated, so that only two levels are excited by the pulse. Of course the formalism is readily modifiable if we are to excite more than two levels.

The level structure of IBr and other diatomic molecules can accommodate these stringent demands. This results from the presence of perturbations between levels belonging to different electronic states. Thus, whereas the spacing between adjacent vibrational levels belonging to the same electronic state is much larger than a few  $\text{cm}^{-1}$  (which guarantees their required isolation), coincidental near degeneracy between levels belonging to different electronic states may occur. In IBr such perturbations occur between some highly excited  $X(^1\Sigma_0)$  vibrational levels and levels of the  $A(^3\Pi_1)$  state.

The situation is illustrated in Fig. 1. For example, the  $X(v=93, J=1)$ ,  $A(v=21, J=1)$  levels and the  $X(v=97, J=1)$ ,  $A(v=24, J=1)$  levels are  $1.0 \text{ cm}^{-1}$  and  $1.1 \text{ cm}^{-1}$  apart, respectively. (In all the calculations performed here, the  $|E_g\rangle$  state is assumed to be in the  $J=0$  state,  $|E_1\rangle$  and  $|E_2\rangle$  in the  $J=1$  state, and  $|E_m, q^- \rangle$  in the  $J=0$  state. Henceforth, we shall therefore omit the rotational quantum number notation.)

The  $X$  and  $A$  levels do not remain pure. Rather, they mix due to coupling between the electronic and nuclear angular moments. As a result, both the  $X$  levels, which borrow intensity from the  $X \rightarrow A$  transition dipole operator, and the  $A$  levels are optically accessible (at around  $14\,300 \text{ cm}^{-1}$ ) from the ground state.

The mixing between the  $A$  and  $X$  levels enters the calculation of the  $\mu(i, g)$  matrix elements of Eq. (4). In order to account for it we write each of the pair of levels of Eq. (1) as a linear combination of  $A$  and  $X$  states,

$$|E_1\rangle = b_{A,1}|E_{A,m}\rangle + b_{X,1}|E_{X,l}\rangle, \quad (9a)$$

$$|E_2\rangle = b_{A,2}|E_{A,m}\rangle + b_{X,2}|E_{X,l}\rangle, \quad (9b)$$

Assuming that  $\langle E_{X,l}|\mu|E_g\rangle = 0$  (since  $|E_g\rangle \equiv |E_{X,0}\rangle$ ) and  $l$  is typically  $\approx 90$ , the  $\mu(i, g)$  matrix elements are simply given as

$$\mu(i, g) = b_{A,i}\langle E_{A,m}|\mu|E_g\rangle; \quad i=1, 2. \quad (10a)$$

Using the Franck Condon approximation we further reduce this expression to

$$\mu(i, g) = b_{A,i}\mu_{A,X}\langle E_{A,m}|E_g\rangle; \quad i=1, 2, \quad (10b)$$

where  $\mu_{A,X}$  is an average electronic matrix element.

The exact value of the  $\mu_{A,X}$  constant is irrelevant for the yield equations, within first-order perturbation theory for the interaction with the excitation pulse, because its square simply multiplies the whole probability expression of Eq. (8). The calculation of the photodissociation yield thus depends on knowing the  $b_{A,i}$  coefficients and the  $\langle E_{A,m}|E_g\rangle$  overlap integrals. The latter, as discussed below, are calculable in a straightforward manner, using uniform Airy functions.

In order to evaluate the remaining  $b_{A,i}$  coefficients, we use Eqs. (9) to form a set of  $2 \times 2$  secular equations. These are solved for  $E_1, E_2$ , and the  $b_{A,i}$  coefficients in terms of the unperturbed  $E_{A,m}$  and  $E_{X,l}$  eigenvalues and the perturbation matrix element  $H_{m,l}$ . We obtain in the usual way that

$$E_i = 0.5\{E_{A,m} + E_{X,l} \pm [(E_{A,m} - E_{X,l})^2 + 4H_{m,l}^2]^{1/2}\};$$

$$i=1, 2, \quad (11)$$

and

$$b_{A,1} = \cos \theta; \quad b_{A,2} = \sin \theta;$$

$$b_{X,1} = -\sin \theta; \quad b_{X,2} = \cos \theta, \quad (12a)$$

where

$$\tan \theta = (E_{A,m} - E_1)/H_{m,l}. \quad (12b)$$

The unperturbed  $E_{A,m}$  and  $E_{X,l}$  eigenvalues are obtained using WKB quantization. The respective eigenfunctions  $\langle R|E_{A,m}\rangle$  and  $\langle R|E_{X,l}\rangle$  are accurately given in terms of uniform Airy<sup>8</sup> functions expressed about the inner and outer turning points and matched at some midpoint.<sup>9</sup> These eigenfunctions are needed for both calculating the  $\langle E_{A,m}|E_g\rangle$  overlap integrals, discussed above, as well as for the  $H_{m,l}$  perturbation matrix elements, which are simply written, using the Condon approximation, as

$$H_{m,l} \equiv \langle E_{A,m}|H|E_{X,l}\rangle \approx H_{A,X}\langle E_{A,m}|E_{X,l}\rangle. \quad (13)$$

As indicated in Eq. (13), the perturbation matrix elements depend, in addition to the overlap integral, on the average non-Born-Oppenheimer interaction term  $H_{A,X}$ . We obtain this term by fitting it to observed level spacing between the  $E_1$  and  $E_2$  levels. The value  $H_{A,X} = 170 \text{ cm}^{-1}$  was found to give reasonable agreement with observed spacings between a number of perturbed pairs in the energetic region of  $\approx 14\,300 \text{ cm}^{-1}$  above  $E_g$ .

A number of other terms must be computed as well. Specifically, the control probabilities in Eq. (8) involve the dissociation amplitudes that depend upon the bound-free  $\mu(q, n, i)$ ,  $i=1, 2$ , matrix elements. Using Eqs. (9) we have that the required matrix elements are given by

$$\mu(q, n, i) = b_{A,i}\langle E, n, q^-|\mu|E_{A,m}\rangle$$

$$+ b_{X,i}\langle E, n, q^-|\mu|E_{X,l}\rangle. \quad (14)$$

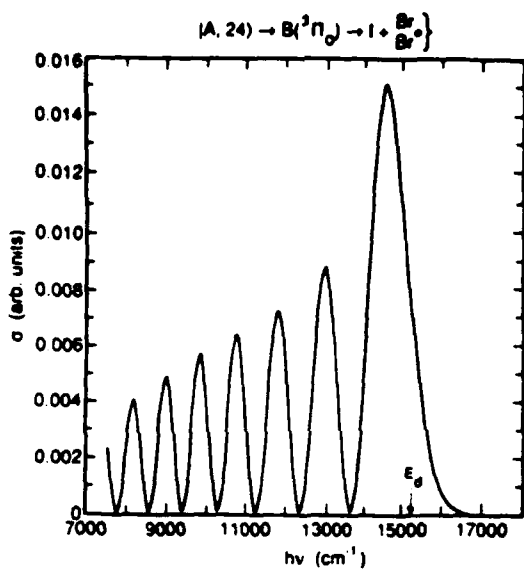


FIG. 2. Calculated total cross section for the photodissociation of the  $|E_{A,24}\rangle$  state to yield  $I + \text{Br}, \text{Br}^*$  as a function of the photon frequency. The center frequency ( $E_d = 15\,230\text{ cm}^{-1}$ ) of the  $\epsilon_d$  dissociation pulse is marked.

Both the  $\langle E, n, q^- | \mu | E_{A,m} \rangle$  and  $\langle E, n, q^- | \mu | E_{X,l} \rangle$  matrix elements were calculated exactly using the artificial channel method.<sup>10</sup>

In Figs. 2 and 3 we examine the absolute magnitude of these matrix elements by plotting the ( $X; l = 97$ ) and ( $A; m = 24$ ) absorption cross sections as a function of  $E$ . That is,

$$\sigma(E|X, l) \equiv 8\pi^3 \omega_{E,l} / c \sum_{n,q} |\langle E, n, q^- | \mu | E_{X,l} \rangle|^2, \quad (15a)$$

$$\sigma(E|A, m) \equiv 8\pi^3 \omega_{E,m} / c \sum_{n,q} |\langle E, n, q^- | \mu | E_{A,m} \rangle|^2. \quad (15b)$$

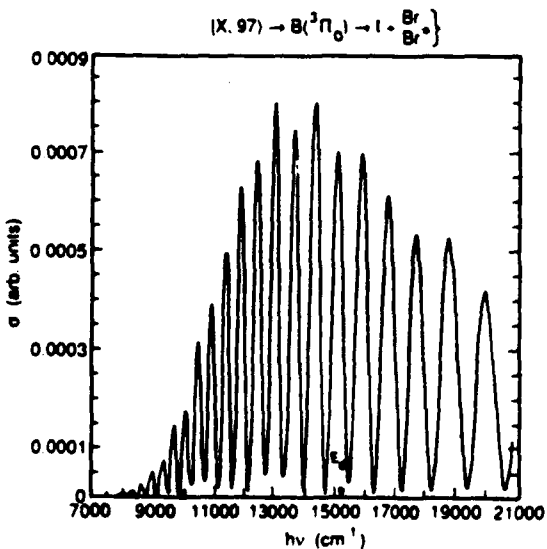


FIG. 3. As in Fig. 2, but for the  $|E_{X,97}\rangle$  state.

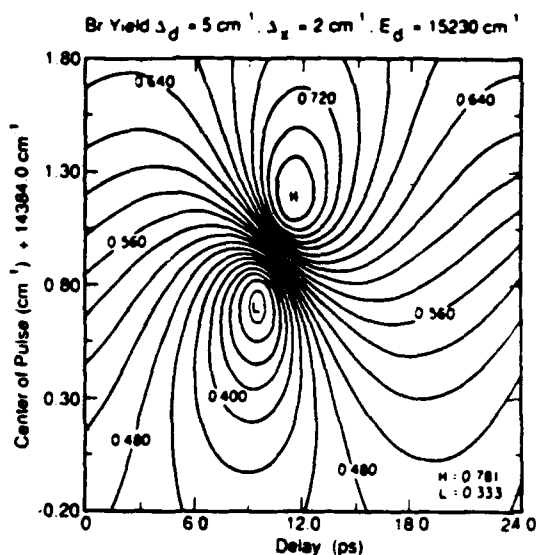


FIG. 4. Computed control over the Br yield  $[= \text{Br}/(\text{Br} + \text{Br}^*)]$  as a function of  $E_d$ —the excitation-pulse detuning, and  $\tau$ —the time delay between the pulses, using the  $|E_{X,97}\rangle$  and  $|E_{A,24}\rangle$  levels, with  $E_d = 15\,230\text{ cm}^{-1}$  and  $\Delta_d = 5\text{ cm}^{-1}$ .

As is clear from the figures, these spectra are very oscillatory, due to the oscillatory nature of the highly excited  $|E_{A,24}\rangle$  and  $|E_{X,97}\rangle$  levels. The artificial channel method obviates the need for first calculating these wavefunctions, then calculating the continuum wavefunctions and then integrating over the product. Rather, the matrix elements are obtained directly in a single calculation involving both the bound and continuum potentials. (In fact, the Morse wavefunctions analytic expressions and finite difference methods for generating diatomic bound wavefunctions become unreliable for such highly excited states. This is indeed the reason why the uniform Airy functions are used for the bound-bound overlap integral calculations.)

Having obtained  $\langle E, n, q^- | \mu | E_{A,m} \rangle$  and  $\langle E, n, q^- | \mu | E_{X,l} \rangle$  we can, using Eqs. (12) and (14), generate the  $\mu(q, n, i)$  matrix elements. These, together with  $\mu(i, g)$  of Eq. (10) and the laser parameters defining  $\epsilon_x$  and  $\epsilon_d$  enter into the expression for  $P(q, n | E)$  [Eq. (8)] and hence into the integrated probability  $P(q)$  derived from it. Results of the  $P(q)$  calculations are discussed below.

## B. Yield control in $I\text{Br}$

In Figs. 4–6 we plot  $P(q = \text{Br})$ , the integrated yield to form ground state Br atoms, as a function of  $E_d$ , the excitation pulse center frequency, and  $\tau$ , the delay time between the  $\epsilon_x(t)$  and  $\epsilon_d(t)$  pulses. The three plots differ in the length of the  $\epsilon_d(t)$  pulse; i.e., the pulse gets shorter, and consequently the bandwidth gets wider, in going from Fig. 4 to Fig. 6. The effect of changing this parameter is quite striking: The Br yield  $[= \text{Br}/(\text{Br} + \text{Br}^*)]$  is seen to vary from 36% to 76% for the  $\Delta_d = 5\text{ cm}^{-1}$  case (see Fig. 4); from 21% to 86% for the  $\Delta_d = 10\text{ cm}^{-1}$  case (see Fig. 5); and reaches almost complete control, 6%–91%, for the  $\Delta_d = 20\text{ cm}^{-1}$  case (see Fig. 6).

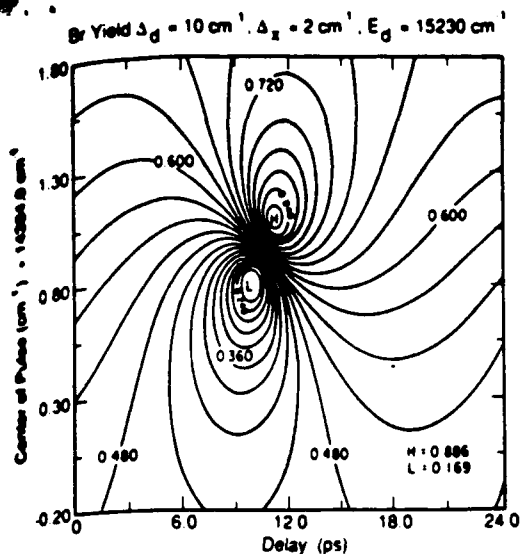


FIG. 5. As in Fig. 4, but with  $\Delta_d = 10 \text{ cm}^{-1}$ .

The reason that the dissociation laser pulse width has such a dramatic effect is that by increasing the width we eliminate uncontrollable photodissociation contributions (which we term satellites) that accompany the controlled process. As can be seen from Eq. (8), if  $\epsilon_d(\omega_{E_1})$  is much smaller than  $\epsilon_d(\omega_{E_2})$ , or *vice versa*, the interference term of Eq. (8) is virtually eliminated, as is our ability to control the process. This always occurs at the satellites that are the very red edge of the energy integral over  $P(q, n | E)$ , where  $\epsilon_d(\omega_{E_2}) \ll \epsilon_d(\omega_{E_1})$ , and the very blue edge, where  $\epsilon_d(\omega_{E_2}) \gg \epsilon_d(\omega_{E_1})$ . Making the pulse width  $\Delta_d$  large relative to the  $E_1$ - $E_2$  level spacing guaranteed that the integrated  $P(q, n | E)$  probability in the satellite regions is negligible relative to the integrated probability in the "control" region, where  $\epsilon_d(\omega_{E_2}) \approx \epsilon_d(\omega_{E_1})$ .

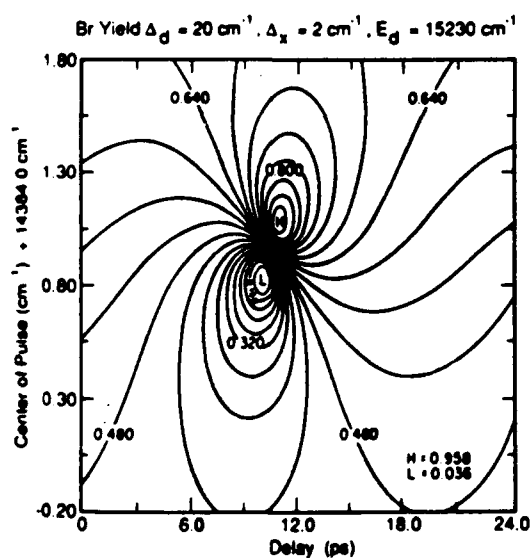


FIG. 6. As in Fig. 4, but with  $\Delta_d = 20 \text{ cm}^{-1}$ .

To conclude this section, we emphasize that the potential curves and most other parameters in our calculation are known and that the nuclear dynamics has been solved exactly. Although we have only looked at the  $J = 0 \rightarrow J = 1$  process, it is our experience<sup>11</sup> that the region of optimal control varies quite slowly with  $J$ . This is due to the fact that ratios such as  $\mu(1,g)/\mu(2,g)$  and  $\mu(q,m,1)/\mu(q,m,2)$  appearing in our control equations [Eqs. (4)-(8)] vary quite slowly with  $J$ . Thus, provided one works with a well-cooled beam, the conclusions reached here for the  $J = 0 \rightarrow J = 1$  transitions are expected to hold in real experimental situations. This situation will be further studied in a future publication.<sup>11</sup>

### III. PROPOSED EXPERIMENT

The principles of coherent control have now been established in a number of papers.<sup>1</sup> We believe that this IBR study should motivate experimental work to demonstrate this effect and, in what follows, we present a sketch of an experiment. Specifically, we briefly discuss the dissociation system and the detection system.

As a possible candidate for a picosecond laser system one may wish to consider a frequency-doubled mode-locked Nd-Yag laser simultaneously pumping two dye lasers. One dye laser is used to generate the excitation pulse, the other, operating at a slightly different frequency (to avoid further excitation of the ground state to the same levels pumped by the first pulse), the dissociating pulse. Picosecond pulses generated in this manner can be made to be transform limited. Indeed, one of the reasons we have chosen IBR is that it can be controlled by picosecond pulses that are usually Gaussian and transform limited. Clearly, in the scheme outlined above, no chirping is necessary.

The train of pulses emanating from the two dye lasers should be spatially united in a co-propagating geometry, on a cell containing IBR vapors. The latter feature insures that the  $k \cdot R$  part of the phase, introduced in the excitation phase, exactly cancels the  $k \cdot R$  part of the phase introduced by the dissociating pulse.

The essential control parameters can be readily varied. A time delay between the two pulse trains may be introduced by changing the optical paths of one color relative to the other. The center of the excitation pulse ( $E_x$ ) can be changed by fine tuning the first dye laser over a range of  $1-2 \text{ cm}^{-1}$ .

In order to detect the products, one must be able to measure both the  $\text{Br}^*$  and  $\text{Br}$  species. This can be achieved by MPI or LIF using vuv lasers, both standard techniques in modern labs. Alternatively one may use CARS spectroscopy with two beams differing in frequency by the  $\text{Br}^*$ - $\text{Br}$  energy difference. The remarkable range of control expected from our Figs. 4-6 should be readily observable.

### IV. SUMMARY

We have shown that a two-pulse scheme, in the picosecond domain, is capable of providing enormous control over the yield of atomic products in the photodissociation of IBR. The scheme is both practical and straightforward

and we urge experimental verification of the principle of coherent control in this setting.

#### ACKNOWLEDGMENTS

This work was supported by the U.S. Office of Naval Research under Contract No. N00014-87-J-1204, and by the Minerva Foundation, Munich, F.R.G. M.S. wishes to acknowledge partial support from the Director, Office of Energy Research, Office of Basic Energy Sciences, Chemical Sciences Division of the U.S. Department of Energy under Contract No. DE-AC03-76SF00098.

<sup>1</sup>(a) P. Brumer and M. Shapiro, *Chem. Phys. Lett.* **126**, 541 (1986); (b) P. Brumer and M. Shapiro, *Disc. Faraday Soc.* **82**, 177 (1987); (c) C. Asaro, P. Brumer, and M. Shapiro, *Phys. Rev. Lett.* **60**, 1634 (1988); (d) M. Shapiro, J. Hepburn, and P. Brumer, *Chem. Phys. Lett.* **149**, 451 (1988); (e) G. Kurizki, M. Shapiro, and P. Brumer, *Phys. Rev. (B)* **39**, 3435 (1989); (f) M. Shapiro and P. Brumer, *J. Chem. Phys.* **90**, 6179 (1989); (g) T. Seideman, M. Shapiro, and P. Brumer, *J. Chem. Phys.* **90**, 7132 (1989); (h) P. Brumer, and M. Shapiro, *Accounts Chem. Res.*

**22**, 407 (1989); (i) P. Brumer and M. Shapiro, *Chem. Phys.* **139**, 221 (1989).

<sup>2</sup>(a) D. J. Tannor and S. A. Rice, *J. Chem. Phys.* **83**, 5013 (1985); (b) D. J. Tannor, R. Kosloff, and S. A. Rice, *J. Chem. Phys.* **85**, 5803 (1986); (c) D. J. Tannor and S. A. Rice, *Adv. Chem. Phys.* **78**, 441 (1988).

<sup>3</sup>T. A. Holme and J. S. Hutchinson, *Chem. Phys. Lett.* **124**, 181 (1986); see, however, T. A. Holme and J. S. Hutchinson, *Chem. Phys. Lett.* **148**, 354 (1988) and related comment in Ref. 2(c).

<sup>4</sup>S. Shi, A. Woody, and H. Rabitz, *J. Chem. Phys.* **88**, 6870 (1988).

<sup>5</sup>J. L. Krause, M. Shapiro, and P. Brumer, *J. Chem. Phys.* **92**, 1126 (1990).

<sup>6</sup>For pre-1986 literature on this topic, see, e.g., (a) *Photoselective Chemistry*, Vols. I and II, edited by J. Jortner, R. D. Levine, and S. A. Rice (Wiley, New York, 1981); (b) P. R. Brooks, R. F. Curl, and T. C. Maguire, *Ber. Bunsenges. Phys. Chem.* **86**, 401 (1982); (c) T. F. George, *J. Phys. Chem.* **86**, 10 (1982).

<sup>7</sup>H. Bony, A. Yogeve, and M. Shapiro, *Chem. Phys. Lett.* **107**, 603 (1984).

<sup>8</sup>R. E. Langer, *Trans. Am. Math. Soc.* **34**, 447 (1932); **37**, 397 (1935); W. H. Miller, *J. Chem. Phys.* **48**, 464 (1968).

<sup>9</sup>T. Seideman and M. Shapiro, *J. Chem. Phys.* **88**, 5525 (1988).

<sup>10</sup>M. Shapiro, *J. Chem. Phys.* **56**, 2582 (1972); see, also, M. Shapiro and R. Bersohn, *Ann. Rev. Phys. Chem.* **33**, 409 (1982).

<sup>11</sup>C. K. Chan, P. Brumer, and M. Shapiro, to be published.

## Quantum beats induced by partially coherent laser sources

Xue-Pei Jiang and Paul Brumer

*Chemical Physics Theory Group, Department of Chemistry, University of Toronto, Toronto, Ontario, Canada M5S 1A1*

Received 28 January 1991; in final form 27 February 1991

We consider the effect of the partial coherence of the excitation light source on the characteristics of quantum beats in isolated molecules. Using a variant of a phase diffusion model we show that the laser incoherence can induce two distinctly different types of behavior, depending upon the relative location of the pulse carrier frequency and the excited molecular eigenstates, as well as upon the Franck-Condon factors for excitation. The approach is applied to analyze both transform limited and partially coherent excitation in the  $C(^1B_2)$  state in  $SO_2$ , providing previously unavailable spectroscopic parameters.

### 1. Introduction

Quantum beats, which constitute one of the simplest manifestations of quantum interference, have been observed in a wide variety of systems including subatomic, atomic and molecular systems as well in the condensed phases [1-7]<sup>†1</sup>. Of particular interest to this paper are quantum beats in the time-resolved fluorescence spectroscopy of isolated molecules [3,4,8], an observational tool which provides a sensitive probe of quasiperiodic excited state dynamics. In such an experiment an excitation light pulse prepares a linear superposition of rovibronic excited states. The molecular coherence established in the prepared state is reflected in the fluorescence emission as quantum beats.

It is well known that both the state created by photon excitation and any subsequent measurement depend upon the characteristics of the excitation source. For example, a completely chaotic source will produce a stationary mixture of eigenstates whereas a transform limited pulse produces a pure quantum state with associated time evolution. Picosecond and femtosecond sources can be well characterized and tend to have minimum incoherence. General light sources, however, such as nanosecond pulses or dye lasers without an étalon, are generally partially coherent, i.e. not transform limited<sup>†2</sup>. We show below that laser incoherences of this kind have a significant effect on the modulation depth of the induced quantum beats. In particular we provide a useful theory and methodology for analyzing quantum beats arising from excitation with partially coherent sources. In doing so we also call attention to possible difficulties associated with neglecting the effect of the electric field amplitude in analyses of quantum beats arising from excitation with transform limited sources. Numerical studies are also presented which show that quantum beat data display distinctive pattern changes with changing laser coherence, depending upon the location of the laser central frequency relative to the eigenstates which are excited, as well as the Franck-Condon factors for excitation. Finally, the theory is applied to analyze data on  $SO_2$ , extracting new information about coupling in this molecule.

<sup>†1</sup> For a comprehensive review see ref. [8].

<sup>†2</sup> Indeed such incoherences have been advantageously utilized to obtain coherent information. See ref. [9].

## 2. Theory

### 2.1. Exact eigenstate basis

The theory of fluorescence quantum beats is most transparent in the exact eigenstate basis set which can be worked out by either conventional time-dependent perturbation method or Green function formalism [10]. Both approaches lead to the fluorescence intensity  $I(t)$  being given by the square of the projection of the created wavefunction onto the final states. That is,  $I(t)$ , barring a multiplicative constant, is given by

$$I(t) = \sum_n |\langle g_n | \mu | \psi(t) \rangle|^2, \quad (1)$$

where  $|g_n\rangle$  are the energy eigenstates of the ground electronic state and  $|\psi(t)\rangle$  is the time-evolved excited state, which was prepared as  $|\psi(0)\rangle$  by the laser pulse.

Consider then a state prepared by excitation from a ground level  $|g_0\rangle$  with a weak coherent pulse, so that first-order perturbation theory is valid. Under these conditions [11]:

$$\begin{aligned} |\psi(t)\rangle &= \sum_j c_j |j\rangle \exp(-\frac{1}{2}\Gamma_j t) \exp(-iE_j t/\hbar) \\ &= \frac{\sqrt{2\pi}}{i\hbar} \sum_j |j\rangle \langle j | \mu | g_0 \rangle \epsilon(\omega_{jg}) \exp(-\frac{1}{2}\Gamma_j t) \exp(-iE_j t/\hbar), \end{aligned} \quad (2)$$

where  $|j\rangle$  denotes a rovibrational level of the excited electronic state of energy  $E_j$ ,  $\omega_{jg} = (E_j - E_{g_0})/\hbar$ ,  $\Gamma_j$  is the lifetime of state  $j$  and  $\epsilon(\omega_{jg})$  is the electric field amplitude of the light source at frequency  $\omega_{jg}$ . Note the dependence of the created state on the electric field amplitude, a feature which persists as long as the pulse is not infinitely fast. This feature, frequently neglected in quantum beat analyses, is carefully included throughout this treatment.

Using eqs. (1) and (2) we have

$$I(t) = \frac{2\pi}{\hbar^2} \sum_n \left| \sum_j \langle g_n | \mu | j \rangle \langle j | \mu | g_0 \rangle \epsilon(\omega_{jg}) \exp(-iE_j t) \exp(-\frac{1}{2}\Gamma_j t) \right|^2. \quad (3)$$

Eq. (3) only applies if the ket  $|\psi(0)\rangle$  is defined, i.e. if the laser source is fully coherent (i.e. transform limited). If this is not the case then we can generalize eq. (1) to

$$I(t) = \sum_n \text{Tr} [ | \mu g_n \rangle \langle \mu g_n | \rho(t) ], \quad (4)$$

where  $\rho(t)$  is the time evolution of the molecular density matrix  $\rho(0)$  formed by the partially coherent pulse at  $t=0$ . The quantity  $\rho(0)$  is the natural generalization of  $|\psi(0)\rangle \langle \psi(0)|$  to the incoherent case. Specifically [12],

$$\begin{aligned} \rho(0) &= -\frac{2\pi}{\hbar^2} \sum_j \sum_k \langle j | \mu | g_0 \rangle \langle g_0 | \mu | k \rangle \langle \epsilon(\omega_{jg}) \epsilon^*(\omega_{kg}) \rangle |j\rangle \langle k|, \\ \rho(t) &= -\frac{2\pi}{\hbar^2} \sum_j \sum_k \langle j | \mu | g_0 \rangle \langle g_0 | \mu | k \rangle \langle \epsilon(\omega_{jg}) \epsilon^*(\omega_{kg}) \rangle |j\rangle \langle k| \exp[-\frac{1}{2}(\Gamma_j + \Gamma_k)t] \exp(-i\omega_{jk}t), \end{aligned} \quad (5)$$

where  $\omega_{jk} = (E_j - E_k)/\hbar$  and  $\langle \epsilon(\omega_{jg}) \epsilon^*(\omega_{kg}) \rangle$  denotes averaging over the ensemble which embodies the statistics of the partially coherent field. Combining eqs. (4) and (5) gives the general expression for the fluorescence emission spectrum associated with a state created by a partially coherent source.

Below we examine experimental quantum beat data in  $\text{SO}_2$ , induced by both coherent and partially coherent sources. The coherent data were well fit [4] by a three-level model, i.e. a single  $|g_0\rangle = |g\rangle$  excited to produce

a superposition of two excited states, denoted  $|1\rangle$ ,  $|2\rangle$ , with fluorescence emission back to  $|g\rangle$ . To recover this model from eqs. (3)–(5) requires that we assume that  $\langle g_n|\mu|j\rangle$  is well approximated as  $\langle g|\mu|j\rangle$  for all  $n$ . In this case  $I(t)$  is given, for the coherent and partially coherent excitations respectively, in accordance with eqs. (3)–(5) by

$$I_{\text{coh}}(t) = |\langle g|\mu|1\rangle|^4 |\epsilon(\omega_{1g})|^2 \exp(-\Gamma_1 t) + |\langle g|\mu|2\rangle|^4 |\epsilon(\omega_{2g})|^2 \exp(-\Gamma_2 t) \\ + 2|\langle g|\mu|1\rangle \langle 2|\mu|g\rangle|^2 \exp[-\frac{1}{2}(\Gamma_1 + \Gamma_2)t] \text{Re}\{\epsilon(\omega_{1g})\epsilon^*(\omega_{2g}) \exp[-i(E_1 - E_2)t/\hbar]\}, \quad (6a)$$

$$I_{\text{incoh}}(t) = |\langle g|\mu|1\rangle|^4 \langle |\epsilon(\omega_{1g})|^2 \rangle \exp(-\Gamma_1 t) + |\langle g|\mu|2\rangle|^4 \langle |\epsilon(\omega_{2g})|^2 \rangle \exp(-\Gamma_2 t) \\ + 2|\langle g|\mu|1\rangle \langle 2|\mu|g\rangle|^2 \exp[-\frac{1}{2}(\Gamma_1 + \Gamma_2)t] \text{Re}\{\langle \epsilon(\omega_{1g})\epsilon^*(\omega_{2g}) \rangle \exp[-i(E_1 - E_2)t/\hbar]\}. \quad (6b)$$

For the computations described below the pulse is assumed Gaussian so that

$$\epsilon(\omega_n) = \frac{1}{\sqrt{2\pi}} \int_{-\infty}^{\infty} \exp(i\omega_n t) \epsilon(t) dt, \quad j=1, 2, \quad (7a)$$

with

$$\epsilon(t) = E_0 \exp(-t^2/\tau^2) \exp[-i\omega_0 t + i\alpha(t)]. \quad (7b)$$

Here  $\alpha(t)$  is a constant phase for coherent light sources and a stochastic variable for partially coherent sources.

In the partially coherent case we adopt a Gaussian variant of the phase diffusion model to simulate both the pulse shape and the field coherence [12], giving the following correlation function:

$$\langle \epsilon(\omega_n)\epsilon^*(\omega_m) \rangle = \frac{E_0^2 \tau T}{\sqrt{2\pi}} \exp[i(\omega_n - \omega_m)t_0] \exp[-\frac{1}{2}\tau^2(\omega_n - \omega_m)^2] \exp[-\frac{1}{2}T^2(\omega_n + \omega_m - 2\omega_0)^2], \quad (8)$$

where  $\tau$  and  $\tau_c$  are the pulse duration and the correlation decay time and  $T$ , related to the laser frequency profile [12], is given by

$$T = \tau\tau_c / (\tau^2 + \tau_c^2)^{1/2}. \quad (9)$$

Inserting eq. (8) into eq. (6b) gives the explicit form for  $I_{\text{incoh}}(t)$ .

## 2.2. Zeroth-order two-state basis

In this section we provide useful expressions for the analysis of fluorescence from partially coherent sources using the alternate interacting-zeroth-order-states viewpoint. In this popular approach [3,8] the true molecular eigenstates  $|1\rangle$  and  $|2\rangle$  result from diagonalizing the intramolecular interaction  $V_{ij}$  between the zeroth-order states denoted  $|s\rangle$  and  $|l\rangle$ . That is

$$|1\rangle = D'_{1s}|s\rangle + D'_{1l}|l\rangle, \quad |2\rangle = D'_{2s}|s\rangle + D'_{2l}|l\rangle, \\ |s\rangle = D_{1s}|1\rangle + D_{2s}|2\rangle, \quad |l\rangle = D_{1l}|1\rangle + D_{2l}|2\rangle, \quad (10)$$

where the orthogonality of  $\{D\}$  implies that  $\{D\}^T = \{D'\}$  and where the exact values of  $\{D\}$  depend upon the  $V_{ij}$ . Note that the crucial parameters to be determined experimentally, from the zeroth-order-basis viewpoint, are the mixing coefficients  $D_{js}$ ,  $D_{jl}$  (or  $D'_{js}$ ,  $D'_{jl}$ ) since they provide insight into the coupling between the pumped state  $|s\rangle$  (see below) and the "background state"  $|l\rangle$ . The standard model assumes that  $|s\rangle$  and  $|l\rangle$  are rovibronic states belonging to the electronic surface and that only  $|s\rangle$  is radiatively coupled to the ground state  $|g\rangle$ . That is,  $\langle g|\mu|s\rangle \neq 0$  and  $\langle g|\mu|l\rangle = 0$  so that the prepared state, assuming two levels excited is (from eqs. (2) and (10))

$$|\psi(0)\rangle = (\sqrt{2\pi}/i\hbar) \langle s|\mu|g\rangle [D'_{1s}\epsilon(\omega_{1g})|1\rangle + D'_{2s}\epsilon(\omega_{2g})|2\rangle]. \quad (11)$$

To recover  
 $|\mu|j\rangle$  for all  
 rdance with

(6a)

(6b)

(7a)

(7b)

ent sources.  
 ate both the

(8)

ency profile

(9)

ent sources  
 : molecular  
 : roth-order

(10)

1 upon the  
 viewpoint,  
 re pumped  
 $|l\rangle$  are ro-  
 und state  
 (from eqs.

(11)

Then, using eqs. (6) and (10) we have the time dependence of the fluorescence intensity associated with coherent and partially coherent source excitation, in terms of the zeroth-order states, being given by

$$I_{\text{coh}}(t) = |D_{1s}|^4 |\epsilon_1|^2 \exp(-\Gamma_1 t) + |D_{2s}|^4 |\epsilon_2|^2 \exp(-\Gamma_2 t) \\
+ 2 \operatorname{Re} \{ |D_{1s}|^2 |D_{2s}|^2 \epsilon_1 \epsilon_2^* \exp[-\frac{1}{2}(\Gamma_1 + \Gamma_2)t] \exp[i(E_1 - E_2)t/\hbar] \} \\
= |\bar{D}_{1s}|^4 \exp(-\Gamma_1 t) + |\bar{D}_{2s}|^4 \exp(-\Gamma_2 t) \\
+ 2 \operatorname{Re} \{ |\bar{D}_{1s}|^2 |\bar{D}_{2s}|^2 \exp[-\frac{1}{2}(\Gamma_1 + \Gamma_2)t] \exp[i(E_1 - E_2)t/\hbar] \}, \quad (12)$$

where  $\epsilon_j = \epsilon(\omega_{\mu j})$  and  $|\bar{D}_{j\mu}|^2 = |D_{j\mu}|^2 \epsilon_j$  and

$$I_{\text{incoh}}(t) = |D_{1s}|^4 \langle |\epsilon_1|^2 \rangle \exp(-\Gamma_1 t) + |D_{2s}|^4 \langle |\epsilon_2|^2 \rangle \exp(-\Gamma_2 t) \\
+ 2 \operatorname{Re} \{ |D_{1s}|^2 |D_{2s}|^2 \langle \epsilon_1 \epsilon_2^* \rangle \exp[-\frac{1}{2}(\Gamma_1 + \Gamma_2)t] \exp[i(E_1 - E_2)t/\hbar] \}. \quad (13)$$

Eqs. (12) and (13) neglect the overall multiplicative constant  $-(2\pi/\hbar^2) |\langle s|\mu|g \rangle|^2$ .

Note that both eqs. (12) and (13) constitute extensions of the traditional two-level zeroth-order-basis model result, eq. (13) insofar as it applies to partially coherent sources and eq. (12) in that it properly includes the effect of the electric field amplitude. The standard literature result [4] obtains in the latter case if, for example, one assumes a  $\delta(t)$  pulse excitation which gives  $\epsilon(\omega_{1g}) = \epsilon(\omega_{2g})$  and hence

$$I_{\text{coh}}(t) \propto |D_{1s}|^4 \exp(-\Gamma_1 t) + |D_{2s}|^4 \exp(-\Gamma_2 t) + 2 |D_{1s} D_{2s}|^2 \exp[-\frac{1}{2}(\Gamma_1 + \Gamma_2)t] \cos(\omega_{12}t). \quad (14)$$

Results below suggest that use of this formula to extract molecular coupling parameters is highly suspected.

### 3. Dependence on $\tau_c$ and application to $\text{SO}_2$

The fluorescence decay of the  $\tilde{C}(^1B_2)$  state of  $\text{SO}_2$  in a beam has been examined by Wallace and co-workers [4] using a Nd:YAG-pumped tunable dye excitation laser of  $\tau = 5$  ns duration. Experiments were done using two different cavity configurations, one with an étalon which gives an essentially transform-limited pulse and the other without an étalon, generating a partially coherent pulse. Both configurations show fluorescence decay with quantum beats of identical periods but with a modulation depth which decreases significantly upon introduction of laser incoherence. Below we analyze both the coherent and partially coherent data and extract new and useful information regarding the prepared state and mixing coefficients in  $\text{SO}_2$ . Prior to doing so we correct an error in the data analysis of ref. [4]. Specifically, they analysed the data generated by the coherent pulse by doing a numerical fit in which both system parameters and those of a Gaussian instrument response function [4.13] were varied. We repeated this computation, correcting a numerical error and have obtained the following parameters (see fig. 1): response function width, 4.0 ns;  $\omega_{12} = 0.00835 \text{ cm}^{-1}$ ,  $\Gamma_1 = 1/50$  ns,  $\Gamma_2 = 1/71.4$  ns, and  $|\bar{D}_{1s}/\bar{D}_{2s}| = 2.2$ .

Consider then the content of this result, typical of those obtained in the standard analysis of quantum beats prepared with transform limited pulses. As is evident from eq. (11), the value of  $|\bar{D}_{1s}/\bar{D}_{2s}|$  determined in this fit provides the (absolute values of the) coefficients of the state prepared by the coherent source, but does not provide the desired molecular mixing coefficient ratio  $D_{1s}/D_{2s}$  since the  $\bar{D}_{j\mu}$  contain the unknown  $\epsilon(\omega_{\mu j})$ . Barring phases, these quantities could be determined if there were an experimental way to adjust the detuning (i.e. the relative locations of  $\omega_0$  and the bound states). However, this is generally unknown, the common technique being to vary  $\omega_0$  until one achieves maximum intensity of the excitation laser or maximum quantum beat signal. This is often presumed to correspond to the case of central tuning, i.e. the laser frequency is assumed tuned

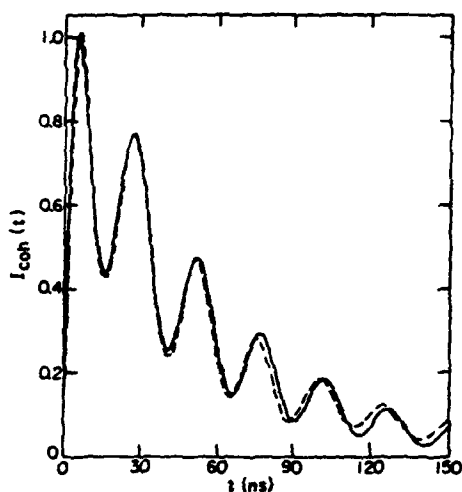


Fig. 1. Best fit (solid curve) to  $\text{SO}_2$  fluorescence emanating from excitation in a coherent pulse experiment. Experimental data are shown dashed and parameters are given in the text.

to the middle of the pair of the excited states. Further,  $\epsilon(\omega_{1g})$  and  $\epsilon(\omega_{2g})$  are often assumed equal, on the basis of an argument that the pulse is ultrafast. However, we will show below that an assumption of  $\epsilon(\omega_{1g}) = \epsilon(\omega_{2g})$  is incorrect for the experiments done on  $\text{SO}_2$ , for example, and that this has important consequences for extracting desired molecular parameters.

Specifically, we used the models described above (eq. (6)) to fit the  $\text{SO}_2$  fluorescence data associated with both the coherent and partially coherent excitation. We obtain, using the model for the pulse discussed above (eqs. (7) and (8)), and the observed power spectrum width of  $0.5 \text{ cm}^{-1}$ , that the field decay time  $\tau_c$  of the partially coherent source is 0.18 ns. Further, in accord with ref. [4], we assume that  $\omega_0$  for both the transform-limited and the partially coherent pulses are the same. In addition, we choose the width of the instrument response function for the partially coherent case to be 3 ns, rather than the 4 ns corresponding to the coherent pulse case. This is not unreasonable since the power varies significantly between these two pulses. The fit we obtain to the experimental results, shown later below, justifies these parameter choices. Note that because the constraint  $|\bar{D}_{1z}/\bar{D}_{2z}| = 2.2$  (obtained from the coherent excitation case) links the two parameters  $|D_{1z}/D_{2z}|$  and  $\omega_0$ , the numerical fit to the observed  $I_{\text{incoh}}$  is actually conducted in one-parameter space.

The numerical fits reveal interesting behavior which is quite general. Specifically, we find that if  $|D_{1z}| \approx |D_{2z}|$  (and hence  $|D_{1x}| \approx |D_{2x}|$ ) then the quantum beat modulation depth is relatively insensitive to variations in  $\tau_c$  (for examples see figs. 2a and 2b). However, when  $D_{1z}$  and  $D_{2z}$  are substantially different then the modulation depth can depend sensitively on the value  $\tau_c$ . That is, in zeroth-order language, two equally bright excited states show little  $\tau_c$  dependence, whereas one-bright plus one-dark-eigenstate (which implies weak interaction between two zeroth-order states) can show strong  $\tau_c$  dependence. However, even in the latter case, we find two different patterns of beat signals as a function of the incoherence parameter  $\tau_c$ , depending upon the location of the central frequency  $\omega_0$  relative to the two levels  $|E_1\rangle$  and  $|E_2\rangle$ . Specifically, if  $\omega_0$  causes excitation to the center (or near center) of the two bound states then the modulation is large and relatively insensitive to  $\tau_c$  (see fig. 2c). However, if  $\omega_0$  corresponds to off-center tuning then we find large modulation depths for the coherent excitation and decreasing modulation depths<sup>23</sup> with decreasing  $\tau_c$  (fig. 2d). These computations are consistent with eq. (13) in which the degree of modulation (defined as the ratio of cross and diagonal terms) is proportional to the ratio  $R$

<sup>23</sup> Note that the modulation depth appears to approach a constant as  $\tau_c$  gets smaller. That is, the quantum beat persists even as one approaches the chaotic source case of  $\tau_c = 0$ . Examination of eqs. (13) and (8) shows that the origin of this behavior lies in the  $T$  dependence of both the diagonal (proportional to  $\langle |\epsilon_i|^2 \rangle$ ) as well as the interference terms in eq. (13).

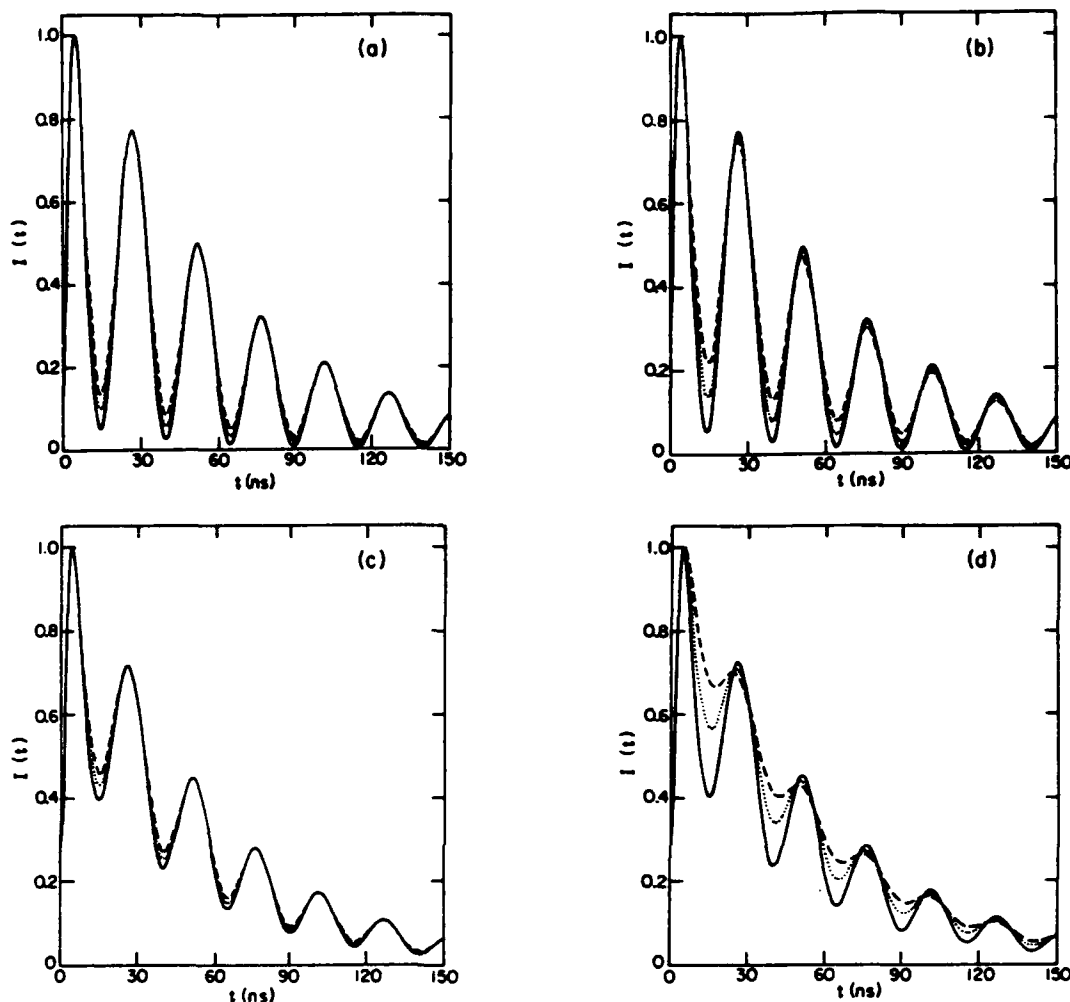


Fig. 2. Dependence of beat patterns on  $\tau_c$ . Panels (a), (b), (c) and (d) correspond to different detunings and  $|D_{1s}/D_{2s}|$  ratios. Notation for different values of  $\tau_c$  is as follows (—) = 100 ns, (···) = 5 ns, (---) = 1.5 ns. Data for  $\tau_c = 0.18$  ns (not shown) are virtually indistinguishable from the  $\tau_c = 1.5$  ns case. (a)  $|D_{1s}/D_{2s}| = 1.2$ , central tuning, i.e.  $\omega_0 = 0$ ; (b)  $|D_{1s}/D_{2s}| = 1.2$ , off-central tuning with  $\omega_0$  resonant with level  $|E_2\rangle$ , i.e.  $\omega_0 = |\omega_{21}| = 0.0042 \text{ cm}^{-1}$ ; (c)  $|D_{1s}/D_{2s}| = 2.2$ , central tuning  $\omega_0 = 0$ ; (d)  $|D_{1s}/D_{2s}| = 2.2$ , off-central tuning with  $\omega_0 = 0.011 \text{ cm}^{-1} > |\omega_{21}|$ . In all cases the width of the Gaussian instrumental response function is taken to be 3 ns.

$$R = 2 \operatorname{Re}(|D_{1s}|^2 |D_{2s}|^2 \langle \epsilon_1, \epsilon_2^* \rangle) / (|D_{1s}|^4 \langle |\epsilon_1|^2 \rangle + |D_{2s}|^4 \langle |\epsilon_2|^2 \rangle). \quad (15)$$

Using eqs. (7) and (8) shows that for the case of central tuning  $R = \exp(\frac{1}{2} T^2 \omega_{12}^2)$  and varies only slightly with  $\tau_c$ , from 1.17 to 1, for the  $\text{SO}_2$  case. For the case of off-center tuning with one dominant  $|D_i|$  coefficient, however,  $R$  shows much larger variation. For example, for  $\omega_0 = \omega_2$ ,  $R = \exp(\frac{1}{2} T^2 \omega_{12}^2)$ , which varies between 1.61 and 1. (In actuality the computed modulation extent is larger than this estimate, a consequence of the Gaussian convolution whose primary effect is to reduce the height of the first peak of the beat signals.)

The essential point then is that observing substantial changes in the modulation depth of the quantum beat fluorescence signal is evidence for off-center excitation of two states with substantially different values of  $D_{1s}$  and  $D_{2s}$ . The  $\text{SO}_2$  data show precisely this strong variation of modulation depth with  $\tau_c$ , consistent with the

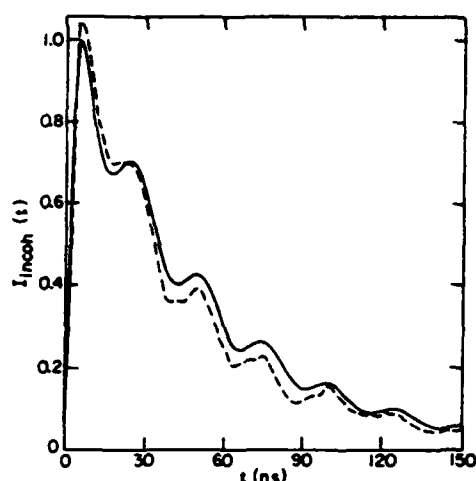


Fig. 3. Best fit (solid curve) to  $\text{SO}_2$  fluorescence emanating from excitation in a partially coherent pulse experiment. Experimental data are shown dashed and parameters are given in the text.

case of off-center tuning. More specifically, our fit to the experimental partially coherent data for  $\text{SO}_2$ , shown in fig. 3, gives  $\omega_0 = 0.011 \text{ cm}^{-1}$  and  $|D_{1z}/D_{2z}| = 3.66$ . Since  $\omega_0 > \frac{1}{2}\omega_{12}$  the laser frequency profile has its maximum at an energy which is larger than that of *both*  $|E_1\rangle$  and  $|E_2\rangle$ . Further, the computed  $|D_{1z}/D_{2z}|$  ratio, with a dominant  $|D_{1z}|$  indicates a small interaction of states from the viewpoint of the zeroth-order state model. Therefore, the combination of fluorescence from excitation with a coherent and partially coherent source has provided new information on the important term,  $|D_{1z}/D_{2z}|$ . In principle, it also can be used to determine the absolute energies of the excited states. However, the pulse frequency is known only to  $0.1 \text{ cm}^{-1}$ , a considerable uncertainty compared to the beat frequency is  $0.0085 \text{ cm}^{-1}$ . This uncertainty limits our ability to extract the bound state locations.

#### 4. Summary

Fluorescence spectroscopy with a transform limited excitation source measures the beat frequency, decay constants of each individual level and the ratio  $|\bar{D}_{1z}/\bar{D}_{2z}|$ . Here we have shown that quantum beat studies utilizing partially coherent sources can also be analyzed, using the approach developed here, to obtain similar data, although with possibly less precision due to the fluctuations inherent in the partial coherent source. Two characteristically different patterns have emerged in our examination of the dependence of quantum beat modulation depths on excitation laser coherence (i.e.  $\tau_c$ ): (1) a modulation depth which is generally insensitive to  $\tau_c$ , corresponding either to large interaction between zeroth-order levels or central tuning, and (2) strong dependence of the modulation on  $\tau_c$ , corresponding to off-central tuning and small interaction between zeroth-order levels, as is the case for the analyzed  $\text{SO}_2$  experiment. Thus, experiments that observe quantum beats with modulation depths which are smaller than that calculated on the basis of a coherent excitation source are suggestive of a case (2) situation. Several such cases have been reported in the literature [8] and might benefit from being reanalyzed in terms of the partially coherent model which we have introduced.

In addition, we have emphasized that even the analyses of quantum beat data obtained with a transform limited excitation source should take proper account of the electric field contributions in order to properly extract the desired  $|D_{1z}/D_{2z}|$  mixing coefficients.

Finally we remark that although our application has been to two-state quantum beats the general formalism we have presented applies to the multistate case as well.

### Acknowledgement

We are grateful to Dr. D. Gruner, Dr. M. Ivanco and Processor S.C. Wallace, for helpful discussions. This work was supported by the US Office of Naval Research under contract number N00014-87-J-1204 and by the Ontario Laser and Lightwave Research Centre.

### References

- [1] S. Haroche, *Am. Phys.* 6 (1971) 189.
- [2] M.J. Rosker, F.W. Wise and C.L. Tang, *Phys. Rev. Letters* 57 (1986) 321;  
M. Mitsunaga and C.L. Tang, *Phys. Rev. A* 35 (1987) 1720;  
I.A. Walmsley and C.L. Tang, *J. Chem. Phys.* 92 (1990) 1568;  
Y.J. Yan and S. Mukamel, *Phys. Rev. A* 41 (1990) 6485.
- [3] W.R. Lambert, P.M. Felker and A.H. Zewail, *J. Chem. Phys.* 75 (1981) 5958;  
J. Chaiken, M. Gurnick and J.D. McDonald, *J. Chem. Phys.* 74 (1981) 106;  
P.M. Felker and A.H. Zewail, *Phys. Rev. Letters* 53 (1984) 501; *J. Chem. Phys.* 82 (1985) 2975, 2992.
- [4] M. Ivanco, J. Hager, W. Sharfin and S.C. Wallace, *J. Chem. Phys.* 78 (1983) 6531.
- [5] Y.X. Yan, L.T. Chent and K.A. Nelson, in: *Advances in nonlinear spectroscopy*, eds. R.J.H. Clark and R.E. Hester (Wiley, New York, 1988);  
K.A. Nelson and E.P. Ippen, *Advan. Chem. Phys.* 75 (1989) 1.
- [6] D. McMorrow, W.T. Lotshaw and G.A. Kenney-Wallace, *Chem. Phys. Letters* 145 (1988) 309;  
C. Kalpouzos, D. McMorrow, W.T. Lotshaw and G.A. Kenney-Wallace, *Chem. Phys. Letters* 155 (1989) 240.
- [7] V. Langer, H. Stolz and W. von der Osten, *Phys. Rev. Letters* 64 (1990) 854;  
E.O. Göbel, K. Leo, T.C. Damen, J. Shah, S. Schmitt-Rink, W. Schäfer, J.F. Müller and K. Köhler, *Phys. Rev. Letters* 64 (1990) 1801.
- [8] P.M. Felker and A.H. Zewail, *Advan. Chem. Phys.* 70 (1988) 265.
- [9] M.A. Dugan, J.S. Melinger and A.C. Albrecht, *Chem. Phys. Letters* 148 (1988) 411;  
Z.Q. Huang, Y.J. Xie, G.L. Huang and H.S. Kwok, *Opt. Letters* 15 (1990) 501;  
G. Vemuri, R. Roy and G.S. Agarwal, *Phys. Rev. A* 41 (1990) 2749;  
Th. Haslwanter, H. Ritsch, J. Cooper and P. Zoller, *Phys. Rev. A* 38 (1988) 5652;  
N. Morita and T. Yajima, *Phys. Rev. A* 30 (1984) 2525;  
Y. Nomura, M. Fujii, Y. Fujimura, M. Ito and A.C. Albrecht, *Multiphoton Processes Conference, Gordon Conference* (1990), preprint.
- [10] K.F. Freed and A. Nitz, *J. Chem. Phys.* 73 (1980) 4765;  
D. Gruner, Ph.D. Dissertation, University of Toronto Canada (1988).
- [11] R.D. Taylor and P. Brumer, *Discussions Faraday Soc.* 75 (1983) 117.
- [12] X-P. Jiang and P. Brumer, *J. Chem. Phys.*, in press.
- [13] C.A. Langhoff, *Chem. Phys.* 20 (1977) 357.

# Controlled photon induced symmetry breaking: Chiral molecular products from achiral precursors

Moshe Shapiro

Chemical Physics Department, Weizmann Institute of Science, Rehovot, Israel 76100

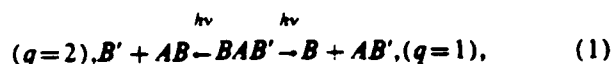
Paul Brumer

Chemical Physics Theory Group, Department of Chemistry, University of Toronto, Toronto M5S 1A1, Canada

(Received 15 August 1991; accepted 18 September 1991)

The existence and role of enantiomers, i.e., nonidentical pairs of chiral molecules related to one another through reflection, stands as one of the fundamental broken symmetries in nature.<sup>1</sup> It has motivated a longstanding interest in asymmetric synthesis, i.e., a process which preferentially produces a specific chiral species. It is a longstanding belief<sup>2</sup> that asymmetric synthesis must necessarily involve either chiral reactants, or chiral external system conditions such as chiral crystalline surfaces. In this paper we show that preferential production of a chiral photofragment can occur even though the parent molecule is not chiral. In particular two results are demonstrated: (1) photodissociation, using plane polarized light, of a prochiral molecule containing two enantiomers is shown to yield different cross sections for the production of right and left handed products, when the products are  $m_j$  selected; and (2) that this natural symmetry breaking may be enhanced and controlled using coherent lasers. Our treatment constitutes a major extension of the "coherent control" approach<sup>3</sup> to affecting molecular dynamics.<sup>4</sup>

Below we demonstrate the theory for the photodissociation of  $BAB'$  to two different arrangement channels,



where  $q$  defines the product arrangement channel and  $BAB'$  denotes a molecule, or a molecular fragment, which is symmetric with respect to reflection  $\sigma$  across the plane which interchanges the enantiomers  $B$  and  $B'$  (e.g., Ref. 5). The existence of this plane implies that the point group of the reactant is at least  $C_s$ . We sketch the theory, an extension of Ref. 3, for controlling the branching and, in doing so, expose the natural symmetry breaking associated with photodissociation to selected  $m_j$  states.

Consider a molecule  $BAB'$ , initially ( $t=0$ ) in eigenstate  $|E_g\rangle$  of Hamiltonian  $H_M$ , which is subjected to two sequential transform limited light pulses. The total Hamiltonian is of the form

$$H = H_M + V = H_M - \mu[\bar{\epsilon}(t) + \bar{\epsilon}^*(t)], \quad (2)$$

where  $\mu$  is the dipole operator along the electric field direction. The field  $\bar{\epsilon}(t)$  consists of two temporally separated pulses  $\bar{\epsilon}(t) = \bar{\epsilon}_x(t) + \bar{\epsilon}_d(t)$ , with the Fourier transform of  $\bar{\epsilon}_x(t)$  denoted  $\epsilon_x(\omega)$ , etc. For convenience these are chosen as Gaussian pulses peaking at  $t = t_x$  and  $t_d$ , respectively. The  $\bar{\epsilon}_x(t)$  pulse lifts the system to the excited electronic states with nuclear eigenfunctions  $|E_k\rangle$  and  $\bar{\epsilon}_d(t)$  induces a

transition back to the lower surface via stimulated emission. The fields are sufficiently weak for perturbation theory to be valid, and we assume no temporal overlap between the two pulses. The state prepared after the  $\bar{\epsilon}_x(t)$  pulse, whose width is chosen to excite only two levels  $|E_1\rangle$  and  $|E_2\rangle$ , is given in first order perturbation theory as

$$|\phi(t)\rangle = |E_g\rangle e^{-iE_g t/\hbar} + c_1 |E_1\rangle e^{-iE_1 t/\hbar} + c_2 |E_2\rangle e^{-iE_2 t/\hbar},$$

$$c_k = (\sqrt{2\pi/\hbar}) \langle E_k | \mu | E_g \rangle \epsilon_x(\omega_{kg}), \quad (3)$$

with  $\omega_{kg} = (E_k - E_g)/\hbar$ . Subsequently, the system is subjected to a  $\bar{\epsilon}_d(t)$  and its wave function, expanded in a complete set of continuum eigenstates  $|E, n, q\rangle$  labeled by energy  $E$ , arrangement channel label  $q$  and remaining labels  $n$  is then

$$|\psi(t)\rangle = |\phi(t)\rangle + \sum_{n,q} \int dE B(E, n, q | t) |E, n, q\rangle e^{-iEt/\hbar}. \quad (4)$$

We require below the probability  $P(E, m, q)$  of forming product in arrangement channel  $q$  at energy  $E$  with total fragment angular momentum projection  $m$ , along a space fixed axis. Using first order perturbation theory and the rotating wave approximation in conjunction with Eq. (4), gives

$$P(E, m, q) = \sum_n' |B(E, n, q | t = \infty)|^2$$

$$= (2\pi/\hbar^2) \sum_n' \left| \sum_{k=1,2} c_k \langle E, n, q^- | \mu | E_k \rangle \times \epsilon_d(\omega_{EE_k}) \right|^2, \quad (5)$$

where  $\omega_{EE_k} = (E - E_k)/\hbar$ ,  $c_k$  is given by Eq. (3) and where the prime denotes summation over all quantum numbers  $n$  (including scattering angles) other than  $m_j$ .

Expanding the square and using the Gaussian pulse shape gives

$$P(E, m, q) = (2\pi/\hbar^2) \{ |c_1|^2 \mu_{1,1}^{(q)\dagger} \epsilon_1^2 + |c_2|^2 \mu_{2,2}^{(q)\dagger} \epsilon_2^2$$

$$+ 2 |c_1 c_2|^2 \epsilon_1 \epsilon_2 \mu_{1,2}^{(q)\dagger} \cos(\omega_{2,1}(t_d - t_x))$$

$$+ \alpha_{1,2}^{(q)}(E) + \phi \}, \quad (6)$$

where  $\epsilon_i = |\epsilon_d(\omega_{EE})|$ ,  $\omega_{2,1} = (E_2 - E_1)/\hbar$  and the phases  $\phi$ ,  $\alpha_{1,2}^{(q)}(E)$  are defined by

$$\begin{aligned} \langle E_1 | \mu | E_g \rangle \langle E_r | \mu | E_2 \rangle &\equiv |\langle E_1 | \mu | E_g \rangle \langle E_r | \mu | E_2 \rangle| e^{i\phi}, \\ \mu_{i,k}^{(q)}(E) &\equiv |\mu_{i,k}^{(q)}(E)| e^{i\alpha_{i,k}^{(q)}(E)} \\ &= \sum_n \langle E,n,q^- | \mu | E_i \rangle \langle E_k | \mu | E,n,q^- \rangle. \quad (7) \end{aligned}$$

Integrating over  $E$  to encompass the width of the second pulse, assumed sufficiently small so that  $\mu_{i,k}^{(q)}(E)$  can be assumed constant, and forming the ratio

$$Y = P(q=1, m_j) / [P(q=1, m_j) + P(q=2, m_j)],$$

gives the quantity shown controllable below.

In general control arises from the possibility of manipulating, in the laboratory, the quantum interference term in Eq. (6). Specifically,<sup>3</sup> the product ratio  $Y$  can be varied by changing the delay time  $\tau = (t_d - t_x)$  or ratio  $x = |c_1/c_2|$ , the latter by detuning the initial excitation pulse. Active control over the products  $B + AB'$  vs  $B' + AB$ , and hence control over left vs right handed products, will result as long as  $P(q=1, m_j)$  and  $P(q=2, m_j)$  have different functional dependences on  $x$  and  $\tau$ .

We now show that  $P(q=1, m_j)$  is indeed different from  $P(q=2, m_j)$  for the  $B'AB$  case. We do this by examining the behavior of  $c_k$  and  $\mu_{i,k}^{(q)}$  for  $|E_1\rangle$  and  $|E_2\rangle$  of different symmetry with respect to the reflection  $\sigma$ . For simplicity we restrict attention to  $BAB'$  belonging to point group  $C_n$ , the smallest group possessing the required symmetry plane. We rely primarily upon symmetry arguments but resort to detailed manipulations on a model three body problems when necessary to gain insight. Such a model has two identical terminal atoms which are nevertheless labeled differently in the computation. Further, we focus upon transitions between electronic potential energy surfaces of similar species, e.g.,  $A'$  to  $A'$  or  $A''$  to  $A''$  and assume the ground vibronic state to be of species  $A'$ . Similar arguments apply for larger groups containing  $\sigma$ , to ground vibronic states of odd parity, and to transition between electronic states of different species.

**Excitation coefficients  $c_k$ :** Components of  $\mu$  lying in the symmetry plane, denoted  $\mu_\sigma$ , transform as  $A'$  and are symmetric with respect to reflection whereas the component perpendicular to the symmetry plane, denoted  $\mu_\sigma$ , is antisymmetric ( $A''$ ). Hence  $\langle E_k | \mu | E_g \rangle = \langle E_k | \mu_\sigma + \mu_\pi | E_g \rangle$ , and hence  $c_k$  is nonzero for transitions between vibronic states of the same symmetry due to the  $\mu_\pi$  component, and nonzero for transitions between vibronic states of different symmetry due to the  $\mu_\sigma$  component. The latter is common in IR spectroscopy. In electronic spectroscopy such transitions result from the non Franck-Condon Herzberg-Teller intensity borrowing<sup>6</sup> mechanism. Thus, the excitation pulse can create an  $|E_1\rangle$ ,  $|E_2\rangle$  superposition consisting of two states of different reflection symmetry and hence a state which no longer displays the reflection symmetry of the Hamiltonian.

**Cumulative matrix elements  $\mu_{i,k}^{(q)}$ :** In contrast to the bound states, the continuum states of interest  $|E,n,q^- \rangle$

are neither symmetric nor antisymmetric. Rather,  $\sigma |E,n,q=1^- \rangle = |E,n,q=2^- \rangle$  and vice versa. Such a choice is possible because of the exact degeneracies which exist in the continuum. To examine  $\mu_{i,k}^{(q)}$  we introduce symmetric and antisymmetric continuum eigenfunctions of  $\sigma$ ,  $|\psi^s \rangle = (|E,n,q=1^- \rangle + |E,n,q=2^- \rangle)/2$  and  $|\psi^a \rangle = (|E,n,q=1^- \rangle - |E,n,q=2^- \rangle)/2$ . Assuming  $|E_1\rangle$  is symmetric and  $|E_2\rangle$  antisymmetric, rewriting  $|E,n,q^- \rangle$  as a linear combination of  $|\psi^s \rangle$  and  $|\psi^a \rangle$ , and adopting the notation  $A_{i2} = \langle \psi^s | \mu_\sigma | E_2 \rangle$ ,  $S_{o1} = \langle \psi^a | \mu_\pi | E_1 \rangle$ , etc., we have, after elimination of null matrix elements,

$$\begin{aligned} \mu_{11}^{(q)} &= \sum' [ |S_{11}|^2 + |A_{o1}|^2 \pm A_{o1} S_{11}^* \pm A_{o1}^* S_{11} ], \\ \mu_{22}^{(q)} &= \sum' [ |A_{22}|^2 + |S_{22}|^2 \pm A_{22} S_{22}^* \pm A_{22}^* S_{22} ], \quad (8) \\ \mu_{12}^{(q)} &= \sum' [ S_{11} A_{22}^* + A_{o1} S_{22}^* \pm S_{11} S_{22}^* \pm A_{o1} A_{22}^* ], \end{aligned}$$

where the plus sign applies for  $q=1$  and the minus sign for  $q=2$ . Equation (8) displays two noteworthy features:

(1)  $\mu_{kk}^{(1)} \neq \mu_{kk}^{(2)}$ . That is, the system displays *natural symmetry breaking* in photodissociation from state  $|E_k\rangle$ , with right- and left-handed product probabilities differing by  $2\Sigma \text{Re}(S_{11}^* A_{o1})$  for excitation from  $|E_1\rangle$  and  $2\Sigma \text{Re}(A_{22} S_{22}^*)$  for excitation from  $|E_2\rangle$ . Note that these symmetry breaking terms may be relatively small since they rely upon non Franck-Condon contributions. However,

(2)  $\mu_{12}^{(1)} \neq \mu_{12}^{(2)}$ . Thus laser controlled symmetry breaking, which depends upon  $\mu_{12}^{(q)}$  in accordance with Eq. (6), is therefore possible, allowing enhancement of the enantiomer ratio for the  $m_j$  polarized product.

To demonstrate the extent of expected control, as well as the effect of  $m_j$  summation, we considered a model of the enantiomer selectively, i.e., HOH photodissociation<sup>7</sup> in three dimensions, where the two hydrogens are assumed distinguishable. The computation is in accord with state-of-the-art formalism and computational machinery.<sup>7,8</sup> Consider the generic matrix element between  $|E,n,q^- \rangle = |\psi^-(q, E, \hat{k}, v, j, m_j)\rangle$  and the bound state  $|E\rangle = |\Phi(E, \mathcal{M}, J, \rho, p_i)\rangle$ , where the scattering direction  $\hat{k}$ , vibrational and rotational product quantum numbers  $v, j$  and projection  $m_j$  are explicitly indicated, as are the initial bound state angular momentum  $J$ , space fixed  $z$  projection  $\mathcal{M}$ , and parity  $p_i$ . We have

$$\begin{aligned} &\langle \psi^-(q, E, \hat{k}, v, j, m_j) | \mu | \Phi(E, \mathcal{M}, J, \rho, p_i) \rangle \\ &= \left( \frac{\rho k_{vj}}{2\pi^2 \hbar^2} \right)^{1/2} \sum_{\lambda} (2J+1)^{1/2} (-1)^{M_i - j - m_j} \\ &\quad \times D_{\lambda, M_i}^J(\phi_k, \theta_k, 0) D_{-j - m_j, -m_j}^J(\phi_k, \theta_k, 0) \\ &\quad \times t^{(q)}(E, J, v, j, \lambda | E, J, \rho, p_i), \quad (9) \end{aligned}$$

where  $D$  are the rotation matrices,  $\rho$  is the reduced mass,  $k_{vj}$  the momentum of the products and  $t^{(q)}(E, J, v, j, \lambda | E, J, \rho, p_i)$  is proportional to the partial wave matrix element<sup>8</sup>  $\langle \psi^-(q, E, J, \mathcal{M}, \rho, v, j, \lambda) | \mu | \Phi(E, \mathcal{M}, J, \rho, p_i) \rangle$

Here  $\lambda$  is the helicity associated with total  $J$  along the body fixed axis of product separation.

Equation (9) allows the construction of product ma-

trix elements which comprise the  $\mu_{ik}^{(q)}$ . The generic matrix element product, integrated over scattering angles and averaged over initial<sup>9(a)</sup>  $M_k = M_p$  is<sup>9(b)</sup>

$$(2J_i + 1)^{-1} \sum_{M_i} \int d\hat{k} \langle \Phi(E_k, M_p, J_k, p_k) | \mu | \psi^-(q', E, \hat{k}, v, j, m_j) \rangle \langle \psi^-(q, E, \hat{k}, v, j, m_j) | \mu | \Phi(E_p, M_p, J_p, p_p) \rangle$$

$$= (-1)^{m_j} \frac{16\pi^2 v p}{k^2 (2J_i + 1)} \sum_{v_j} k_{v_j} \sum_{\lambda, \lambda'} [(2J + 1)(2J' + 1)]^{1/2} \sum_{\mu=0,2} (-1)^{(\lambda - \lambda' + J + J' + J)} (2\mu + 1) \begin{pmatrix} J & J' & \mu \\ \lambda & -\lambda' & \lambda' - \lambda \end{pmatrix}$$

$$\times \begin{pmatrix} j & j & \mu \\ -\lambda & \lambda' & \lambda - \lambda' \end{pmatrix} \begin{pmatrix} j & j & \mu \\ -m_j & m_j & 0 \end{pmatrix} \begin{pmatrix} 1 & 1 & \mu \\ 0 & 0 & 0 \end{pmatrix} \begin{pmatrix} 1 & 1 & \mu \\ J & J' & J_i \end{pmatrix} t^{(q)}(E, J, v, j, \lambda, p | E, J, p_i) t^{(q')*}(E, J', v, j, \lambda', p | E, J', p_k). \quad (10)$$

Here  $J_i = J_k$  has been assumed for simplicity. These equations, in conjunction with the artificial channel method<sup>8</sup> for computing the  $t$  matrix elements, were used to compute the ratio  $Y$  of the HO + H (as distinct from the H + OH) product in a fixed  $m_j$  state. Specifically, Fig. 1 shows the result of first exciting the superposition of symmetric plus asymmetric vibrational modes [(1,0,0) + (0,0,1)] with  $J_i = J_j = 0$  in the ground electronic state, followed by dissociation at 70 700  $\text{cm}^{-1}$  to the  $B$  state using a pulse width of 200  $\text{cm}^{-1}$ . Results show that varying the time delay between pulses allows for controlled variation of  $Y$  from 61% to 39%!

Finally we sketch the effect of a summation over product  $m_j$  states on symmetry breaking and chirality control. In this regard the three body model is particularly informative. Specifically, note that Eq. (8) provides  $\mu_{ik}^{(q)}$  in terms of products of matrix elements involving  $|\psi^a\rangle$  and  $|\psi^b\rangle$ . Focus attention on those products which involve both wave functions, e.g.,  $A_{a1}S_{j1}^*$ . These matrix element products can be written in the form of Eq. (10) where  $q$  and  $q'$  now refer to the antisymmetric or symmetric continuum states, rather than channels 1 and 2. Thus, for example,  $A_{a1}S_{j1}^*$  results from using  $|\psi^a\rangle$  in Eq. (9) to form

$A_{a1}$  and  $|\psi^a\rangle$  to form  $S_{j1}^*$ . The resultant  $A_{a1}S_{j1}^*$  has the form of Eq. (10) with  $t^{(q)}$  and  $t^{(q')}$  associated with the symmetric and antisymmetric continuum wave functions, respectively. Consider now the effect of summing over  $m_j$ . Standard formulae<sup>7,8</sup> imply that this summation introduces a  $\delta_{\mu,0}$  which, in turn forces  $\lambda = \lambda'$  via the first and second  $3j$  symbol in Eq. (10). However, a rather involved argument<sup>10</sup> shows that  $t$  matrix elements associated with symmetric continuum eigenfunctions and those associated with antisymmetric continuum eigenfunctions must have  $\lambda$  of different parities. Hence, summing over  $m_j$  eliminates all contributions to Eq. (8) which involve both  $\psi^a$  and  $\psi^b$ . Specifically, we find<sup>10</sup> after  $m_j$  summation,

$$\mu_{ii}^{(1)} = \mu_{ii}^{(2)} = \sum [ |S_{ii}|^2 + |A_{ii}|^2 ], \quad (11a)$$

$$\mu_{12}^{(1)} = \mu_{12}^{(2)} = \sum [ S_{i1}A_{j1}^* + A_{i1}S_{j1}^* ]. \quad (11b)$$

That is, natural symmetry breaking is lost [Eq. (11a)] upon  $m_j$  summation, both channels  $q = 1$  and  $q = 2$  having equal photodissociation probabilities, and control over the enantiomer ratio is lost since the interference terms [Eq. (11b)] no longer distinguish the  $q = 1$  and  $q = 2$  channels.<sup>11</sup>

Having thus demonstrated the principle of  $m_j$  selected enantiomer control it remains to determine the extent to which realistic systems can be controlled. Further computations are therefore planned.

We gratefully acknowledge support from the U. S. Office of Naval Research, under Contract No. N00014-90-J-1014.

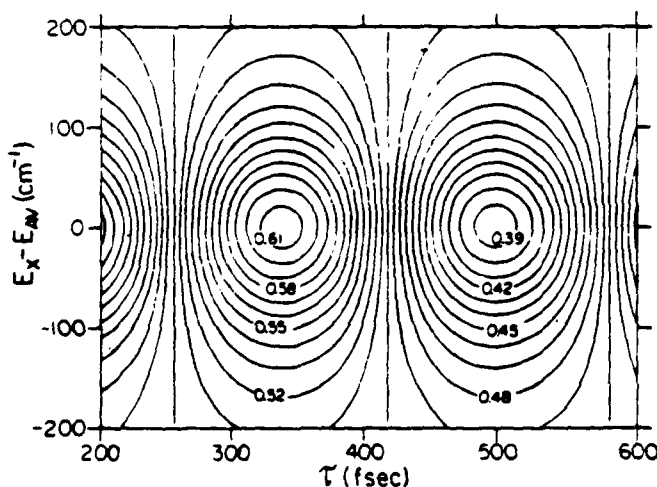


FIG. 1. Contour plot of percent HO + H (as distinct from H + OH) in HOH photodissociation. Ordinate is the detuning from  $E_{th} = (E_2 - E_1)/2$ , abscissa is time between pulses.

<sup>1</sup> L. D. Barron, *Molecular Light Scattering and Optical Activity* (Cambridge University, Cambridge, MA, 1982); R. G. Woolley, *Adv. Phys.* **25**, 27 (1975); *Origins of Optical Activity in Nature*, edited by D. C. Walker (Elsevier, Amsterdam, 1979).

<sup>2</sup> For a discussion see L. D. Barron, *Chem. Soc. Rev.* **15**, 189 (1986). For historical examples see J. A. Bel, *Bull. Soc. Chim. Fr.* **22**, 337 (1874); J. H. Van't Hoff, *Die Lagerung der Atome und Raume*, 2nd ed. (1894), p. 30.

<sup>3</sup> (a) For an introduction to coherent control see P. Brumer and M. Shapiro, *Acc. Chem. Res.* **22**, 407 (1989); (b) T. Seideman, M. Shapiro, and P. Brumer, *J. Chem. Phys.* **90**, 7132 (1989); (c) C. K. Chan,

P. Brumer, and M. Shapiro, *ibid.* **94**, 2688 (1991), and references therein.

<sup>4</sup>The reliance of coherent control on a small number of participating bound states of specific symmetries is central to the application described herein. As such it is distinct, for example, from the alternative control method of D. Tannor and S. A. Rice [*J. Chem. Phys.* **85**, 5805 (1986)] which utilizes localized wave packets involving large numbers of excited bound states.

<sup>5</sup>An example, although requiring a slight extension of the *BAB* notation, is the Norrish type II reaction:  $D(\text{CH}_2)_2\text{CO}(\text{CH}_2)_2D'$  dissociating to  $D\text{CHCH}_2 + D'(\text{CH}_2)_2\text{COCH}_3$  and  $D'\text{CHCH}_2 + D(\text{CH}_2)_2\text{COCH}_3$ , where *D* and *D'* are enantiomers.

<sup>6</sup>J. M. Hollas, *High Resolution Spectroscopy* (Butterworths, London, 1982).

<sup>7</sup>E. Segev and M. Shapiro, *J. Chem. Phys.* **77**, 5604 (1982)

<sup>8</sup>G. G. Balint-Kurti and M. Shapiro, *Chem. Phys.* **61**, 137 (1981)

<sup>9</sup>(a)  $M = V_k$  since both  $|E_1\rangle$  and  $|E_2\rangle$  arise by excitation, with linearly polarized light, from a common eigenstate. (b) Equation (10) is a generalized version of Eq. (48), Ref. 8.

<sup>10</sup>M. Shapiro and P. Brumer (unpublished).

<sup>11</sup>As an aside we note that control is not possible in collinear models since, in that case,  $\mu_x$  and  $\mu_z$  cannot both couple to the same electronically excited state.

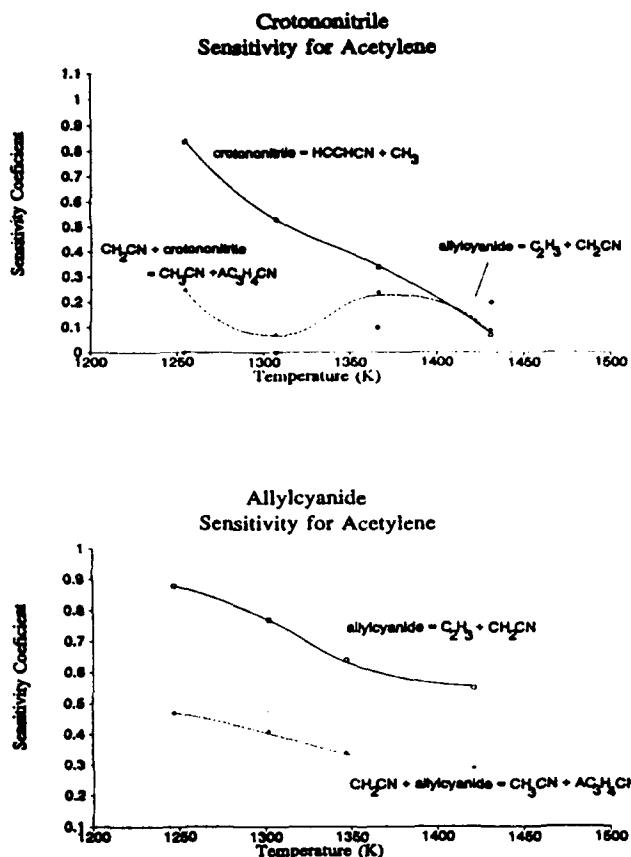


Figure 14. Variation with temperature of sensitivity coefficients for the designated species. Only the most sensitive reactions are shown.

abstraction reaction of cyanomethyl radicals with crotononitrile, reaction 27.

From Figure 13 it may be seen that two reactions have high sensitivities for HCN production. These are the unimolecular fission of allyl cyanide into cyanomethyl and vinyl radicals (reaction -13) and reaction 50, the addition of H atoms to the nitrile

group of allyl cyanide. Rate of production analysis indicates that a significant reaction flux to HCN flows through reaction 77, the disproportionation reaction of two cyanomethyl radicals to form HCN and acrylonitrile.

From Figure 11 it may be seen that the sensitivity of acrylonitrile toward the rate of the allyl cyanide initiation reaction



exceeds unity. This implies that the reaction is slightly branching in nature. This can arise if the vinyl radical initially produced in (-13) decomposes sufficiently rapidly to  $\text{C}_2\text{H}_2 + \text{H}$ .

### Conclusions

The butenenitriles undergo thermal decomposition between 1200 and 1500 K at about 20 atm pressure and at residence times from 650 to 750  $\mu\text{s}$ . Isomerization precedes thermal decomposition. The decomposition is free radical in nature, with a major chain mechanism involving the cyanomethyl radical, leading to the production of acetonitrile and acetylene. Other reaction pathways have been identified involving H-atom additions to the reactant isomers. Several nitrogen-containing radicals including cyanomethyl, cyanovinyl, and cyanoallyl, together with their hydrocarbon counterparts, methyl, vinyl, and allyl, play important roles in the pyrolysis mechanism.

Pyrolysis of the butenenitriles can be satisfactorily modeled by a detailed kinetic mechanism involving the aforementioned radicals and hydrogen atoms. Yields of most major and minor decomposition products exhibit kinetics of formation approximately first order in the initial concentration of the starting butenenitrile isomer. The outstanding exception is acetonitrile, whose kinetics are largely influenced by cyanomethyl radical abstraction. Arrhenius parameters for initiation reactions of the butenenitriles can be obtained from experiment and kinetic modeling.

**Acknowledgment.** We thank Drs Robin Walsh and Peter Nelson for helpful discussions. Dr. Nelson also assisted with GCMS analyses. Mr. M. Esler is thanked for research assistance. Financial support of the ARC and CSIRO/University of Sydney Collaborative Funds are gratefully acknowledged.

**Registry No.** (Z)- $\text{H}_3\text{CCH}=\text{CHCN}$ , 1190-76-7; (E)- $\text{H}_3\text{CCH}=\text{CHCN}$ , 627-26-9;  $\text{H}_2\text{C}=\text{CHCH}_2\text{CN}$ , 109-75-1;  $\text{NCCH}_2$ , 2932-82-3; H, 12385-13-6.

## Laser-Induced Unimolecular Isomerization: Theory and Model Applications

Daniel Gruner,\* Paul Brumer,

Chemical Physics Theory Group, Department of Chemistry, University of Toronto, Toronto, M5S 1A1 Canada

and Moshe Shapiro

Department of Chemical Physics, Weizmann Institute of Science, Rehovot, Israel (Received: July 1, 1991)

We show that stimulated emission pumping provides a means of inducing cis-trans isomerization in isolated molecules. The method relies solely upon the characteristics of stationary molecular eigenstates and utilizes pulses in the nanosecond regime. The theory is supported with computations on the vibrational manifold of a model polyatomic.

### 1. Introduction

Until recently, there has been little progress in resolving the problem of controlling unimolecular reactions with lasers. Recently, however, there have been a number of promising proposals for controlling chemical reactions.<sup>1,2</sup> In this paper we propose

a laser-based approach to inducing isomerization in polyatomic molecules. However, unlike our previous work,<sup>1</sup> the method described here relies entirely upon simple properties of stationary states and not upon the coherence properties of the molecules and of the radiation field. Specifically, our technique consists of the preparation of the molecule in a stationary (except for spontaneous emission) excited state, followed by selective stimulated emission

(1) Brumer, P.; Shapiro, M. *Chem. Phys. Lett.* 1986, 126, 541. Brumer, P.; Shapiro, M. *Faraday Discuss. Chem. Soc.* 1986, 82, 177. Shapiro, M.; Brumer, P. *J. Chem. Phys.* 1986, 84, 4103. Asaro, C.; Brumer, P.; Shapiro, M. *Phys. Rev. Lett.* 1988, 60, 1634. Shapiro, M.; Hepburn, J.; Brumer, P. *Chem. Phys. Lett.* 1988, 149, 451. Shapiro, M.; Brumer, P., to be published.

(2) Tannor, D. J.; Rice, S. A. *J. Chem. Phys.* 1985, 83, 5013. Lami, A.; Villani, G. *J. Phys. Chem.* 1988, 92, 4348.

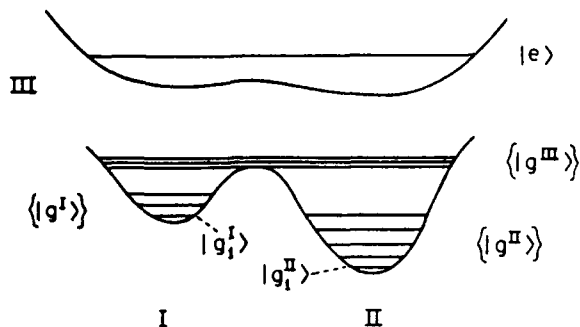


Figure 1. Schematic potential energy diagram representing the molecular isomerization coordinate as a cut through the electronic potential surfaces. Regions I and II denote the different isomers, while region III represents molecular energy levels above the isomerization barrier where conformational identity is lost. Ground vibronic levels are denoted by  $|g\rangle$ , and  $|e\rangle$  represents excited vibronic levels.

pumping to the desired final state. What is particularly significant is our preparation of stationary states instead of time-dependent initial zeroth-order states. Such an approach automatically bypasses any difficulties associated with intramolecular vibrational dynamics and fast time scales. In essence, isomer selectivity lies in frequency control and in properties of exact molecular eigenstates.

The basic technique for control is outlined in section 2, followed, in section 3, by calculations on a simplified three-level two-laser model which allows us to gain insight into the problem of controlled photoisomerization. Section 4 contains the description, and results, of calculations performed on a model polyatomic system, illustrating the possibilities afforded by this method. The model is based upon, but far simpler than, the stilbene molecule for which there is a vast array of data available and for which stimulated emission pumping has already been experimentally demonstrated.<sup>3</sup>

## 2. Branching in Unimolecular Isomerization

In this section we describe the nature of isomerization in an isolated molecule using a simple one-dimensional model; the ideas are, however, completely general.

Consider a system, in the Born–Oppenheimer approximation, which has two electronic states and for which there is a significant barrier to isomerization in the ground electronic state. Figure 1 depicts the reaction coordinate for such a simple system; there may or may not be a barrier to isomerization in the excited state. We assume that the probability of tunneling through the ground-state barrier at room temperature is negligible so that two thermally stable isomers exist. The two wells are therefore effectively uncoupled at low energies, and the low-lying exact eigenstates of the molecular Hamiltonian are localized in either of the two wells (regions I and II in Figure 1). This description is, however, inappropriate for the eigenstates that are close to the top of the barrier and above it. In these cases (region III in Figure 1) the probability density is distributed over the full conformational space of the molecule, and one can no longer distinguish stable isomers. Similarly, if the excited electronic state has a barrier, the same description applies, with the system losing its conformational identity when excited above the barrier to isomerization.

Isomerization can then take place by several different routes, e.g., (1) excitation to a high-lying vibronic state of the ground electronic surface which lies above the barrier, followed by collisional quenching; (2) tunneling through the ground-state barrier (highly unlikely unless the energy of the system is close to the top of the barrier); or (3) by electronic excitation to a vibronic state above the isomerization barrier in the excited potential surface, followed by fluorescence or collisional deexcitation. Each of these different routes will result in different cis/trans products ratios, and traditional methods for controlling this ratio are limited to varying gross properties such as excitation energy, temperature, or pressure. For example, in electronic excitation (route 3 above)

in the absence of collisions, as discussed in detail in section 2.1, the product yield is completely determined by the nature of the excited state and by the radiative transition matrix elements between this state and the ground states. Hence we have virtually no control over cis/trans product ratios in this case. Prior to discussing control of the cis/trans ratio we first describe this situation, where emission from the excited state is spontaneous and hence uncontrolled.

**2.1. Uncontrolled Isomerization.** To understand the physics we first consider an uncontrolled experiment corresponding to excitation from a ground-state  $|g\rangle$  to a single vibronic level of an excited electronic state  $|e\rangle$ , followed by spontaneous emission. Specifically, a molecule is prepared at  $t = t_0$  in a single excited energy eigenstate by a device such as a sharp laser; when the laser is turned off, the molecule is left in a quasistationary state that can only decay by spontaneous emission. We emphasize that the molecule system is dynamics-free (barring emission) after excitation, since it is a single exact energy eigenstate of the molecular Hamiltonian. Subsequent to excitation the state vector can then be written as ( $t \geq t_0$ )

$$|\Psi(t)\rangle = a(t)|e\rangle + \sum_i b_i^I(t)|g_i^I\rangle + \sum_j b_j^{II}(t)|g_j^{II}\rangle + \sum_k b_k^{III}(t)|g_k^{III}\rangle \quad (1)$$

with the initial condition, immediately after preparation, of

$$|\Psi(t=t_0)\rangle = a(t_0)|e\rangle = |e\rangle \quad (2)$$

Here the superscript in  $|g_f^I\rangle$  denotes one of the three regions I, II, or III of the ground state. The fluorescence rate  $S_f^I$  into state  $i$  of the ground vibronic states  $f$  ( $f = I, II, III$ ) is given by the rate of change of the population of these states, brought about by the spontaneous fluorescent decay of the excited vibronic state:

$$S_f^I(t \geq t_0) = |a(t_0)|^2 \gamma_f^I e^{-\Gamma(t-t_0)} \quad f = I, II, III \quad (3)$$

Here  $\Gamma = \sum_i \gamma_i^I + \sum_j \gamma_j^{II} + \sum_k \gamma_k^{III}$  is the total decay constant for the excited state  $|e\rangle$ , whose coefficient  $a(t)$  evolves as

$$a(t \geq t_0) = a(t_0) e^{-(\Gamma/2 + i\omega_e)(t-t_0)} \quad (4)$$

and

$$\gamma_f^I = \frac{e^2}{3\epsilon_0\pi\hbar c^3} (\omega_e - \omega_i)^3 | \langle g_f^I | D | e \rangle |^2 \quad (5)$$

with  $\omega_e = E_e/\hbar$  and  $\omega_i = E_i/\hbar$  and  $D$  is the dipole moment operator. The total probability  $R^I(\tau)$  that after a certain time  $\tau$  the system will have decayed by spontaneous emission to stable conformations I is then

$$R^I(\tau) = \sum_i R_i^I(\tau) = \sum_i \int_{t_0}^{t_0+\tau} S_i^I(t) dt = a(t_0) \frac{1 - e^{-\Gamma\tau}}{\Gamma} \sum_i \gamma_i^I \quad (6)$$

and similarly for conformer II:

$$R^{II}(\tau) = a(t_0) \frac{1 - e^{-\Gamma\tau}}{\Gamma} \sum_j \gamma_j^{II} \quad (7)$$

Clearly, it is only the relative fluorescence rates into the different states that determine the product ratios in this simple uncontrolled photoinduced process.

Generalizing this result to arbitrary excited states (e.g., superposition states, coherent or otherwise) produced by different excitation processes is straightforward. For example, if the excited state is a mixed state comprised of  $|e_n\rangle$ , the discussion above carries forward essentially unchanged, with the inclusion of an extra sum over the different excited states  $|e_n\rangle$

$$R^f(\tau) = \sum_n \sum_i R_{n,i}^f(\tau) = \sum_n a_n(t_0) \frac{1 - e^{-\Gamma_n\tau}}{\Gamma_n} \sum_i \gamma_{n,i}^f, \quad f = I, II \quad (8)$$

where  $\gamma_{n,i}^f$  is given by eq 5 with  $|e\rangle$  replaced by  $|e_n\rangle$  and  $\omega_e$  by  $E_{e_n}/\hbar$ . If, however, the initial state is a coherent superposition  $|\Psi(t_0)\rangle = \sum_n a_n(t_0)|e_n\rangle$ , the time evolution of the prepared state is more complicated, with the probabilities now given by

$$R^f(\tau) = \sum_i \left[ \sum_n R_{n,i}^f(\tau) + \sum_{n \neq m} R_{nm,i}^f(\tau) \right] \quad (9)$$

(3) Suzuki, T.; Mikami, N.; Ito, M. *Chem. Phys. Lett.* 1985, 120, 333.

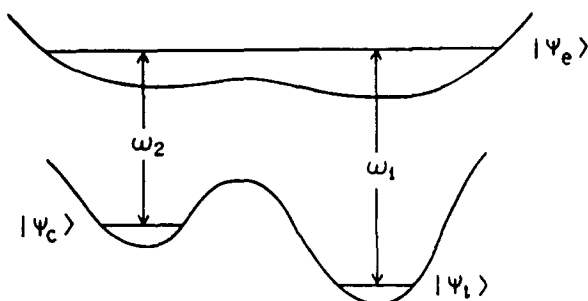


**Figure 2.** Simplified potential energy diagram for a model three-level, two-laser system. Computations are for parameters of case 2, section 4. That is, the system transition frequencies are  $\omega_1 = 33\,128.46\text{ cm}^{-1}$ ,  $\omega_2 = 33\,001.90\text{ cm}^{-1}$ . Oscillator strengths for the electronic transitions: 0.825 727 for cis vs. 1.364 626 for trans. Overlap integrals:  $|\langle\psi_i|\psi_c\rangle| = 2.417 \times 10^{-2}$ ,  $|\langle\psi_c|\psi_e\rangle| = 6.546 \times 10^{-3}$ .

where the first term is the same as eq 8, and the summand in the second (interference) term is<sup>4</sup>

$$R_{nm}^f(\tau) = \text{Re} \frac{ie^2}{3\pi\epsilon_0\hbar c^3} a_n^*(t_0) a_m(t_0) \langle e_n | D | g_i \rangle \langle g_i | D | e_m \rangle \times \\ \left[ \frac{1 - e^{-(\Gamma_n + \Gamma_m)\tau/2} e^{i\omega_{nm}\tau}}{\omega_{nm} + \frac{i}{2}(\Gamma_n + \Gamma_m)} \right] \quad (10)$$

with  $\omega_{nm} = \omega_{e_n} - \omega_{e_m}$ . Here  $a_n(t_0)$  is the coefficient of  $|e_n\rangle$  at time zero and  $\Gamma_n$  is the decay rate from this level.

It is clear from this discussion that once the excited state is defined the product ratios are determined. Thus, the extent of our control over these ratios in this standard approach is limited to our ability to produce and choose the well-defined excited states. For example, suppose  $R^{II} \ll R^I$  (i.e., the transition matrix elements between the excited state and states of type  $|g^{II}\rangle$  are much smaller than those with states  $|g^I\rangle$ ) for most of the  $|e\rangle$  states accessible from the initial configuration I. Under these circumstances it is difficult to use this route to produce excess conformation II. Below, we demonstrate how this situation may be altered.

**2.2. Controlled Isomerization.** Our proposal is to use stimulated-emission-pumping to induce the system into the desired particular conformation, from the prepared state  $|e\rangle$  as follows.

The molecule is first prepared in an excited stationary state  $|e\rangle$  using a narrow band laser. Then, a laser pulse is tuned to a well defined emission line (e.g.,  $|g^I\rangle \leftarrow |e\rangle$  or  $|g^{II}\rangle \leftarrow |e\rangle$  in Figure 1), stimulating the downward transition to the chosen ground vibronic state at a rate competitive to, or faster than, that for spontaneous emission. This route allows for production of the desired conformation but it is qualitatively clear that a number of conditions must be met. We list them below and investigate them quantitatively in sections 3 and 4:

1. The stimulated transition rate to the desired state must be comparable to, or faster than, the spontaneous emission rate.

2. The duration of the down-pumping pulse must be short compared to the natural lifetime of the excited state  $|e\rangle$ .

3. The emission line of interest must be isolated, that is, must not have lines belonging to the "other" conformation closer to it than the width of the pulse. Indeed, it is this feature, i.e., that conformations may have sufficiently different emission frequencies, that is the essence of this entire control scheme.

Conditions 2 and 3 are not necessarily independent since the pulse frequency width is inversely proportional to the pulse duration, or wider, depending on the laser operation conditions. In order to satisfy condition 1, while keeping the pulse short, one need only have a laser with a photon number density  $\gg 1$  in the mode of interest, as the stimulated transition rate is proportional to the photon number (intensity). However, if the laser intensity is too high, oscillations in the state populations can arise (Rabi

oscillations), making the controlled production of a particular state more cumbersome and possibly inefficient. Thus, numerical studies are required and carried out below. These calculations are of two types. The first is an analytic solution in the dressed states approximation for the simplest possible system, i.e., three levels. The second are computations on a model polyatomic system.

The numerical calculations are based upon the Schrödinger equations of motion for the coefficients of the state vector  $|\Psi(t)\rangle$ , eqs 11–12, in the presence of a coherent transform-limited pulse, in the Weisskopf–Wigner approximation. That is,

$$i\hbar \frac{d}{dt} \beta_f^i(t) = 2e \sum_n e^{-i\omega_n t} \{ \langle g_i | D | e_n \rangle \cdot \text{Re } \mathcal{E}_p(t) \} \alpha_n(t), \\ f = \text{I, II, III} \quad (11)$$

$$i\hbar \frac{d}{dt} \alpha_n(t) = \\ 2e \sum_f \sum_i e^{i\omega_n t} \{ \langle e_n | D | g_i \rangle \cdot \text{Re } \mathcal{E}_p(t) \} \beta_f^i(t) - \frac{1}{2} \hbar \Gamma_n \alpha_n(t) \quad (12)$$

Here  $\omega_{ni} = (E_{e_n} - E_{g_i})/\hbar$  and

$$\alpha_n(t) = a_n(t) e^{i\omega_n t}$$

$$\beta_f^i(t) = b_f^i(t) e^{i\omega_n t}, \quad f = \text{I, II, III}$$

and  $\mathcal{E}_p(t)$  is the time-varying amplitude of that part of the electric field corresponding to the laser pulse. The notation  $f = \text{I, II, III}$  identifies the three regions depicted in Figure 1. These equations can be solved numerically, or approximately (if the laser intensity is not too high) using perturbation theory. An application of the technique to a polyatomic model is given in section 4. First, however, we focus on insight afforded by a simple three-level system.

### 3. Three-Level Two-Laser Dressed Model

The case of a three-level system subjected to two laser frequencies has been the subject of extensive, often highly detailed, studies.<sup>5</sup> Radmore and Knight<sup>6</sup> have studied the population dynamics of a three-level system using the dressed state approach. The study we present in this section is similar in approach, and serves to illustrate the amount of population shifting among the three levels that can be achieved by careful control over the laser frequencies and intensities. Here we focus on the simple physics of the system in order to illustrate our control technique in its simplest form. Consider a simple three-level model system (see Figure 2), consisting of the following molecular states: (1) a ground state  $|\psi_i\rangle$  modeling one isomer, (2) a ground state  $|\psi_c\rangle$  modeling the other isomer, and (3) the excited state  $|\psi_e\rangle$ , which has nonzero dipole matrix elements to both  $|\psi_i\rangle$  and  $|\psi_c\rangle$ . Two laser fields are used, each tuned to one of the system transition frequencies (i.e.,  $\omega_1 = \omega_{ie}$  and  $\omega_2 = \omega_{ce}$ ), with variable intensities and duration of interaction with the molecule.

In the limit of high laser intensities, as is the case for the present example, it is most convenient to describe the system in terms of the dressed-molecule approach.<sup>5,6</sup> This approach yields energy eigenstates of the molecule + radiation field, which are only coupled by spontaneous emission. As will be shown below, we can, for the purpose of our discussion, neglect the very small spontaneous emission coupling.

In the uncoupled molecule–radiation field basis, the full Hamiltonian  $\hat{H}$  (molecule + lasers) matrix is block diagonal, with the blocks being  $3 \times 3$  matrices. The only coupling between the blocks is through spontaneous emission<sup>5</sup> and a representative Hamiltonian block is

(5) See, e.g.: Ho, T.; Chu, S. *Phys. Rev.* **1985**, *A33*, 377, and references therein as well as Hioe, F. T.; Eberly, J. H. *Phys. Rev. Lett.* **1981**, *47*, 838. For a general dressed molecule discussion see: Cohen-Tannoudji, C. In *Frontiers in Laser Spectroscopy*; Balian, R., Haroche, S., Liberman, S., Eds.; North-Holland: Amsterdam, 1977; Vol. 1.

(6) Radmore, P. M.; Knight, P. L. *J. Phys.* **1982**, *B15*, 561.

$$\hat{H} = \hat{H}^0 + \hat{H}^1 = \begin{pmatrix} H_{tt}^0 & 0 & H_{te}^1 \\ 0 & H_{cc}^0 & H_{ce}^1 \\ H_{et}^1 & H_{ec}^1 & H_{ee}^0 \end{pmatrix} \quad (13)$$

where  $H_{tt}^0 = \langle t | \hat{H}^0 | t \rangle$ , etc. Here  $\hat{H}^0$  is the uncoupled molecule-radiation field Hamiltonian, and  $|t\rangle$ ,  $|e\rangle$ , and  $|c\rangle$  are (product) eigenstates of  $\hat{H}^0$ . Specifically, using number states for the description of the laser fields, we can write the zeroth-order states (i.e., eigenstates of  $\hat{H}^0$ ) corresponding to one block of the Hamiltonian as

$$\begin{aligned} |t\rangle &= |\psi_t\rangle |n_1\rangle |n_2\rangle \\ |c\rangle &= |\psi_c\rangle |n_1 - 1\rangle |n_2 + 1\rangle \\ |e\rangle &= |\psi_e\rangle |n_1 - 1\rangle |n_2\rangle \end{aligned} \quad (14)$$

$|t\rangle$  corresponds to the molecule being in the trans ground state  $|\psi_t\rangle$  in the presence of  $n_1$  photons of laser 1 (of frequency  $\omega_1$ ), and  $n_2$  photons of laser field 2 (frequency  $\omega_2$ ); in  $|e\rangle$  the molecule has been excited to state  $|\psi_e\rangle$  with laser 1 losing one photon and laser 2 remaining the same as for  $|t\rangle$ , while in  $|c\rangle$  the molecule is in the cis ground state, having emitted one photon into field 2, and field 1 having the same number of photons as in state  $|e\rangle$ . Note our use of curved braces in, e.g.,  $|t\rangle$ , to denote a state of molecule and radiation field.

These zeroth-order states yield the following Hamiltonian matrix elements:

$$H_{tt}^0 = \hbar(\omega_t + n_1\omega_1 + n_2\omega_2) = E_0$$

$$H_{cc}^0 = \hbar[\omega_c + (n_1 - 1)\omega_1 + (n_2 + 1)\omega_2] = E_0$$

$$H_{ee}^0 = \hbar[\omega_e + (n_1 - 1)\omega_1 + n_2\omega_2] = E_0 \quad (15)$$

$$H_{et}^1 = H_{te}^1 = ie \left( \frac{\hbar\omega_1}{2\epsilon_0 V} \right)^{1/2} \epsilon_1 \cdot \mathbf{D}_{et} n_1^{1/2} = ie \mathcal{E}_1 \cdot \mathbf{D}_{et} \quad (16)$$

$$H_{ec}^1 = H_{ce}^1 = ie \left( \frac{\hbar\omega_2}{2\epsilon_0 V} \right)^{1/2} \epsilon_2 \cdot \mathbf{D}_{ec} (n_2 + 1)^{1/2} = ie \mathcal{E}_2 \cdot \mathbf{D}_{ec} \quad (17)$$

where  $\mathbf{D}_{et} = \langle e | \mathbf{D} | t \rangle$ , etc.

Diagonalizing the Hamiltonian matrix produces the eigenvalues

$$E_1 = E_0 + K; \quad E_2 = E_0; \quad E_3 = E_0 - K \quad (18)$$

and associated eigenvectors

$$|\psi_1\rangle = \frac{1}{K\sqrt{2}} [H_{te}^1 |t\rangle + H_{ce}^1 |c\rangle] + \frac{1}{\sqrt{2}} |e\rangle \quad (19)$$

$$|\psi_2\rangle = \frac{1}{K} [H_{ce}^1 |t\rangle - H_{te}^1 |c\rangle] \quad (20)$$

$$|\psi_3\rangle = \frac{1}{K\sqrt{2}} [H_{te}^1 |t\rangle + H_{ce}^1 |c\rangle] - \frac{1}{\sqrt{2}} |e\rangle \quad (21)$$

where  $K = [|H_{te}^1|^2 + |H_{ce}^1|^2]^{1/2}$ .

A general time-dependent state of the molecule + laser system can now be described in terms of these eigenstates as

$$|\Psi(t)\rangle = \sum_{i=1}^3 e^{-iE_i t/\hbar} C_i |\psi_i\rangle \quad (22)$$

As an example, consider the case where the molecule is initially (just before the laser fields are turned on) in the  $|t\rangle$  ground configuration. That is,

$$|\Psi_i(t=0)\rangle = |t\rangle = \frac{H_{te}^1}{K\sqrt{2}} [|\psi_1\rangle + |\psi_3\rangle] + \frac{H_{ce}^1 \sqrt{2}}{H_{te}^1} |\psi_2\rangle \quad (23)$$

this state evolves as

$$|\Psi_i(t)\rangle = \frac{H_{te}^1}{K\sqrt{2}} [e^{-iE_1 t/\hbar} |\psi_1\rangle + e^{-iE_3 t/\hbar} |\psi_3\rangle] + \frac{H_{ce}^1 \sqrt{2}}{H_{te}^1} e^{-iE_2 t/\hbar} |\psi_2\rangle \quad (24)$$

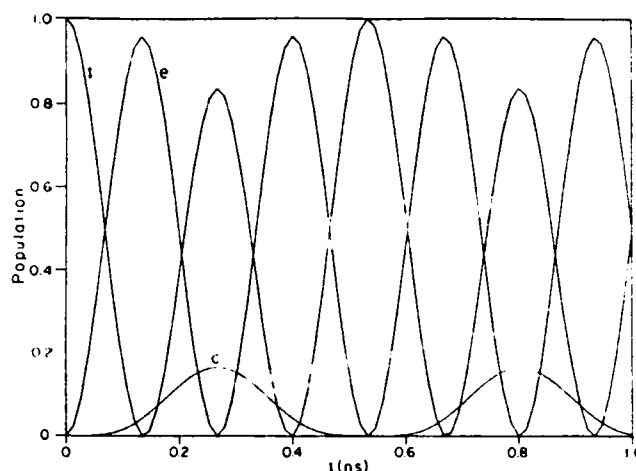


Figure 3. Time evolution of the zeroth-order state populations in the three-level two-laser system. The curve corresponding to  $|b_t(t)|^2$ , i.e., the population of the state  $|t\rangle$ , is labeled with a 't', and similarly for the populations of the states  $|c\rangle$  and  $|e\rangle$ . Laser intensities:  $I_1 = 1.0 \times 10^{10}$  W m $^{-2}$ ,  $I_2 = 1.0 \times 10^{10}$  W m $^{-2}$ .

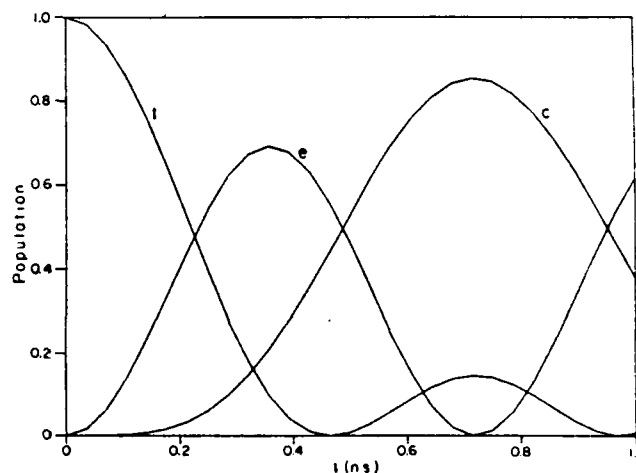


Figure 4. As in Figure 3 but with  $I_1 = 1.0 \times 10^9$  W m $^{-2}$ ,  $I_2 = 1.0 \times 10^{10}$  W m $^{-2}$ .

Substituting for the dressed eigenstates in terms of the uncoupled states (eqs 19–21) we obtain

$$e^{-iE_0 t/\hbar} |\Psi_i(t)\rangle = b_t(t) |t\rangle + b_c(t) |c\rangle + a_e(t) |e\rangle \quad (25)$$

where

$$b_t(t) = \frac{|H_{te}^1|^2 \cos(Kt/\hbar) + |H_{ce}^1|^2}{K^2} \quad (26)$$

$$b_c(t) = \frac{H_{te}^1 H_{ce}^1 [\cos(Kt/\hbar) - 1]}{K^2} \quad (27)$$

$$a_e(t) = -\frac{iH_{te}^1 \sin(Kt/\hbar)}{K} \quad (28)$$

Thus, the populations of the zeroth-order states evolve as the square of the moduli of the coefficients  $b_t(t)$  and  $a_e(t)$  and are clearly periodic. We can see from eq 27 that the population of state  $|c\rangle$  is maximum when  $Kt/\hbar = (2n + 1)\pi$ , and that by properly controlling the relative intensities of the two lasers (i.e., the values of  $H_{te}^1$  and  $H_{ce}^1$ ), as well as their duration, one can induce a *complete*  $|t\rangle$  to  $|c\rangle$  conformational inversion of the molecule.

Figures 3–5 show the time evolution of the zeroth-order state populations. The values used for the system parameters are given in the caption of Figure 2, and correspond to case 2 of the model molecule of section 4. The  $|\psi_1\rangle$ ,  $|\psi_2\rangle$ , and  $|\psi_3\rangle$  states model, respectively, the vibrationless level of the trans ground state, the vibrationless level of the cis ground state, and the excited state  $|e^*\rangle$  of the polyatomic model (see section 4). The intensity of the

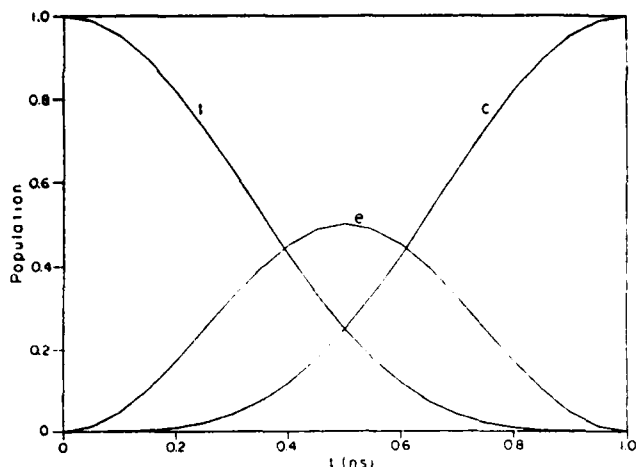


Figure 5. As in Figure 3 but with  $I_1 = 4.472 \times 10^8 \text{ W m}^{-2}$ ,  $I_2 = 1.0 \times 10^{10} \text{ W m}^{-2}$ .

laser tuned to the  $|\psi_c\rangle \leftrightarrow |\psi_e\rangle$  transition ( $\omega_2$ ) is kept constant at  $I_2 = 1.0 \times 10^{10} \text{ W m}^{-2}$ , while that of the other laser, tuned to the  $|\psi_t\rangle \leftrightarrow |\psi_e\rangle$  transition ( $\omega_1$ ), decreases from Figure 3 to Figure 5. In Figure 3 the system oscillates mainly between states |t) and |e), with little population being channeled into |c). A factor of 10 decrease in  $I_1$  results in Figure 4, where the two transitions have comparable Rabi frequencies, and a near-complete conformational inversion is seen at  $t \sim 0.7 \text{ ns}$ . By a further decrease in  $I_1$  one can achieve full conformational inversion as seen in Figure 5, where the system is totally in the |c) state at  $t = 0.914 \text{ ns}$ .

The neglect of spontaneous emission in this experiment can be justified by noting that, in the absence of radiation, a system prepared initially in state |c) would, after 1 ns, lose only 1.15% of its population to spontaneous radiative decay (for values of the decay constants see section 4). This is clearly negligible when compared with the large population oscillations induced by the lasers.

In order for this control scheme to work when applied to real molecules, fulfillment of the same conditions as those described in section 2 is required. That is, the laser intensities must be high enough to make the stimulated transition rates faster than (or at least competitive to) the spontaneous emission, the pumped lines must be isolated (i.e., the three molecular levels which our scheme uses must be clearly resolvable with the lasers used), and the light duration must be short compared to the natural lifetime of the excited state. All these conditions are satisfied by our model, which uses the same molecular parameters as the model system of case 2 in section 4 below. There, the spectral lines of interest are well isolated, and the natural lifetime of the excited state is  $\sim 86 \text{ ns}$ , about 2 orders of magnitude longer than the interaction duration needed to achieve full conformational inversion at the laser powers used here ( $\sim 1 \text{ ns}$  for laser intensities  $I_1 \sim 0.5 \times 10^8 \text{ W m}^{-2}$  and  $I_2 = 1.0 \times 10^{10} \text{ W m}^{-2}$ ).

The lasers used in the present calculations are available in the laboratory. The sole experimental issue to be dealt with is that of timing, i.e., controlling the duration of the interaction between the molecule and the laser fields, as well as the relative phases of the lasers, in order to "stop" the Rabi oscillations at the precise point of the desired population ratio. This timing is important because of the frequency width induced by the light pulse. If the light pulses are too short, a decrease in spectral resolution ensues, resulting in the possible loss of isomerization control. This decrease-of-spectral-resolution difficulty manifests itself when the three level model is extended to realistic models, as described below.

#### 4. A Polyatomic Model

Given the insights afforded by the three-level system we examine, in this section, results of controlled photoisomerization as applied to a model polyatomic system. This system is based on data from cis-trans stilbene isomerization, but in no sense in-

corporates the real physics of this molecule. Rather, the main point of this study is to explore the extent to which conditions for controlled isomerization exist in polyatomic systems. In doing so we neglect polyatomic rotation; we comment on this approximation in the summary of this paper.

**4.1. The Model.** We base the molecular model on Warshel's<sup>7</sup> semiempirical (consistent force field<sup>8</sup>) quantum mechanical calculation of ground and first excited electronic potential surfaces for *trans*- and *cis*-stilbene. To minimize computational cost we use this approach to provide input for a *harmonic potential surface*, i.e., equilibrium conformations, normal modes, and vibrational frequencies for the different electronic states. The harmonic surfaces, which we recalculated using Warshel's QCFF/PI program, are used as the basic building blocks of our model, thus retaining the full dimensionality of the problem. We assume the following:

1. A large potential barrier to isomerization in the ground electronic state, so that thermally stable *cis* and *trans* isomers exist and tunneling is precluded at the energies of interest. The ground electronic state is thus described by independent multidimensional harmonic oscillators for each of the two conformers, with localized energy eigenstates.

2. The first singlet excited electronic state, on the other hand, is either devoid of a barrier or has a small one. Indeed since our concern is with states that span the full conformational space of the molecule, in order to apply the technique of section 2 to the isomerization, the details of the barrier shape and size are relatively unimportant, as long as we consider states of high enough vibrational energy. The QCFF/PI semiempirical excited-state potential harmonic surfaces for *cis*- and *trans*-stilbene provide a first approximation to these states. These were then slightly modified to provide a reasonably good fit to the experimental spectra in accordance with the discussion later below.

The modified QCFF/PI results provide only a start on the excited vibronic states which are considerably more difficult to model than those of the ground electronic state since it is necessary to account for the region bridging the isomers. We summarize the argument and observations that led us to the simplifying approximation for the excited-state wave functions given in eq 29. First, analysis of the modified QCFF/PI results showed an almost one to one correspondence between normal vibrations of the *cis* and *trans* conformations, in the sense that the relative motion of the individual atoms in specific normal modes is similar for both conformations. Second, we also found that motion along the reaction coordinate, i.e., torsion about the ethylene bond in stilbene, is represented mainly by one normal mode, with two or three other modes having only a small component in that direction. Accordingly, we make the assumption that isomerization corresponds to motion in one normal mode (the one with the large torsional component about the ethylene bond), while all the other modes are harmonic, uncoupled and orthogonal to the reactive mode.

It is obvious that a normal mode, which by definition represents low-amplitude vibration, is not a good representation of the isomerization, since the latter involves both large-amplitude motion and periodic torsional motion about the ethylene bond. This would suggest the use of a hindered-rotor potential to describe the isomerization coordinate. The full excited-state vibrational eigenfunctions of the model molecule would then be products of  $(3N - 7)$ -dimensional harmonic oscillator wave functions  $|\psi_{\text{harmonic}}\rangle$  (corresponding to the harmonic part of the potential) times the reactive mode wave functions  $|\psi_{\text{react}}\rangle$  (i.e., the hindered-rotor eigenfunctions). In going from one conformation to the other (*cis* or *trans* or vice versa), i.e., moving in the direction of the reactive mode, each harmonic normal mode of one conformation correlates with a corresponding mode in the other conformation, with the same number of quanta in each mode. The calculation of the overlap matrix elements required below could be simplified by expanding the (one-dimensional) hindered-rotor eigenfunctions

(7) Warshel, A. *J. Chem. Phys.* 1975, 62, 214.

(8) Warshel, A. In *Modern Theoretical Chemistry, Vol. 7: Semiempirical Methods of Electronic Structure Calculation. Part A: Techniques*; Segal, G. A., Ed.; Plenum Press: New York, 1977.

in terms of the cis + trans harmonic oscillator wavefunctions of the reactive mode, which form a complete basis. This would reduce the overlap problem to that of evaluating harmonic polyatomic Franck-Condon factors, which we can do very efficiently.<sup>9</sup>

Although the above procedure is desirable in practice, the experimental information on molecules like *cis*-stilbene is very scant, so that one can neither infer the proper coefficients nor their energies for such a linear combination of states. Therefore, it is not unreasonable to assume that the major term in the basis set expansion consists of equal contributions from those harmonic cis and trans states of the reactive mode,  $|\phi_{\text{react}}^{\text{cis}}\rangle$  and  $|\phi_{\text{react}}^{\text{trans}}\rangle$ , which are closest in energy to the hindered-rotor state of interest. As such, we approximate the excited vibronic states of the model by

$$|e^{\pm}\rangle = \frac{1}{\sqrt{2}} (|\psi_{\text{harmonic}}^{\text{cis}}\rangle |\phi_{\text{react}}^{\text{cis}}\rangle \pm |\psi_{\text{harmonic}}^{\text{trans}}\rangle |\phi_{\text{react}}^{\text{trans}}\rangle) \quad (29)$$

with corresponding energies

$$E^+ = \min(E^{\text{cis}}, E^{\text{trans}}), \quad E^- = \max(E^{\text{cis}}, E^{\text{trans}}) \quad (30)$$

Here  $E^{\text{cis}}$  and  $E^{\text{trans}}$  are respectively the energies of the cis and trans  $(3N-6)$ -dimensional harmonic states which constitute the linear combination  $|e^{\pm}\rangle$ , as obtained from the QCFF/PI calculation of the excited electronic state.

Equation 29 contains only the bare essentials of the character of the exact molecular vibrational states in the excited electronic state. Nevertheless, it suffices as a useful first step in the examination of conditions for laser induced isomerization, described below.

**4.2. Spectra.** In order to assess the suitability of a molecule for isomerization control, it is necessary to acquire a reasonably detailed understanding of its molecular spectroscopy, and to determine which vibronic transitions are the most useful for the application of this technique. In this section we present the absorption and some single-vibronic-level (SVL) emission spectra (purely harmonic) for the two separate conformations of the model. The oscillator strengths for the electronic transitions are given by the QCFF/PI program<sup>8</sup> and used without modification. Although we are not attempting a realistic model of a molecule,<sup>10,11</sup> it is useful to attempt an approximation to a real system such as stilbene. Hence, we use experimental spectral data to adjust the calculated stilbene QCFF/PI surfaces, as described below. We report spectra below simply as Franck-Condon (FC) factors for absorption or emission; that is, we do not take any line broadening or resolution factors into account.

(i) **The Model Trans Configuration.** Very good experimental spectra for *trans*-stilbene are available<sup>12-16</sup> including the absorption, fluorescence excitation, and dispersed fluorescence spectra of the jet-cooled molecule. Much of this has been assigned using Warshel's calculations.<sup>7,17</sup> The spectra we have calculated by directly using the QCFF/PI normal modes and equilibrium nuclear configurations do not adequately reproduce the experimental intensity patterns. Thus, we altered the surfaces to fit the intensity data, specifically, by modifying the excited-state equilibrium conformation.

Little effort was required to fit the calculated spectra to major features of the experimental spectra. This procedure is described

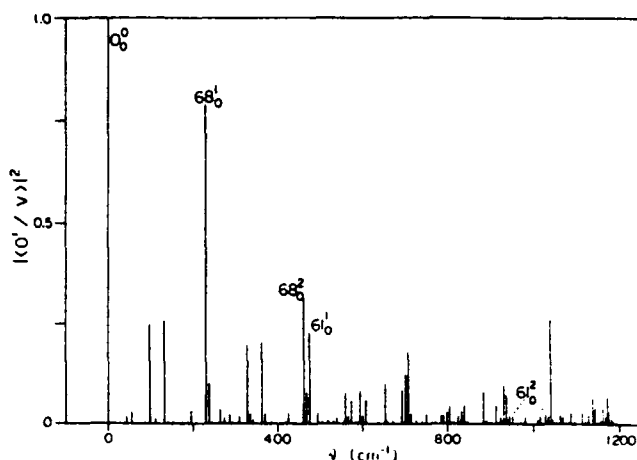


Figure 6. Absorption FC factors for the trans model, from the vibrationless level in the ground electronic state to vibronic levels of the first excited singlet. Frequencies are relative to the origin of the electronic transition. Maximum FC factor =  $3.418 \times 10^{-2}$ . Excited-state normal frequencies:  $\nu_{61} = 475.669 \text{ cm}^{-1}$ ,  $\nu_{68} = 230.825 \text{ cm}^{-1}$ .

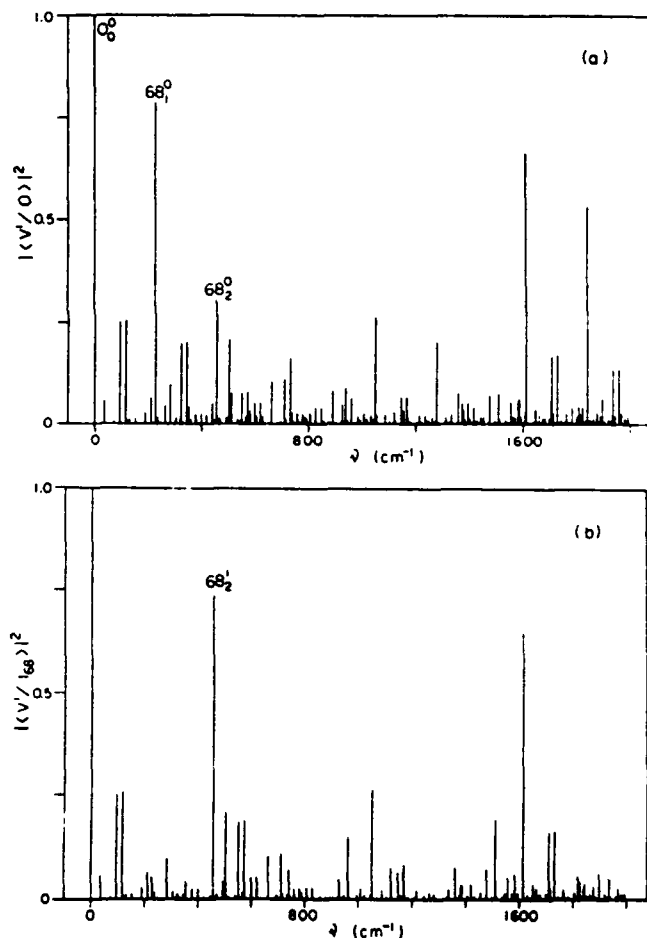


Figure 7. Emission FC factors for the trans-model. Ground state normal frequencies:  $\nu_{68} = 228.634 \text{ cm}^{-1}$ . (a) Emission from the vibrationless level in the first excited singlet state to vibronic levels of the ground electronic state. Frequencies are relative to the origin of the electronic transition. Maximum FC factor =  $3.418 \times 10^{-2}$ . (b) Emission from the state with one quantum in the  $C_2C_2\phi$  bending mode ( $\nu_{23}^{13}$  or our mode 68). Frequencies are relative to the  $68_0^1$  transition. Maximum FC factor =  $2.700 \times 10^{-2}$ .

in detail elsewhere.<sup>4</sup> However, it is of sufficient general interest to warrant displaying some results. As an example, consider Figure 6 which is the fitted absorption FC spectrum for the trans model, from the vibrationless level in the ground electronic state to vibronic levels of the first excited singlet. The spectrum compares

(9) Gruner, D.; Brumer, P. *Chem. Phys. Lett.* 1987, 138, 310.

(10) Orlandi, G.; Siebrand, W. *Chem. Phys. Lett.* 1975, 30, 352.

(11) For example, the need for double excitations in the CI is discussed by: Hemley, R. J.; Leopold, D. G.; Vaida, V.; Karplus, M. *J. Chem. Phys.* 1985, 82, 5379.

(12) Syage, J. A.; Lambert, Wm. R.; Felker, P. M.; Zewail, A. H.; Ilchstrasser, R. M. *Chem. Phys. Lett.* 1982, 88, 266.

(13) Syage, J. A.; Felker, P. M.; Zewail, A. H. *J. Chem. Phys.* 1984, 81, 4685.

(14) Syage, J. A.; Felker, P. M.; Zewail, A. H. *J. Chem. Phys.* 1984, 81, 4706.

(15) Zwier, T. S.; Carrasquillo, E.; Levy, D. H. *J. Chem. Phys.* 1983, 78, 5493.

(16) Amirav, A.; Jortner, J. *Chem. Phys. Lett.* 1983, 95, 295.

(17) Such assignments often show frequencies which are too high. Hemley et al.<sup>16</sup> report that their newer PPP/CI program, which is essentially an improved QCFF/PI, also produces somewhat high normal frequencies.

very favorably with the experimental data shown in Figure 4 of ref 12, showing the same trends for the dominant peaks and a similar sort of background. Mode 61, which corresponds to the reactive mode (i.e., torsion about the ethylene bond), has been enhanced in this fit; this line is not unambiguously identified in ref 12.

The excited-state equilibrium conformation resulting from this fit was used to calculate the FC factors for emission from single vibronic levels of the excited electronic state, as shown in Figure 7. The fluorescence FC factors for the vibrationless level of  $S_1$  are plotted in Figure 7a, while emission from the state with one quantum in the  $C_2C_2\phi$  bending mode ( $\nu_{25}$  of ref 13, or our mode 68), which forms the major progression in both absorption and emission, is shown in Figure 7b. These can be favorably compared to the corresponding bottom two spectra in Figure 7 and the top spectrum in Figure 1a of ref 12. As one can readily observe, the same trends in the spectral progressions are evident, e.g., the line corresponding to the  $61_1^1$  transition (or  $25_1^1$  in Syage et al.'s notation<sup>13</sup>) is noticeably absent.

The obtained fit is quite good. A better fit than that presented here is certainly possible, but the nature of our model does not warrant the effort.

(ii) **Model Cis Configuration.** The situation regarding *cis*-stilbene<sup>2</sup> is quite different than that for *trans* since high-resolution experimental data for the *cis* form are unavailable. Hence, the QCFF/PI calculations were used directly.

The absorption (8a) and SVL fluorescence (8b) FC spectra of the *cis* model are shown in Figure 8. Note the low values for the FC factors relative to those of the *trans* model. Figure 9 shows the SVL fluorescence spectra (emission Franck-Condon factors) from levels with one and two quanta of excitation in the reactive mode (our mode 61), for both *trans* and *cis* model stilbene. The oscillator strength for the *cis* model electronic transition is also substantially lower than for the *trans* ( $0.825727$  for *cis* vs.  $1.364626$  for *trans*).

**4.3. Stimulated Emission and Branching Control.** We present here results on controlled isomerization in our model polyatomic. In order to investigate the variety of behavior which can be observed, we devised two models differing by the different assignments of the *cis* electronic transition energy,  $\omega_{0cis}^0$ . Parameter values for the two cases are as follows:

**Case 1.** The origin of the *cis* transition was set at  $\omega_{0cis}^0 = 30000$   $\text{cm}^{-1}$ , the approximate origin<sup>18</sup> in diphenylmethane. For the *trans*,  $\omega_{0trans}^0 = 32234.2$   $\text{cm}^{-1}$ , equal to the actual  $S_1 \leftarrow S_0$  transition origin.<sup>13</sup> The zero-point energy difference in the ground electronic state, as calculated by the QCFF/PI program, is  $E_{0cis} - E_{0trans} = 2126.56$   $\text{cm}^{-1}$ , in good accord with the  $S_0$  potential energy diagrams in refs 11 and 13.

**Case 2.** Here we set the *cis* origin at  $\omega_{0cis}^0 = 32000$   $\text{cm}^{-1}$ , equal to the approximate  $S_1 \leftarrow S_0$  origin in gaseous *cis*-stilbene.<sup>19</sup> The origin  $\omega_{0trans}^0$  is the same as in case 1, so that the ground zero point energy difference becomes  $E_{0cis} - E_{0trans} = 126.56$   $\text{cm}^{-1}$ . The relative energies of the excited electronic potential surfaces for the *cis* and *trans* model are the same in both cases studied.

The initially prepared excited eigenstate of the model molecule is chosen as the linear combination

$$|e^+\rangle = \frac{1}{\sqrt{2}} [|2_{61}\rangle_{cis} + |2_{61}\rangle_{trans}] \quad (31)$$

i.e., the combination of the *cis* and *trans* states with 2 quanta of excitation in the  $S_1$  vibrational mode 61, which corresponds to the isomerization coordinate. The remaining oscillators are in their ground states. The energy of this excited state is then  $2\omega_{61trans}^0 = 894.2616$   $\text{cm}^{-1}$  above the *trans*  $S_1$  origin and  $1001.9016$   $\text{cm}^{-1}$  above the *cis*  $S_1$  origin. Experimental preparation of such a state in our model systems would not pose a problem, since (see Figures 6 and 8a) the  $61_2^2$  transition is well isolated in both the *cis* and *trans* model. That is, although the vibrational density of states at the energy corresponding to the state  $|e^+\rangle$  is  $\sim 40$  states/ $\text{cm}^{-1}$ ,

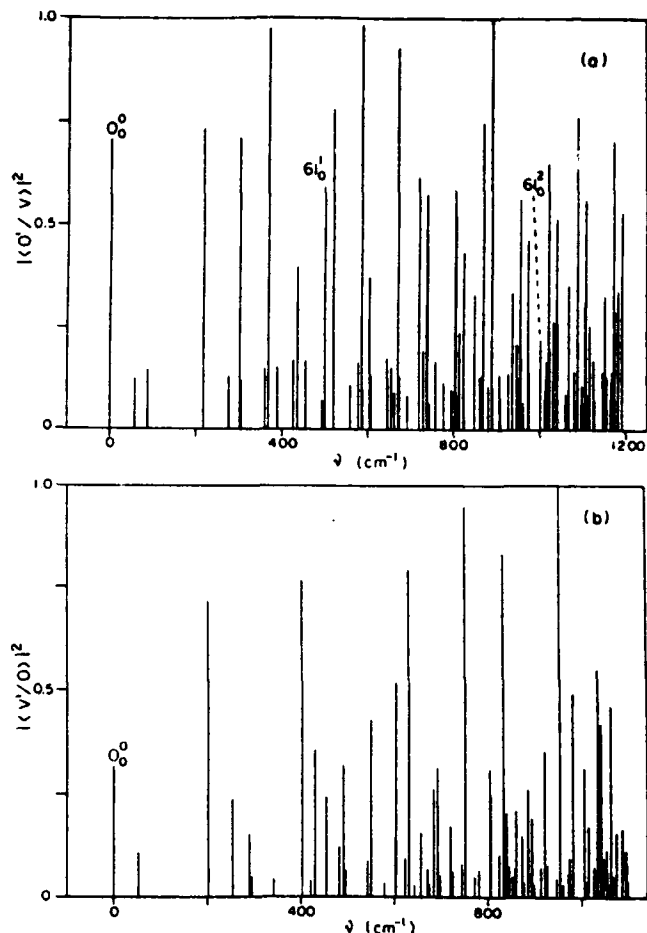


Figure 8. (a) Absorption FC spectrum for the *cis* model from the vibrationless level of the ground electronic state to vibronic levels of the first excited singlet. Frequencies are relative to the origin of the *cis* electronic transition. Excited-state frequencies:  $\nu_{61} = 500.950$   $\text{cm}^{-1}$ ,  $\nu_{68} = 218.240$   $\text{cm}^{-1}$ . Maximum FC factor =  $3.864 \times 10^{-4}$ . (b) Emission FC factors for *cis*-model stilbene from the vibrationless level in the first excited singlet state to vibronic levels of the ground electronic state. Frequencies are relative to the origin of the electronic transition. Ground-state frequencies:  $\nu_{61} = 537.462$   $\text{cm}^{-1}$ ,  $\nu_{68} = 201.333$   $\text{cm}^{-1}$ . Maximum FC factor =  $8.609 \times 10^{-4}$ .

only a single state lying within the frequency width associated with a reasonably sharp laser has a significant Franck-Condon factor with the ground state. We therefore simply assume this as our initial state for the stimulated emission pumping calculations described below.

We present below stimulated emission spectra from the state  $|e^+\rangle$  (eq 31) produced with a laser pulse  $\mathcal{E}_p(t) = \mathcal{E}_0 \sin \omega_L t$  of duration  $t_p = 100$  ps. To obtain this result we assume  $|e^+\rangle$  to be first prepared and then compute the stimulated depopulation of the initial state for laser pulses centered at each transition frequency by solving the equations of motion (eqs 11 and 12) to first order in time-dependent perturbation theory.<sup>20</sup> The use of perturbation theory is justified as long as the excited-state depopulation remains small, as in the case in our calculations. For example, using a laser power of  $10^9$   $\text{W m}^{-2}$ , the depopulation is less than 10% for all but the strongest transitions, and less than 1% for the weaker *cis* transitions. The spontaneous emission contribution to eq 12 was neglected, since the natural radiative lifetime of the excited state is  $\sim 100$  times longer than the duration of the pulse. One obtains, for the coefficients of the ground states (see eq 11)

$$\beta_i(t) = \frac{e \langle g_i^0 | D | e^+ \rangle \cdot \mathcal{E}_0}{2i\hbar} \left[ \frac{1 - e^{i(\omega_0 + \omega_L)t}}{\omega_{ie} + \omega_L} - \frac{1 - e^{i(\omega_0 - \omega_L)t}}{\omega_{ie} - \omega_L} \right] \quad (32)$$

(18) Dyck, R. H.; McClure, D. S. *J. Chem. Phys.* 1962, 36, 2326.

(19) Greene, B. I.; Farrow, R. C. *J. Chem. Phys.* 1983, 78, 3336.

(20) Taylor, R. D.; Brumer, P. *Faraday Discuss. Chem. Soc.* 1983, 75, 117.

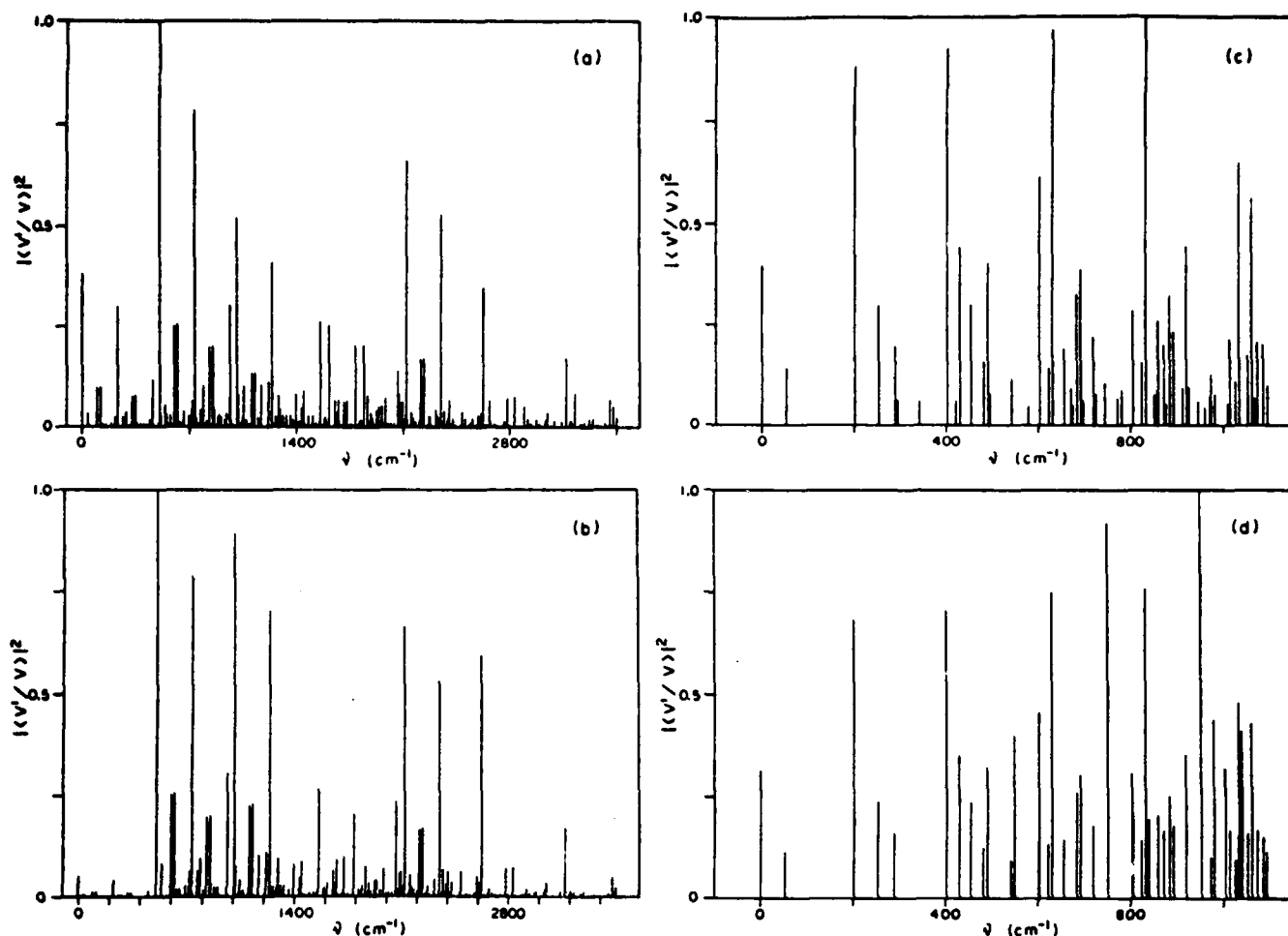


Figure 9. Single vibronic level fluorescence (Franck-Condon) spectra from levels with one and two quanta of excitation in the reactive mode (no. 61): (a) trans 61<sup>1</sup>; (b) trans 61<sup>2</sup>; (c) cis 61<sup>1</sup>; (d) cis 61<sup>2</sup>. The ordinates are normalized to (a)  $2.054 \times 10^{-2}$ , (b)  $1.270 \times 10^{-2}$ , (c)  $5.745 \times 10^{-4}$ , (d)  $2.711 \times 10^{-4}$ .

where  $\omega_{ie} = \omega_{ij} - \omega_e < 0$  for stimulated emission. In addition, we neglect the smaller second term in the brackets in eq 32, in accord with the resonance approximation.<sup>21</sup>

The total excited-state depopulation  $R_{stim}(t, \omega)$  is given by

$$R_{stim}(t, \omega) = \sum_i \sum_j |\beta_j^i(t)|^2 \quad (33)$$

with similar definitions for the probabilities of producing a ground-state molecule in a particular conformation (i.e.,  $f = I, II$ ). In the Condon approximation, and assuming the polarization of the field is parallel to the electronic dipole moment of the molecule  $\mu_{el}$  we therefore have

$$R_{stim}^f(t, \omega) = \left( \frac{e\mu_{el} \mathcal{E}_0}{2\hbar} \right)^2 \sum_i |\langle g_j^i | e^+ \rangle|^2 \left( \frac{\sin [(\omega_{ie} + \omega)t/2]}{(\omega_{ie} + \omega)/2} \right)^2 \quad (34)$$

The results of our calculations for the system parameters defined above follow. In each case the number of ground levels had to be restricted to allow effective calculation. The criterion used to restrict the number of states to be included was that the overlaps of the excited state with ground vibronic states are largest for states with small number of quanta. As verified in our calculations, the neglected overlaps are indeed extremely small.

(f) *Case 1.* In this case, using eq 8 and including in the sums over the damping coefficients all the states discussed below, the spontaneous trans/cis ratio is determined to be

$$\frac{R_{spont}^{trans}(t_p)}{R_{spont}^{cis}(t_p)} = \frac{\sum_i \gamma_i^{trans}}{\sum_j \gamma_j^{cis}} = \frac{24869086.0 \text{ s}^{-1}}{407916.9 \text{ s}^{-1}} = 61.0 \quad (35)$$

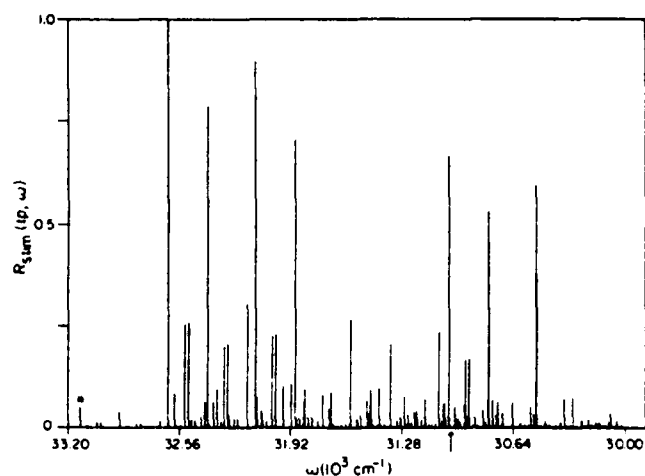


Figure 10. Case 1: Stimulated emission spectrum of the model polyatomic excited to  $|e^+\rangle$ , for sinusoidal laser pulses of duration,  $t_p = 100$  ps, centered at the transition frequencies. Laser intensity =  $1 \times 10^8$  W  $m^{-2}$ . The asterisk marks the origin of the trans transitions, i.e., the line  $61_0^2$ , with frequency =  $33128.46 \text{ cm}^{-1}$ . The origin of the cis transitions,  $61_0^1$ , at a frequency of  $31001.90 \text{ cm}^{-1}$ , is marked with an arrow. Maximum actual depopulation =  $3.593 \times 10^{-2}$ .

That is, trans heavily predominates in spontaneous emission. The key question is therefore whether we can stimulate production of the cis conformer. We show below that this is, in fact, not a suitable case for laser induced isomerization.

Figure 10 shows the spectrum of  $|e^+\rangle$  stimulated down to the ground electronic state. Approximately 35 000 transitions to both cis and trans conformers are included. The calculation is restricted

(21) Cohen-Tannoudji, C.; Diu, B.; Laloe, F. *Quantum Mechanics*, Wiley-Interscience: New York, 1977.

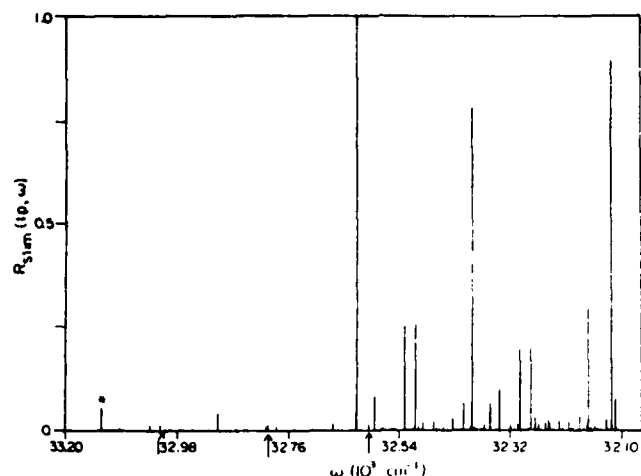


Figure 11. Case 2: Stimulated emission spectrum for the model polyatomic excited to  $je^+$ , for sinusoidal laser pulses of duration  $t_p = 100$  ps, centered at the transition frequencies (i.e., not continuously swept). Laser intensity =  $1 \times 10^9$  W m $^{-2}$ . The asterisk marks the origin of the trans transitions, i.e., the line  $\nu_{61}^2$ , with frequency =  $33\,128.46$  cm $^{-1}$ . Some of the cis transitions that can be used for selective stimulated emission pumping are marked as follows: (a) the cis origin,  $\nu_{61}^2$ , at a frequency of  $33\,001.90$  cm $^{-1}$ ; (b)  $\nu_{61}^2 \nu_{68}^2$ , with frequency =  $32\,800.57$  cm $^{-1}$ ; (c)  $\nu_{61}^2 \nu_{68}^2$ , with frequency =  $32\,599.23$  cm $^{-1}$ . Maximum actual depopulation =  $2.190 \times 10^{-1}$ .

to ground vibronic states as follows: (i) for the cis model, states with up to 4 quanta of excitation in each vibrational mode were included; (ii) for the trans model, the restriction was much more severe, with only states with up to 2 quanta per mode and a maximum total number of vibrational quanta (summed over all modes) of 3. With these constraints there are 7652 states in the first 1100 cm $^{-1}$  of the cis ground state (the full state count is 13010), and 32339 states in the first 3500 cm $^{-1}$  of the trans ground state (an estimate of the total number of states,<sup>22</sup> gives  $\sim 10^9$  states in this energy range). The density of  $S_0$  trans states in the vicinity of the origin for the cis transitions ( $31\,001.90$  cm $^{-1}$ ), i.e., between 2100 and 2200 cm $^{-1}$  of vibrational energy above the zero-point level, is approximately<sup>22</sup>  $3.5 \times 10^4$  states/cm $^{-1}$ . In addition, the transitions to the cis conformation are quite weak relative to those to the trans conformation (by as much as 2 orders of magnitude). The latter feature, coupled with the high density of trans states, makes the selective production of the cis isomer impractical by the method of section 2.

It is true that we can use stimulated emission pumping to enhance the trans yield, but this is not of much interest in this case since the ratio of trans to cis produced by spontaneous emission is already quite large.

(ii) Case 2. In this case the model parameters are such that the origin for the cis transitions is moved, relative to case 1, closer to that for the trans. As a consequence, a whole new range of possibilities for isomerization control opens up. A computation similar to that above shows that the trans still dominates in spontaneous emission, with a spontaneous trans/cis ratio  $R_{\text{spont}}^{\text{trans}}(t_p)/R_{\text{spont}}^{\text{cis}}(t_p) = 24.0$  so that the issue is to show enhanced cis production.

The stimulated emission spectrum for this case is presented in Figure 11, and includes transitions to all states in the energy range shown containing up to 4 quanta of vibrational excitation per mode for both cis and trans (there are 13 146 such states in the first 1100 cm $^{-1}$  of the trans ground state, and 7652 in the first 1100 cm $^{-1}$  of the cis). It is evident from Figure 11 that the density of significant transitions, in the first 550 cm $^{-1}$ , is low enough to allow selective down pumping of isolated lines with reasonable lasers. Some of the cis transitions that can be used for selective stimulated emission pumping are marked in the figure. Table I lists the

TABLE I: Polyatomic Model, Case 2: Stimulated Emission Probabilities for Excitation to  $je^+$ , Corresponding to the First 550 cm $^{-1}$  of the Spectrum of Figure 11<sup>a</sup>

$\omega$ , cm $^{-1}$	$R_{\text{stim}}^{\text{trans}}(t_p, \omega)$	$R_{\text{stim}}^{\text{cis}}(t_p, \omega)$
33 128.46	$1.1800 \times 10^{-2}$	0
33 091.92	$1.5577 \times 10^{-3}$	0
33 033.08	$2.9836 \times 10^{-3}$	0
33 011.85	$3.0412 \times 10^{-3}$	0
33 001.90	0	$1.4774 \times 10^{-3}$
32 949.81	$2.5519 \times 10^{-4}$	$5.3766 \times 10^{-4}$
32 916.46	$7.6867 \times 10^{-4}$	0
32 899.83	$9.2890 \times 10^{-3}$	0
32 863.29	$1.2263 \times 10^{-3}$	0
32 844.97	$1.0369 \times 10^{-3}$	$4.7894 \times 10^{-9}$
32 844.93	$1.1120 \times 10^{-3}$	$2.3676 \times 10^{-9}$
32 804.44	$2.3488 \times 10^{-3}$	$1.7777 \times 10^{-7}$
32 800.57	$1.3211 \times 10^{-7}$	$3.2069 \times 10^{-3}$
32 783.21	$2.4157 \times 10^{-3}$	$4.8533 \times 10^{-12}$
32 783.19	$2.3690 \times 10^{-3}$	$2.0654 \times 10^{-10}$
32 748.47	$1.0208 \times 10^{-6}$	$1.1216 \times 10^{-3}$
32 712.47	$2.3131 \times 10^{-6}$	$7.5686 \times 10^{-4}$
32 687.83	$6.1009 \times 10^{-6}$	0
32 687.80	$5.9826 \times 10^{-6}$	0
32 671.19	$3.6066 \times 10^{-3}$	$1.4347 \times 10^{-9}$
32 670.96	$5.0795 \times 10^{-4}$	$8.5253 \times 10^{-8}$
32 624.65	$8.4739 \times 10^{-4}$	$1.8576 \times 10^{-11}$
32 624.53	$9.4882 \times 10^{-3}$	$1.8645 \times 10^{-12}$
32 624.02	$2.1896 \times 10^{-1}$	0
32 623.45	$4.4414 \times 10^{-3}$	0
32 623.22	$3.5243 \times 10^{-3}$	0
32 623.20	$3.6138 \times 10^{-3}$	0
32 623.18	$3.4013 \times 10^{-3}$	0
32 616.34	$8.1628 \times 10^{-4}$	$8.8838 \times 10^{-8}$
32 616.29	$8.7540 \times 10^{-4}$	$6.5691 \times 10^{-8}$
32 599.45	$1.0849 \times 10^{-4}$	$6.4656 \times 10^{-4}$
32 599.45	$1.0850 \times 10^{-4}$	$6.6118 \times 10^{-4}$
32 599.33	$7.5285 \times 10^{-7}$	$2.4854 \times 10^{-3}$
32 599.23	$2.9021 \times 10^{-7}$	$3.3036 \times 10^{-3}$
32 588.00	$7.9790 \times 10^{-4}$	$1.2746 \times 10^{-11}$
32 587.49	$1.8411 \times 10^{-2}$	$3.8202 \times 10^{-11}$

<sup>a</sup> For comparison, the spontaneous emission probabilities, for  $t_p = 0.1$  ns, are  $R_{\text{spont}}^{\text{trans}}(t_p) = 1.1110 \times 10^{-3}$  and  $R_{\text{spont}}^{\text{cis}}(t_p) = 4.6283 \times 10^{-5}$ .

stimulated transition probabilities to both trans and cis final ground-state conformations,  $R_{\text{stim}}^{\text{trans}}(t_p, \omega)$  and  $R_{\text{stim}}^{\text{cis}}(t_p, \omega)$ , for all the major lines in the first 550 cm $^{-1}$  of the spectrum. Note that for most of the lines described in Table I there is some probability for stimulated emission to both conformations, even though each of the spectral transitions on which the laser pulses are centered corresponds to a *single* conformation. This is due to the lifetime broadening of the laser, which results in more than one emission line being under the laser bandwidth.

Consider, for example, the ground-state populations obtained by centering the laser pulse on the cis transition  $\nu_{61}^2 \nu_{68}^2$  at  $32\,599.23$  cm $^{-1}$ . Here the stimulated production of trans conformer is 4 orders of magnitude smaller than that of cis at this frequency—see Table I. For the laser power used ( $10^9$  W m $^{-2}$ ) we can make the production of cis ground state occur at a rate comparable to the spontaneous production of trans ground molecules. Increasing the laser power will proportionately increase the stimulated rates (eq 34), enabling the enhancement of the cis/trans product ratio. Similarly dramatic results can be obtained by tuning the down pumping laser to other predominantly cis transitions, e.g., the cis origin  $\nu_{61}^2$  at  $33\,001.90$  cm $^{-1}$ . Results on induced isomerization for this case have already been provided in section 3 where full conformational inversion has been shown possible.

## 5. Summary

In this paper we have suggested a means of using stimulated emission pumping to control isomerization in isolated molecules. Specifically, one first excites the molecule to a single excited vibronic eigenstate with a sharp laser and then uses stimulated emission pumping to pump the system down to the desired isomer. The approach (although not necessarily our computations) is based

(22) Using the algorithm of: Whitten, G. Z.; Rabinovitch, B. S. *J. Chem. Phys.* 1963, 38, 2466.

(23) Yoshihara, K.; Namiki, A.; Sumitani, M.; Nakashima, N. *J. Chem. Phys.* 1979, 71, 2892.

entirely upon exact molecular eigenstates and recognizes the differences in energy levels between cis and trans isomers of the same molecule. We have emphasized the importance, for experimental demonstration of this cis/trans control, of a number of molecular features reiterated below.

Specifically, one must be able to produce a *single excited molecular eigenstate* which spans the full conformational space of the molecule, i.e., a state above or close to the top of the barrier to isomerization in the excited electronic state. This necessitates that any barrier in the excited state be low enough that the vibronic state density permits the excitation of a single energy eigenstate. Further, in order to be able to influence the product ratio for the isomerization reaction, there must be relatively isolated transitions to states of the desired conformation. These conditions were not met by the first example in section 4.3 but the second example, where the molecular features were more favorable, showed considerable control over the cis/trans ratio.

The conditions on the molecular parameters go hand-in-hand with those that must be imposed on the exciting and down pumping lasers, the power and duration of which must be such that "clean" transitions are pumped and the pumping must occur at a rate faster than that for spontaneous emission.

To simplify the computations we have considered a model without vibrational motion. Including rotations is necessary, of course,

in any analysis of a real molecular system. However, the essential principles outlined in this paper are unaltered by including rotations. The principal effect of incorporating rotations would be to increase the state density, necessitating use of longer pulses to isolate individual states.

This paper also contains extensive calculations on two versions of a model which were designed to examine features of polyatomic molecules which are of importance to the feasibility of laser-induced isomerization. Case 1, for example, showed extensive interleaving of cis and trans transitions so that effective control is difficult to achieve. This was not the situation for case 2 which has a smaller difference in the cis and trans equilibrium energies and which allows for extensive trans-cis induced isomerization. Thus, we anticipate that laser-induced isomerization will be experimentally demonstrable for molecules with level structures similar to those of case 2.

*Acknowledgment.* We thank the donors of the Petroleum Research Fund, administered by the American Chemical Society, and the US Office of Naval Research, under contract No. N00014-90-J-1014, for support of this research. We also thank Professor A. Warshel for a copy of his QCFF/PI program and for his advice on its implementation.

Registry No. *trans*-Stilbene, 103-30-0; *cis*-stilbene, 645-49-8.

## A High-Temperature Photochemistry Study of the Reaction between Ground-State Cu Atoms and N<sub>2</sub>O from 470 to 1340 K

A. S. Narayan, Peter M. Futerko, and Arthur Fontijn\*

*High-Temperature Reaction Kinetics Laboratory, The Isermann Department of Chemical Engineering, Rensselaer Polytechnic Institute, Troy, New York 12180-3590 (Received: July 15, 1991; In Final Form: August 26, 1991)*

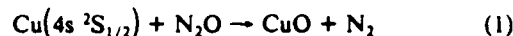
The Metals-HTP (high-temperature photochemistry) technique has been adapted for studies with thermally unstable reactants, here N<sub>2</sub>O. The rate coefficients for the reaction  $\text{Cu}(4s^2S_{1/2}) + \text{N}_2\text{O} \rightarrow \text{CuO} + \text{N}_2$  from 470 to 1190 K are best fitted by  $k_1(T) = 1.7 \times 10^{-10} \exp(-5129 \text{ K}/T) \text{ cm}^3 \text{ molecule}^{-1} \text{ s}^{-1}$  with  $2\sigma$  precision limits varying from  $\pm 8$  to  $\pm 18\%$ , depending on temperature, and corresponding  $2\sigma$  accuracy limits of  $\pm 22$  to  $\pm 27\%$ . It is shown that this expression correlates well with data on a series of other metal atom-N<sub>2</sub>O reactions. Above about 1190 K, the Arrhenius plot shows distinct upward curvature, which may be due to a contribution to the observed rates of vibrationally excited N<sub>2</sub>O in bending modes. For the entire 470-1340 K range the measurements are best described by  $k_1(T) = 3.04 \times 10^{-20} T^{2.97} \exp(-3087 \text{ K}/T) \text{ cm}^3 \text{ molecule}^{-1} \text{ s}^{-1}$  with estimated  $2\sigma$  accuracy limits of  $\pm 22$  to  $\pm 28\%$ .

### 1. Introduction

Recently, we reported on the development of the Metals-HTP (high-temperature photochemistry) technique,<sup>1</sup> to complement our well-established HTFFR (high-temperature fast-flow reactor) method for studying reactions of metallic and other refractory species. Metals-HTP differs from regular HTP<sup>2,3</sup> in that metal salts are evaporated in the apparatus to replace permanent gases as atom precursors. In HTP techniques, atoms are produced photolytically and the reactions are observed in real time in the same volume element in which they are formed; pressures that can be utilized range from about 40 mbar to around atmospheric, and wall reactions are negligible. In HTFFR experiments, atoms

or radicals are produced upstream of the reaction zone by evaporative<sup>4,5</sup> or microwave<sup>6</sup> methods and pressures are typically in the 5-80 mbar range.

In the first Metals-HTP study we made measurements on the termolecular  $\text{Na} + \text{O}_2 + \text{N}_2 \rightarrow \text{NaO}_2 + \text{N}_2$  reaction. Here we report on the first bimolecular reaction studied by this technique



No previous studies on this reaction have been reported, but more metal atom oxidation reactions with N<sub>2</sub>O have been studied than with any other oxidant, (see e.g. ref 4 and section 3), which allows

(1) Marshall, P.; Narayan, A. S.; Fontijn, A. *J. Phys. Chem.* 1990, 94, 2998.

(2) Mahmud, K.; Kim, J.-S.; Fontijn, A. *J. Phys. Chem.* 1990, 94, 2994.

(3) Ko, T.; Marshall, P.; Fontijn, A. *J. Phys. Chem.* 1990, 94, 1401.

(4) Fontijn, A.; Felder, W. In *Reactive Intermediates in the Gas Phase: Generation and Monitoring*; Setser, D. W., Ed.; Academic: New York, 1979; Chapter 2.

(5) Slavejkov, A. G.; Stanton, C. T.; Fontijn, A. *J. Phys. Chem.* 1990, 94, 3347.

(6) Slavejkov, A. G.; Fontijn, A. *Chem. Phys. Lett.* 1990, 165, 375.

# LASER CONTROL OF MOLECULAR PROCESSES

Paul Brumer

Chemical Physics Theory Group, Department of Chemistry,  
University of Toronto, Toronto, Canada M5S 1A1

Moshe Shapiro

Chemical Physics Department, The Weizmann Institute of Science,  
Rehovot, Israel 76100

KEY WORDS: chemical reactions, coherent control, optimal control, pulse shaping

## INTRODUCTION

The last 20 years have seen enormous strides in our understanding of the detailed dynamics of elementary chemical reactions (1-3). With this understanding well in hand, attention has turned to controlling, rather than passively observing, molecular collision processes. Theoretical and computational advances, supported by preliminary experimental results, now clearly indicate that efficient control over molecular processes is possible. We review these advances in detail below.

The primary goal of practical chemistry is to produce desired molecular products in substantial yield. For decades, enhanced productivity was attained by thermodynamic techniques, e.g. variations in pressure and temperature. Recently, efforts have been directed toward using properties of lasers to enhance desired product yield selectively. Initial efforts attempted to utilize high laser power (4-5c) to manipulate molecules; control was based on introducing into the system Hamiltonian, laser-molecule coupling terms of comparable size to interatomic potentials. A second thrust, "mode-selective excitation," emphasized selective excitation of particular bonds, which encourage reaction toward one channel. These

AUP  
72 COLINGWOOD ST  
MIDLAND CT  
Please return this slip on receipt

EX APR 1992

**URGENT**

**PROOFS - DO NOT DELAY**

Author

efforts were generally unsuccessful, although a few recent studies on molecules, in which local modes are excited (6-8), have shown some success.

These approaches attempted to take advantage of the power and frequency resolution of the laser. However, as we have recently shown (9-24), a third property, laser coherence, proves far more useful in the control of molecular processes. Specifically, manipulation of material phases, through use of laser phase, provides a general route for controlling molecular processes. We provide details of this approach in the next section. In the third section, we describe related contributions introduced from other perspectives, with a specific focus on pulse-shaping methods and optimal control theory. In the interest of historical accuracy, references (9-24) are referred to as work on the method of coherent control (CC).

## COHERENT RADIATIVE CONTROL OF MOLECULAR PROCESSES

Coherent radiative control of chemical reactions, which has been developed over the last five years (9-24), affords a direct method for controlling reaction dynamics by using coherence properties of weak lasers, with a large range of yield control expected in laboratory scenarios. In addition, the CC theory provides deep insights into the essential features of reaction dynamics and quantum interference, which are necessary to achieve control over elementary chemical processes. Below, we provide a schematic overview of coherent radiative control, including the general principles, and a survey of several experimental scenarios, which implement the principles of coherent control.

### The Essence of Control: Quantum Interference

Consider a chemical reaction that, at total energy  $E$ , produces several distinct products. The total Hamiltonian is denoted  $H = H_0 + V_q$ , where  $H_0$  is the Hamiltonian of the separated products in the arrangement channel labeled by  $q$ , ( $q = 1, 2, \dots$ ), and  $V_q$  is the interaction between products in arrangement  $q$ . We denote eigenvalues of  $H_0$  by  $|E, n, q^0\rangle$ , where  $n$  denotes all quantum numbers other than  $E$  (including scattering angles). Eigenfunctions of  $H$ , which correlate with  $|E, n, q^0\rangle$  at large product separation, are labeled  $|E, n, q^-\rangle$ . By definition of the minus states, a state prepared experimentally as a superposition  $|\psi(t=0)\rangle = \sum_n c_n |E, n, q^-\rangle$  has probability  $|c_n|^2$  of forming product in channel  $q$ , with quantum numbers  $n$ . Thus, control over the probability of forming a product in any asymptotic state is equal to the probability of initially forming the appropriate minus state that correlates with the desired product. The essence of control, therefore, lies in forming the desired linear

combination at the time of preparation. The essence of the coherent radiative control approach is to utilize phase and intensity properties of laser excitation to alter the character of the prepared state, so that production of the desired product is enhanced.

Note that a proper analysis of the relationship between the state of the molecule to be excited and the desired product is built upon the molecular eigenstates  $|E, n, q^-\rangle$ . Qualitative thinking in mode-selective chemistry, however, relies upon the idea of using lasers to excite specific bonds or modes in the reactant molecule in order to drive a reaction in a desired direction. The brief remarks above, elaborated upon elsewhere (18), make clear that the proper modes to excite in order to produce product in arrangement  $q$  are the eigenfunctions  $|E, n, q^-\rangle$ , the system's natural modes, if you will. (For a related discussion of the role of bound eigenstates in controlled *cis-trans* isomerization, see Ref. 25.) Thus, the extent to which excitation of some zeroth order state  $|\chi\rangle$  is successful in promoting reaction to the desired product  $q$  depends entirely on the extent to which  $|\chi\rangle$  overlaps  $|E, n, q^-\rangle$ .

Many of the proposed CC scenarios rely upon a simple way of achieving active control over the prepared state and product. Specifically, active control over products is achieved by driving an initially pure molecular state through two or more independent coherent optical excitation routes. The resultant product probability displays interference terms between these two routes, whose magnitude and sign depend upon laboratory parameters. Thus, product probabilities can be directly manipulated in the laboratory.

This approach has a well-known analogy: The interference between paths as a beam of either particles or of light passes through a double slit. In that instance, source coherence leads to either constructive or destructive interference, manifest as patterns of enhanced or reduced probabilities on an observation screen. With CC, the overall coherence of a pure state plus laser source allows for the constructive or destructive manipulation of probabilities in product channels.

Consider, as an example of coherent control, a specific scenario for unimolecular photoexcitation (13, 21) (Figure 4b), in which a system, initially in pure state  $|E\rangle$ , is excited to energy  $E$ , by simultaneous application of two CW fields  $\epsilon(t) = \epsilon_1 \epsilon_2 \cos[(\omega_1 + \theta_1)t] + \epsilon_1 \epsilon_2 \cos[(\omega_1 + \theta_2)t]$ , thus providing two independent, optically driven routes from  $|E\rangle$  to  $|E, n, q^-\rangle$ . Here,  $\epsilon_i$  ( $i = 1, 2$ ) denotes a unit vector in the  $i$ th field direction.

Straightforward perturbation theory, valid for the weak fields under consideration, gives the probability  $P(E, q; E_i)$  of forming product at energy  $E$  in arrangement  $q$  as

4b  
↑  
"b"

$$P(E, q; E_i) = P_3(E, q; E_i) + P_{13}(E, q; E_i) + P_1(E, q; E_i). \quad 1.$$

Here,  $P_3(E, q; E_i)$  is the probability arising from the one-photon route,

$$P_3(E, q; E_i) = \left( \frac{\pi}{\hbar} \right) \epsilon_i^2 \sum_{\mu} |\langle E, n, q^- | (\hat{\epsilon}_3 \cdot \mu)_{e, g} | E_i \rangle|^2, \quad 2.$$

where  $\mu$  is the electric dipole operator, and

$$\langle \hat{\epsilon}_3 \cdot \mu \rangle_{e, g} = \langle e | \hat{\epsilon}_3 \cdot \mu | g \rangle, \quad 3.$$

where  $|g\rangle$  and  $|e\rangle$  are the ground and excited electronic state wavefunctions, respectively. The second term is the photodissociation contribution from the three-photon route, given by

$$P_{13}(E, q; E_i) = \left( \frac{\pi}{\hbar} \right) \epsilon_i^2 \sum_{\mu} |\langle E, n, q^- | T | E_i \rangle|^2, \quad 4.$$

with

$$T = (\hat{\epsilon}_1 \cdot \mu)_{e, g} (E_i - H_g + 2\hbar\omega_1)^{-1} (\hat{\epsilon}_1 \cdot \mu)_{e, g} (E_i - H_e + \hbar\omega_1)^{-1} (\hat{\epsilon}_1 \cdot \mu)_{e, g}. \quad 5.$$

The final and most significant term  $P_{13}(E, q; E_i)$  arises from one-photon-three-photon interference:

$$P_{13}(E, q; E_i) = -2 \left( \frac{\pi}{\hbar} \right) \epsilon_i \epsilon_1^2 \cos(\theta_3 - 3\theta_1 + \delta^{\{q\}}) |F^{\{q\}}| \quad 6.$$

with the amplitude  $|F^{\{q\}}|$  and phase  $\delta^{\{q\}}$  defined by

$$|F^{\{q\}}| \exp(i\delta^{\{q\}}) = \sum_{\mu} \langle E_i | T | E, n, q^- \rangle \langle E, n, q^- | (\hat{\epsilon}_3 \cdot \mu)_{e, g} | E_i \rangle. \quad 7.$$

The branching ratio  $R_w$  for channels  $q$  and  $q'$ , can then be written as

$$R_w = \frac{P(E, q; E_i)}{P(E, q'; E_i)} = \frac{F^{\{q\}} - 2x \cos(\theta_3 - 3\theta_1 + \delta^{\{q\}}) \epsilon_0^2 |F^{\{q\}}| + x^2 \epsilon_0^2 F^{\{q\}2}}{F^{\{q'\}} - 2x \cos(\theta_3 - 3\theta_1 + \delta^{\{q'\}}) \epsilon_0^2 |F^{\{q'\}}| + x^2 \epsilon_0^2 F^{\{q'\}2}}, \quad 8.$$

where

$$F^{\{q\}} = \left( \frac{\hbar}{\pi} \right)^2 \frac{P_3(E, q; E_i)}{\epsilon_3^2},$$

$$F^{\{q'\}} = \left( \frac{\hbar}{\pi} \right)^2 \frac{P_3(E, q'; E_i)}{\epsilon_1^2}, \quad 9.$$

with  $F^{\{q\}}$  and  $F^{\{q'\}}$  defined similarly. Here,  $x = \epsilon_1^2/\epsilon_3$ , with  $\epsilon_1 = \epsilon \epsilon_0$ ; the quantity  $\epsilon_0$  essentially carries the unit for the electric field.

Both the numerator and denominator of Equation 8 display the canonical CC form, i.e. independent contributions from more than one route, modulated by an interference term. Because the interference term is controllable through variation of laboratory parameters (here, the relative intensity and relative phase of the two lasers), so, too, is the product ratio  $R$ .

As an example of this scenario, consider the photodissociation of IBr to produce I + Br and I + Br\*, obtained computationally with high quality potential surfaces and accurate photodissociation methods. A typical result is shown in Figure 1, which provides a contour plot of the Br yield as a function of relative laser phase and amplitude. The results show extensive control over the product ratio, with the yield ranging from 25–95% as relative laser phase and intensity are varied. Similar results are shown in Figure 2, but with the case of initial rotational state  $J = 42$ . Remarkably, no loss of control results from the extensive  $m$ , averaging included in the latter computation, nor is any strong  $J$  dependence evident.

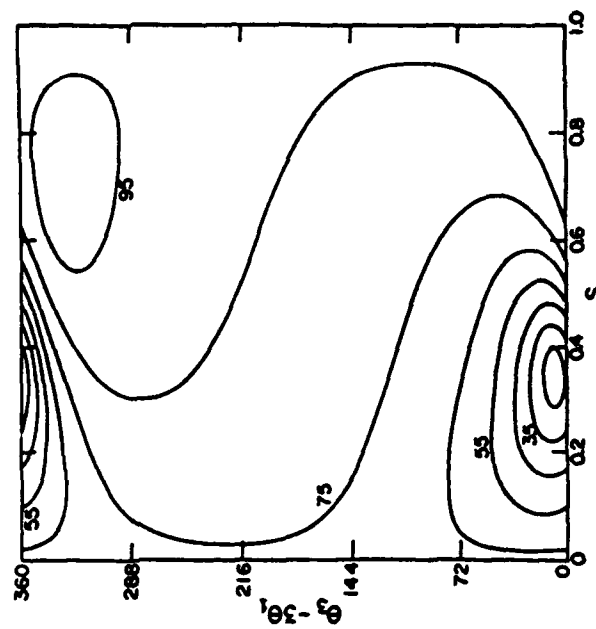


Figure 1 Contour plot of the yield of  $\text{Br}^*(2P_{1/2})$  as a function of relative phase angle and relative intensity [ $S = x^2/(1+x^2)$ ] IBr photodissociation from an initial state in  $X^1\Sigma_g^+$  with  $v = 0$ ,  $J = 1$ ,  $M_l = 0$ . Results arise from simultaneous  $(\omega_1, \omega_2)$  excitation ( $\omega_3 = 3\omega_1$ ) with  $\omega_1 = 6637.5 \text{ cm}^{-1}$ . (From Ref. 21; reprinted with permission of the American Physical Society.)

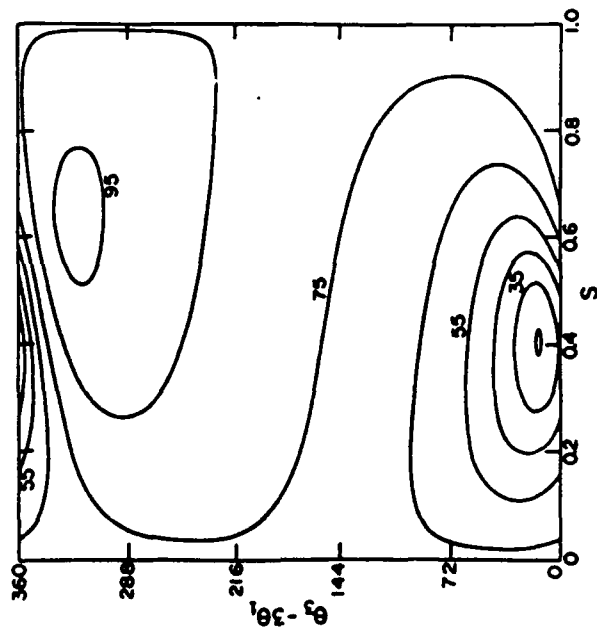


Figure 2 As in Figure 1, but  $M_f$  averaged with  $J_f = 42$ . (From Ref. 21; reprinted with permission of the American Physical Society.)

A related CC scenario (24), which invokes resonant two-photon + two-photon excitation routes, has proven to be equally impressive in a study of  $\text{Na}_2$  photodissociation. This particular approach has the advantage of canceling out possible deleterious effects caused by laser jitter, as well as providing a means of selective excitation from a thermal sample.

This three-photon + one-photon scenario has now been experimentally implemented in studies of Hg and HCl ionization through a resonant bound Rydberg state (26, 28). Specifically, in the work of Gordon and colleagues (27, 28), HCl is excited to a selected rotational state in the  $^3\Sigma^-(\Omega^+)$  manifold using  $\omega_1 = 336$  nm;  $\omega_2$  is obtained by third harmonic generation in a Krypton gas cell. The relative phase of the light fields was then varied by passing the beams through a second gas cell and varying the gas pressure. The population of the resultant Rydberg state was interrogated by ionizing to  $\text{HCl}^+$  with an additional photon. This REMPI type experiment showed that the  $\text{HCl}^+$  ion probability depended upon both the relative phase and intensity of the two exciting lasers, in accord with the theory described above. Figure 3 illustrates a sample result, in which the  $\text{HCl}^+$  signal oscillates as a function of gas pressure, i.e. as

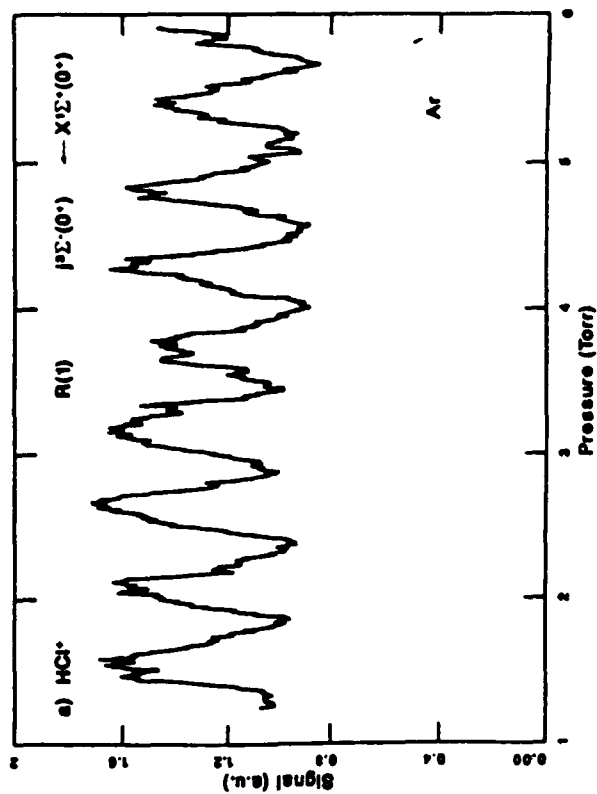


Figure 3 Modulation of  $\text{HCl}^+$  signal as a function of Argon gas pressure in the one-photon + three-photon excitation, and subsequent photoionization, of HCl. (From Ref. 28.)

a function of relative laser phase. In this case, control is achieved by simultaneous excitation to a nondegenerate bound state. As a consequence, there is no sum over  $n$  in Equations 2, 4, and 7; hence,  $|F^{(q)}F^{(p)}| = |F^{(q)}|^2$ . Satisfaction of this Schwartz equality ensures that the probability of forming the HCl Rydberg state can be varied over the full range of zero to unity (9). Specifically, setting  $\theta, -3\theta, = -\delta^{(q)}$  and  $\epsilon_3^2/\epsilon_1^2 = F^{(q)}/F^{(p)}$  gives zero probability in channel  $q$ . A similar phase control experiment has been performed on atoms in the simultaneous three-photon + five-photon ionization of Hg (26). Although the effect of the relative laser intensity was not studied, the  $\text{Hg}^+$  ionization probability was shown to be a function of relative phase of the two lasers. Because excitation is nonresonant in this case, this experiment shows the feasibility of control over continuum channels via interfering optical excitation routes.

In another laboratory study, photocurrent directionality, which we predicted to be achievable in semiconductors by using CC techniques with no bias voltage (14), has recently been demonstrated by using one-photon + two-photon interferences (29).

These experiments clearly show that coherent control of simple molec-

ular processes through quantum interference of multiple optical excitation routes is both feasible and experimentally observable. Further experimental studies designed to show control over processes with more than one product channel are in progress by several experimental groups.

*The Essential Principle and Assorted CC Scenarios*

The three-photon + one-photon case is but one example of a scenario that embodies the essential principle of coherent control, i.e. that coherently driving a pure state through multiple optical excitation routes to the same final state allows for the possibility of control. Given this general principle, numerous scenarios may be proposed to obtain control in the laboratory. Such scenarios must, however, properly account for several factors that reduce or eliminate control. We briefly discuss four such features.

1. Adherence to selection rule requirements: Control requires that the interference term [e.g.  $F^2$ ] arising between optical routes is nonzero. In general, this is the case only if the various optical excitation routes satisfy specific rules regarding conserved integrals of motion. For example, consider the one-photon + three-photon case discussed above. Here, excitation from, for example,  $J = 0$ , where  $J$  is the rotational angular momentum, yields  $J = 1$  for the one-photon route, and  $J = 1$  and  $J = 3$  for the three-photon route. Selection rules are such that only final states with the same  $J$ , here  $J = 1$ , interfere.

2. Minimize extraneous and parasitic uncontrolled satellites: The  $J = 3$  state created by three-photon absorption in the above scenario is an example of a satellite state, i.e. an uncontrolled (and, hence, undesired) product state that arises in the course of the photoexcitation. Effective scenarios must ensure that such contributions are small, compared with the controlled component.

3. Ensure properly treated laser spatial dependence and phase jitter: Because the ability to manipulate the laser relative phase accurately is crucial to CC, one must account for all laboratory features that affect the phase. For example, scenarios must be designed to eliminate effects caused by the  $\mathbf{k} \cdot \mathbf{R}$  spatial dependence of the laser phase. Not to do so would result in the diminution of the control that results from the variation of this term over the molecule beam-laser beam intersection volume.

4. Allow maintenance of coherence over time scale associated with any true relaxation processes, e.g. collisions: Proposed scenarios must maintain phase coherence in the face of possibly dephasing effects (e.g. collisions or partial laser coherence). The collision and laser incoherence studies mentioned below indicate that control can survive moderate levels of such phase destructive processes (15).

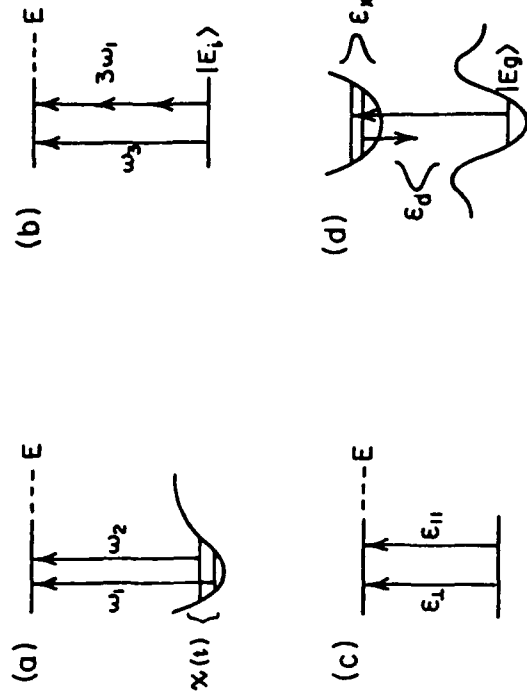


Figure 4 Assorted coherent control scenarios.

Thus far, we have proposed several different scenarios for coherent control. They are summarized in Figure 4 and discussed briefly below.

Figure 4b shows the three+one-photon route discussed above. The original CC scenario (9) is shown in Figure 4b in which two bound states prepared in a superposition state  $|\chi(t)\rangle = c_1|E_1\rangle + c_2|E_2\rangle$  are photo-dissociated with two fields  $\epsilon(t) = \epsilon_1 \cos[(\omega_1 + \theta_1)t] + \epsilon_2 \cos[(\omega_2 + \theta_2)t]$ , which lift the levels to energy  $E$  (undesired satellite excitations are not indicated in the figure, but are included in the full computation). An analysis of this very basic scenario (9) gives the probability  $P(E, q)$  of forming product in product arrangement channel  $q$  as

$$P(E, q; E_i) = \epsilon_1^2 \mu_{i,1}^{(q)} + 2\epsilon_1 \epsilon_2 \cos(\theta_1 - \theta_2 + \alpha_i^{(q)}(E)) |\mu_{i,2}^{(q)}|^2 + \epsilon_2^2 \mu_{i,2}^{(q)} \quad 10.$$

where

$$\mu_{i,k}^{(q)}(E) \equiv |\mu_{i,k}^{(q)}(E)| e^{i\alpha_i^{(q)}(E)} = \sum_n \langle E, n, q^- | \mu | E_i \rangle \langle E_k | \mu | E, n, q^- \rangle \quad 11.$$

Here forming the ratio as in Equation 8 shows that the ratio is a function of the relative laser phase  $\theta_1 - \theta_2$  and relative laser intensity  $(\epsilon_1/\epsilon_2)^2$ . This basic mechanism (9) has been examined in the gas phase, primarily for the photodissociation of  $\text{CH}_3\text{I}$  to form  $\text{CH}_3 + \text{I}$  versus  $\text{CH}_3 + \text{I}^*$ , both in the absence (9, 10) and presence (15) of collisions. In the former case, sub-

above

4b

4a

NO

[i.e.  $\frac{q}{k}(\epsilon)$ ]

Resulting

stantial control (e.g. 35–75% of  $I^0$ ) was obtained by varying the field properties. In the latter case, saturating the transition between the two bound levels allowed for the maintenance of control into the range of reasonable temperatures (15). That is, as long as coherence survives, control persists.

A theoretically straightforward extension of this scenario to include far more levels and dissociating laser frequencies is conceptually enlightening. Specifically, for the case in which there are  $N$  final product states, the use of  $N$  bound states in the initial superposition, followed by excitation with an equal number of frequencies carrying all levels to energy  $E$ , allows for total control (i.e. 0–100%) over the product arrangement channels. This result provides a useful theorem, which proves total control in the perturbation theory regime.

The two-level scenario (Equation 10) has also been applied (30) to examine photodissociation and control of Na<sub>2</sub>, where stimulated emission pumping is used to prepare the ground state superposition, and control over atomic products is examined. Results show a wide range of control for excitation from initial pairs of vibrationally excited levels. In addition, this scenario has been suggested as a means of controlling currents in semiconductors without bias voltage (14). Basically, we form a superposition of bound states of a shallow donor. Photoionizing the superposition leads to three terms, similar to those in Equation 11. Two terms correspond to photoionization of the individual levels, and the third to interference between them. Only the third term, controllable by manipulating relative laser intensity and phase, is anisotropic, thus leading to a directional current that is controllable. Finally, Mandel and coworkers (31a,b) have independently examined this scenario for the case of three bound levels, with attention focused on absorption of radiation into the uppermost level. Simple considerations show the ability to suppress absorption to the upper level, which leads to interesting suggestions for lasing without population inversion.

We note one final application in the domain of CW lasers (12). Specifically, the scenario in Figure 4b may be simplified to that shown in Figure 4c, in which the two independent optical routes to the continuum are the parallel and perpendicular components of a single electric field. Control here is also achieved by varying the relative field intensities and phases, which is equivalent to varying the degree of laser elliptic polarization. However, control is restricted to the product ratio in the differential cross-section; the interference contribution to the total cross-section vanishes, because these two routes reach different values of the angular momentum projection  $M_J$ . Results in this case show that total control (variations of the yield from 0–100%) results for diatomics initially in a well-defined  $M_J$

state. If this is not the case, then control survives for some  $M_J$  averaged cases, such as  $\Sigma \rightarrow \Pi$  transitions.

Developments in pulsed-laser technology may be used to advantage in a straightforward modification of the above scenario, as shown in Figure 4d. Specifically, the superposition state preparation and subsequent excitation with frequencies  $\omega_1, \omega_2$  may both be carried out by using pulsed lasers in accord with Figure 4d. In this instance, the frequencies required to excite to energy  $E$  are contained within the second excitation pulse, which also creates product, and the associated interference contributions over a wider energy range. Multiple excitation paths are contained within this overall pump-pump excitation scheme and serve to introduce the necessary interfering coherent paths.

In general, the initial excitation pulse,  $\bar{\epsilon}_x(t)$ , creates a linear superposition state in the excited state, and the temporally separated dump pulse,  $\bar{\epsilon}_d(t)$ , brings the system to  $E$ , where product is energetically accessible. The state prepared after the  $\bar{\epsilon}_x(t)$  is given in first order perturbation theory by

$$|\phi(t)\rangle = |E_p\rangle e^{-iE_p t/\hbar} + \sum_j c_j |E_j\rangle e^{-iE_j t/\hbar} \quad 12a.$$

with

$$c_j = (\sqrt{2\pi/\hbar}) \langle E_j | \mu | E_p \rangle \epsilon_x(\omega_{jp}) = d_j \rho_x(\omega_{jp}) \quad 12b.$$

where  $\omega_{jp} = (E_j - E_p)/\hbar$ , the excitation frequency to level  $|E_p\rangle$ , and where  $d_j$  is defined by the second equality. Note that  $\epsilon_x(\omega)$  or  $\epsilon_d(\omega)$  denote the Fourier transform of the respective laser pulse.

Subsequently, the system is subjected to the dump pulse, and perturbation theory, plus the rotating wave approximation, gives the probability  $P(E, q)$  of forming product in arrangement channel  $q$  at energy  $E$  as

$$P(E, q) = (2\pi/\hbar^2) \sum_j \left| \sum_n c_n \langle E, n, q^- | \mu | E_j \rangle \epsilon_d(\omega_{Ej}) \right|^2 \quad 13.$$

where  $\omega_{Ej} = (E - E_j)/\hbar$ , and  $c_j$  is given by Equation 12.

Expanding the square gives the canonical form

$$\begin{aligned} P(E, q) &= (2\pi/\hbar^2) \sum_{ij} c_i c_j^* \epsilon_d(\omega_{Ej}) \epsilon_d^*(\omega_{Ei}) \mu_{ij}^{(q)}(E) \\ &= (2\pi/\hbar^2) \sum_{ij} d_i d_j^* \epsilon_x(\omega_{jp}) \epsilon_x^*(\omega_{ip}) \epsilon_d(\omega_{Ej}) \epsilon_d^*(\omega_{Ei}) \mu_{ij}^{(q)}(E). \end{aligned} \quad 14.$$

Equation 14 shows coherence created in the initial excitation, which is subsequently utilized to alter the product state in the deexcitation step. Because picosecond pulses are easily generated, it is important to note that

it suffices to create this coherence by excitation of only two levels (16, 19). Under these circumstances, and assuming Gaussian pulses for convenience,  $P(E, q)$  is given by

$$P(E, q) = (2\pi/\hbar^2) [|c_{11}|^2 \mu_{11}^{(0)} + |c_{22}|^2 \mu_{22}^{(0)} + 2|c_{12}|^2 \mu_{12}^{(0)} e^{-i\phi}] \cos(\omega_2 \Delta t + \alpha_{12}^{(0)}(E) + \beta), \quad (15)$$

with  $\Delta t = (t_2 - t_1)$  and  $\langle E_1 | \mu | E_2 \rangle \langle E_2 | \mu | E_1 \rangle \equiv |E_1 \mu E_2| |E_2 \mu E_1| e^{i\phi}$ . Integrating over  $E$  to encompass the width of the second pulse produces  $P(q)$ ; the controllable quantity of interest is then the yield  $Y = P(q)/(\sum_i P_i(q))$ .

The laboratory control parameters are the time delay  $\Delta t$  between the pulses and the coefficients  $c_i$  of the initially created superposition, controlled via properties of the initial excitation pulse. Below, the latter is varied by changing the energy of the excitation pulse.

The scenarios involving two bound levels described above are not restricted to two-state problems. Rather, we recognize that two levels are sufficient to carry the necessary phase information to allow control over the relative yield. That is, lasers with narrow frequency profiles (i.e. long pulses in time) are sufficient. Indeed, as the molecules increase in size, and the density of states increases, longer and longer pulses could be used, and two intermediate levels retained. There appears little advantage to the inclusion of more than two levels, a situation that would result if the pulses were considerably shorter in time.

We have applied this scenario to model  $DH_2$  (16), to IBR photo-dissociation (19), and to selective bond breaking in HOD photo-dissociation. Figure 5 illustrates sample results for the IBR case, in which a contour plot of the Br yield is shown as a function of the energy of the excitation pulse and the delay time between the two pulses. Control is almost complete, with relatively small changes in the detuning or in the time delay, which is in the convenient picosecond domain, thus resulting in yields that vary from 4–96%.

In a related study, Metiu & Engel (33) have examined the effect of pump coherence on pump-probe experiments, in which the pump causes molecular predissociation. In this case, their initial excitation prepares a linear combination of continuum, rather than bound, states, which are subsequently pumped to a higher state. The studies show, in accordance with the discussion above, that the coherence established by the pump leads to oscillations in the dependence of the two-pulse laser-induced fluorescence signal on the delay time between pulses.

In a rather unique application of this coherent control scenario, we have examined the possibility of bond breaking in the prochiral molecule ABA',

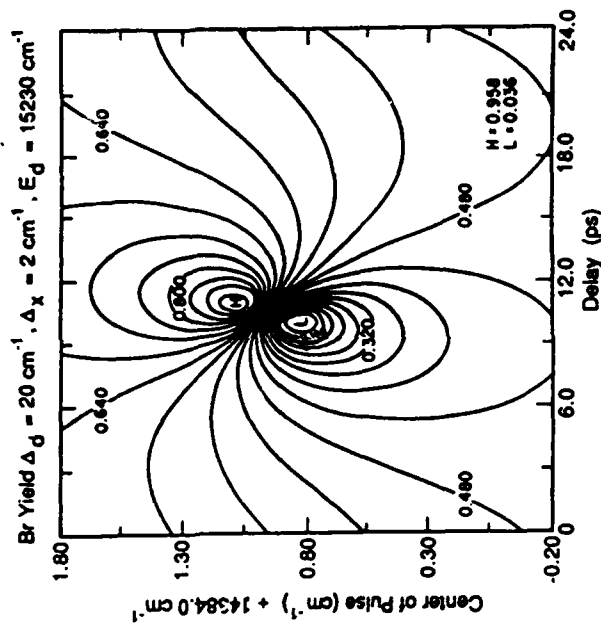


Figure 5 Contour plot of the yield of Br in the photodissociation of IBR, which uses the scheme in Figure 4d. Control parameters are the energy of the excitation pulse and the time delay between pulses. Also shown are the widths  $\Delta_n$ ,  $\Delta_s$  of the excitation and dump pulses. (From Ref. 19; reprinted with permission of the American Physical Society.)

where A and A' are enantiomers (34). Control over channel yield would correspond to the ability to alter the yield of  $A + BA'$  versus  $AB + A'$ , i.e. controlled production of a given enantiomer via a nonchiral external perturbation, starting with an achiral molecule. [One example, which requires a slight extension of the BAB' notation, is the Norrish type II reaction:  $D(CH_2)_3CO(CH_2)_2D'$ , which dissociates to  $DCHCH_2 + D'(CH_2)_3COCH_3$  and  $D'CHCH_2 + D(CH_2)_3COCH_3$ , where D and D' are enantiomers.] Studies show that such control could be achieved when the observation is restricted to states with well-defined projection of the total angular momentum (i.e.  $M_J$ ) along the z axis (34).

This pump-dump type scheme has also been applied to control bimolecular reactions (22). In this case, the initial excitation is from the continuum ground electronic state to a bound excited electronic state, followed by a dump back down to the ground electronic state. Significant control results only in the energy domain that is essentially below reaction threshold. Above threshold, the interference term does not effectively compete with the energetically allowed reaction.

Studies of the pump-dump scenario that use very large numbers of intermediate levels  $|E_i\rangle$  have been independently developed and advocated by Rice and coworkers (35-39). In this instance, the initially created state is spatially localized, as is the wavefunction that results from the subsequent deexcitation. This is achieved by using ultrafast laser pulses, which create states over numerous levels. This approach is discussed in further detail in the next section.

Finally, Jiang, Shapiro, and Brumer have studied the effect of partial laser coherence on this scenario. In this case, Equation 14 is extended to include partial coherence by averaging the laser field over an ensemble of phases and intensities that model the density matrix of the laser field; that is, Equation 14 becomes

$$P(E, g) = (2\pi/\hbar^2) \sum_{ij} d_i d_j^* \langle \epsilon_i(\omega_{ij}) \epsilon_j^*(\omega_{ij}) \rangle \langle e_A(\omega_{EE}) e_B^*(\omega_{EE}) \rangle \mu_{ij}^{(g)}(E) \quad 16.$$

with the frequency-frequency correlation functions given by models discussed elsewhere (40, 41). The results of model computational studies suggest that modest amounts of laser incoherence in the excitation pulse can be tolerated. Significantly larger amounts of incoherence in the de-excitation pulse allow control to persist, as long as the matrix elements  $\mu_{ij}^{(g)}(E)$  do not vary significantly over the width of the deexcitation pulse.

### The Status of Coherent Control

We have provided a capsule summary of the current status of coherent control of chemical reactions and molecular processes. Three essential points should be emphasized: Theoretical studies show that control over molecular processes, via simple quantum interference, is possible. Computational results show that such control can be extensive, with achievable variations in yield close to the full possible range of 0-100%. And, experimental studies have shown that the proposed CC scenarios are feasible in the laboratory.

## PULSE SHAPING AND OPTIMAL CONTROL THEORY

Concurrent with ideas in CC, Rice, Tannor, and coworkers (35-37) initiated an alternative approach to molecular control. Their original idea was to use a (Gaussian) pulse to create a localized wavepacket ... a bound excited state. Then, during the very short residence time of the wavepacket above the exit channel of the product of interest, they "dumped" it down on the ground state by using a second strong pulse (35). This scheme has obvious appeal, but even their initial variational analysis indicated that it

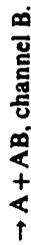
is unclear which pulses would best do the job. For example, the wavepacket, once created, is expected to disperse quickly and not remain localized. The solution to this problem was to abandon intuition [often based on classical simulations (35, 36)] in favor of a more systematic pulse optimization scheme, i.e. the use of optimal control theory (OCT) methods (38, 39), emanating from the work of Rabitz and coworkers (43-52) and Manz and coworkers (53-59).

In the next section, we first outline the general principles of OCT, as emerging from the work of the various groups involved in the field, and then analyze specific cases.

### General Principles of OCT

Whereas CC is a linear theory, in which one maximizes the long-time  $P(E, g; E_i)$  probabilities by using weak fields, OCT is a nonlinear theory involving strong laser pulses, in which one attempts to attain these, as well as more general, objectives. Most such general objectives can be expressed as the production of a specified wavefunction  $\Phi$  at a specified time  $t_f$ , given a wavefunction  $\Psi(t_0)$  at time  $t_0$ . Clearly, because of the more general scope, even the partial attainment of such an objective usually results in the loss of the relative simplicity of the perturbative regime.

The general principles of OCT are best understood via a case study presented by Rice and coworkers (38, 39), in which the objective is to concentrate a wavefunction in one of the exit channels of a bifurcating chemical reaction:



Defining this wavefunction as  $\Phi$ , the objective is to maximize

$$J = \langle \Psi(t_f) | P | \Psi(t_f) \rangle \quad 17.$$

where  $P \equiv |\Phi\rangle \langle \Phi|$  is a projection operator on the state of interest.

The maximization of  $J$  is subject to a set of physical and practical constraints that make the optimization problem meaningful. For example, we usually wish to solve the optimization problem for a laser pulse of a given total energy  $\bar{\epsilon}$ . This results in the (practical) constraint equation,

$$\int_{t_0}^{t_f} dt |\epsilon(t)|^2 - \bar{\epsilon} = 0. \quad 18.$$

Dynamics are introduced as an additional constraint. In this case, it is that  $\Psi$  is a solution of the time dependent Schrödinger equation,

$$[i\hbar\partial/\partial t - H(t)]\Psi = 0.$$

For example, in the two-state problem considered by Tannor and coworkers (35-37), Kosloff et al (38), Seideman et al (16), and Levy et al (19),  $\Psi$  is a two-component state-vector

$$\Psi \equiv \begin{pmatrix} \psi_a \\ \psi_b \end{pmatrix}$$

and  $H(t)$ —the full time-dependent Hamiltonian—is a  $2 \times 2$  matrix,

$$H(t) \equiv \begin{pmatrix} H_a & -\mu_{ab} \cdot \epsilon(t) \\ -\mu_{ba} \cdot \epsilon^*(t) & H_b \end{pmatrix}$$

where  $\mu_{ab}$  is the transition dipole moment of Equation 3.

The problem of maximizing the objective  $J$ , subject to the above constraints, is transformed into an unconstrained problem by adding Equations 18 and 19, multiplied respectively by  $\lambda$  and  $i\langle\chi|$ , where  $\chi$  is a two-component state-vector,

$$\chi \equiv \begin{pmatrix} \chi_a \\ \chi_b \end{pmatrix},$$

to Equation 17. The resulting unconstrained objective,

$$J = \langle \psi(t_f) | P | \psi(t_f) \rangle + \lambda \left[ \int_{t_0}^{t_f} |\epsilon(t)|^2 - \epsilon \right] + i \int_{t_0}^{t_f} dt [\langle \chi | i\hbar\partial/\partial t - H | \psi \rangle + c.c.], \quad 22.$$

is maximized by imposing the  $\delta J = 0$  condition. When this is done, it follows from Equation 22 that (38)

$$i\hbar\partial\chi/\partial t = H\chi,$$

with the boundary condition,

$$\chi(t_f) = P\psi(t_f).$$

The optimum field is then related to the above solutions and  $\lambda$  as

$$\epsilon(t) = O(t)/\lambda,$$

where

$$O(t) = i[\langle \chi_a | \mu_{ab} | \psi_b \rangle - \langle \psi_a | \mu_{ba} | \chi_b \rangle].$$

$\lambda$  can now be obtained by substituting Equation 24a in Equation 18 as

$$\lambda = \pm \frac{\left( \int_{t_0}^{t_f} dt |O(t)|^2 \right)^{1/2}}{\left( \int_{t_0}^{t_f} dt |O(t)|^2 \right)^{1/2}}, \quad 25a.$$

and  $\epsilon(t)$  can be written in a closed form, obtained from Equations 24a and 25a, as

$$\epsilon(t) = O(t) \left( \int_{t_0}^{t_f} dt |O(t)|^2 \right)^{-1/2}. \quad 25b.$$

The above set of equations gives rise to an iterative procedure, which starts by guessing some  $\epsilon(t)$  function. One then determines  $H(t)$ , by using Equation 21, and  $\psi(t)$ , by propagating it from  $t_0$  to  $t_f$  by using Equation 19. The final value of  $\chi$ , which, by Equation 23b gives  $\psi(t_f)$ , is used to obtain  $\chi(t)$  from Equation 23a for all  $t < t_f$ . An improved guess for  $\epsilon(t)$  is obtained from Equations 24b and 25b, and the whole procedure is repeated until convergence.

This is essentially the procedure adopted by Kosloff et al (38), who studied the  $\text{HHD} \rightarrow \text{H}_2 + \text{D}$ ,  $\text{H} + \text{HD}$  dissociation reaction; Amstrup et al (42) who studied the control of the  $\text{HgAr}$  and  $\text{I}_2$  photodissociation; Hartke et al (56), who looked at the control of the  $\text{Br}^*/\text{Br}$  branching ratio in the photodissociation of  $\text{Br}_2$ ; and Jin et al (57), who studied the control of population inversion between two displaced harmonic oscillators. In all cases, it is possible to increase the yield of the desired product appreciably by optimizing the pulse shape. Although the increase in yield relative to the zero order guess is dramatic, the final selectivity is often much less than that obtained in the linear regime by the CC procedure. This has been explicitly shown in the HHD case for the Rice-Tannor potential (16).

The fact that OCT may sometimes give poorer results than CC arises from the difficulty involved in globally maximizing the objective functional and from the nonlinear nature of the theory. Even the choice of constraints, such as the range of laser power via the energy (Equation 18), seriously affects the solution. Thus, for example, weak-field CC results, which give superior yield control, will not emerge from the standard strong field considerations of OCT. Indeed, the very existence of a unique solution is not guaranteed. This point has been investigated in the context of square integrable functions by Peirce et al (45) and for unbounded systems by Rice and coworkers (50, 51), who proved the existence of an optimal solution under certain conditions. In contrast, Yao et al (52) show that

nonlinearities may give rise to multiple solutions, each of which produces exactly the same physical effect on the molecule.

As Kosloff et al (38) have discussed, global optimization is a difficult procedure, which involves search in a complex function space. (See, however, Ref. 57 for a description of an improved search routine that uses conjugate gradient methods.) The search is difficult, because each step necessitates solving the time-dependent Schrödinger equation, which although done very efficiently, is still time consuming (60-62).

An additional complication arises because of uncertainties in the parameters of the system to be optimized, the most obvious such parameter being the Hamiltonian itself (interaction potentials are only rarely known to sufficient accuracy). In CC, the experimentalist does not really need a theoretical evaluation of the molecular matrix elements that appear in the control equations (e.g. Equations 8 and 15). Rather, if necessary, these parameters, which are coefficients of a quadratic expression, can be evaluated experimentally, by making a preliminary scan of the external laser parameters and fitting to the quadratic form. By contrast, OCT, which is a nonlinear theory and necessitates the full solution of the Schrödinger equation at every iteration stage, is much more sensitive to these uncertainties. This point has been thoroughly analyzed by Dahleh et al (49), who proposed strategies for designing optimal pulses that would be least sensitive to errors in the molecular Hamiltonians. Basically, they recommend pulses that prohibit the wavepacket from venturing into regions of uncertainty.

The pulses recommended by Dahleh et al (49) may not always yield the best results as far as objectives. In fact, Rice and coworkers (38, 39) show great sensitivity of the outcome to even slight changes in pulse shapes. The frequency and time representation of their optimal pulses shows surprisingly small difference between pulses designed to select the AA + B channel versus the AB + A channel. This means that one has to tailor these pulses very carefully to achieve the desired product. Thus, in spite of the great progress in pulse shaping (63-65d), the resulting optimal fields may be difficult to generate in the lab because of their complexity. This problem can be made easier by smoothing the pulses. As Amstrup et al (42) have shown (66a) it is often possible to do almost as well as in the full optimization by restricting the last stages of the iteration to a search in a space spanned by two Gaussian pulses.

There is, as yet, no direct experimental confirmation of the effect of the pulse shapes recommended by OCT. The role of the phase between two pulses, predicted in CC studies (16, 19, 34) and in OCT by Rice and coworkers (38, 39), has been confirmed experimentally by Fleming et al (66a,b), who showed that fluorescence from I<sub>2</sub> in the B-state is influenced by constructive or destructive interference between two wavepackets

induced by two phase-locked excitation pulses. (For a study of the dependence of the sensitivity of such experiments to the potential energy surfaces, see Ref. 67.) The study of Fleming et al ties in with a large volume of work on wavepacket interferometry in atoms (68-70), as well as with the femtochemistry experiments of Zewail and coworkers (71a-d), where similar effects were seen in absorption.

### Case Studies in Pulse Shaping

Perhaps the simplest objective is to control the population of a given vibrational state. The interest in this topic dates back to the early days of Infrared Multi-Photon Dissociation (IRMPD) (72). The idea was to populate a given vibrational state preferentially, "before intra-molecular vibrational relaxation (IVR) sets in." Thus, one could "beat" IVR by populating a given level while it remains "pure."

Whenever the lowest (*N*) order perturbation theory for the *N*-photon problem is valid, it is possible to generate a zero-order bright state. This can be shown as follows: We write every (field-free) energy eigenstate  $|E_n\rangle$  as a linear combination of a bright state  $|\phi\rangle$ , and dark states,  $|X_m\rangle$ ,

$$|E_n\rangle = |\phi\rangle \langle\phi|E_n\rangle + \sum_m b_{m,n} |X_m\rangle, \quad 26.$$

where the dark states are defined such that,

$$\langle E_i | T^{(N)}(\omega) | X_m \rangle \approx 0, \quad 27.$$

with  $|E_i\rangle$  denoting the initial state. Here,  $T^{(N)}(\omega)$  is the lowest order *N*-photon transition operator (the *N*-photon analogue of the three-photon operator of Equation 5), given by

$$T^{(N)}(\omega) = \prod_{k=1,2,\dots,N-1} [\hat{\epsilon} \cdot \mu(E_k - H + k\hbar\omega)]^k |\hat{\epsilon} \cdot \mu\rangle, \quad 28.$$

where *H* is the field free Hamiltonian for one or more electronic states. For one-photon transition  $T^{(N)}(\omega) = \hat{\epsilon} \cdot \mu$ .

An optical pulse

$$\epsilon(t) = \int d\omega \epsilon(\omega) [\exp(-i\omega t) + c.c.], \quad 29.$$

where  $t \equiv t - z/c$ , and *z* is the direction of propagation, will create, in the perturbative limit at the end of the pulse, a superposition-state of the form,

$$\begin{aligned} |\psi(t)\rangle &= \frac{2\pi i}{\hbar} \sum_n \hat{\epsilon}^{(N)}(\omega_n) |E_n\rangle \langle E_n | T^{(N)}(\omega_n) | E_i \rangle \exp(-iE_n t/\hbar) \\ &= \frac{2\pi i}{\hbar} \sum_n \langle \phi | T^{(N)}(\omega_n) | E_i \rangle \hat{\epsilon}^{(N)}(\omega_n) | E_n \rangle \langle E_n | \phi \rangle \exp(-iE_n t/\hbar). \end{aligned} \quad 30.$$

where  $\omega_n \equiv [(E_n - E_0)/N\hbar]$ ,  $\tilde{\epsilon}(\omega_n) \equiv \epsilon(\omega_n) \exp(i\omega_n \tau/c)$ . We have used Equation 27 in the last equality.

If the band-width of the pulse is large enough (i.e. a sufficiently short pulse), and  $\omega_n$  is far from an intermediate resonance (or the power broadening is large enough to smooth out such resonances), we can assume that  $T^{(M)}(\omega_n) \tilde{\epsilon}^*(\omega_n)$  varies more slowly with  $n$  than  $\langle E_n | \phi \rangle$ . Under these circumstances, we can take  $T^{(M)}(\omega_n) \tilde{\epsilon}^*(\omega_n)$  out of the sum of Equation 30, as some constant  $T^{(M)}(\bar{\omega}) \tilde{\epsilon}^*(\bar{\omega})$ , and obtain

$$|\psi(t)\rangle = \frac{2\pi i}{\hbar} \langle \phi | T^{(M)}(\bar{\omega}) | E_n \rangle \tilde{\epsilon}^*(\bar{\omega}) \sum_n \langle E_n | \phi \rangle \exp(-iE_n t/\hbar) \quad 31.$$

$$= \frac{2\pi i}{\hbar} \langle \phi | T^{(M)}(\bar{\omega}) | E_n \rangle \tilde{\epsilon}^*(\bar{\omega}) \exp(-iHt/\hbar) |\phi\rangle. \quad 31.$$

It follows from Equation 31 that immediately after the pulse ( $t = 0$ )

$$|\psi(0)\rangle = A |\phi\rangle, \quad 32.$$

where  $A = 2\pi i/\hbar \langle \phi | T^{(M)}(\bar{\omega}) | E_n \rangle \tilde{\epsilon}^*(\bar{\omega})$ . Hence, we see that in the perturbative regime, a short enough pulse can, indeed, create the pure zero-order bright state at  $t = 0$ .

Postponing the discussion of whether this zero-order state is desired, from the photochemical point of view, we note that this result can be generalized to the multiphoton case for strong fields. Larsen & Bloembergen (73) noted that an  $M$ -level oscillator with the right anharmonicity,

$$E_v = E_0 + \hbar\nu[\omega_{1,0} - \Delta^*(v-1)], \quad 33.$$

where  $\omega_{1,0}$  is a basic harmonic frequency and  $\Delta^*$  is the anharmonicity constant, which is driven from the ground state by a CW field

$$\epsilon(t) = \epsilon_0 \cos(\omega t), \quad 34.$$

is equivalent to a two-level system. This can be shown by expanding the system wavefunction in  $\phi_v$ —the energy eigenstates of the oscillator,

$$|\psi(t)\rangle = \sum_v a_v \phi_v \exp(-iE_v t/\hbar). \quad 35.$$

The set of coupled equations for the  $a_v$  coefficients assumes the form,

$$i \frac{d}{dt} a_v = [(n-v) - S_n] a_v - F_0 [(v+1)^{1/2} a_{v+1} + v^{1/2} a_{v-1}],$$

$$v = 0, 1, 2, \dots, M, \quad 36.$$

where,  $\tau \equiv \Delta^* t$  is a dimensionless time,

$$S_n \equiv n-1 - (\omega_{1,0} - \omega)/\Delta^*,$$

and

$$F_0 \equiv \mu_{1,0} \epsilon_0 / (2\hbar \Delta^*) \quad 38.$$

is a dimensionless "Rabi frequency."

If  $F_0 \ll 1$ , the above set of equations is identical to a two-level system,

$$i \frac{d}{dt} a_0 = -F_0^n a_n,$$

$$i \frac{d}{dt} a_n = S_n a_n - F_0^n a_0, \quad 39.$$

where,

$$F_0^n = F_0^n / [(n-1)!(n!)^{1/2}]. \quad 40.$$

These equations are solved in the usual way to yield,

$$P_n(\tau) \equiv |a_n(\tau)|^2 = (F_0^n / \Omega_n)^2 \sin^2 \Omega_n \tau \quad 41.$$

where

$$\Omega_n = \left\{ [S_n(n/2) + (F_0^n)^2]^{1/2} \right\} N_0 - \text{used later} \quad 42.$$

is the  $n$ -photon Rabi frequency.

When  $\omega$  is tuned to the  $n$ -photon resonance frequency,

$$\omega = \omega_{1,0} - \Delta^*(n-1), \quad 43.$$

$S_n = 0$ , and  $P_n(\tau)$  reaches unity for  $\tau_p = \pi/(2\Omega_n)$ . Because the validity of this result depends on  $F_0 \ll 1$ ,  $\tau_p \gg 1$  and the time taken to attain complete population transfer to the  $n$ th level is very long. The same applies to the use of optimal pulses in populating rotational states (48) and to the use of adiabatic switching (78-79), by which one can transfer populations to any desired level by using two coherent CW beams. If one wants to "beat" IVR, these times are not fast enough.

Larsen & Bloembergen (73) found that an increase in  $F_0$ , which shortens  $\tau_p$ , results in complete loss of selectivity. Basically, the power broadening increases so much that all  $n$ -photon resonances overlap. The situation has been remedied by Paramonov et al (74a-c) who showed, in complete agreement with the argument given above for the population of a bright state, that the use of a short pulse does not result in the coalescence of the  $n$ -photon resonances, even when  $F_0$  is increased. This results in selective excitation, which is achieved over very short times (essentially the pulse duration).

Paramonov used a laser pulse of the form,

$$\epsilon(t) = \epsilon_0 \sin^2(\alpha t) \cos(\omega t), \quad 44.$$

with  $\alpha \ll \omega$ . The set of equations analogous to Equation 36 is now of the form,

$$i \frac{d}{dt} a_v = [(n-v) - S_n] v a_v - F_0 \sin^2 \left( \frac{\alpha t}{\Delta} \right) [(v+1)^{1/2} a_{v+1} + v^{1/2} a_{v-1}],$$

$$v = 0, 1, 2, \dots, M. \quad 45.$$

When these equations are solved, it is possible to excite any level  $n$  preferentially, depending on the values of  $\omega$ ,  $F_0$ , and  $\alpha$  (74a-c).

The pulse considered by Paramonov can be thought of as a sum of three rectangular pulses,

$$\epsilon(t) = \epsilon_0 \{ 2 \cos(\omega t) - \cos[(\omega + \alpha)t] - \cos[(\omega - \alpha)t] \}, \quad 46.$$

which have two additional frequencies, as compared with the pulse of Equation 34. Thus, on top of the shortness of the pulse, multiphoton excitation with  $\sin^2(\alpha t)$  modulation is more efficient, because it provides additional frequencies that help overcome bottlenecks. In fact, a pulse of the type,

$$\epsilon(t) = \epsilon_0 \sin^{2m}(\alpha t) \cos(\omega t), \quad 47.$$

which has also been considered by Paramonov & Savva (75), has, depending on the value of  $m$  and  $\alpha$ , all the "right" resonance frequencies for a sequential multiphoton process, as

$$\epsilon(t) = \epsilon_0 \sum_{k=-m}^m C_k \cos[(\omega + 2k\alpha)t]. \quad 47$$

By comparing  $\omega + 2k\alpha$  with the level spacing  $\omega_{1,0} - 2v\Delta^0$ , we see that all the anharmonic frequencies, up to level  $m$ , are contained in the pulse, provided we choose  $\alpha = \Delta^0$ .

The numerical simulation of Paramonov and coworkers (74-75), which was later confirmed by Manz and coworkers (53, 54, 59) via OCT, show that this effect, though important (in accordance with the sequential model, the excitation of the  $m$ th resonance occurs toward the end of the pulse), is not as important as the introduction of a continuum of frequencies afforded by the leading and trailing edges of the pulse. This is in agreement with the above-mentioned perturbative treatment of the  $n$ -photon pulsed excitation.

Theoretical studies of tailored frequency chirped pulse excitation of diatomic dissociation have been carried out by Chelkowski et al (76). Here,

as in the above work, the high field pulse is tailored, with frequency decreasing as a function of time, so that the pulse is resonant with transitions between higher lying diatomic levels at later times. The result is an increase of dissociation rates by many orders of magnitude over unchirped pulses. In an extension to vibrational excitation (77), chirped intense infrared fields were used in a computation to excite and dissociate the CH bond in the local mode molecule HCN selectively.

Consider now the *raison d'être* for producing a single excited vibrational state. If we are not interested in photochemistry, i.e. we just want to control populations of stable molecules, then no more need be said. In fact, as shown by Shi et al (44, 46), who used classical OCT, it is possible to control the vibrational states of local bonds in a chain of harmonic oscillators. However, if we are interested in photochemistry, then this goal requires further consideration.

In photochemistry, the production of a single excited vibrational state may lead to the desired product in excitation + dissociation or excitation + reaction schemes. This is particularly true for local-mode type molecules, such as HOD. As shown theoretically by Zhang & Imre (80) and Engel & Schinke (81), and later confirmed experimentally by Vander Wal et al (8) and Bar et al (7), excitation of the OH stretch results in marked enhancement of the A-state H + OD photodissociation channel. Vibrational excitation can also have a strong inhibitory effect, which also results in great selectivity, as shown recently for the B-state photodissociation of HOD (82). Recently, Zare and coworkers (83), in confirming the theoretical predictions of Schatz et al (84) and Clary (85), demonstrated that excitation of either the OH or the OD bond leads to selective enhancement of the H + HOD reaction: When the OH bond is excited, the reaction yields  $H_2 + OD$ ; when the OD bond is excited, H reacts with HOD to form the HD + OH product.

Rather than affect the excitation for the  $v = 4$  state of HOD by overtone excitation, as done by Crim and coworkers (6a-c, 8), or to the  $v = 1$  state by Raman pumping, as done by Bar et al (7), Manz and coworkers (59) showed that strong optimized pulse can also achieve selective excitation.

All these cases consider local mode molecules (86). In HOD, for example, the large frequency difference between the OH and OD oscillators maintains the local nature of the excitation, and one need not worry about IVR. Similar dynamic separability exists if one excites a resonance state that displays local behavior. Such is the case studied by Joseph & Manz (55) for an ABA type molecule, in which a neat separation between an asymmetric and symmetric vibrational resonances exists.

In the context of IRMPD, the main argument often given for using short laser pulses is to try to complete the excitation rapidly, so as to beat

IVR. However, as we have shown, the preparation of a zero-order state at  $t = 0$  does not guarantee overcoming IVR (18, 87). In fact, as discussed in the context of CC, the quantum yield to forming various photochemical channels is entirely contained in the  $|E, n, q\rangle$  states. As shown in Equation 31, the production of  $|\phi\rangle$  at  $t = 0$  is a result of forming a linear combination of many of these energy eigenstates. Is it possible that  $\sum_{n,q} \int dE_{n,q}(E) |E, n, q\rangle$  will do better than its average constituent  $|E, n, q\rangle$  states? Obviously not. Expressed in another way, the amplitude populating the  $n$  and  $q$  channels as  $t \rightarrow \infty$  is already dictated by the "on-the-energy-shell"  $d_{n,q}(E)$  coefficients. Asymptotically, the Hamiltonian commutes with the channel indices— $q$  and  $n$ . Hence, these quantities are entirely independent of the spreading in energy space. As a result, the production of a pure zero-order state does nothing to enhance the yield of photochemical reactions beyond that achievable over a series of CW preparations with different frequencies.

## SUMMARY

In sharp contrast to the situation of less than ten years ago, the future of laser control over chemical reactions and molecular processes is bright. Recent advances in theory have focused attention upon the importance of molecular and laser coherence in both molecular dynamics and control schemes. Simultaneously, experimental techniques have advanced to the stage at which coherence is becoming a manageable laboratory variable. As a consequence, significant strides in this new area of coherence chemistry (17) are anticipated over the next decade.

## ACKNOWLEDGMENTS

We acknowledge support from the US Office of Naval Research, under contract numbers N00014-87-J-1204 and N00014-90-J-1014.

## Literature Cited

1. Levine, R. D., Zewail, A. H., El-Sayed, M. A., eds. 1991. Bernstein memorial issue on molecular dynamics, *J. Phys. Chem.* 95: 7961-8422
2. Manz, J., Parmentier, C. S., eds. 1989. Mode selectivity in unimolecular reactions, *Chem. Phys.* 139: 1-239
3. Ben-Shaul, A., Haas, Y., Kompa, K. L., Levine, R. D. 1981. *Lasers and Chemical Change*. Berlin: Springer
- 4a. Gudzenko, L. I., Yakovlenko, S. I. 1972. *Sov. Phys. JETP* 35: 877
- 4b. Yakovlenko, S. I. 1973. *Sov. Phys. JETP* 37: 1019
- 4c. Lisitsa, V. S., Yakovlenko, S. I. 1974. *Sov. Phys. JETP* 39: 759
- 4d. Harris, S. E., Lidow, D. B. 1974. *Phys. Rev. Lett.* 33: 674
- 4e. Wetner, J. 1980. *J. Chem. Phys.* 72: 2856
- 4f. Kroll, N. M., Watson, K. M. 1973. *Phys. Rev. A* 8: 804; Kroll, N. M., Watson, K. M. 1976. *Phys. Rev. A* 13: 1018

← *Spds* →

- 4g. Lau, A. M. F. 1976. *Phys. Rev. A* 13: 139; Lau, A. M. F. 1978. *Phys. Rev. A* 18: 172; Lau, A. M. F. 1981. *Phys. Rev. A* 25: 363
- 5a. George, T. F., Zimmerman, I. H., Yuan, J. M., Laing, J. R., deVries, P. L. 1977. *Acc. Chem. Res.* 10: 449
- 5b. deVries, P. L., George, T. F. 1979. *Faraday Disc. Chem. Soc.* 67: 129
- 5c. Bandrauk, A. D., ed. 1988. *Atomic and Molecular Processes with Short Intense Laser Pulses*. New York: Plenum
- 6a. Crim, F. F. 1984. *Annu. Rev. Phys. Chem.* 35: 647; Crim, F. F. 1990. *Science* 249: 1387
- 6b. Likar, M. D., Baggott, J. E., Sinha, A., Tichich, T. M., Vander Wal, R. L., Crim, F. F. 1988. *J. Chem. Soc. Faraday Trans. 2* 84: 1483
- 6c. Vander Wal, R. L., Scott, J. L., Crim, F. F. 1990. *J. Chem. Phys.* 92: 803
7. Bar, I., Cohen, Y., David, D., Rosenwaks, S., Valentini, J. J. 1990. *J. Chem. Phys.* 93: 2146; Bar, I., Cohen, Y., David, D., Rosenwaks, S., Valentini, J. J. 1991. *J. Chem. Phys.* 95: 3341
8. Vander Wal, R. L., Scott, J. L., Crim, F. F., Weide, K., Schintke, R. 1991. *J. Chem. Phys.* 94: 3548
9. Brumer, P., Shapiro, M. 1986. *Chem. Phys. Lett.* 126: 541
10. Brumer, P., Shapiro, M. 1987. *Faraday Disc. Chem. Soc.* 82: 177
11. Shapiro, M., Brumer, P. 1986. *J. Chem. Phys.* 84: 4103
12. Asaro, C., Brumer, P., Shapiro, M. 1988. *Phys. Rev. Lett.* 60: 1634
13. Shapiro, M., Hepburn, J. W., Brumer, P. 1988. *Chem. Phys. Lett.* 149: 451
14. Kuritzki, G., Shapiro, M., Brumer, P. 1989. *Phys. Rev. B* 39: 3435
15. Shapiro, M., Brumer, P. 1989. *J. Chem. Phys.* 90: 6179
16. Seideman, T., Shapiro, M., Brumer, P. 1989. *J. Chem. Phys.* 90: 7132
17. Brumer, P., Shapiro, M. 1989. *Acc. Chem. Res.* 22: 407
18. Brumer, P., Shapiro, M. 1989. *Chem. Phys.* 139: 221
19. Levy, I., Shapiro, M., Brumer, P. 1990. *J. Chem. Phys.* 93: 2493
20. Shapiro, M., Brumer, P. 1992. *J. Chem. Phys.* Submitted
21. Chan, C. K., Brumer, P., Shapiro, M. 1991. *J. Chem. Phys.* 94: 2688
22. Krause, J. L., Shapiro, M., Brumer, P. 1990. *J. Chem. Phys.* 92: 1126
23. Deleted in proof
24. Chen, Z., Brumer, P., Shapiro, M. 1992. *Phys. Rev. Lett.* Submitted
25. Gruner, D., Brumer, P., Shapiro, M. 1992. *J. Phys. Chem.* 96: 281
26. Chen, C., Yin, Y.-Y., Elliott, D. S.
1990. *Phys. Rev. Lett.* 64: 507; 1990. 65: 1737
27. Park, S. M., Lu, S.-P., Gordon, R. J. 1991. *J. Chem. Phys.* 94: 8622
28. Lu, S.-P., Park, S. M., Xie, Y., Gordon, R. J. 1992. *J. Chem. Phys.* Submitted
29. Baranova, B. A., Chudinov, A. N., Zel'dovich, B. Ya. 1990. *Opt. Commun.* 79: 116
30. Dods, J. 1992. MSc dissertation. Univ. Toronto
- 31a. Kocharovskaya, O., Li, R.-D., Mandel, P. 1990. *Opt. Commun.* 77: 215
- 31b. Kocharovskaya, O., Mandel, P. 1991. *Opt. Commun.* 84: 179
32. Deleted in proof
33. Metiu, H., Engel, V. 1990. *J. Opt. Soc. B* 7: 1709; Engel, V., Metiu, H. 1991. *J. Chem. Phys.* 95: 3444
34. Shapiro, M., Brumer, P. 1991. *J. Chem. Phys.* 95: 8658
35. Tannor, D. J., Rice, S. A. 1985. *J. Chem. Phys.* 83: 5013
36. Rice, S. A., Tannor, D. J., Kosloff, R. 1986. *J. Chem. Soc. Faraday Trans. 2* 82: 2423; Tannor, D. J., Kosloff, R., Rice, S. A. 1986. *J. Chem. Phys.* 85: 5805
37. Tannor, D. J., Rice, S. A. 1988. *Adv. Chem. Phys.* 70: 441
38. Kosloff, R., Rice, S. A., Gaspard, P., Tersigni, S., Tannor, D. J. 1989. *Chem. Phys.* 139: 201
39. Tersigni, S., Gaspard, P., Rice, S. A. 1990. *J. Chem. Phys.* 93: 1670
40. Jiang, X.-P., Brumer, P. 1991. *J. Chem. Phys. Lett.* 180: 222
41. Jiang, X.-P., Brumer, P. 1991. *J. Chem. Phys.* 94: 5833
42. Amstrup, B., Carlsson, R. J., Matro, A., Rice, S. A. 1991. *J. Phys. Chem.* 95: 8019
43. Shi, S., Woody, A., Rabitz, H. 1988. *J. Chem. Phys.* 88: 6870
44. Shi, S., Rabitz, H. 1989. *Chem. Phys.* 139: 185
45. Peirce, A. P., Dahleh, M. A., Rabitz, H. 1988. *Phys. Rev. A* 37: 4950
46. Shi, S., Rabitz, H. 1990. *J. Chem. Phys.* 92: 364
47. Burnee, J. G. B., Rabitz, H. 1990. *J. Math. Phys.* 31: 1253
48. Judson, R. S., Lehmann, K. K., Rabitz, H., Warren, W. S. 1990. *J. Mol. Struct.* 223: 425
49. Dahleh, M., Peirce, A. P., Rabitz, H. 1990. *Phys. Rev. A* 42: 1065
50. Zhao, M., Rice, S. A. 0000. *J. Chem. Phys.* Submitted
51. Rice, S. A. 1991. In *Mode Selective Chemistry*, ed. J. Jortner, R. D. Levine, B. Pullman, p. 485. Dordrecht: Kluwer
52. Yao, K., Shi, S., Rabitz, H. 1990. *Chem. Phys.* 150: 373
53. Jakubetz, W., Just, B., Manz, J.,

- Schreier, H.-J. 1990. *J. Phys. Chem.* 94: 2294
54. Jakubetz, W., Manz, J., Mohan, V. 1989. *J. Chem. Phys.* 90: 3686
55. Joseph, T., Manz, J. 1986. *Mol. Phys.* 57: 1149
56. Hartke, B., Kolba, E., Manz, J., Schor, H. H. R. 1990. *Ber. Bunsenges. Phys. Chem.* 94: 1312
57. Jin, Y., Tannor, D. J., Somloi, J., Lornicz, A. 0000. *J. Chem. Phys.* Submitted
58. Combariza, J. E., Just, B., Manz, J., Paramonov, G. K. 1991. *J. Phys. Chem.* 95: 10351
59. Combariza, J. E., Daniel, C., Just, B., Kadez, E., Kolba, E., et al. 1992. In *Isotope Effects in Chemical Reactions and Photoassociation Processes, ACS Symp. Ser.*, ed. J. A. Kaye. Washington, DC: Am. Chem. Soc.
- 60a. Kosloff, D., Kosloff, R. 1983. *J. Comput. Phys.* 52: 35; Kosloff, R., Kosloff, D. 1983. *J. Chem. Phys.* 79: 1823
- 60b. Kosloff, R. 1988. *J. Phys. Chem.* 92: 2087
61. Kosloff, R., Tal-Ezer, H. 1986. *Chem. Phys. Lett.* 127: 223
62. Lefortier, C., et al. 1991. *J. Comput. Phys.* 94: 59
63. Weiner, A. M., Leaird, D. E., Wiederrecht, G. P., Nelson, K. A. 1990. *Science* 247: 1317
- 64a. Weiner, A. M., Heritage, J. P., Thurston, R. N. 1986. *Opt. Lett.* 11: 153
- 64b. Weiner, A. M., Heritage, J. P. 1987. *Phys. Rep. Appl.* 22: 1619
- 65a. Spano, F., Haner, M., Warren, W. S. 1987. *Chem. Phys. Lett.* 135: 97
- 65b. Haner, M., Warren, W. S. 1988. *Appl. Phys. Lett.* 52: 1459
- 65c. Haner, M., Spano, F., Warren, W. S. 1986. In *Ultrafast Phenomena V*, ed. G. R. Fleming, A. Siegman, pp. 514-17. Berlin: Springer-Verlag
- 65d. Warren, W. S., Silver, M. S. 1988. *Adv. Chem. Res.* 12: 247
- 66a. Scherer, N. F., Ruggiero, A. J., Du, M., Fleming, G. R. 1990. *J. Chem. Phys.* 93: 856
- 66b. Scherer, N. F., Carlson, R. J., Maitro, A., Du, M., Ruggiero, A. J., et al. 1991. *J. Chem. Phys.* 95: 1487
67. Bavi, R., Engel, V., Metiu, H. 1992. *J. Chem. Phys.* Submitted
- 68a. Parter, J., Stroud, C. R. Jr. 1986. *Phys. Rev. Lett.* 56: 716
- 68b. Yeazell, J. A., Stroud, C. R. Jr. 1988. *Phys. Rev. Lett.* 60: 1494
- 69a. Albert, G., Ritch, H., Zoller, P. 1986. *Phys. Rev. A* 34: 1058
- 69b. Henle, W. A., Ritch, H., Zoller, P. 1987. *Phys. Rev. A* 36: 683
70. Fedorov, M. V., Movsesian, A. M. 1988. *J. Opt. Soc. Am. B* 5: 850
- 71a. Zewail, A. H. 1988. *Science* 242: 1645
- 71b. Zewail, A. H., Bernstein, R. B. 1988. *Chem. Eng. News* 66(45): 24
- 71c. Rosker, M. J., Dantus, M., Zewail, A. H. 1988. *J. Chem. Phys.* 89: 6113, 6128
- 71d. Bowman, M. J., Dantus, M., Zewail, A. H. 1989. *Chem. Phys. Lett.* 161: 297
72. Ragratskhvili, V. N., Letokhov, V. S., Mekarov, A. A., Ryabov, E. A. 1984. *Laser Chem.* 4: 311
73. Larsen, D. M., Bloembergen, N. 1976. *Opt. Commun.* 17: 254
- 74a. Paramonov, G. K., Savva, V. A. 1983. *Phys. Lett. A* 97: 340
- 74b. Paramonov, G. K., Savva, V. A., Samson, A. M. 1985. *Infrared Phys.* 25: 201
- 74c. Paramonov, G. K. 1990. *Chem. Phys. Lett.* 169: 573; Paramonov, G. K. 1991. *Phys. Lett. A* 152: 191
75. Paramonov, G. K., Savva, V. A. 1984. *Chem. Phys. Lett.* 107: 394
76. Chelkowski, S., Bandrauk, A. D., Corkum, P. B. 1990. *Phys. Rev. Lett.* 65: 2355
77. Chelkowski, S., Bandrauk, A. D. 1991. *Chem. Phys. Lett.* 186: 284
- 78a. Kuzninin, M. V., Sazonov, V. N. 1980. *Zh. Eksp. Teor. Fiz.* 79: 1759
- 78b. Hioe, F. T. 1983. *Phys. Lett.* 99A: 150
- 78c. Hioe, F. T., Eberly, J. H. 1984. *Phys. Rev. A* 29: 1164
79. Gaubatz, U., Rudecki, P., Schiekemann, S., Bergmann, K. 1990. *J. Chem. Phys.* 92: 5363
80. Zhang, J., Imre, D. G. 1988. *Chem. Phys. Lett.* 149: 233; Imre, D. G., Zhang, J. 1989. *Chem. Phys.* 139: 89
81. Engel, V., Schinke, R. 1988. *J. Chem. Phys.* 88: 6831
82. Shapiro, M. 1992. In *Mechanisms for Isotopic Enrichment in Photodissociation Reactions, ACS Symp. Ser.*, ed. J. A. Kaye. Washington, DC: Am. Chem. Soc.
83. Bronikowski, M. J., Simpson, W. R., Girard, B., Zare, R. N. 1991. *J. Chem. Phys.* 95: 8647
84. Schatz, G. C., Colton, M. C., Grant, J. L. 1984. *J. Phys. Chem.* 88: 2971
85. Clary, D. C. 0000. *J. Chem. Phys.* Submitted
86. Jaffe, C., Brumer, P. 1980. *J. Chem. Phys.* 73: 5645
87. Shapiro, M., Brumer, P. 1986. *J. Chem. Phys.* 84: 540



## Abstract

The quantum scattering theory of resonant two photon ( $\omega_1 + \omega_2$ ) dissociation is developed and applied to  $\text{Na}_2$  photodissociation. In the energy range considered photodissociation primarily occurs via excitation to the  $A^1\Sigma_u^+$  state, intersystem crossing to the  $b^3\Pi_u$  state and subsequent excitation to the triplet continuum. Photodissociation probabilities to produce  $\text{Na}(3s) + \text{Na}(3d)$ ,  $\text{Na}(3s) + \text{Na}(4s)$  and  $\text{Na}(3s) + \text{Na}(3p)$  are reported as a function of both  $\omega_1$  and  $\omega_2$ . Characteristic features due to spin-orbit coupling and to multiple product production are observed and discussed.

## I Introduction

Photodissociation has emerged as an informative approach to the study of molecular structure, interactions and dynamics<sup>1</sup>. Typical studies now utilize laser sources to initiate one photon absorption to the continuum, with dynamics and products studied via a variety of detection methods. Additional interest in laser initiated photodissociation has arisen as a result of recent ideas in the coherent radiative control of photodissociation<sup>2</sup>, a technique for using laser and molecular coherence to alter the relative product yield in photon initiated dynamics.

The availability of increased laser power motivates interest in multiphoton induced dissociation, with two photon processes being the subject of this paper. The theory and application to Na<sub>2</sub> discussed here also provide part of the theoretical basis for a second paper<sup>3</sup> which shows how resonant two photon absorption may be used to provide a means of controlling molecular processes in a *thermally equilibrated systems*, affording an enormous improvement in coherent control technology.

In this paper we develop the theory of two photon dissociation, discuss the artificial channel method<sup>4</sup> as applied to treat this problem and apply the method to the photodissociation of Na<sub>2</sub>, a problem currently under experimental study<sup>5</sup>. In addition to providing a direct link with these experiments, the study of the Na<sub>2</sub> two photon dissociation provides insight into the spin-orbit coupling between the Na<sub>2</sub>  $^1\Sigma_u^+$  and  $^3\Pi_u$  electronic states, which has been the subject of a series of studies<sup>6, 7</sup>. Here we treat this coupling nonperturbatively and find that the dissociation probability is sensitive to the strength of the spin-orbit interaction, providing direct information on the magnitude of this interaction.

The paper is organized as follows: in the next section, we describe the quantum scat-

tering theory of photodissociation and derive explicit formulae for the resonant two-photon processes. The artificial channel method, which provides a direct numerical method to compute the two-photon dissociation amplitudes, is explained. Aspects of the  $\text{Na}_2$  numerics and the artificial channel method for two photon dissociation are discussed in Section 3. Numerical results are discussed in Section 4.

## II Quantum Scattering Theory and Two-Photon Dissociation

### II.1 Formalism

Consider the photodissociation of a molecule  $AB$ . The Hamiltonian  $H_M$  can be conveniently written as the sum of the nuclear kinetic parts,  $K, k$ , and the electronic part  $H_{el}(\mathbf{q}|\mathbf{R}, \mathbf{r})$ ,

$$H_M = K(\mathbf{R}) + k(\mathbf{r}) + H_{el}(\mathbf{q}|\mathbf{R}, \mathbf{r}), \quad (1)$$

where  $\mathbf{R}$  is the displacement vector between  $A$  and  $B$ ,  $\mathbf{r}$  are the remaining nuclear coordinates, and  $\mathbf{q}$  denotes the collection of all electronic coordinates. As the molecule dissociates, ( $R \rightarrow \infty$ ),  $H_M$  approaches its asymptotic form  $H_M^\infty$  while  $H_{el}(\mathbf{q}|\mathbf{R}, \mathbf{r})$  approaches  $h_{el}(\mathbf{q}, \mathbf{r})$ ,

$$\lim_{R \rightarrow \infty} H_M = H_M^\infty, \quad (2)$$

$$H_M^\infty = K(\mathbf{R}) + [k(\mathbf{r}) + h_{el}(\mathbf{q}, \mathbf{r})], \quad (3)$$

where the term in the bracket of the right hand side of Eq.(3) is the Hamiltonian of the fragments  $A$  and  $B$ .

The Hamiltonian of the total system, the molecule plus the radiation field, can be written as

$$H = H_0 + V \quad (4)$$

$$H_0 = H_M + H_R \quad (5)$$

where  $H_R$  is the radiation Hamiltonian, and  $V$  is the molecule-radiation interaction which can be expressed in the electric dipole approximation as

$$V = -\boldsymbol{\mu} \cdot \mathbf{E}, \quad \mathbf{E} = i \sum_k \epsilon_k (\mathbf{e}_k a_k - \mathbf{e}_k^* a_k^\dagger). \quad (6)$$

Here  $\boldsymbol{\mu}$  is the electric dipole operator,  $\epsilon_k = (2\pi\omega_k/L^3)^{1/2}$ , and  $\mathbf{e}_k$  and  $\omega_k$  are the polarization vector and angular frequency of mode  $k$ , respectively. We set  $\hbar = 1$  throughout the paper.

Consider photodissociation, i.e.<sup>8</sup>, a transition from a molecular bound state  $|E_i\rangle$  to dissociating states  $|E, \mathbf{m}^- \rangle$ , where  $|E_i\rangle$  and  $|E, \mathbf{m}^- \rangle$  are orthogonal eigenstates of  $H_M$  with discrete energy  $E_i$  and continuous energy  $E$ , respectively:

$$H_M |E_i\rangle = E_i |E_i\rangle \quad (7)$$

$$H_M |E, \mathbf{m}^- \rangle = E |E, \mathbf{m}^- \rangle, \quad (8)$$

The notation  $\mathbf{m}^-$  implies the incoming boundary condition that at large  $R$  the states  $|E, \mathbf{m}^- \rangle$  approach well-defined asymptotic states  $|E, \mathbf{m} \rangle$ , which are eigenstates of the asymptotic Hamiltonian  $H_M^\infty$

$$H_M^\infty |E, \mathbf{m} \rangle = E |E, \mathbf{m} \rangle. \quad (9)$$

The quantity  $\mathbf{m}$ , being good quantum number of  $H_M^\infty$ , specifies, apart from energy  $E$ , the states  $|E, \mathbf{m} \rangle$  of the fragment products and includes the arrangement channel label.

The presence of radiation is conveniently described by field modes characterized by occupation quantum number  $n_k$  of a Fock state  $|n_k\rangle$  with energy  $n_k\omega_k$ . (Later, we will deal with the case in which the field is described by a coherent state.) In the multimode case the notation  $n_k$  is to be understood as the set of quantum numbers specifying each of the modes in the collective state  $|\{n_k\}\rangle \equiv |n_1, n_2, \dots\rangle$ , and  $n_k\omega_k$  is understood to imply the sum  $\sum_k n_k\omega_k$ . The eigenstates of  $H_0$ , which do not include the molecule-radiation field coupling, are the direct product of the molecular and photon states; e.g.,  $|E, m^-\rangle|n_k\rangle$  and  $|E_i\rangle|n_k\rangle$ , denoted by  $|(E, m^-), n_k\rangle$  and  $|E_i, n_k\rangle$ , respectively.

The dynamics of photodissociation is completely described<sup>9a</sup> by the fully interacting state  $|(E, m^-), n_k^-\rangle$  of the total Hamiltonian  $H$ , which satisfies the eigenequation:

$$H|(E, m^-), n_k^-\rangle = (E + n_k\omega_k)|(E, m^-), n_k^-\rangle. \quad (10)$$

Again, the minus superscript on  $n_k$  in the fully interacting state  $|(E, m^-), n_k^-\rangle$  suggests the boundary condition that when the radiative interaction  $V$  is switched off, the incoming state  $|(E, m^-), n_k^-\rangle$  becomes the non-interacting state  $|(E, m^-), n_k\rangle = |E, m^-\rangle|n_k\rangle$ .

To obtain an explicit expression for the two photon dissociation probability we proceed in two steps. First, we sketch a derivation, somewhat different from that previously given<sup>9a</sup>, showing that the photodissociation amplitude is given by  $\langle(E, m^-), n_k^-|V|E_i, n_i\rangle$  and contains all orders of the molecule-field interaction. Then we restrict attention to the two photon case to obtain an explicit expression, and computational technique, for the two photon photodissociation amplitude.

Consider then the system initially in the state  $|\psi(0)\rangle = |E_i, n_i\rangle$ . The time evolution of the system is given by

$$|\psi(t)\rangle = \exp(-iHt)|\psi(0)\rangle. \quad (11)$$

Our primary interest is to study transitions into the continuum subspace of the system as  $t \rightarrow \infty$ . Expanding  $U(t) = \exp(-iHt)$  in terms of the fully interacting incoming states Eq.(10) gives

$$|\psi(t)\rangle = \sum_{\mathbf{m}, n_k} \int dE \exp(-i(E + n_k \omega_k)t) |(E, \mathbf{m}^-), n_k^- \rangle \langle (E, \mathbf{m}^-), n_k^- | E_i, n_i \rangle. \quad (12)$$

The overlap integral  $\langle (E, \mathbf{m}^-), n_k^- | E_i, n_i \rangle$  can be evaluated by noting that  $\langle (E, \mathbf{m}^-), n_k^- |$  satisfies the Lippmann-Schwinger equation<sup>8</sup>

$$\langle (E, \mathbf{m}^-), n_k^- | = \langle (E, \mathbf{m}^-), n_k | + \langle (E, \mathbf{m}^-), n_k^- | V G_0(E^+ + n_k \omega_k) \quad (13)$$

where  $G_0(E) = 1/(E - H_0)$  is the Green function associated with  $H_0$ , and  $E^+$  denotes  $E + i\epsilon$  ( $\epsilon \rightarrow 0^+$  at the end of the computation). Using Eq. (13) and state orthogonality, we have

$$\langle (E, \mathbf{m}^-), n_k^- | E_i, n_i \rangle = \frac{\langle (E, \mathbf{m}^-), n_k^- | V | E_i, n_i \rangle}{E^+ - E_i - (n_i \omega_i - n_k \omega_k)}. \quad (14)$$

To obtain the desired long time result we substitute Eq.(14) into Eq.(12), perform the integration and let  $t \rightarrow \infty$ . The contributions to the integration come from the poles of the integrand Eq.(14) in the lower half of the complex  $E$  plane, and are given by  $[E_i + (n_i \omega_i - n_k \omega_k) - i\epsilon]$  and by the poles of  $\langle (E, \mathbf{m}^-), n_k^- | V | E_i, n_i \rangle$  in that half-plane. The latter contain an imaginary part which contributes an exponentially decaying term to the integration, and hence vanishes in the long time limit. The final result is then

$$\lim_{t \rightarrow \infty} |\psi(t)\rangle = -2\pi i \sum_{\mathbf{m}, n_k} |(E, \mathbf{m}^-), n_k^- \rangle \langle (E, \mathbf{m}^-), n_k^- | V | E_i, n_i \rangle \exp[-i(E + n_k \omega_k)t], \quad (15)$$

where  $E$  is constrained by the on-resonance condition

$$E = E_i + (n_i \omega_i - n_k \omega_k). \quad (16)$$

The quantity  $\langle (E, \mathbf{m}^-), n_k^- | V | E_i, n_i \rangle$  in Eq.(15) includes all orders of interaction  $V$  and, as the photodissociation amplitude, contains all information required for the complete description of the photodissociation cross section. Different photodissociation processes (e.g. involving different photon numbers) result in different structures for  $\langle (E, \mathbf{m}^-), n_k^- | V | E_i, n_i \rangle$ . For one-photon dissociation processes, the complete theory has been developed<sup>9</sup>, as has the perturbative non-resonant three photon case<sup>10</sup>. Below we consider two-photon processes and obtain an explicit form for photodissociation amplitude. This form allows considerable insight into the nature of the photodissociation and also provides the basis for partial wave resolution required to obtain computational results.

Note that Eq.(13) is displayed in terms of the Green function  $G_0$  of the free Hamiltonian  $H_0$ . To evaluate  $\langle (E, \mathbf{m}^-), n_k^- | V | E_i, n_i \rangle$ , we reexpress it in terms of the Green function  $G$  of the full Hamiltonian  $H$ :

$$\langle (E, \mathbf{m}^-), n_k^- | = \langle (E, \mathbf{m}^-), n_k | + \langle (E, \mathbf{m}^-), n_k | V G(E^+ + n_k \omega_k) \quad (17)$$

where  $G(E^+) \equiv 1/(E^+ - H)$ . On multiplying both sides of Eq.(17) by  $V | E_i, n_i \rangle$ , we obtain

$$\begin{aligned} \langle (E, \mathbf{m}^-), n_k^- | V | E_i, n_i \rangle &= \langle (E, \mathbf{m}^-), n_k | V | E_i, n_i \rangle \\ &+ \langle (E, \mathbf{m}^-), n_k | V G(E^+ + n_k \omega_k) V | E_i, n_i \rangle \end{aligned} \quad (18)$$

Note that the essential result of this equality is to rewrite the matrix elements in terms of the free field states, placing the molecule-radiative coupling entirely into the Green's function.

In two-photon transitions,  $|E_i\rangle$  is assumed not directly coupling to  $|E, \mathbf{m}^- \rangle$  by the radiative interaction  $V$ , but to bound intermediate states  $|E_m\rangle$  of  $H_M$ . Since we assume

that photodissociation does not occur via one photon excitation the first term on the right hand side is negligible compared to the second term. Inserting  $\sum_{E_m, n_m} |E_m, n_m\rangle\langle E_m, n_m|$  between  $V$  and  $G$  and between  $G$  and  $V$  in the second term on the right hand side of Eq.(18), and separating the  $H_M$  diagonal elements from the off-diagonal elements of  $G$ , we obtain

$$\begin{aligned}
& \langle (E, m^-), n_k^- | V | E_i, n_i \rangle \\
&= \sum_{E_m, n_m} \langle (E, m^-), n_k | V | E_m, n_m \rangle \langle E_m, n_m | G | E_m, n_m \rangle \langle E_m, n_m | V | E_i, n_i \rangle \\
&+ \sum_{(E_m, n_m) \neq (E_{m'}, n_{m'})} \langle (E, m^-), n_k | V | E_m, n_m \rangle \langle E_m, n_m | G | E_{m'}, n_{m'} \rangle \langle E_{m'}, n_{m'} | V | E_i, n_i \rangle
\end{aligned} \tag{19}$$

where the argument of  $G$  is  $(E^+ + n_k \omega_k)$ . The off-diagonal elements of  $G$  represent the interactions between two intermediate states and are negligible in the two-photon process if the radiation field intensities are moderate so that the perturbation caused by the interaction  $V$  is smaller than the spacing between  $|E_m, n_m\rangle$  and  $|E_{m'}, n_{m'}\rangle$ . Under these conditions  $\langle E_m, n_m | G | E_{m'}, n_{m'} \rangle \approx \langle E_m, n_m | G_0 | E_{m'}, n_{m'} \rangle = 0$  for  $(E_m, n_m) \neq (E_{m'}, n_{m'})$ . For  $\text{Na}_2$ , the spacing between two adjacent rotational levels of low  $J$  is on the order  $\sim 10^{-1} \text{ cm}^{-1}$ . Thus, as long as the laser intensities are less than  $10^6 \text{ W/cm}^2$ , the condition is fulfilled. (Larger intensities are allowed for higher  $J$ .) For the simplicity of the derivation we assume this condition and neglect the second term on the right hand side of Eq.(19). Note, however, that this assumption is not made in the numerical calculations discussed later below.

To evaluate the diagonal element  $\langle E_m, n_m | G(E^+ + n_k \omega_k) | E_m, n_m \rangle$ , we introduce the

projection operators  $Q$  and  $P$

$$Q = |E_m, n_m\rangle\langle E_m, n_m| \quad (20)$$

$$P = 1 - Q \quad (21)$$

In terms of the projection operators,  $QGQ$  can be written as

$$QG(E)Q = Q[E - H_0 - QR(E)Q]^{-1}Q \quad (22)$$

$$R(E) = V + VP[E - PHP]^{-1}PV \quad (23)$$

where the operator  $R$  will be seen being responsible for the shifts and widths of the intermediate bound states. After letting  $\epsilon$  in  $E^+$  approaches zero, we obtain

$$\begin{aligned} \lim_{\epsilon \rightarrow 0} \langle E_m, n_m | G(E^+ + n_k \omega_k) | E_m, n_m \rangle &= \lim_{\epsilon \rightarrow 0} \langle E_m, n_m | QG(E^+ + n_k \omega_k) Q | E_m, n_m \rangle \\ &= \frac{1}{(E + n_k \omega_k) - (E_m + \delta_m + n_m \omega_m) + i\Gamma_m} \end{aligned} \quad (24)$$

where

$$\delta_m = \text{Re}(\lim_{\epsilon \rightarrow 0} \langle E_m, n_m | R(E + i\epsilon + n_k \omega_k) | E_m, n_m \rangle) \quad (25)$$

$$\Gamma_m = -\text{Im}(\lim_{\epsilon \rightarrow 0} \langle E_m, n_m | R(E + i\epsilon + n_k \omega_k) | E_m, n_m \rangle) \quad (26)$$

are the shift and width of the bound state  $|E_m\rangle$ , respectively. Substituting Eq.(24) into Eq.(19) for the diagonal element and neglecting the off-diagonal elements on the right hand side of the equation, we obtain,

$$\begin{aligned} &\langle (E, m^-), n_k^- | V | E_i, n_i \rangle \\ &= \sum_{E_m, n_m} \frac{\langle (E, m^-), n_k^- | V | E_m, n_m \rangle \langle E_m, n_m | V | E_i, n_i \rangle}{E - (E_m + \delta_m + (n_m \omega_m - n_k \omega_k)) + i\Gamma_m} \end{aligned} \quad (27)$$

Consider now the case of diatomic photodissociation . Here the quantum number  $m$  refers to scattering angles  $\hat{k}$  and the channel index  $q$ , which specifies the states of the

fragment products. To further simplify the result, we denote the first and second photons absorbed by the molecule by  $\omega_1$  and  $\omega_2$ , respectively, and  $|n_i\rangle = |n_1, n_2\rangle$ ,  $|n_m\rangle = |n_1 - 1, n_2\rangle$  and  $|n_k\rangle = |n_1 - 1, n_2 - 1\rangle$ , where  $n_1$  and  $n_2$  are the initial occupation numbers of the field modes  $\omega_1$  and  $\omega_2$ , respectively, and the photon  $\omega_1$  is in resonance with one of the intermediate states. Using the expression Eq.(6) for  $V$  and the on-resonance condition (16), we perform the calculation in the numerator of Eq.(27) with respect to photon states. The result, the negative of  $T_{\hat{k}q,i}^-(E, E_i, \omega_2, \omega_1)$  with

$$T_{\hat{k}q,i}^-(E, E_i, \omega_2, \omega_1) = \sum_{E_m} \frac{\langle E, \hat{k}q^- | \mu_2 \mathcal{E}_2 | E_m \rangle \langle E_m | \mu_1 \mathcal{E}_1 | E_i \rangle}{\omega_1 - \delta E_{m,i} + i\Gamma_m}, \quad (28)$$

has the characteristic form of the product of two transition matrix elements divided by an energy denominator in which proper account is taken of the level width and shift. Here  $E = E_i + \omega_1 + \omega_2$ ,  $\delta E_{m,i} = E_m + \delta_m - E_i$ ,  $\mathcal{E}_i = \sqrt{n_i} \epsilon_i$ , which is the amplitude of the field mode  $\omega_i$ , and  $\delta_m$  and  $\gamma_m$  are given by Eqs.(25) and (26), respectively, with  $|n_m\rangle$  replaced by  $|n_1 - 1, n_2\rangle$ . The  $\mu_1$  and  $\mu_2$  are the components of the dipole moment along the radiation electric-field vectors of the modes  $\omega_1$  and  $\omega_2$ , respectively. For simplicity we assume later that both lasers are linearly polarized and have parallel electric field vectors, along which the space-fixed z-axis is conventionally defined. The dissociation probability of observing the product in channel  $q$  is then of the form

$$\begin{aligned} P^{(q)}(E, E_i, \omega_2, \omega_1) &= \int d\hat{k} \left| T_{\hat{k}q,i}^-(E, E_i, \omega_2, \omega_1) \right|^2 \\ &= \int d\hat{k} \left| \sum_{E_m} \frac{\langle E, \hat{k}q^- | \mu_2 \mathcal{E}_2 | E_m \rangle \langle E_m | \mu_1 \mathcal{E}_1 | E_i \rangle}{\omega_1 - \delta E_{m,i} + i\Gamma_m} \right|^2. \end{aligned} \quad (29)$$

In the above discussion, the states of the external electric field are described by Fock states. This description is appropriate when the laser phases are irrelevant. In cases where the field phases are crucial, such as in two photon coherent radiative control<sup>3</sup>, the field

modes are appropriately described by the coherent states that contain phase information<sup>9</sup>.

For the field mode  $k$ , the coherent state  $|\alpha_k\rangle$  is a superposition of the Fock states<sup>11</sup>

$$|\alpha_k\rangle = \sum_{n_k} P(\alpha_k, n_k) |n_k\rangle \quad (30)$$

where  $P$  is the Poisson distribution function

$$P(\alpha_k, n_k) = \exp(-|\alpha_k|^2/2) \frac{\alpha_k^{n_k}}{\sqrt{n_k!}} \quad (31)$$

with  $\alpha_k = |\alpha_k| \exp(i\theta_k) = \sqrt{\bar{n}_k} \exp(i\theta_k)$ , where  $\theta_k$  and  $\bar{n}_k$  are the phase and average photon number of the mode  $k$ , respectively. In multi-mode case,  $|\alpha_k\rangle$  is replaced by  $|\alpha_1, \alpha_2, \dots\rangle$ ,  $\sum_{n_k}$  by  $\sum_{n_1} \sum_{n_2} \dots$ , and  $P(\alpha_k, n_k)$  by  $P(\alpha_1, n_1)P(\alpha_2, n_2) \dots$ . The initial state of the total system is now described by

$$|\psi(0)\rangle = |E_i, \alpha_i\rangle = \sum_{n_i} P(\alpha_i, n_i) |E_i, n_i\rangle \quad (32)$$

Repeating the derivations from Eqs.(11) to (28) and specifying the field modes as the two modes  $|\alpha_1, \alpha_2\rangle$ , we obtain the wavefunction at the long time limit after the absorption of the two photons from the modes  $\alpha_1$  and  $\alpha_2$ ,

$$\begin{aligned} \lim_{t \rightarrow \infty} |\psi(t)\rangle &= 2\pi i \sum_{\mathbf{m}, n_1, n_2} \sum_{n_1, n_2} |(E, \mathbf{m}^-), n_k^- \rangle \exp[-i(E + \sum_k n_k \omega_k)t] \\ &\langle n_k | n_1 - 1, n_2 - 1 \rangle P(\alpha_1, n_1) \sqrt{n_1} P(\alpha_2, n_2) \sqrt{n_2} \sum_{E_m} \frac{\langle E, \mathbf{m}^- | \mu_2 \epsilon_2 | E_m \rangle \langle E_m | \mu_1 \epsilon_1 | E_i \rangle}{\omega_1 - \delta E_{m,i} + i\Gamma_m} \end{aligned} \quad (33)$$

Substituting into Eq.(33) the equalities  $P(\alpha_1, n_1) \sqrt{n_1} = \alpha_1 P(\alpha_1, n_1 - 1)$  and  $P(\alpha_2, n_2) \sqrt{n_2} = \alpha_2 P(\alpha_2, n_2 - 1)$ , replacing  $n_1 - 1$  and  $n_2 - 1$  in the summations by  $n_1$  and  $n_2$ , respectively, and performing the summation  $\sum_{n_k}$ , we rewrite Eq.(33) as

$$\begin{aligned} \lim_{t \rightarrow \infty} |\psi(t)\rangle &= 2\pi i \sum_{\mathbf{m}} \left\{ \sum_{n_1, n_2} P(\alpha_1, n_1) P(\alpha_2, n_2) |(E, \mathbf{m}^-), (n_1 n_2)^- \rangle \exp[-i(E + n_1 \omega_1 + n_2 \omega_2)t] \right\} \\ &\times T_{\mathbf{m}, i}^c(E, E_i, \omega_2, \omega_1). \end{aligned} \quad (34)$$

Here  $T_{\mathbf{m},i}^c$  is defined by

$$T_{\mathbf{m},i}^c(E, E_i, \omega_2, \omega_1) = \sum_{E_m} \frac{\langle E, \mathbf{m}^- | \mu_2 \tilde{\mathcal{E}}_2 | E_m \rangle \langle E_m | \mu_1 \tilde{\mathcal{E}}_1 | E_i \rangle}{\omega_1 - \delta E_{\mathbf{m},i} + i\Gamma_{\mathbf{m}}} \quad (35)$$

where  $\tilde{\mathcal{E}}_1 = \mathcal{E}_1 \exp(i\theta_1)$  and  $\tilde{\mathcal{E}}_2 = \mathcal{E}_2 \exp(i\theta_2)$ , which are the complex amplitudes of the field modes  $\omega_1$  and  $\omega_2$ , respectively. The state in the brackets in Eq.(34) asymptotically approaches the non-interacting state

$$U_0(t)|(E, \mathbf{m}^-), \alpha_1 \alpha_2) \equiv \exp(-iH_0 t)|(E, \mathbf{m}^-), \alpha_1 \alpha_2),$$

where the radiation is in coherent states. Hence the coefficient  $T_{\mathbf{m},i}^c(E, E_i, \omega_2, \omega_1)$  in the equation is the desired photodissociation amplitude to the state  $|(E, \mathbf{m}^-), \alpha_1 \alpha_2)$ . Note that the amplitude  $T_{\mathbf{m},i}^c$  in Eq.(35) differs from that in Eq. (28) only by the inclusion of the phase in Eq.(34). We will use the latter in the present paper, and the former in the subsequent paper<sup>3</sup>, where phases are relevant.

### III Two-Photon Dissociation of Na<sub>2</sub>

Na<sub>2</sub> has been the subject of both one photon<sup>12</sup> and two photon dissociation experiments<sup>13</sup>. In addition theoretical studies on Na<sub>2</sub> one photon dissociation are available<sup>14</sup>. Here we consider photodissociation of Na<sub>2</sub> by the resonant absorption of two visible photons. The resonant absorption not only greatly enhances dissociation probabilities, but provides selective excitation of molecules out of the thermal distribution, a property which is of great importance for the control of reactions in a realistic environment.

The electronic potential curves<sup>15</sup> of Na<sub>2</sub> relevant for this study are shown in Fig. 1. The energetics are such that upon absorption of the photon  $\omega_1$ , the molecule, initially in the bound state  $|E_i\rangle$  of  ${}^1\Sigma_g^+$ , is excited to an intermediate bound state  $|E_m\rangle$ , which is a

superposition of the  $A^1\Sigma_u^+$  and  $b^3\Pi_u$ , as discussed below. Subsequently absorption of the second photon  $\omega_2$  lifts the system to the dissociating state  $|E, \hat{k}q^- \rangle$ .

Dissociation of  $\text{Na}_2$  in the energy range of interest yields:



where the channel index  $q$  is either  $3p$ ,  $4s$  or  $3d$ . Below we consider energy regimes  $\omega_1$  from 16500 to 18680  $\text{cm}^{-1}$  and  $\omega_2$  from 10000 to 22000  $\text{cm}^{-1}$ . Usually more than one electronic state correlates with a dissociation product [see Fig. 1]. Note, however, that the dominant contributions to the  $\text{Na}(3p)$ ,  $\text{Na}(4s)$  and  $\text{Na}(3d)$  dissociation come from  $^3\Pi_g$ ,  $^3\Sigma_g^+$  and  $^3\Pi_g$  states. The other curves, although included in the computation, make insignificant contributions due to substantially less favorable Franck-Condon factors.

### III.1 Spin-Orbit Coupling

Since the first photon  $\omega_1$  carries the system to the region of the  $^1\Sigma_u^+$ ,  $^3\Pi_u^+$  states, the spin-orbit coupling between these zeroth order states plays an important role in the two photon dissociation. In this section we analyze the photodissociation in terms of the zeroth order states by diagonalizing the spin-orbit interaction. In the computation later below, the diagonalization is carried out numerically and nonperturbatively.

To examine the coupling we divide the electronic Hamiltonian into an electrostatic part  $H_{es}$ , which provides the electrostatic nuclear potentials, and the spin-orbital coupling  $H^{so}$  so that the molecular Hamiltonian  $H_M$  becomes

$$H_M = H_M^0 + H^{so} \quad (37)$$

where  $H_M^0 = K(\mathbf{R}) + H_{es}$ . Now define  $|E_{m_1}, ^1\Sigma_u^+ \rangle$  and  $|E_{m_3}, ^3\Pi_u \rangle$  as the eigenstates of  $H_M^0$  [Eq.(37)] with electronic wavefunctions corresponding to the  $^1\Sigma_u^+$  and  $^3\Pi_u$  states,

respectively;

$$H_M^0 |E_{m_1}, {}^1\Sigma_u^+\rangle = E_{m_1} |E_{m_1}, {}^1\Sigma_u^+\rangle \quad (38)$$

$$H_M^0 |E_{m_3}, {}^3\Pi_u\rangle = E_{m_3} |E_{m_3}, {}^3\Pi_u\rangle, \quad (39)$$

For simplicity, these states are denoted by  $|E_{m_1}\rangle$ ,  $|E_{m_3}\rangle$  with the subscripts  $m_1$  and  $m_3$  serving as reminders of the singlet and triplet state character. Typical high lying zeroth order energy levels, used below, are shown in Table 1. The true intermediate states  $|E_m\rangle$ , being eigenstates of  $H_M$ , are the superposition states

$$|E_m^\pm\rangle = A^\pm |E_{m_1}\rangle + B^\pm |E_{m_3}\rangle. \quad (40)$$

where the states in both sides of the equation implicitly have the same rotational quantum number,  $J_m$ , since the spin-orbit interaction is  $J$ -independent. By diagonalizing the spin-orbit interaction, the perturbed energies  $E_m^\pm$  and the mixing coefficients  $A^\pm$  and  $B^\pm$  are expressed in terms of the unperturbed energies  $E_{m_1}$  and  $E_{m_3}$  and the matrix element of the spin-orbit interaction

$$V_{so} \equiv \langle E_{m_1} | H^{so} | E_{m_3} \rangle = \langle {}^1\Sigma_u^+ | H^{so} | {}^3\Pi_u \rangle \langle v_{m_1} | v_{m_3} \rangle, \quad (41)$$

where  $\langle v_{m_1} | v_{m_3} \rangle$  is the overlap of the vibrational wavefunctions between the two states, and  $\langle {}^1\Sigma_u^+ | H^{so} | {}^3\Pi_u \rangle = 5.91 \text{ cm}^{-1}$ . The results are

$$E_m^\pm = \frac{1}{2} \left\{ E_{m_1} + E_{m_3} \pm [(E_{m_1} - E_{m_3})^2 + 4V_{so}^2]^{1/2} \right\} \quad (42)$$

$$A^+ = \frac{(E_m^+ - E_{m_3})}{\sqrt{(E_m^+ - E_{m_3})^2 + V_{so}^2}}, \quad B^+ = \frac{V_{so}}{\sqrt{(E_m^+ - E_{m_3})^2 + V_{so}^2}} \quad (43)$$

$$A^- = \frac{(E_m^- - E_{m_3})}{\sqrt{(E_m^- - E_{m_3})^2 + V_{so}^2}}, \quad B^- = \frac{V_{so}}{\sqrt{(E_m^- - E_{m_3})^2 + V_{so}^2}}. \quad (44)$$

Typical  $V_{so}$  values (See Table 2) range from 0.01 to 1.0  $\text{cm}^{-1}$ , depending on the wavefunction overlap. Inserting Eq.(40) into Eq.(29), we rewrite the probability

$$P^{(q)}(E, E_i, \omega_2, \omega_1) = \mathcal{E}_1^2 \mathcal{E}_2^2 \int d\hat{\mathbf{k}} \left| \sum_{E_{m_1}, E_{m_3}} \left( \frac{A^+ B^+ \langle E, \hat{\mathbf{k}}q^- | \mu_2 | E_{m_3} \rangle + (A^+)^2 \langle E, \hat{\mathbf{k}}q^- | \mu_2 | E_{m_1} \rangle}{\omega_1 - \delta E_{m,i}^+ + i\Gamma_m^+} \right. \right. \\ \left. \left. + \frac{A^- B^- \langle E, \hat{\mathbf{k}}q^- | \mu_2 | E_{m_3} \rangle + (A^-)^2 \langle E, \hat{\mathbf{k}}q^- | \mu_2 | E_{m_1} \rangle}{\omega_1 - \delta E_{m,i}^- + i\Gamma_m^-} \right) \langle E_{m_1} | \mu_1 | E_i \rangle \right|^2. \quad (45)$$

where  $\delta E_{m,i}^\pm = E_m^\pm + \delta_m^\pm - E_i$ , and  $\delta_m^\pm$  and  $\Gamma_m^\pm$  are the shifts and widths of the states  $|E_m^\pm\rangle$ . The states  $|E_{m_1}\rangle$  and  $|E_{m_3}\rangle$  possess the same rotational quantum number  $J_m$  and the summation over  $J_m$  is implicitly incorporated in the sum in Eq. (45).

In accord with Eq.(45), the probability  $P^{(q)}(E, E_i, \omega_2, \omega_1)$  should display the following structure as a function of the photon energy  $\hbar\omega_1$ : for a given  $J_m$ ,  $P^{(q)}$  shows a double-peak at  $\omega_1 = \delta E_{m,i}^+$  and  $\delta E_{m,i}^-$  if  $(E_{m_1} - E_{m_3}) \leq 2V_{so}$ , i.e., if  $|E_{m_1}\rangle$  and  $|E_{m_3}\rangle$  are strongly coupled. The distance between the pair of peaks is  $[(E_{m_1} - E_{m_3})^2 + 4V_{so}^2]^{1/2}$ , from which the spin-orbit interaction  $V_{so}$  may be extracted. Alternatively, if  $(E_{m_1} - E_{m_3}) \gg 2V_{so}$ , i.e. if the  $|E_{m_1}\rangle, |E_{m_3}\rangle$  coupling is weak, then  $E_m^\pm$  approaches  $E_{m_1}$  and  $E_{m_3}$ , and the coefficient  $A^-$  vanishes at  $E_m^- = E_{m_3}$ . The peak at  $\omega_1 = E_{m_1} - E_i$  predominates over that at  $\omega_1 = E_{m_3} - E_i$ , leading to a single peak of  $P^{(q)}$  as a function of  $\omega_1$ . Note that since the  $E_{m_3}(J_m), E_{m_1}(J_m)$  spacing depends on the rotational quantum number  $J_m$ , the location of the double-peak changes as a function of rotational temperature. That is, a pair of the rovibronic states  $(E_{m_3}(J_m), E_{m_1}(J_m))$  that are strongly coupled for a particular  $J_m$  may be weakly coupled at a different  $J'_m$ , and vice-versa. As a consequence the location of the doublet would shift from  $\delta E_{m,i}^\pm$  to some  $\delta E_{m,i}^{\pm'}$ , as  $J_m$  changes to  $J'_m$ . This behavior is indeed observed in the computations presented in Section 4.

### III.2 Computational Details

To compute the required photodissociation probability we utilize the artificial channel method, which provides a means of rewriting the photodissociation problem, i.e. a half collision process, in terms of a full collision problem, and permits the use of full collision computational methods to compute the photodissociation amplitudes in a way which avoids integrations over highly oscillatory continuum matrix elements. The technique<sup>4</sup> works by introducing an artificial open channel that couples to the physical bound states. As a result the artificial channel serves as an incoming channel of a full collision problem, the physical continua serve as outgoing channels, and the physical bound states become poles at positive energies. The resultant problem is then amenable to treatment by full collision problem techniques.

To see the general structure, consider an artificial channel  $|A\rangle$  which is weakly coupled to  $|E_i, n_i\rangle$  by an artificial interaction  $\langle E_i, n_i|W|A\rangle$ . This interaction can be regarded as a component of the interaction  $V$  which connects  $|A\rangle$  and  $|E_i, n_i\rangle$  only and thus does not affect the couplings between the physical states. Further, to avoid the disturbance to  $|E_i, n_i\rangle$  caused by the introduction of  $W$ , the element  $\langle A|W|E_i, n_i\rangle$  is set to zero in the computation. A rough derivation of the method results from multiplying the Lippmann-Schwinger equation [Eq. (13)] by  $V|A\rangle$  to give:

$$\langle (E, m^-), n_k^- |V|A\rangle = \sum_{E_i} \frac{\langle (E, m^-), n_k^- |V|E_i, n_i\rangle \langle E_i, n_i|W|A\rangle}{E^+ - E_i - (n_i\omega_i - n_k\omega_k)} \quad (46)$$

where we have used  $\langle E_i, n_i|W|A\rangle = \langle E_i, n_i|V|A\rangle$ . That is,  $W$  is the component of  $V$  which couples the artificial channel to the initial bound state. The left hand side of Eq. (46) defines the  $T$ -matrix element  $T_{m_n, A}$  between the two open states of the artificial

full-collision problem and can be computed accurately by utilizing well-developed collision techniques. Because we have set  $\langle A|W|E_i, n_i\rangle = 0$ , the poles at  $T_{m n_k, A}$  have no width. The residue of  $T_{m n_k, A}$  at  $E = E_i + (n_i \omega_i - n_k \omega_k)$  gives the requisite photodissociation amplitude  $\langle (E, m^-), n_k^- | V | E_i, n_i \rangle$  at the on-resonance condition. For a more complete derivation the reader is referred to Ref. 4.

The argument above applies to different photodissociation processes (e.g., one-photon, two-photon processes, etc.), and the computational procedures of the method are similar: we expand the full interacting state  $|(E, m^-), n_k^- \rangle$  in terms of the non-interacting states  $|E_i, n_i\rangle$ ,  $|E_m, n_m\rangle$  and  $|(E, m^-), n_k\rangle$ , where the molecule states contain rotational, electronic and radial parts with the radial parts, serving as expansion coefficients, to be determined. Substituting the expansion into Eq. (10) and performing the calculations over photon states gives a set of coupled equations for the molecular states. Adding the artificial channel to the coupled equations and solving the resultant equations for the  $T_{m n_k, A}$  numerically, gives  $\langle (E, m^-), n_k^- | V | E_i, n_i \rangle$  according to Eq.(46), or in the two photon case, the amplitude  $T_{k q, i}^c(E, E_i, \omega_2, \omega_1)$  [Eq.(28)].

Specifically, the electronic states are chosen as eigenstates of the electrostatic Hamiltonian  $H_{es}$ , and they generate the bound and continuous nuclear-electronic wave functions in Eq.(28). The rotational functions are chosen as the parity adapted rotation matrices<sup>16</sup> defined as

$$D_{\lambda, M}^{J p}(\Omega) = t_\lambda \left[ D_{\lambda, M}^J(\Omega) + (-1)^\lambda p D_{-\lambda, M}^J(\Omega) \right], \quad p = \pm 1 \quad (47)$$

whose parity under inversion is given by  $p(-1)^J$ . Here  $D_{m, m}^J$  are the rotation matrices of Edmonds<sup>17</sup>,  $\Omega$  are the Euler angles which specify the rotation that takes the space-fixed to the molecule-fixed coordinate system,  $J$  and  $M$  are the angular momentum and its

projection along the space-fixed z-axis, respectively,  $\lambda (= |\Lambda + \Sigma|)$  is the absolute value of the projection of  $J$  on the internuclear axis, which is a function of the electronic state, and  $t_\lambda = \sqrt{\frac{1}{2}}$  for  $\lambda \neq 0$  and  $t_\lambda = \frac{1}{2}$  for  $\lambda = 0$ . For the  $^1\Sigma$  electronic states,  $\lambda = 0$  only, and  $D_{\lambda,M}^{Jp}$  reduces to  $D_{0,M}^J$  with  $p = 1$ .

The notation  $|E_i\rangle$  and  $|E_m\rangle$  are extended to properly include the full complement of quantum numbers, i.e., they are denoted  $|E_i, J_i, M_i\rangle$  and  $|E_m, J_m, M_m\rangle$ . Therefore, we have<sup>16</sup>

$$\langle R, \Omega | E_i, J_i, M_i \rangle = \sqrt{\frac{2J_i + 1}{8\pi^2}} D_{0,M_i}^{J_i}(\Omega) |i\rangle \Phi_i^{J_i}(R) / R \quad (48)$$

$$\langle R, \Omega | E_m, J_m, M_m \rangle = \sqrt{\frac{2J_m + 1}{8\pi^2}} D_{\lambda_m, M_m}^{J_m p_m}(\Omega) |m\rangle \Phi_{\lambda_m, m}^{J_m p_m}(R) / R \quad (49)$$

$$\begin{aligned} \langle R, \Omega | E, \hat{k}q^- \rangle &= \sum_{J, M, p, \lambda \geq 0} \frac{\sqrt{2\mu k_q (2J + 1)}}{h} D_{\lambda, M}^{Jp}(\theta_k, \phi_k, 0) \\ &\times \sum_{\xi} \sqrt{\frac{2J + 1}{8\pi^2}} D_{\lambda, M}^{Jp}(\Omega) |\xi\rangle \Phi_{\lambda, \xi}^{(Jpq)^-}(R) / R \end{aligned} \quad (50)$$

where  $(\theta_k, \phi_k)$  are the scattering angles in the  $\hat{k}$  direction, and the curved kets stand for the (electrostatic) electronic states, in which  $|i\rangle = |^1\Sigma_g^+\rangle$ ,  $|m\rangle$  is  $|m_1\rangle = |^1\Sigma_u^+\rangle$  or  $|m_3\rangle = |^3\Pi_u^+\rangle$ , and  $|\xi\rangle$  denotes electronic states that correlate with the specific product in channel  $q$ . The radial parts of the expansion,  $\Phi_i^{J_i}(R)$ ,  $\Phi_{\lambda_m, m}^{J_m p_m}(R)$  and  $\Phi_{\lambda, \xi}^{(Jpq)^-}(R)$ , are the nuclear-vibrational wavefunctions of the bound states and continua.

Inserting Eqs.(48)-(50) into Eq.(28), we first perform the integration over the rotational wavefunctions in the interaction matrix elements and separate geometric factors from physical elements to give terms like

$$\begin{aligned} &\frac{\sqrt{(2J + 1)(2J_m + 1)}}{8\pi^2} \int d\Omega D_{\lambda, M}^{Jp}(\Omega) (\xi | \mu_2 \mathcal{E}_2 | m) D_{\lambda_m, M_m}^{J_m p_m}(\Omega) \\ &= (-1)^{-M} \begin{pmatrix} J & 1 & J_m \\ -M & 0 & M_m \end{pmatrix} V_{\xi, m}(Jp\lambda, J_m) \end{aligned} \quad (51)$$

$$\begin{aligned}
& \frac{\sqrt{(2J_m+1)(2J_i+1)}}{8\pi^2} \int d\Omega D_{\lambda_m, M_m}^{J_m p_m}(\Omega) (m|\mu_1 \mathcal{E}_1|i) D_{0, M_i}^{J_i}(\Omega) \\
& = (-1)^{-M_m} \begin{pmatrix} J_m & 1 & J_i \\ -M_m & 0 & M_i \end{pmatrix} V_{m,i}(J_m, J_i). \tag{52}
\end{aligned}$$

Here, we have introduced the reduced radiative interaction elements  $V_{\xi, m}$  and  $V_{m, i}$ ,

$$\begin{aligned}
V_{\xi, m}(J p \lambda, J_m) & = (-1)^{\lambda} t_{\lambda} t_{\lambda_m} \sqrt{(2J+1)(2J_m+1)} \sum_{K=0, \pm 1} [1 + p p_m (-1)^{J+J_m+K+1}] \\
& \times \left[ \begin{pmatrix} J & 1 & J_m \\ -\lambda & K & \lambda_m \end{pmatrix} + (-1)^{\lambda} p \begin{pmatrix} J & 1 & J_m \\ \lambda & K & \lambda_m \end{pmatrix} \right] (\xi|\mu_K(R)|m) \mathcal{E}_2 \tag{53}
\end{aligned}$$

$$\begin{aligned}
V_{m, i}(J_m, J_i) & = (-1)^{\lambda_m} t_{\lambda_m} \sqrt{(2J_m+1)(2J_i+1)} \sum_{K=0, \pm 1} [1 + p_m (-1)^{J_m+J_i+K+1}] \\
& \times \left[ \begin{pmatrix} J_m & 1 & J_i \\ -\lambda_m & K & 0 \end{pmatrix} + (-1)^{\lambda_m} p_m \begin{pmatrix} J_m & 1 & J_i \\ \lambda_m & K & 0 \end{pmatrix} \right] (m|\mu_K(R)|i) \mathcal{E}_1, \tag{54}
\end{aligned}$$

where  $\mu_K(R)$  are components of the dipole moment (assumed all equal in the computation below) in the body-fixed frame. For  $|m_1\rangle$  electronic state,  $\lambda_m = 0$  only; for  $|m_3\rangle$  state,  $\lambda_m$  can be 0 and 1, but only the former couples with  $|m_1\rangle$  by the spin-orbit interaction<sup>7</sup>. We thus take  $\lambda_m = 0$ . The expressions (53) and (54) imply the selection rules:  $p_m = (-1)^{J_m+J_i+1}$ ,  $p = p_m (-1)^{J+J_m+1}$  (for  $\lambda = \lambda_m$ ) and  $p = p_m (-1)^{J+J_m}$  (for  $|\lambda - \lambda_m| = 1$ ).

With these, we then rewrite the photodissociation amplitude  $T_{\mathbf{k}q, i}$  in Eq.(28) as

$$\begin{aligned}
T_{\mathbf{k}q, i}(E, E_i, \omega_2, \omega_1) & = \sum_{J, p, \lambda \geq 0} \sum_{E_m, J_m} \begin{pmatrix} J & 1 & J_m \\ -M_i & 0 & M_i \end{pmatrix} \begin{pmatrix} J_m & 1 & J_i \\ -M_i & 0 & M_i \end{pmatrix} \\
& \times \frac{\sqrt{2\mu k_q (2J+1)}}{h} D_{\lambda, M_i}^{J p}(\theta_k, \phi_k, 0) \mathbf{t}(E, E_m, E_i; J, J_m, J_i; p \lambda q) \tag{55}
\end{aligned}$$

where  $E = E_i + \omega_1 + \omega_2$ , and  $\mathbf{t}(E, E_m, E_i; J, J_m, J_i; p \lambda q)$  is the reduced matrix element of the resonant two-photon photodissociation, which is computed by the artificial channel method. The set of the differential equations for the computation of the reduced  $\mathbf{t}$ -matrix element is comprised of the equations for  $\Phi_i^{J_i}(R)$ ,  $\Phi_{\lambda_m, m}^{J_m p_m}(R)$  and  $\Phi_{\lambda, \xi}^{(J p q)-}(R)$ , with coupling due to the reduced radiative interaction elements,  $V_{\xi, m}$  and  $V_{m, i}$ , and the spin-orbit

interaction, plus the equation for the artificial channel. One example of such a set of the equations is described in detail in Ref.18.

Finally, inserting Eqs.(55) into Eq.(29) and integrating over scattering angles we obtain the dissociation probability explicitly as

$$P^{(q)}(E, E_i, \omega_2, \omega_1) = \frac{8\pi\mu k_q}{h^2} \frac{1}{2J_i + 1} \sum_{M_i} \sum_{J, p, \lambda \geq 0} \times \left| \sum_{E_m, J_m} \begin{pmatrix} J & 1 & J_m \\ -M_i & 0 & M_i \end{pmatrix} \begin{pmatrix} J_m & 1 & J_i \\ -M_i & 0 & M_i \end{pmatrix} t(E, E_m, E_i; J, J_m, J_i; p\lambda q) \right|^2 \quad (56)$$

where no polarization of the molecule prior to excitation is assumed.

## IV Results and Discussion

We have used the artificial channel method to compute the resonant two-photon dissociation probability  $P^{(q)}(E, E_i, \omega_2, \omega_1)$  [Eq.(56)] for Na<sub>2</sub>. The data for the potential curves and transition dipole moments are taken from the work of Schmidt and Meyer<sup>15</sup>.

The frequency  $\omega_1$  is chosen to selectively excite a specific vib-rotational state by choosing small detuning  $\Delta = \omega_1 - \delta E_{m,i}$ , significantly enhancing the photodissociation rate as long as the line width  $\Gamma_m$  is less than  $\Delta$ . For Na<sub>2</sub>, with laser intensity less than 10<sup>6</sup> W/cm<sup>2</sup>,  $\Gamma_m$  (and  $\delta_m$ ) are order of magnitude of 10<sup>-2</sup> cm<sup>-1</sup>, the latter being smaller than the energy separation of adjacent rotational lines of low  $J$ . Under these conditions excitation of a single rotational line out of the initial thermal distribution can be achieved. Hence below we choose the laser intensities as 5×10<sup>5</sup> W/cm<sup>2</sup> to be consistent with this intensity constraint.

Consider first Figure 2a which shows  $P^{(q)}(E, E_i, \omega_2, \omega_1)$  vs.  $\omega_1$  for an arbitrary constant  $\omega_2 = 16777.1$  cm<sup>-1</sup>. Here  $q$  corresponds to the 3p channel and the initial state is chosen

as  $v = 0, J_i = 0$ . The probability  $P^{(q)}$  appears as a set of peaks of varying intensity corresponding to the excitation to vibrational energy levels with varying  $v_m$  and  $J_m = 1$ . Of considerable interest is the doublet at  $\omega_1 \approx 17,080 \text{ cm}^{-1}$ , shown on an expanded scale in Fig. 2b. A similar structure appears for  $q = 4s$ , shown in Fig. 3. In both cases the doublet is found to be substantially stronger than the single peaks, the distance between the double peaks is  $1.9 \text{ cm}^{-1}$  and the width of the individual peaks corresponds to power broadening at the incident laser field strength.

The doublet peaks clearly reflect strong spin-orbit coupling between vib-rotational levels of the  $^1\Sigma_u^+$  and  $^3\Pi_u$  states. Specifically note (Table 1) that all levels of  $^1\Sigma_u^+$  from  $v_{m_1} = 18$  to 35, except  $v_{m_1} = 23$ , are sufficiently well separated energetically to be weakly coupled to the levels of  $^3\Pi_u$ . The exception is  $v_{m_1} = 23$ , which is nearly degenerate ( $0.6 \text{ cm}^{-1}$  apart) with the  $v_{m_3} = 26$  level of  $^3\Pi_u$ . Both the spacing between the doublet ( $1.9 \text{ cm}^{-1}$ ) and its frequency location is consistent with Eq. (45), assuming this assignment. Thus, in accord with Eq.(45) we see a series of the single-peaks and one double-peak in  $P^{(q)}(E, E_i, \omega_2, \omega_1)$  when  $\omega_1$  is scanned. In addition, we note that Eq.(45) has terms containing the factors  $A^+B^+$  and  $A^-B^-$  which contribute to photodissociation through the triplets states  $^3\Pi_g$  or  $^3\Sigma_g^+$ , while the terms containing the factors  $(A^+)^2$  and  $(A^-)^2$  contribute through the singlet states. Our numerical results show that the primary photodissociation contribution is via the triplet states. Therefore, since the first photon carries the system to the singlet state, the two photon  $\text{Na}_2$  photodissociation is seen to occur via intersystem crossing between the  $|E_{m_1}, ^1\Sigma_u^+\rangle$  and  $|E_{m_3}, ^3\Pi_u\rangle$  states.

With increasing initial rotational state the  $P^{(q)}$  spectrum becomes more complex. Figure 4a shows  $P^{(3p)}(E, E_i, \omega_2, \omega_1)$  vs.  $\omega_1$  with  $\omega_2$  as above but for the case of  $J_i = 9$ .

Only a narrow  $\omega_1$  scan, about  $v_{m_1} = 31$  (Figure 4a) and  $v_{m_1} = 32$  (Figure 4b) are shown. The former shows a set of two lines corresponding to transitions to  $J_m = 8$  and 10 whereas the latter displays more complex structure resulting from the splitting of the  $J_m = 10$  line. Once again, the results show agreement with Tables 1 and 2 insofar as the location of the doublet has shifted to a frequency corresponding to the regime of strongly coupled  $v_{m_1} = 32$  of  $^1\Sigma_u^+$  and  $v_{m_3} = 33$  of  $^3\Pi_u$  for  $J_m = 10$ . Further, the reduced splitting ( $1.1 \text{ cm}^{-1}$ ) in accord with Eq. (45).

Consider now the photodissociation probability with  $\omega_1$  fixed and  $\omega_2$  variable. Figure 5 shows a series of cases for excitation from  $v_i = \bar{\phantom{v}}$ ,  $J_i = 0$  where  $\omega_1$  is resonant with successively higher  $v_{m_1}$  ( $J_m = 1$ ) levels. In each case  $P^{(q)}(E, E_i, \omega_2, \omega_1)$  is shown as a function of  $\omega_2$  for all three products  $q = 3p, 4s, 3d$ . The degree of the detunings  $\Delta$  are in the same order of magnitude in the figures. The general features of each of these curves is similar and readily explained in terms of the Franck-Condon principle and the oscillatory character of the wavefunctions from which photodissociation occurs. For example the number of oscillations in  $P^{(q)}(E, E_i, \omega_2, \omega_1)$  increases with increasing  $v_{m_1}$ , reflecting the increasingly oscillatory character of intermediate bound state wavefunction. Note also that  $P^{(4s)}$  and  $P^{(3p)}$  behave similarly as a function of  $\omega_2$  (except for the sharp cutoff of  $P^{(4s)}$  at the  $4s$  threshold), since the potentials of  $^3\Pi_g$  and  $^3\Sigma_g^+$  states are similar in the regime where  $\omega_2$  is scanned. Dissociation to  $\text{Na}(3d)$  occurs only at higher  $\omega_2$  and overlaps the energy region of  $\text{Na}(4s)$  and  $\text{Na}(3p)$  only at larger  $\omega_1$ , (e.g.  $v_{m_1} = 35$  in Fig. 5d), when the intermediate bound state wavefunction becomes sufficiently broad in  $r$ .

These results are confined to the case of  $v_i = 0$ . Preliminary results on higher  $v_i$  (realized in a heat pipe, for example), show an increase in  $P^{(q)}$ . For example, at  $v_i = 5$

$P^{(q)}$  for the  $v_{m_1} = 35$  case is a factor of  $10^4$  larger than that at  $v_i = 0$ , a consequence of improved Franck-Condon overlap in the initial  $\omega_1$  excitation. The relevance of these probabilities in the control of photodissociation will be discussed elsewhere<sup>3</sup>.

## V Conclusions

We have derived a consistent non-perturbative theory of two photon dissociation and applied it to the photodissociation of  $\text{Na}_2$ . Illumination with the first photon in the 500 to 610 nm regime, widely available with conventional dye lasers, leads to excitation to the  $A^1\Sigma_v^+$  state, followed by intersystem crossing to the  $b^3\Pi_u$  state and subsequent dissociation. With the second photon again in the convenient 600 ~ 690 nm region we see significant photodissociation intensity to three different atomic products.

The efficient two photon dissociation probabilities obtained for  $\text{Na}_2$  serves as input to a new coherent control scenario in which we demonstrate control over systems initially in thermal equilibrium. This scenario and its ramifications are to be discussed elsewhere<sup>3</sup>.

## Acknowledgements

We thank J. Dods for useful discussions about  $\text{Na}_2$ . This work was supported by the U.S. Office of Naval Research under contract number N00014-90-J-1014.

## References

- [1] See, e.g. *Advances in Chemical Physics*, volume 60, (Wiley, N.Y., 1985)
- [2] P. Brumer and M. Shapiro, *Chem. Phys. Lett.* **126** 541 (1986); P. Brumer and M. Shapiro, *Faraday Discuss. Chem. Soc.* **82** 177, (1986); M. Shapiro and P. Brumer, *J. Chem. Phys.* **84** 4103 (1986); M. Shapiro, J. Hepburn and P. Brumer, *Chem. Phys. Letters* **149** 451 (1988); C. Asaro, P. Brumer and M. Shapiro, *Phys. Rev. Lett.* **60** 1634 (1988); P. Brumer and M. Shapiro, *Chem. Phys.* **139** 221 (1989); T. Seideman, P. Brumer, M. Shapiro, *J. Chem. Phys.* **90** 7132 (1989); I. Levy, M. Shapiro and P. Brumer, *J. Chem. Phys.* **93** 2493 (1990); C. K. Chan, P. Brumer and M. Shapiro, *J. Chem. Phys.* **94** 4103 (1991); J.L. Krause, M. Shapiro and P. Brumer, *J. Chem. Phys.* **92**, 1126 (1990); G. Kurizki, M. Shapiro, and P. Brumer, *Phys. Rev. B* **39**, 3435 (1989); M. Shapiro and P. Brumer, *J. Chem. Phys.*, **90**, 6179 (1989); M. Shapiro and P. Brumer, *J. Chem. Phys.*, **95**, 8658 (1991).
- [3] Z. Chen, P. Brumer and M. Shapiro, (unpublished).
- [4] M. Shapiro, *J. Chem. Phys.* **56** 2582 (1972); M. Shapiro and R. Bersohn, *Ann. Rev. Phys. Chem.* **33** 409 (1982); G. G. Balint-Kurti and M. Shapiro, *Adv. Chem. Phys.* **60** 403, K. P. Lawley, Ed., (Wiley-Interscience Pub., 1986); A. D. Bandrauk and G. Turcotte, *J. Phys. Chem.* **89** 3039 (1985); A. D. Bandrauk and O. Atabek, *Adv. Chem. Phys.* **73** 823, 1989
- [5] I. Sofer *et al.*, (unpublished).

- [6] F. Engelke, H. Hage and C. D. Caldwell, *Chem. Phys.* **64** 221 (1982); K. Shimizu and F. Shimizu, *J. Chem. Phys.* **78** 1126 (1983).
- [7] C. Effantin, O. Babaky, K. Hussein, J. d'Incan and R. F. Barrow, *J. Phys. B* **18** 4077 (1985); J. B. Atkinson, J. Becker and W. Demtroder, *Chem. Phys. Lett.* **87** 92 (1982).  
In this paper we neglect the orbit-rotation coupling which is much smaller than  $V_{so}$ .
- [8] R. D. Levine, *Quantum Mechanics of Molecular Rate Processes*, (Clarendon, Oxford, England, 1969).
- [9] a) G. G. Balint-Kurti and M. Shapiro, *Adv. Chem. Phys.* **60** 403, K. P. Lawley, Ed., (Wiley-Interscience Pub., 1986); b) P. Brumer and M. Shapiro, *Adv. Chem. Phys.* **60** 371, K. P. Lawley, Ed., (Wiley-Interscience Pub., 1986).
- [10] M. Shapiro, J. Hepburn, P. Brumer, *Chem. Phys. Letters*, **149**, 451 (1988).
- [11] R. Loudon, *The Quantum Theory of Light*, (Clarendon, Oxford, 1973).
- [12] See, for example, M. L. Janson and S. M. Papernov, *J. Phys. B* **15** 4175 (1982), and references therein.
- [13] G. Gerber and R. Moller, *Phys. Rev. Lett.* **55** 814 (1985). However, the energy regime in this paper is different from what we consider here.
- [14] J. Dods, M.Sc. Dissertation, University of Toronto, 1992; J. Dods, P. Brumer and M. Shapiro (to be published).
- [15] I. Schmidt, Ph.D. Thesis, Kaiserslautern University, 1987; W. Meyer, Private communication.

- [16] I. Levy and M. Shapiro, *J. Chem. Phys.* **89** 2900 (1988); T. Seideman and M. Shapiro, *J. Chem. Phys.* **94** 7910 (1991).
- [17] A. R. Edmonds, *Angular Momentum in Quantum Mechanics*, 2nd Ed. (Princeton University Press, Princeton, 1960).
- [18] M. Shapiro and H. Bony, *J. Chem. Phys.* **83** 1588 (1985).

Table 1: Na<sub>2</sub> zeroth order bound state energies (in cm<sup>-1</sup>).

$v_m$	$J_m = 1$		$J_m = 10$	
	$^1\Sigma_u^+$	$^3\Pi_u$	$^1\Sigma_u^+$	$^3\Pi_u$
20	10910.4	10427.7	10921.1	10442.5
21	11012.5	10561.6	11023.2	10576.4
22	11114.0	10694.5	11124.6	10709.2
23	11214.8	10826.3	11225.3	10840.9
24	11314.9	10957.1	11325.3	10971.6
25	11414.3	11086.8	11424.7	11101.2
26	11513.0	11215.4	11523.4	11229.8
27	11611.0	11343.0	11621.3	11357.3
28	11708.4	11469.5	11718.6	11483.7
29	11805.0	11594.9	11815.2	11609.1
30	11901.0	11719.3	11911.1	11733.4
31	11996.2	11842.6	12006.3	11856.6
32	12090.7	11964.8	12100.7	11978.7
33	12184.6	12086.0	12194.5	12099.9
34	12277.7	12206.1	12287.6	12219.8
35	12370.1	12325.1	12380.0	12338.7

Table 2: Spin orbit coupling matrix elements  $V_{so} = H_{so} \langle v_{m_3} | v_{m_1} \rangle$  with  $H_{so} = 5.91$

cm<sup>-1</sup>.

$v_{m_3}$ $v_{m_1}$	20	21	22	23	24	25	26	27	28	29	30	31	32	33
20	0.94	0.22	0.95	0.36	0.90	0.59	0.75	0.89	0.40	1.14	0.22	1.07	0.99	0.36
21	0.66	0.68	0.67	0.66	0.76	0.55	0.91	0.33	1.05	0.06	1.08	0.62	0.78	1.18
22	0.15	0.91	0.22	0.92	0.21	0.95	0.91	0.17	0.14	1.01	0.49	0.86	0.92	0.42
23	0.79	0.36	0.86	0.28	0.89	0.28	0.91	0.37	0.88	0.56	0.78	0.82	0.53	1.09
24	0.82	0.42	0.74	0.56	0.68	0.63	0.67	0.64	0.73	0.59	0.85	0.44	1.01	0.14
25	0.30	0.85	0.59	0.88	0.12	0.88	0.22	0.89	0.25	0.92	0.19	0.98	0.38	1.03
26	0.37	0.69	0.62	0.50	0.77	0.34	0.45	0.23	0.89	0.18	0.92	0.22	0.94	0.35
27	0.79	0.11	0.84	0.21	0.78	0.45	0.68	0.60	0.59	0.69	0.56	0.74	0.58	0.75
28	0.76	0.50	0.52	0.74	0.24	0.84	0.03	0.85	0.22	0.82	0.36	0.81	0.44	0.82
29	0.35	0.80	0.08	0.77	0.43	0.60	0.67	0.39	0.79	0.18	0.86	0.03	0.89	0.07
30	0.19	0.68	0.59	0.35	0.79	0.02	0.79	0.34	0.69	0.57	0.54	0.72	0.39	0.81
31	0.62	0.25	0.79	0.23	0.66	0.59	0.38	0.77	0.06	0.81	0.22	0.76	0.44	0.67
32	0.78	0.27	0.59	0.66	0.19	0.78	0.24	0.67	0.56	0.43	0.75	0.16	0.82	0.29
33	0.63	0.65	0.15	0.75	0.36	0.53	0.68	0.16	0.78	0.23	0.68	0.53	0.48	0.73

\*

## VI Figure Captions

Figure 1: Potential Energy Curves for  $\text{Na}_2$

Figure 2: Probability for two photon ( $v_i = 0, J_i=0$ )  $\text{Na}_2$  photodissociation into the  $\text{Na}(3p) + \text{Na}(3s)$  product with  $\omega_2 = 16777.1 \text{ cm}^{-1}$ , as a function of  $\omega_1$ . (a) Over a wide  $\omega_1$  range and (b) in the neighborhood of the doublet. In the former figure the peaks are labeled by the  $v_{m_1}$  state resonant with  $\omega_1$

Figure 3: As in Figure 2, but for the  $\text{Na}(3s) + \text{Na}(4s)$  product.

Figure 4: As in Figure 2, but for the  $\text{Na}(3s) + \text{Na}(4s)$  product and with initial  $J_i=9$ . (a) sample probability in region of a single peak and (b) in region of a doublet.

Figure 5: Probability for two photon  $\text{Na}_2$  photodissociation into assorted atomic products starting in  $v_i = 0, J_i = 0$  as a function of  $\omega_2$  and for various values of  $\omega_1$ . Here  $\omega_1$  is chosen resonant with  $J_m = 1$  and (a)  $v_{m_1} = 17, \Delta = 0.003 \text{ cm}^{-1}$ , (b)  $v_{m_1} = 25, \Delta = 0.004 \text{ cm}^{-1}$ , (c)  $v_{m_1} = 31, \Delta = 0.002 \text{ cm}^{-1}$ , (d)  $v_{m_1} = 35, \Delta = 0.003 \text{ cm}^{-1}$ .

Figure 1

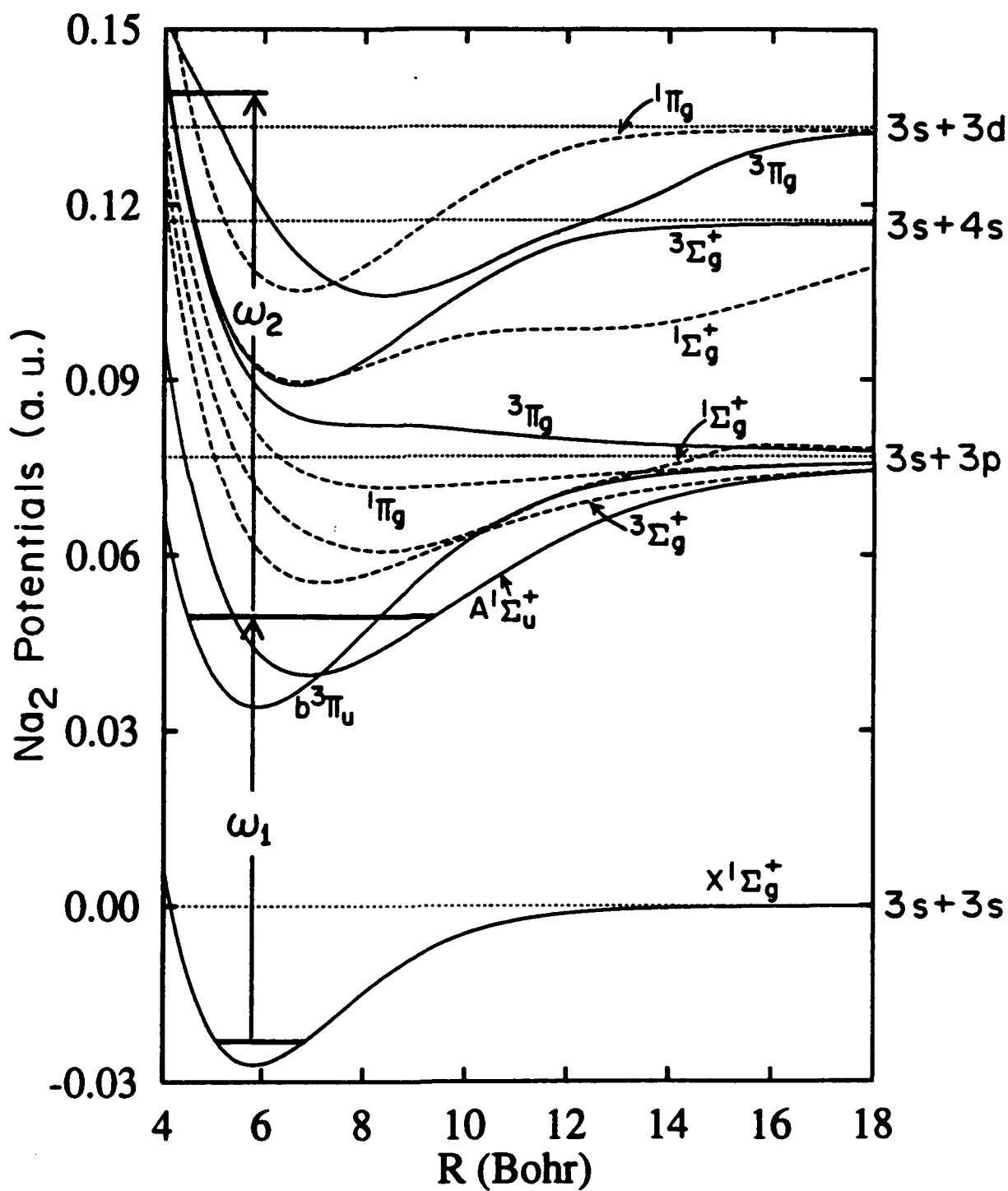


Figure 1

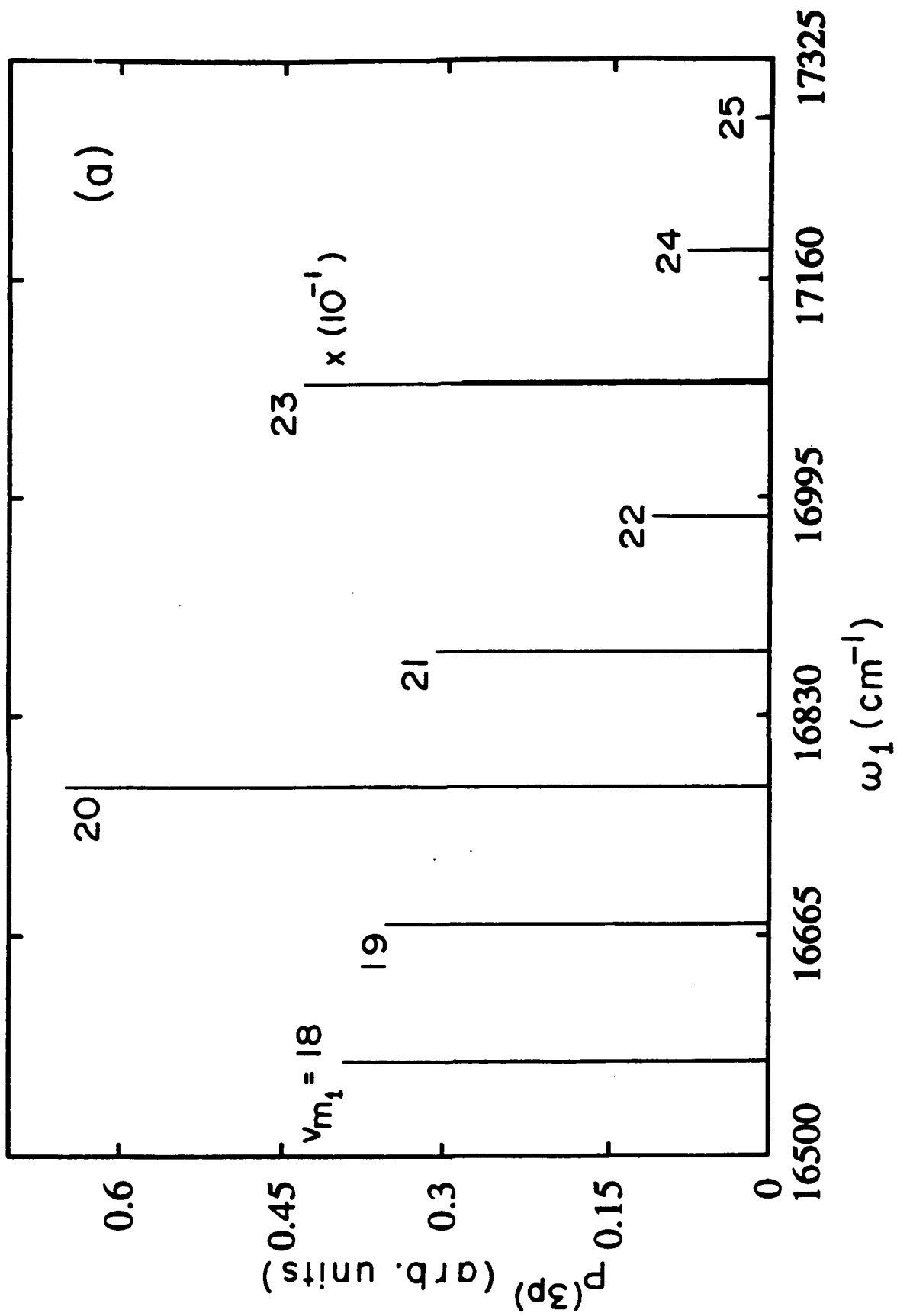


Figure 2a

Figure 2a

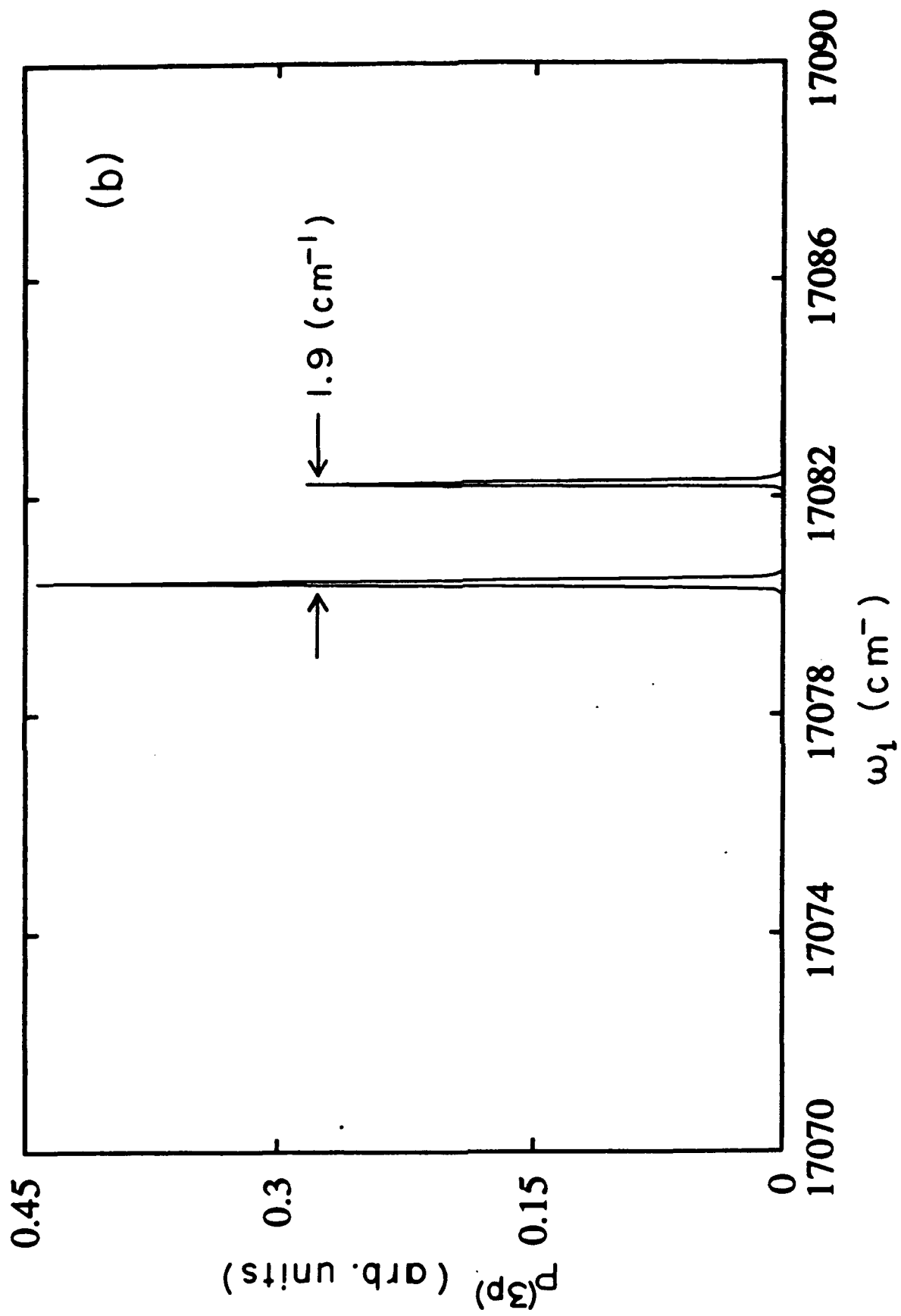


Figure 2b

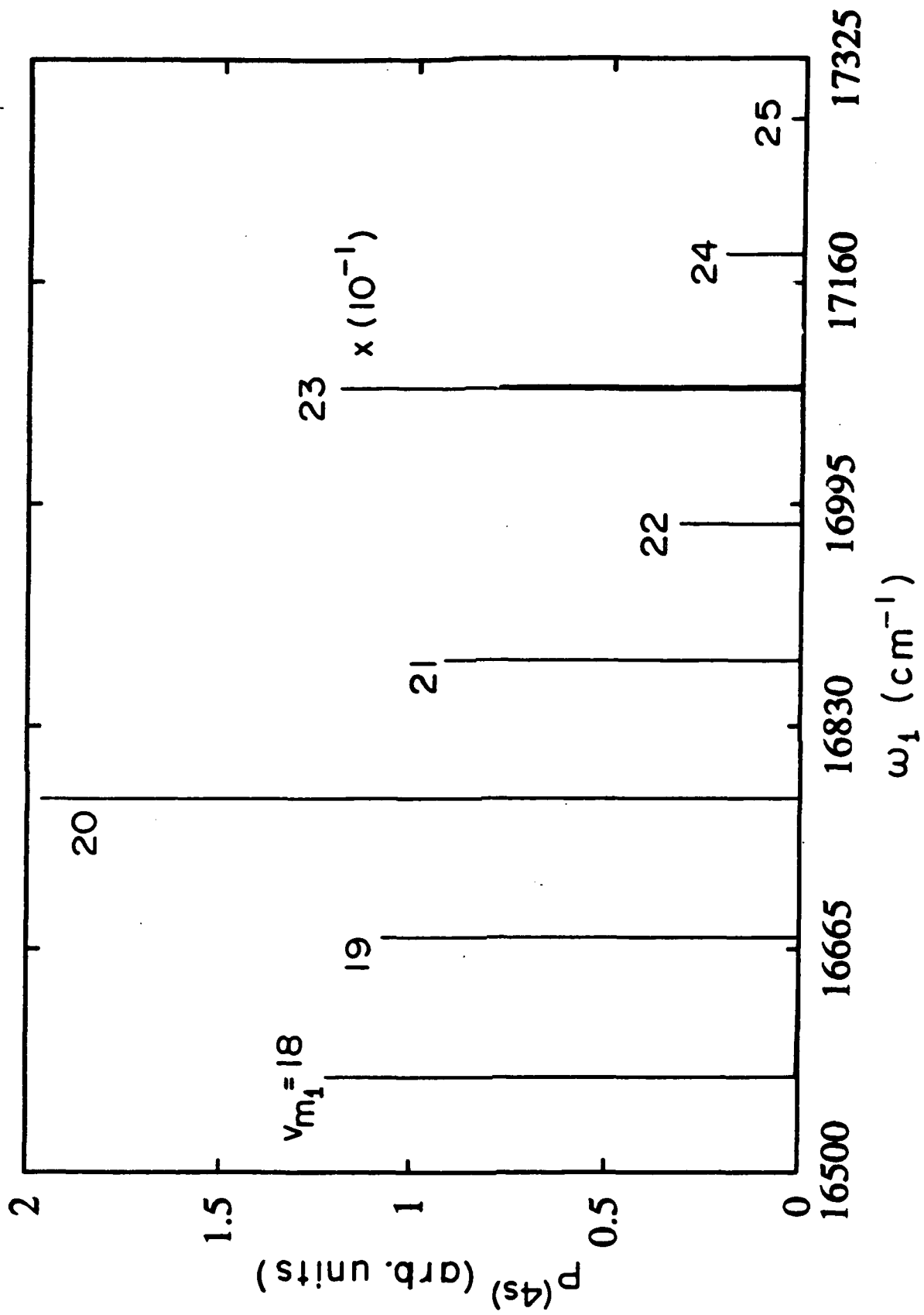


Figure 3

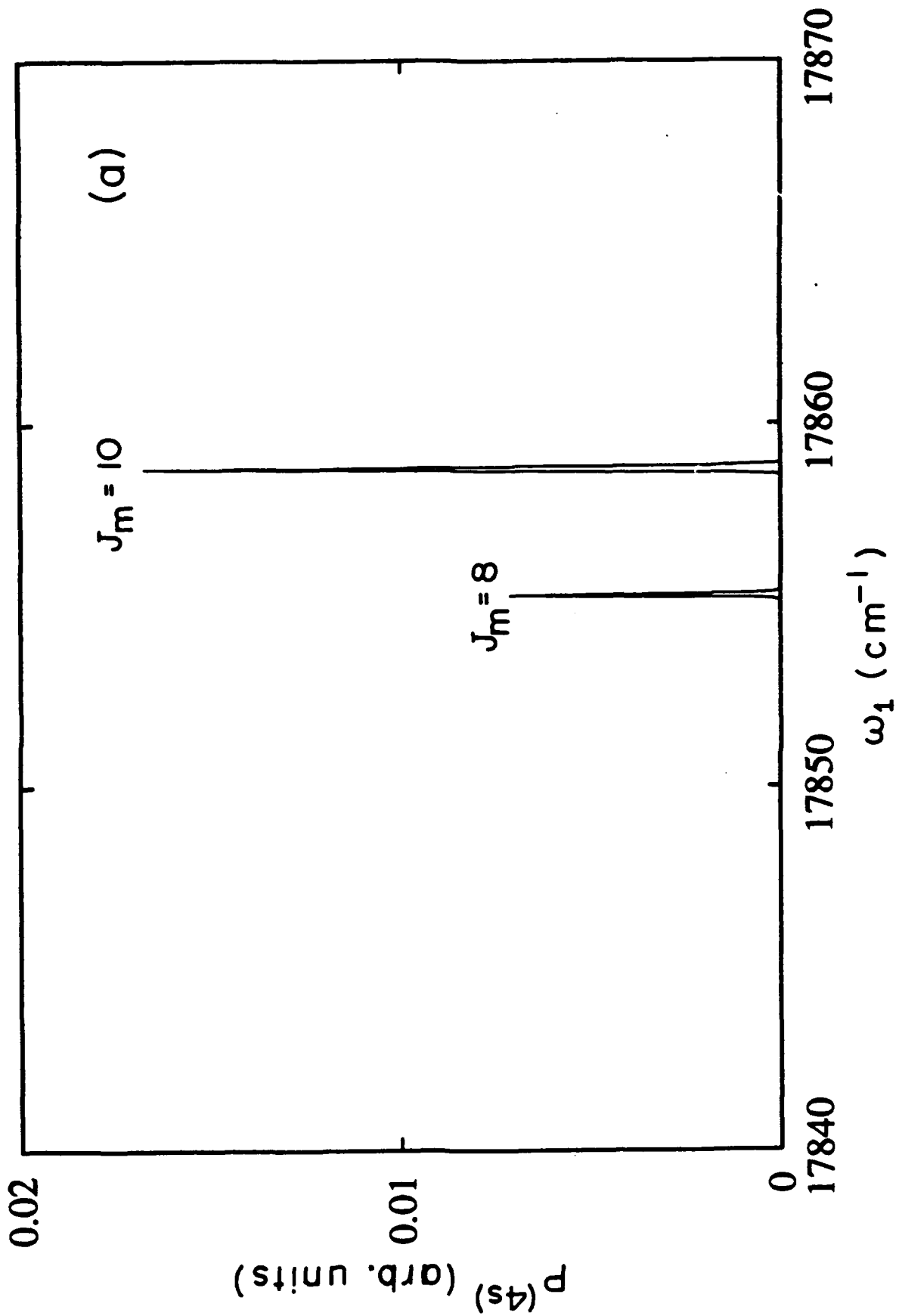


Fig 4a

Figure 4a

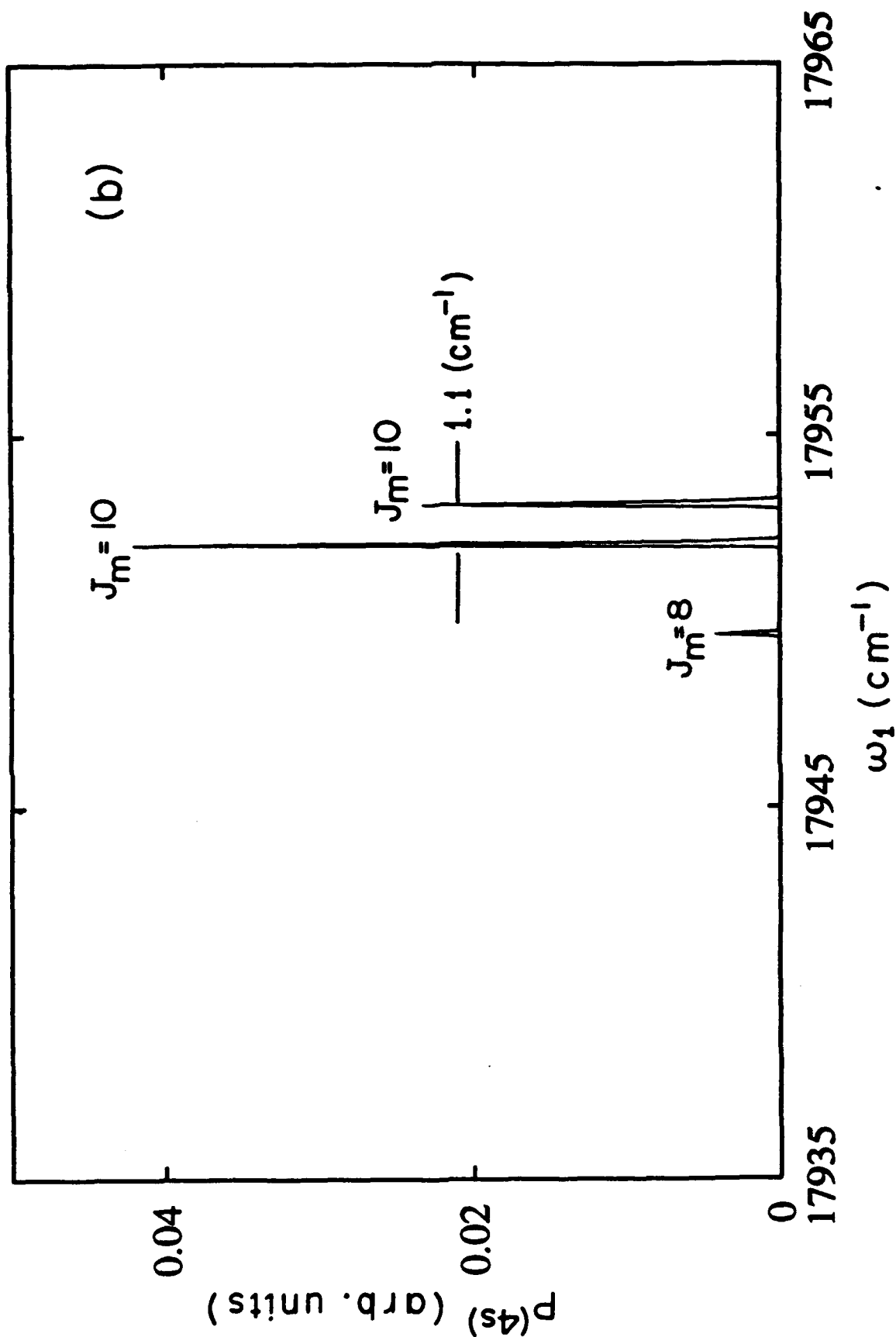


Figure 4b

Figure 4a

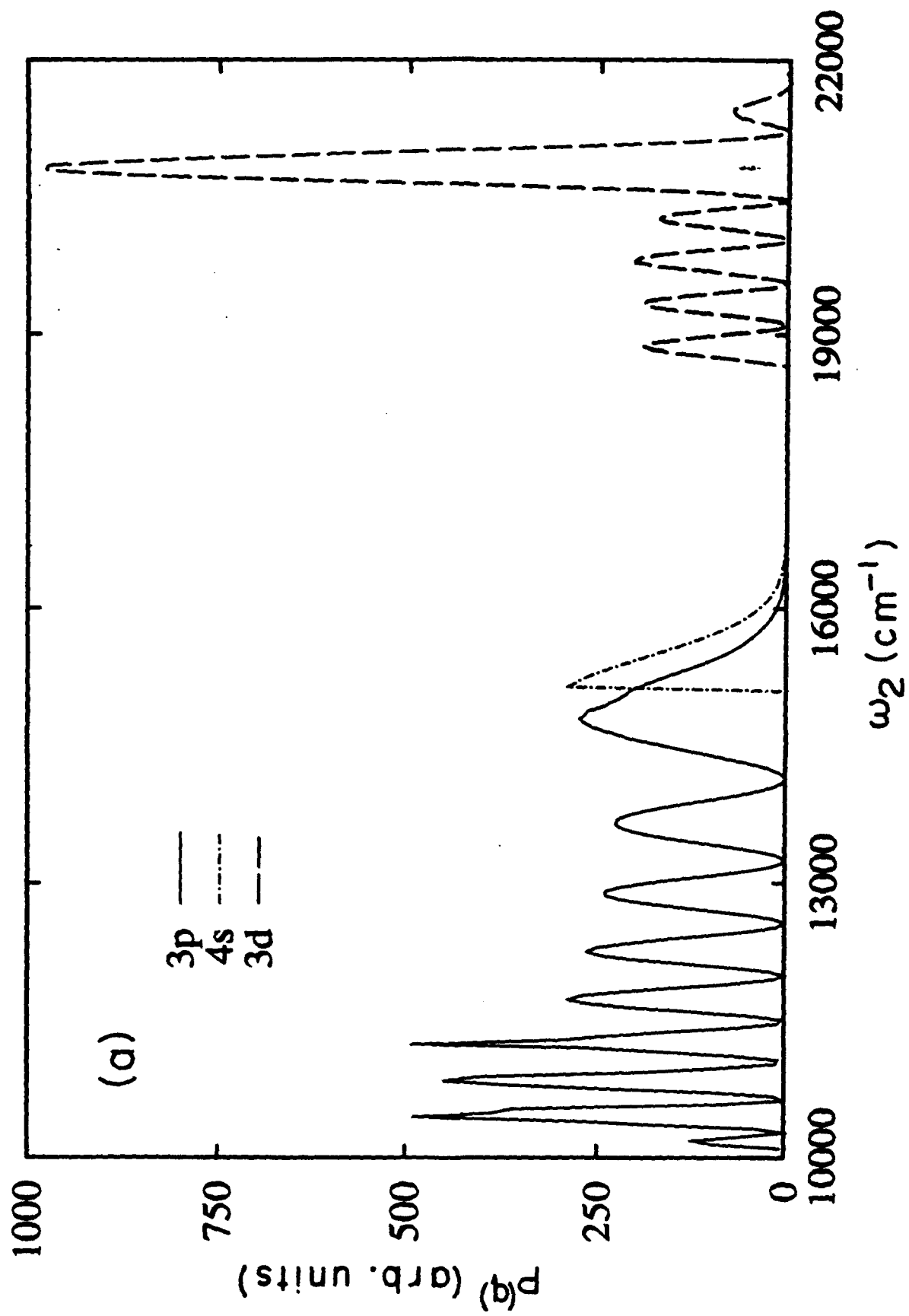


Figure 5a

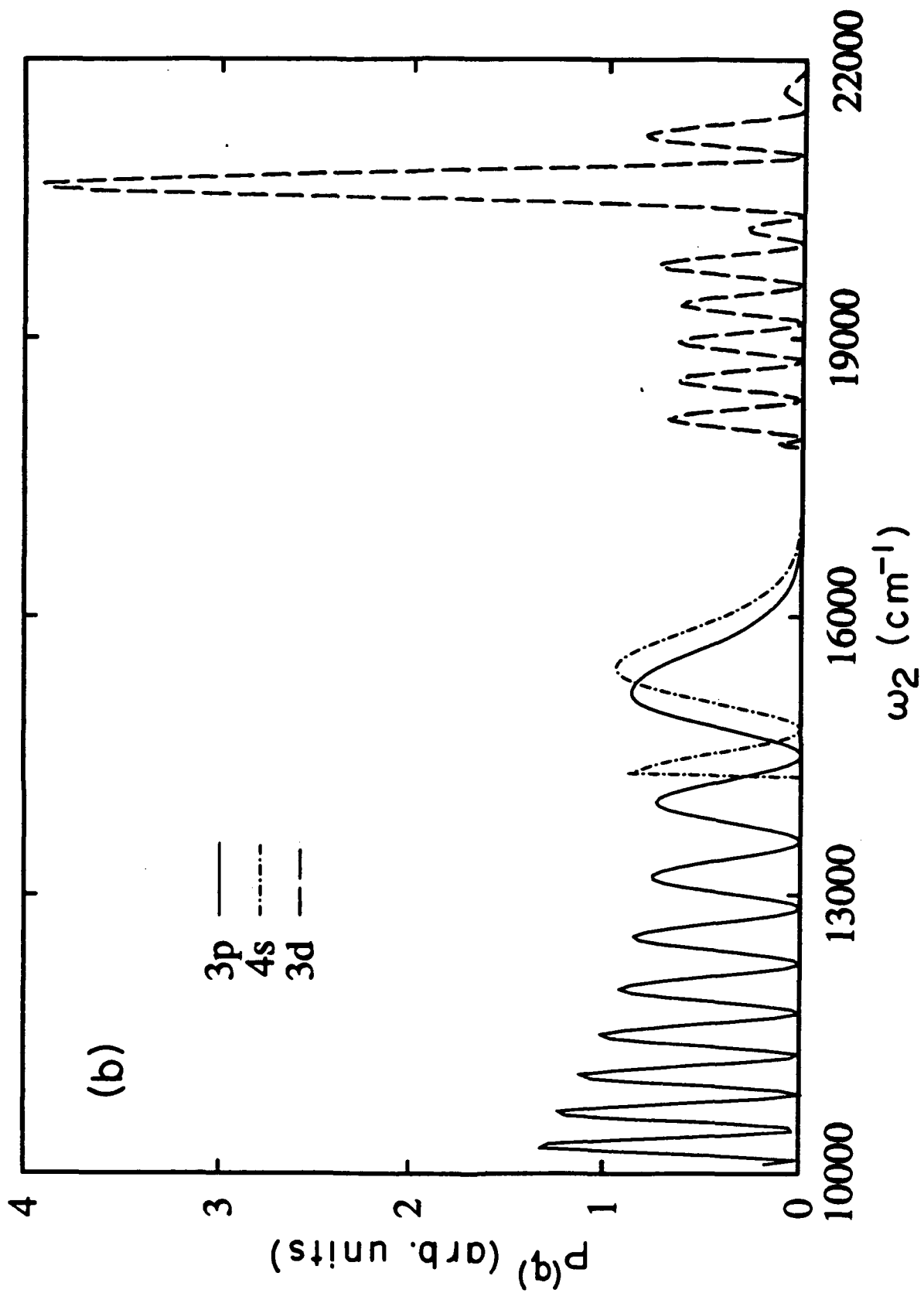


Figure 5b

Figure 5b

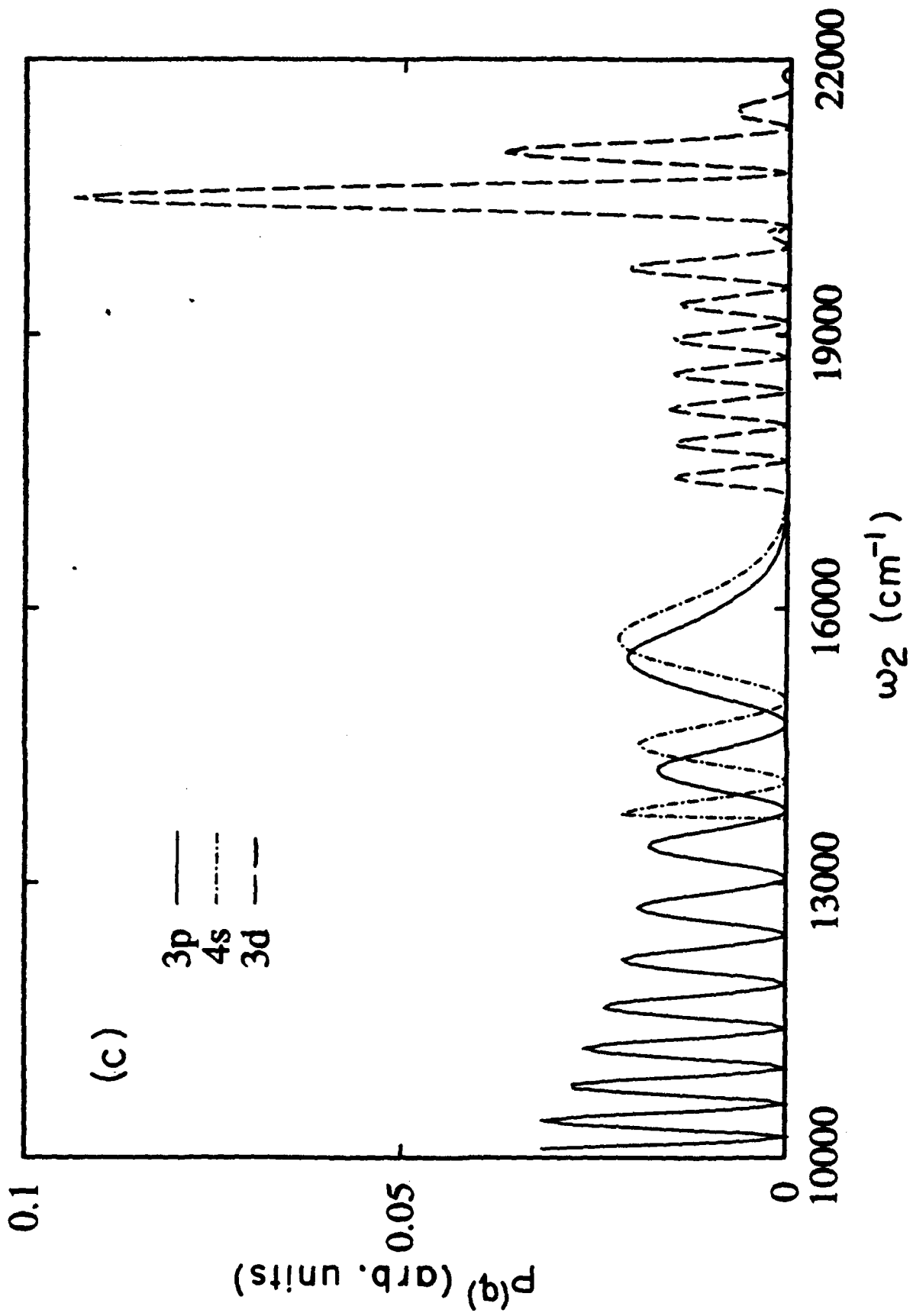


Figure 5c

Figure 5c

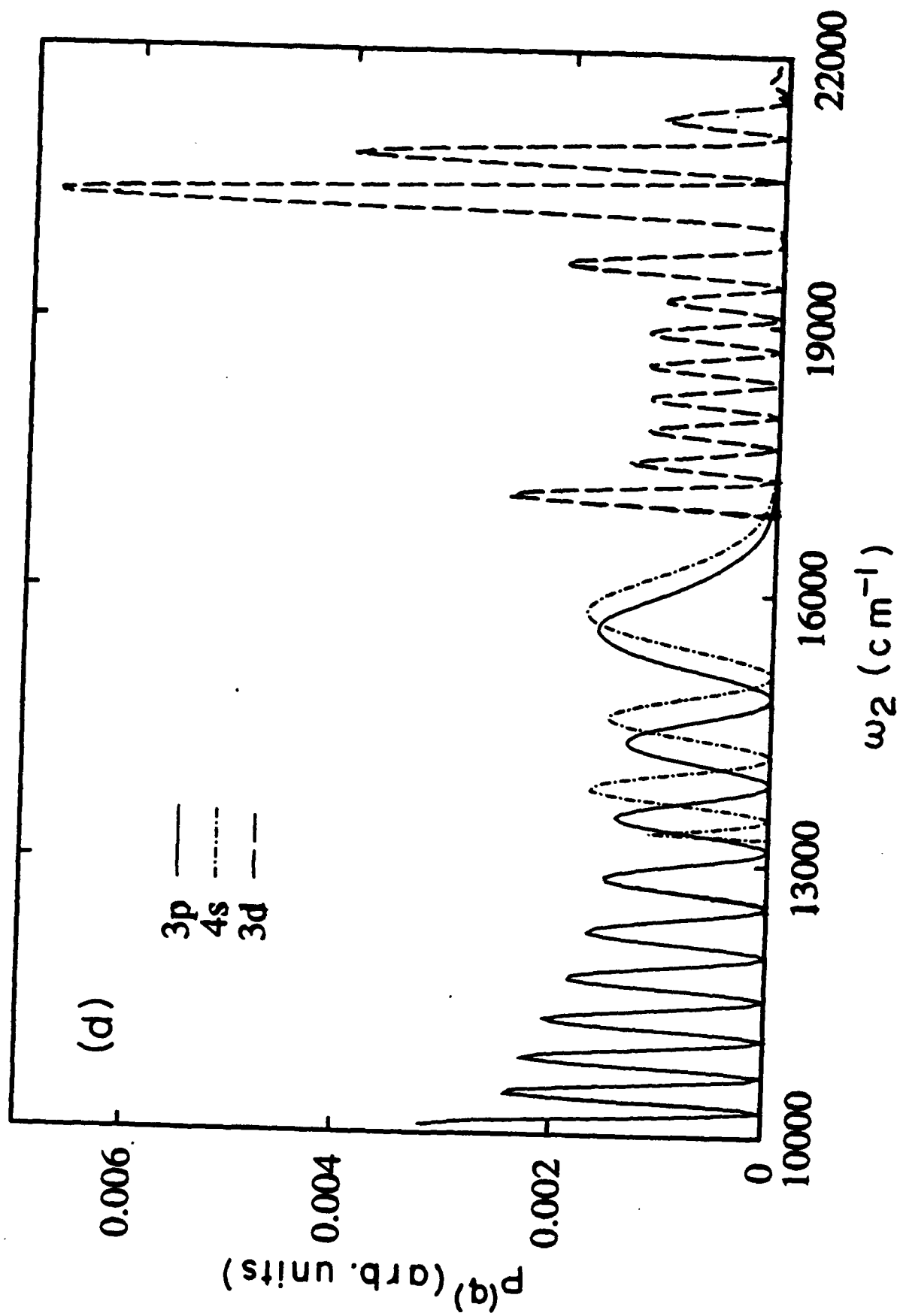


Figure 5d

**Coherent Radiative Control of Molecular Photodissociation  
via Resonant 2-Photon vs. 2-Photon Interference**

**Zhidang Chen, Paul Brumer**

**Chemical Physics Theory Group, Department of Chemistry**

**University of Toronto**

**Toronto M5S 1A1 Canada**

**and**

**Moshe Shapiro**

**Chemical Physics Department, Weizmann Institute of Science,**

**Rehovot, Israel**

**PACS Numbers: 33.80.-b, 34.50.Rk, 33.80.Gj**

## Abstract

We show that resonant 2-photon vs. 2-photon interference provides a means of controlling relative photodissociation cross sections even when the initial molecular system is in a mixed state, e.g. in thermal equilibrium. The resultant technique, which also allows cancellation of incoherences due to laser phase fluctuations and the reduction of uncontrolled background photodissociation contributions, is demonstrated computationally on  $\text{Na}_2$  photodissociation, where a wide range of control over branching into  $\text{Na}(3s) + \text{Na}(4s)$  vs.  $\text{Na}(3s) + \text{Na}(3p)$  is achieved.

*Introduction:* Utilizing and manipulating quantum interference phenomena has become an increasingly important area of atomic and molecular physics as evidenced by advances in quantum devices<sup>1</sup>, atomic and molecular interferometry<sup>2</sup> and coherent radiative control of molecular processes<sup>3</sup>. In the latter case<sup>4,5,6,7,8,9</sup> active control over product cross sections is achieved by driving an initially pure molecular state through two or more independent coherent optical excitation routes to the same final continuum state. If this continuum state can decay into a number of product arrangements then the probability of forming a particular product arrangement displays interference terms between the two routes, whose magnitude and sign depend upon laboratory parameters. Specifically, by manipulating laser parameters one can directly alter the quantum interference terms, and hence manipulate cross sections for various processes.

As in all interference phenomena the known system phase, both molecular and optical, plays a crucial role. Incoherence effects leading to a mixed initial matter-photon state, such as partial laser coherence or an initially mixed molecular state, degrade control in quantum interference based methods. As a consequence, all but one<sup>5</sup> of the previous coherent control scenarios were limited to isolated molecules in a pure state, e.g. molecular beam systems. Here we show that it is possible to maintain control in a molecular system in thermal equilibrium by interfering two distinct resonant two-photon routes to photodissociation. The resonant character of the excitations insure that only a selected state out of the molecular thermal distribution participates in the photodissociation. Hence coherence is re-established by the excitation and maintained throughout the process. The proposed control scenario also provides a method for overcoming destructive interference loss due to phase jitter in the laser source. In addition, we show that this approach allows the reduction of contributions from uncontrolled ancillary photodissociation routes. Computational

results support the feasibility and broad range of control afforded by this approach. Thus, this letter advances a coherent control scenario which eliminates three major incoherence effects and defines a method for controlling molecular reactions in natural environments.

*Resonant Two Photon Dissociation:* Although the control theory we propose is completely general, we focus on the realistic case of two photon photodissociation in  $\text{Na}_2$ . Our recent analysis<sup>10</sup> of resonant two photon dissociation of a diatomic molecule yielded the following results, which serve as input to the coherent control scenario discussed later below. Consider a molecule in a state  $|E_i, J_i, M_i\rangle$  which is subjected to two laser fields and photodissociates to a number of different product channels labeled by  $q$ . Absorption of the first photon of frequency  $\omega_1$  lifts the system to a region close to an intermediate bound state  $|E_m J_m M_m\rangle$ , and a second photon of frequency  $\omega_2$  carries the system to the dissociating states  $|E, \hat{\mathbf{k}}q^-\rangle$ . These continuum states are of energy  $E$  and correlate with the product in arrangement channel  $q$ , in the direction specified by the scattering angles  $\hat{\mathbf{k}} = (\theta_k, \phi_k)$ . Here the  $J$ 's are the angular momentum,  $M$ 's are their projection along the  $z$ -axis, and the values of energy,  $E_i$  and  $E_m$ , include specification of the vibrational quantum numbers. Photon states of the incident lasers are described by the coherent states. Specifically if we denote the phases of the coherent states by  $\phi_1$  and  $\phi_2$ , the wavevectors by  $\mathbf{k}_1$  and  $\mathbf{k}_2$  with overall phases  $\theta_i = \mathbf{k}_i \cdot \mathbf{r} + \phi_i$  ( $i = 1, 2$ ) and the electric field amplitudes by  $\mathcal{E}_1$  and  $\mathcal{E}_2$ , then the probability amplitude for resonant two photon ( $\omega_1 + \omega_2$ ) photodissociation is given<sup>10</sup> by

$$\begin{aligned}
T_{\hat{\mathbf{k}}q,i}(E, E_i J_i M_i, \omega_2, \omega_1) &= \\
&= \sum_{E_m, J_m} \frac{\langle E, \hat{\mathbf{k}}q^- | d_2 \mathcal{E}_2 | E_m J_m M_i \rangle \langle E_m J_m M_i | d_1 \mathcal{E}_1 | E_i J_i M_i \rangle \exp[i(\theta_1 + \theta_2)]}{\omega_1 - (E_m + \delta_m - E_i) + i\Gamma_m} \\
&= \frac{\sqrt{2\mu k_q}}{h} \sum_{J,p,\lambda \geq 0} \sum_{E_m, J_m} \begin{pmatrix} J & 1 & J_m \\ -M_i & 0 & M_i \end{pmatrix} \begin{pmatrix} J_m & 1 & J_i \\ -M_i & 0 & M_i \end{pmatrix} \\
&\times \sqrt{2J+1} D_{\lambda, M_i}^{Jp}(\theta_k, \phi_k, 0) t(E, E_i J_i, \omega_2, \omega_1, q | Jp\lambda, E_m J_m) \exp[i(\theta_1 + \theta_2)] \quad (1)
\end{aligned}$$

Here  $d_i$  is the component of the dipole moment along the electric-field vector of the  $i^{\text{th}}$  laser mode,  $E = E_i + (\omega_1 + \omega_2)$ ,  $\delta_m$  and  $\Gamma_m$  are respectively the radiative shift and width of the intermediate state,  $\mu$  the reduced mass, and  $k_q$  is the relative momentum of the dissociated product in  $q$ -channel. The  $D_{\lambda, M_i}^{Jp}$  is the parity adapted rotation matrix<sup>11</sup> with  $\lambda$  the magnitude of the projection on the internuclear axis of the electronic angular momentum and  $(-1)^{Jp}$  the parity of the rotation matrix. We have set  $\hbar \equiv 1$ , and assumed for simplicity that the lasers are linearly-polarized and their electric-field vectors are parallel. Note that the  $T$ -matrix element in Eq.(1) is a complex quantity, whose phase is the sum of the laser phase  $\theta_1 + \theta_2$  and the molecular phase, i.e. the phase of  $t$ .

The essence of the photodissociation lies in the molecular two photon  $t$ -matrix element whose structure has been analyzed in detail elsewhere<sup>10</sup>. It incorporates integrations over radial nuclear-vibrational wavefunctions of the bound and continuous states in the numerator and contains the essential dynamics of the photodissociation process. Below we compute the  $t$ -matrix elements for  $\text{Na}_2$  exactly by the artificial channel method<sup>10,12</sup>.

The probability of producing the fragments in  $q$ -channel is obtained by integrating the square of Eq.(1) over the scattering angles  $\hat{\mathbf{k}}$ , with the result:

$$\begin{aligned}
P^{(q)}(E, E_i J_i M_i, \omega_2, \omega_1) &= \int d\hat{\mathbf{k}} |T_{\hat{\mathbf{k}}q,i}^{(E, E_i J_i M_i, \omega_2, \omega_1)}|^2 \\
&= \frac{8\pi\mu k_q}{\hbar^2} \sum_{J,p,\lambda \geq 0} \left| \sum_{E_m, J_m} \begin{pmatrix} J & 1 & J_m \\ -M_i & 0 & M_i \end{pmatrix} \begin{pmatrix} J_m & 1 & J_i \\ -M_i & 0 & M_i \end{pmatrix} \right. \\
&\quad \left. \times t(E, E_i J_i, \omega_2, \omega_1, q | J p \lambda, E_m J_m) \right|^2, \tag{2}
\end{aligned}$$

Because the  $t$ -matrix element contains a factor of  $[\omega_1 - (E_m + \delta_m - E_i) + i\Gamma_m]^{-1}$  the probability is greatly enhanced by the approximate inverse square of the detuning  $\Delta = \omega_1 - (E_m + \delta_m - E_i)$  as long as the line width  $\Gamma_m$  is less than  $\Delta$ . Here only the levels closest to the resonance  $\Delta = 0$  contribute significantly to the dissociation probability. *This allows us to selectively photodissociate molecules from a thermal bath, reestablishing coherence necessary for quantum interference based control and overcoming dephasing effects due to collisions.*

*Coherent Control via Resonant 2-photon vs. 2-photon Interference:* The essence of control lies in the simultaneous excitation of a molecule via two or more coherent paths, which introduces a controllable quantum interference term between them<sup>4</sup>. Consider then the following scenario. A molecule is irradiated with three interrelated frequencies,  $\omega_0, \omega_+, \omega_-$  where photodissociation occurs at  $E = E_i + 2\omega_0 = E_i + (\omega_+ + \omega_-)$  and where  $\omega_0$  and  $\omega_+$  are chosen resonant with intermediate bound state levels. The probability of photodissociation at energy  $E$  into arrangement channel  $q$  is then given by the square of the sum of the  $T$  matrix elements from pathway "a" ( $\omega_0 + \omega_0$ ) and pathway "b" ( $\omega_+ + \omega_-$ ). That is the probability into channel  $q$

$$\begin{aligned}
P_q(E, E_i J_i M_i; \omega_0, \omega_+, \omega_-) &\equiv \int d\hat{\mathbf{k}} \left| T_{\hat{\mathbf{k}}q,i}^{(E, E_i J_i M_i, \omega_0, \omega_0)} + T_{\hat{\mathbf{k}}q,i}^{(E, E_i J_i M_i, \omega_+, \omega_-)} \right|^2 \\
&\equiv P^{(q)}(a) + P^{(q)}(b) + P^{(q)}(ab) \tag{3}
\end{aligned}$$

Here  $P^{(q)}(a)$  and  $P^{(q)}(b)$  are the independent photodissociation probabilities associated

with routes  $a$  and  $b$  respectively and  $P^{(q)}(ab)$  is the interference term between them, discussed below. Note that the two  $T$  matrix elements in Eq.(3) are associated with different lasers and as such contain different laser phases. Specifically, the overall phase of the three laser fields are  $\theta_0 = \mathbf{k}_0 \cdot \mathbf{r} + \phi_0$ ,  $\theta_+ = \mathbf{k}_+ \cdot \mathbf{r} + \phi_+$  and  $\theta_- = \mathbf{k}_- \cdot \mathbf{r} + \phi_-$ , where  $\phi_0$ ,  $\phi_+$  and  $\phi_-$  are the photon phases, and  $\mathbf{k}_0$ ,  $\mathbf{k}_+$ , and  $\mathbf{k}_-$  are the wavevectors of the laser modes  $\omega_0$ ,  $\omega_+$  and  $\omega_-$ , whose electric field strengths are  $\mathcal{E}_0, \mathcal{E}_+, \mathcal{E}_-$  and intensities  $I_0, I_+, I_-$ .

The optical path-path interference term  $P^{(q)}(ab)$  is given by

$$P^{(q)}(ab) = 2|F^{(q)}(ab)| \cos(\alpha_a^q - \alpha_b^q) \quad (4)$$

with relative phase

$$\alpha_a^q - \alpha_b^q = (\delta_a^q - \delta_b^q) + (2\theta_0 - \theta_+ - \theta_-). \quad (5)$$

where the amplitude  $|F^{(q)}(ab)|$  and the molecular phase difference  $(\delta_a^q - \delta_b^q)$  are defined by

$$\begin{aligned} & |F^{(q)}(ab)| \exp[i(\delta_a^q - \delta_b^q)] \\ &= \frac{8\pi\mu k_q}{h^2} \sum_{J,p,\lambda \geq 0} \sum_{E_m, J_m} \sum_{E'_m, J'_m} \begin{pmatrix} J & 1 & J_m \\ -M_i & 0 & M_i \end{pmatrix} \begin{pmatrix} J_m & 1 & J_i \\ -M_i & 0 & M_i \end{pmatrix} \begin{pmatrix} J & 1 & J'_m \\ -M_i & 0 & M_i \end{pmatrix} \\ & \times \begin{pmatrix} J'_m & 1 & J_i \\ -M_i & 0 & M_i \end{pmatrix} \mathfrak{t}(E, E_i J_i, \omega_0, \omega_0, q|Jp\lambda, E_m J_m) \mathfrak{t}^*(E, E_i J_i, \omega_-, \omega_+, q|Jp\lambda, E'_m J'_m). \end{aligned} \quad (6)$$

Consider now the quantity of interest, the branching ratio of the product in  $q$ -channel to that in  $q'$ -channel, denoted by  $R_{qq'}$ . Noting that in the weak field case  $P^{(q)}(a)$  is proportional to  $\mathcal{E}_0^4$ ,  $P^{(q)}(b)$  to  $\mathcal{E}_+^2 \mathcal{E}_-^2$ , and  $P^{(q)}(ab)$  to  $\mathcal{E}_0^2 \mathcal{E}_+ \mathcal{E}_-$  we can write

$$R_{qq'} = \frac{\mu_{aa}^{(q)} + x^2 \mu_{bb}^{(q)} + 2x |\mu_{ab}^{(q)}| \cos(\alpha_a^q - \alpha_b^q) + (B^{(q)}/\mathcal{E}_0^4)}{\mu_{aa}^{(q')} + x^2 \mu_{bb}^{(q')} + 2x |\mu_{ab}^{(q')}| \cos(\alpha_a^{q'} - \alpha_b^{q'}) + (B^{(q')}/\mathcal{E}_0^4)} \quad (7)$$

where  $\mu_{aa}^{(q)} = P^{(q)}(a)/\mathcal{E}_0^4$ ,  $\mu_{bb}^{(q)} = P^{(q)}(b)/(\mathcal{E}_+^2 \mathcal{E}_-^2)$  and  $|\mu_{ab}^{(q)}| = |F^{(q)}(ab)|/(\mathcal{E}_0^2 \mathcal{E}_+ \mathcal{E}_-)$  and  $x = \mathcal{E}_+ \mathcal{E}_- / \mathcal{E}_0^2 = \sqrt{I_+ I_-} / I_0$ . The terms with  $B^{(q)}, B^{(q')}$ , described below, correspond to

resonant photodissociation routes to energies other than  $E = E_i + 2\hbar\omega_0$  and hence<sup>13</sup> to terms which do not coherently interfere with the  $a$  and  $b$  pathways. We discuss the minimization of these terms later below. Here we just emphasize that the product ratio in Eq. (7) depends upon both the laser intensities and relative laser phase. Hence manipulating these laboratory parameters allows for control over the relative cross section between channels.

The proposed scenario, embodied in Eq. (7), also provides a means by which control can be improved by eliminating effects due to laser jitter. Specifically, the term  $2\phi_0 - \phi_+ - \phi_-$  contained in the relative phase  $\alpha_a^q - \alpha_b^q$  can be subject to the phase fluctuations arising from laser instabilities. If such fluctuations are sufficiently large then the interference term in Eq.(7), and hence control, disappears<sup>14</sup>. The following experimentally desirable implementation of the above 2-photon plus 2-photon scenario readily compensates for this problem. Specifically, consider generating  $\omega_+ = \omega_0 + \delta$  and  $\omega_- = \omega_0 - \delta$  in a parametric process by passing a beam of frequency  $2\omega_0$  through a nonlinear crystal. This latter beam is assumed generated by second harmonic generation from the laser  $\omega_0$  with the phase  $\phi_0$ . Then<sup>15</sup> the quantity  $2\phi_0 - \phi_+ - \phi_-$  in the phase difference between the  $(\omega_0 + \omega_0)$  and  $(\omega_+ + \omega_-)$  routes is a constant. That is, in this particular scenario, fluctuations in  $\phi_0$  cancel and have no effect on the relative phase  $\alpha_a^q - \alpha_b^q$ . *Thus the 2-photon plus 2-photon scenario is insensitive to the laser jitter of the incident laser fields.*

Finally, this control scheme allows for the controlled reduction of the background contributions  $B^{(q)}$  and  $B^{(q')}$  [Eq. (7)]. These terms include contributions from the resonant photodissociation processes due to absorption of  $(\omega_0 + \omega_-)$ ,  $(\omega_0 + \omega_+)$ ,  $(\omega_+ + \omega_0)$  or  $(\omega_+ + \omega_+)$  which lead to photodissociation at energies  $E_- = E_i + (\omega_0 + \omega_-)$ ,  $E_+ = E_i + (\omega_0 + \omega_+)$ ,  $E_{++} = E_i + (\omega_+ + \omega_+)$ , respectively. Possible non-resonant pathways are negligible by

comparison. Controllable reduction of this background term is indeed possible because  $B^{(q)}$  and  $B^{(q')}$  are functions of  $\mathcal{E}_+$  or  $\mathcal{E}_-$ , while the products resulting from paths  $a$  and  $b$  depend on the product  $\mathcal{E}_+\mathcal{E}_-$ . Thus, changing  $\mathcal{E}_+$  (or  $\mathcal{E}_-$ ) while keeping  $\mathcal{E}_+\mathcal{E}_-$  fixed will not affect the yield from the controllable paths  $a$  and  $b$ , but will affect  $B^{(q)}$ . To this end we introduce the parameters  $\mathcal{E}_b^2 = \mathcal{E}_+\mathcal{E}_-$  with  $\mathcal{E}_-^2 = \eta\mathcal{E}_b^2, \mathcal{E}_+^2 = \mathcal{E}_b^2/\eta$ . The terms  $B^{(q)}$  and  $B^{(q')}$  are the only terms dependent upon  $\eta$  and may be reduced by appropriate choice of this parameter. Numerical examples are discussed below.

*Control of Na<sub>2</sub> Photodissociation.* To examine the range of control afforded by this scheme consider the photodissociation of Na<sub>2</sub> in the regime below the Na(3d) threshold where dissociation is to two product channels Na(3s) + Na(3p) and Na(3s) + Na(4s). Two photon dissociation of Na<sub>2</sub> from a bound state of the  $^1\Sigma_g^+$  state occurs<sup>10</sup> in this region by initial excitation to an excited intermediate bound state  $|E_m J_m M_m\rangle$ . The latter is a superposition of states of the  $A^1\Sigma_u^+$  and  $b^3\Pi_u$  electronic curves, a consequence of spin-orbit coupling. That is, the two photon photodissociation can be viewed<sup>10</sup> as occurring via intersystem crossing subsequent to absorption of the first photon. The continuum states reached in the excitation can be either of singlet or triplet character but, despite the multitude of electronic states involved in the computation, the predominant contributions to the products Na(3p) and Na(4s) are found to come from the  $^3\Pi_g$  and  $^3\Sigma_g^+$  states, respectively. Methods for computing the required photodissociation amplitude, which involves eleven electronic states are discussed elsewhere<sup>10</sup>. Since the resonant character of the two photon excitation allows us to select a single initial state from a thermal ensemble we consider here the specific case of  $v_i = J_i = 0$  without loss of generality, where  $v_i, J_i$  denote the vibrational and rotational quantum numbers of the initial state.

The ratio  $R_{qq'}$  depends on a number of laboratory control parameters including the

relative laser intensities  $x$ , relative laser phase, and the ratio of  $\mathcal{E}_+$  and  $\mathcal{E}_-$  via  $\eta$ . In addition, the relative cross sections can be altered by modifying the detuning. Typical control results are shown in Fig. 1 and 2 which provide contour plots of the Na(3p) yield (i.e., the ratio of the probability of observing Na(3p) to the sum of the probabilities to form Na(3p) plus Na(4s)). The figure axes are the ratio of the laser amplitudes  $x$ , and the relative laser phase  $\delta\theta = 2\theta_0 - \theta_+ - \theta_-$ . Consider first Fig. 1 resulting from excitation with  $\omega_0 = 623.367$  nm and  $\omega_+ = 603.491$  nm, frequencies which are in close resonance with the intermediate states  $v=13$  and 18,  $J_m=1$  of  $^1\Sigma_u^+$ , respectively. The corresponding  $\omega_-$  is 644.596 nm. The yield of Na(3p) is seen to vary from 58% to 99%, with the Na(3p) atom predominant in the products. Although this range is large, variation of the  $\eta$  parameter should allow for improved control by minimizing the background contributions. This improvement is, in fact, not significant in this case since reducing  $\eta$  decreases  $B^{(q)}$  from the  $(\omega_0 + \omega_-)$  route but increases the contribution from the  $(\omega_0 + \omega_+)$  route. By contrast the background can be effectively reduced for the frequencies shown in Fig. 2. Here  $\omega_0 = 631.899$ ,  $\omega_+ = 562.833$  and  $\omega_- = 720.284$  nm in this instance, and with  $\eta = 5$  we achieve a larger range of control, from 30% Na(3p) to 90% as  $\delta\theta$  and  $x$  are varied.

Finally we note that the proposed approach is not limited to the specific frequency scheme discussed above. Essentially all that is required is that the two resonant photodissociation routes lead to interference and that the cumulative laser phases of the two routes be independent of laser jitter. As one sample extension, consider the case where paths  $a$  and  $b$  are composed of totally different photons,  $\omega_+^{(a)}$  and  $\omega_-^{(a)}$  and  $\omega_+^{(b)}$  and  $\omega_-^{(b)}$ , with  $\omega_+^{(a)} + \omega_-^{(a)} = \omega_+^{(b)} + \omega_-^{(b)}$ . Both these sets of frequencies can be generated, for example, by passing  $2\omega_0$  light through nonlinear crystals, hence yielding two pathways whose relative phase is independent of laser jitter in the initial  $2\omega_0$  source. Given these four frequen-

cies we now have an additional degree of freedom in order to optimize control. A sample result is shown in Figure 3 where  $\omega_+^{(a)} = 599.728$ ,  $\omega_-^{(a)} = 652.956$ ,  $\omega_+^{(b)} = 562.833$  and  $\omega_-^{(b)} = 703.140$  nm, and ( $\eta_a = 1/2$ ,  $\eta_b = 10$ ), where  $\eta_a$  and  $\eta_b$  are the analogues of  $\eta$  for the a and b paths, respectively. Here the range of the control is from 14 % to 95 %, i.e. a substantial fraction of total product control and an improvement over the three frequency approach.

In summary, we have described an effective means of eliminating major incoherence effects in radiative control, allowing quantum interference effects to dominate and allowing for coherent control in a natural environment.

### **Acknowledgements**

This work was supported by the U.S. Office of Naval Research under contract number N00014-90-J-1014.

## References

- [1] For example, C. Weisbuch and B. Vinter, "Quantum Semiconductor Structures", (Academic Press, San Diego, 1991).
- [2] O. Carnal and J. Mlynek, Phys. Rev. Lett. **66**, 2689 (1991); D.W. Keith, C.R. Ekstrom, Q.A. Turchette and D.E. Pritchard, Phys. Rev. Lett. **66**, 2693 (1991).
- [3] P. Brumer and M. Shapiro, Annual Reviews of Physical Chemistry, **43**, (1992) (in press).
- [4] See, e.g., P. Brumer and M. Shapiro, Chem. Phys. Lett. **126**, 541 (1986); C. Asaro, P. Brumer and M. Shapiro, Phys. Rev. Lett. **60**, 1634 (1988); T. Seideman, P. Brumer, M. Shapiro, J. Chem. Phys. **90**, 7132 (1989); I. Levy, M. Shapiro and P. Brumer, J. Chem. Phys. **93**, 2493 (1990); C. K. Chan, P. Brumer and M. Shapiro, J. Chem. Phys. **94**, 4103 (1991); G. Kurizki, M. Shapiro, and P. Brumer, Phys. Rev. B **39**, 3435 (1989); M. Shapiro and P. Brumer, J. Chem. Phys., **95**, 8658 (1991).
- [5] M. Shapiro and P. Brumer, J. Chem. Phys., **90**, 6179 (1989). This limited method relies on a scheme where a saturating laser field constantly reestablishes coherence against collisional dephasing effects.
- [6] C. Chen, Y-Y. Yin, and D.S. Elliott, Phys. Rev. Lett., **64**, 507 (1990); Phys. Rev. Lett., **65**, 1737 (1990).
- [7] S.M. Park, S-P. Lu, and R.J. Gordon, J. Chem. Phys., **94**, 8622 (1991); S-P. Lu, S.M. Park, Y. Xie, and R.J. Gordon, (to be published).
- [8] Baranova B.A., Chudinov A.N., and Zel'dovitch B. Ya., Opt. Comm., **79** 116 (1990)

- [9] Tannor D.J., and Rice S.A., *Adv. Chem. Phys.*, **70**, 441 (1988); Kosloff R., Rice S.A., Gaspard P., Tersigni S., and Tannor D.J., *Chem. Phys.* **139**, 201 (1989); Tersigni S., Gaspard P. and Rice S.A., *J. Chem. Phys.*, **93**, 1670 (1990).
- [10] Z. Chen, M. Shapiro and P. Brumer, *J. Chem. Phys.* (submitted).
- [11] I. Levy and M. Shapiro, *J. Chem. Phys.*, **89**, 2900 (1988).
- [12] M. Shapiro, *J. Chem. Phys.*, **56** 2582 (1972); M. Shapiro, R. Bersohn, *Ann. Rev. Phys. Chem.*, **33** 409 (1982).
- [13] M. Shapiro and P. Brumer, *J. Chem. Phys.* **84**, 540 (1986).
- [14] X-P. Jiang, P. Brumer and M. Shapiro (to be submitted)
- [15] M. Schubert and B. Wilhelmi, "Nonlinear Optics and Quantum Electronics", (Wiley, New York, 1986).

### Figure Captions

Figure 1: Contours of equal Na(3p) yield. Ordinate is the relative laser phase and the abscissa is the field intensity ratio  $x$ . Here for  $\omega_0 = 623.367$ ,  $\omega_+ = 603.491$ ,  $\omega_- = 644.596$  nm and  $\eta = 1$ .

Figure 2: As in Figure 1 but for  $\omega_0 = 631.899$ ,  $\omega_+ = 562.833$ ,  $\omega_- = 720.284$  nm and  $\eta = 5$ .

Figure 3: As in Figure 1 but for four field case with  $\omega_+^{(a)} = 599.728$ ,  $\omega_-^{(a)} = 652.956$ ,  $\omega_+^{(b)} = 562.833$ ,  $\omega_-^{(b)} = 703.140$  nm,  $\eta_a = 1/2$  and  $\eta_b = 10$ .

Figure 1

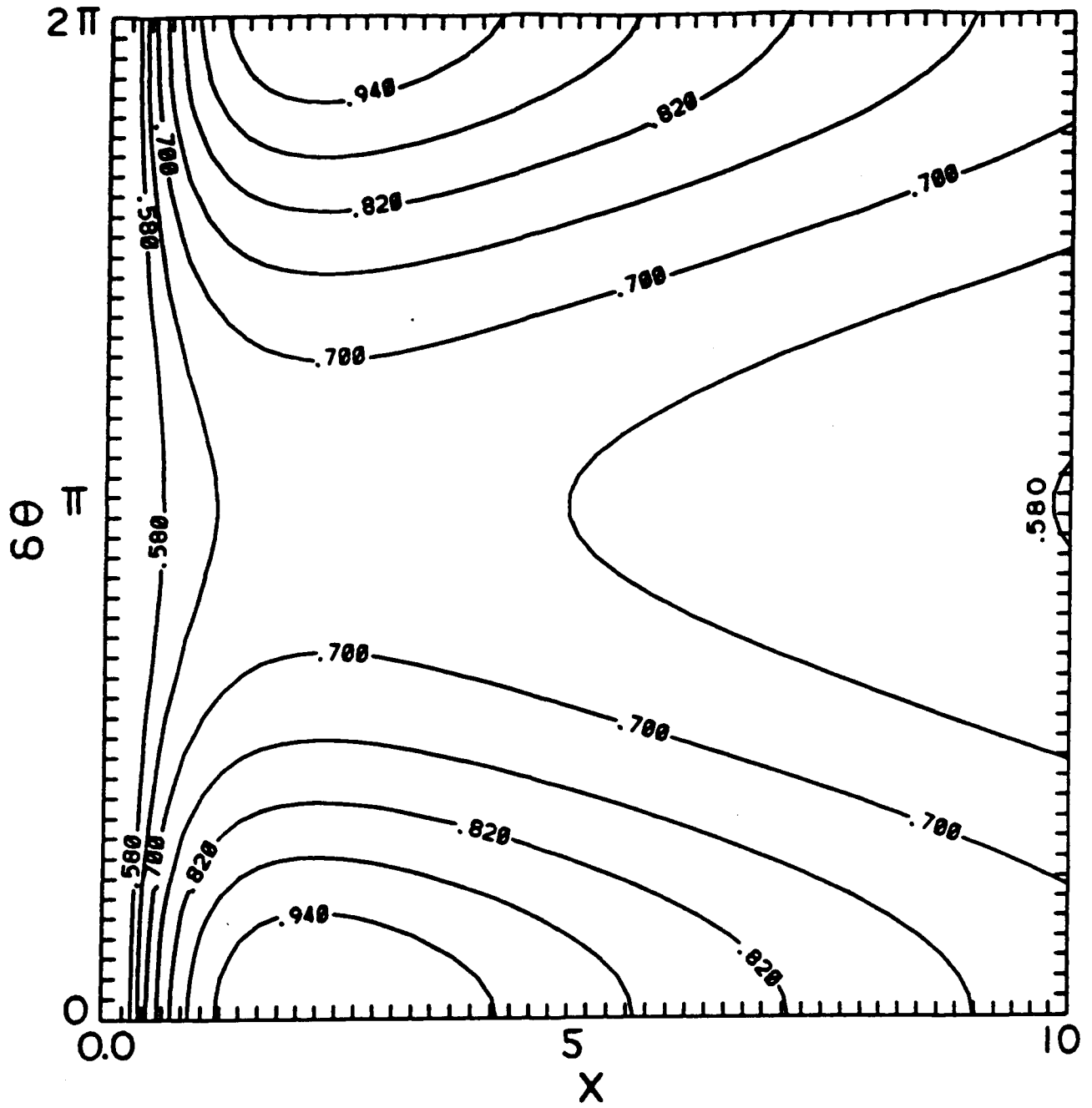
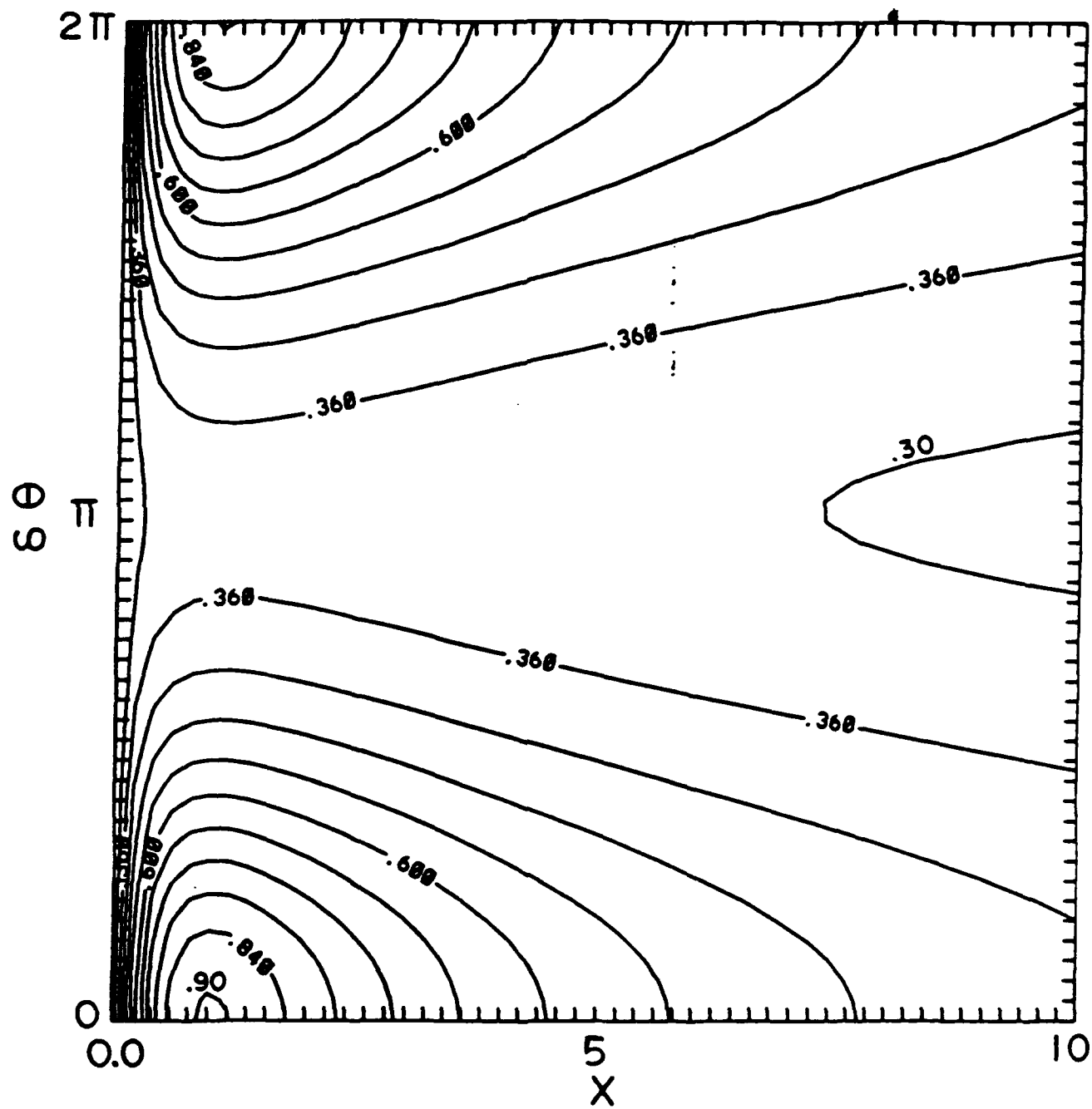


Figure 2





# Three-Dimensional Quantum-Mechanical Computations of the Control of the $\text{H}+\text{OD}\leftarrow\text{DOH}\rightarrow\text{D}+\text{OH}$ Reaction

Moshe Shapiro

Department of Chemical Physics, The Weizmann Institute of Science,  
Rehovot 76100, Israel

and

Paul Brumer

Chemical Physics Theory Group, Department of Chemistry,  
University of Toronto, Toronto M5S 1A1, Canada

## Abstract

A three dimensional quantum mechanical study of the control of a branching photochemical reaction,  $\text{H}+\text{OD}\leftarrow\text{DOH}\rightarrow\text{D}+\text{OH}$ , is presented. It is shown that with two laser pulses, one pulse used to generate a superposition of the (0,2,0) and the (1,0,0) states, and the other, a VUV pulse, used to dissociate the molecule by exciting it to the B-continuum, it is possible to control which of two chemical channels is preferred. The control parameters used are the center frequency of the excitation laser and the time delay between the two pulses. For the above superposition state, a combination of a 200 fsec excitation pulse and a 50 fsec dissociation pulse is found to yield the widest (10% to 90% yield in the  $\text{H}+\text{OD}$  channel) range of control, essentially *irrespective* of the photolysis wavelength.

## 1. Introduction

Control of isotopic branching ratios in polyatomic photofragmentation processes is one of the most demanding *mode specific* tasks. This is especially true when the mass ratio between the two isotopes is close to unity. In the Born-Oppenheimer approximation, differences in the exit-channel potentials that may sometimes enable selectivity are absent in the case of different isotopomers. Conventional methods therefore rely entirely on kinematic factors.

In conventional methods one takes advantage of kinematic factors by using the bound part of the molecular spectrum. This is done by a *pre-excitation* process in which the dissociation step is preceded by an optical transition to one of the bound excited states. The wavelength of the photodissociation step is then tuned to the red-edge of the absorption spectrum, where only the pre-excited state can be energetically dissociated.

If such pre-excitation is associated with excitation of a well localized mode, and if the greater extension of the excited nuclear wavefunction associated with that mode enhances its subsequent dissociation probability, than the process may lead to mode (and isotopic) selectivity. Indeed, this combination of the existence of well localized modes and red-edge effects underlie many of the mode specific dissociations studied in the past, both theoretically<sup>1-4</sup> and experimentally<sup>5-9</sup>.

A prime example of a molecule for which the pre-excitation approach works very well is HOD. This molecule has been studied both theoretically<sup>1, 3, 4</sup> and experimentally<sup>5-9</sup>. Most of these studies concentrated on the A-system dissociation of HOD. It was shown that due to the local nature of the OH and OD bonds, an excitation of a stretch mode results in elongation of either an OH or an OD bond. Such elongations result in a strong increase of

the absorption at the red-edges. Because of the local nature of the pre-excitation, the bond that has been elongated is the one to be dissociated. This is true even if the pre-excitation is only to the first excited state of the bond, although, as pointed out by Imre and Zhang<sup>3</sup> and by Bar et al.,<sup>8</sup> the effect is more pronounced for OH( $v = 1$ ) than for OD( $v = 1$ ). In the case of OD pre-excitation, with photolysis conducted at threshold energies, the effect is mainly felt by exciting HOD to a higher (e.g., the (4,0,0)) level<sup>3, 7</sup>.

An alternative effect, in which one *inhibits* the dissociation of one bond while leaving another unchanged was also shown theoretically to exist in HOD, when excited to the B-state.<sup>10</sup> The inhibitory effect was shown to result in even greater selectivity.

If local modes cannot be identified by the pre-excitation step, or a large amount of mode coupling exists in the excited state, or photodissociation is performed at wavelengths corresponding to the *center* of the absorption continuum, then the above schemes are not expected to work. Unfortunately, most molecules fall into this category.

In recent years, a very general strategy for control which holds the promise of being able to overcome many of these difficulties, has emerged.<sup>11-15</sup> In this scheme, called Coherent Radiative Control (CRC) one uses the laser's phase-coherence to control dissociation processes. It was shown theoretically that molecules may be made to disintegrate in a specific manner, through quantum interference effects, thus overcoming dynamical and statistical biases. Initial experimental verifications of this theory have now been reported.<sup>16-18</sup>

An alternative approach, called Optimal Control Theory (OCT), in which one tries to optimize the laser pulse-shapes in order to achieve certain tasks has also been developed.<sup>19, 20, 21</sup> The importance of relative phase between pulses, common to both the CRC and OCT approaches, has been recently demonstrated experimentally.<sup>22</sup>

None of the CRC or OCT calculations reported thus far have dealt with a photochemical reaction in three dimensions which branches to different chemically distinct species. That CRC is in fact possible for a real three dimensional rotating polyatomic molecule, despite averaging over the (parent molecule and fragments') magnetic ( $M$ ) and other (e.g.,  $j, v$ ) quantum numbers, has been demonstrated in the case of  $\text{CH}_3\text{I}$ .<sup>23</sup> In that case, however,  $\text{CH}_3\text{I}$  disintegrates into only *one* chemically distinct channel, namely that of the  $\text{CH}_3$  and I fragments and control over the fine structure states ( $^2\text{P}_{1/2}$  or  $^2\text{P}_{3/2}$ ) of iodine was demonstrated. Here we show that such  $M, j, v$  averaging does not affect control in the important case of branching into chemically distinct channels.

In the present paper we study the CRC of the B-system photodissociation of HOD,



a process induced by VUV photons ( $h\nu \approx 70000 - 80000\text{cm}^{-1}$ ).

The effect of ordinary pre-excitation of vibrational states on the HOD B-system has already been studied.<sup>1, 24</sup> It was shown that excitation of the bend mode does not result in a dramatic isotope effect<sup>1</sup>, whereas excitation of the stretch modes results in a strong *inhibitory* effect of the mode associated with that excitation.<sup>24</sup> The inhibitory effect is a result of both the validity of the Franck-Condon approximation *and* red-edge effects. Basically, in the B-state of water, the OH bond characteristics (the equilibrium position and the vibrational frequency) are very similar to those of the ground state of  $\text{H}_2\text{O}$  and free  $\text{OH}(A^2\Sigma)$ . As a result, the dissociation process cannot couple different vibrational channels. The same applies to the optical transition process. Therefore, excitation of the OD bond of HOD to  $v = 1$  puts the molecule in a subspace which is essentially decoupled from the  $\text{H} + \text{OD}(v = 0)$  channel. The molecule would dissociate to the  $\text{H} + \text{OD}(v = 1)$

channel, were this channel not closed for  $E_{av} < 2770\text{cm}^{-1}$ , where  $E_{av}$ , the *available energy*, equals  $h\nu - E_{th}$  with  $E_{th}$  being the *threshold energy* for dissociation in the B-state (to the H+OD( $A^2\Sigma$ ) channel). Thus, the excitation completely turns-off the H + OD channel, leaving the D + OH channel as the only possibility. Thus, although excitation of the OD bond does preferentially produce D+OH it does so by an unexpected inhibitory mechanism.

This effect disappears once the H + OD( $v = 1$ ) channel opens, hence the effect strongly depends on the photolysis laser being tuned to the red-edge of the absorption spectrum. This limitation can be overcome by using coherent radiative control techniques: As shown below, with CRC we can achieve chemical selectivity *irrespective* of the photolysis wavelength. We do this by employing a two-pulse control scenario in which the molecule is photodissociated from an intermediate *superposition* state. This scenario has been successfully demonstrated in the collinear reactive regime for the  $\text{DH}_2$  case,<sup>12</sup> and for diatomic electronic branching ratio, for the IBr case.<sup>13</sup> The present study is the first 3D theoretical calculation of two-pulse control of a branching photochemical reaction.

## 2. Two-Pulse Control via a Superposition State

Following Refs. [12, 13], we consider the action of two pulses, one an excitation pulse and one a dissociation pulse, on a molecular system. The pulses are assumed weak enough so that second order perturbation theory applies and the time delay between them is denoted  $\tau$ . The first pulse, an excitation pulse, denoted  $\epsilon_x(t)$ , is used to coherently pump just two excited bound states, thus generating a non-stationary superposition state,

$$|\chi\rangle = c_1|E_1\rangle + c_2|E_2\rangle. \quad (1)$$

The generation of  $|\chi\rangle$  is possible if  $E_1$  and  $E_2$  are within the excitation laser band-width. (For a picosecond laser,  $E_1$  and  $E_2$  can be no more than a few  $\text{cm}^{-1}$  apart). In the second step,  $|\chi\rangle$  is subjected, after some time-delay  $\tau$ , to a second dissociation pulse  $\varepsilon_d(t)$ , which induces a transition to the continuum.

Assuming for simplicity that each pulse, given as,

$$\varepsilon_a(t) = \int d\omega_p \varepsilon_a(\omega_p) \cos(\omega_p t + \mathbf{k} \cdot \mathbf{R} + \phi(\omega_p)) \quad (2)$$

is Gaussian, we have that,

$$\varepsilon_a(\omega_p) = \varepsilon_a(\omega_a) \exp\{-4 \ln 2 [(\omega_p - \omega_a)/\Delta_a]^2\}; \quad a = x, d. \quad (3)$$

where  $a = x$  denotes the excitation pulse,  $a = d$  denotes the dissociation pulse, and  $\omega_p$  is the photon frequency.

With the system initially in a bound state  $|E_g\rangle$ , and given the pulse shape in Eqs. (2)-(3), we readily obtain, within first order perturbation theory, that the  $c_1$  and  $c_2$  coefficients in Eq. (1), are,

$$c_i = 2\pi \mu(i, g) \varepsilon_x(i); \quad i = 1, 2, \quad (4)$$

where  $\mu(i, g) \equiv \langle E_i | \mu | E_g \rangle$ , ( $i = 1, 2$ ) is the transition dipole matrix element between the  $|E_g\rangle$  and  $|E_i\rangle$  states, and

$$\varepsilon_x(i) \equiv \varepsilon_x(\omega_{i,g}) \exp[-i\{\mathbf{k}_{i,g} \cdot \mathbf{R} + \phi(\omega_{i,g})\}]; \quad i = 1, 2. \quad (5)$$

The wavevector  $\mathbf{k}_{i,g}$  is that associated with the  $\omega_{i,g} = (E_i - E_g)/\hbar$  frequency absorbed from the excitation pulse at the end of the transition process.

The time-evolution of  $|\chi\rangle$  from  $t = -\infty$  to  $t = \tau$  causes each  $c_i$  coefficient to acquire an extra phase,

$$c_i(\tau) = c_i \exp(-iE_i\tau/\hbar), \quad i = 1, 2. \quad (6)$$

Assuming that at time  $\tau$  the excitation pulse is over, the probability of dissociating  $|\chi(\tau)\rangle$  to yield a given chemical product  $q$ , with internal quantum numbers  $\mathbf{n}$ , at energy  $E$ , is given, in first order perturbation theory, by,

$$P(q, \mathbf{n}|E) = 4\pi^2 |c_1(\tau)\epsilon_d(1)\mu(q, \mathbf{n}, 1) + c_2(\tau)\epsilon_d(2)\mu(q, \mathbf{n}, 2)|^2, \quad (7)$$

where  $\mu(q, \mathbf{n}, i) \equiv \langle E_i | \mu | E, \mathbf{n}, q^- \rangle$ ,  $|E, \mathbf{n}, q^- \rangle$  denoting a scattering state leading, as  $t \rightarrow \infty$ , to the desired  $\{q, \mathbf{n}\}$  product. In Eq. (7), in analogy with Eq. (5),  $\epsilon_d$  is defined as,

$$\epsilon_d(i) \equiv \epsilon_d(\omega_{E,i}) \exp[-i\{\mathbf{k}_{E,i} \cdot \mathbf{R} + \phi(\omega_{E,i})\}]; \quad i = 1, 2. \quad (8)$$

In order to better analyze the interference inherent in the probability expression of Eq. (7), we separate out the phase factors from the molecular matrix elements. Writing,

$$\mu(q, \mathbf{n}, i) \equiv |\mu(q, \mathbf{n}, i)| \exp[\alpha(q, \mathbf{n}, i)], \quad (9)$$

we can, using Eqs. (5) and (8), expand Eq. (7) to obtain that,

$$P(q, \mathbf{n}|E) = 4\pi^2 \{ |c_1|^2 \epsilon_d^2(\omega_{E,1}) |\mu(q, \mathbf{n}, 1)|^2 + |c_2|^2 \epsilon_d^2(\omega_{E,2}) |\mu(q, \mathbf{n}, 2)|^2 + 2|c_1||c_2|\epsilon_d(\omega_{E,1})\epsilon_d(\omega_{E,2})|\mu(q, \mathbf{n}, 1)||\mu(q, \mathbf{n}, 2)| \cos[\alpha(q, \mathbf{n}, 1) - \alpha(q, \mathbf{n}, 2) - \omega_0\tau] \}, \quad (10)$$

where,  $\omega_0 = (E_2 - E_1)/\hbar$ ,

In deriving Eq. (10), it was assumed that the optical phases of different modes within  $\epsilon_d$  are the same, i.e., that,  $\phi(\omega_{E,1}) = \phi(\omega_{E,2})$ . The same assumption, justified for mode-locked pulses, applies to  $\epsilon_x$ . Notice also that because  $\mathbf{k}_{i,g} \cdot \mathbf{R}$  of Eq. (5) is added to  $\mathbf{k}_{E,i} \cdot \mathbf{R}$  of Eq. (7), all  $\mathbf{R}$ -dependence disappears from Eq. (10), provided that  $\epsilon_x$  and  $\epsilon_d$  are co-propagating.

$P(q)$ , the *total* probability to populate arrangement  $q$ , is obtained from  $P(q, \mathbf{n}, E)$  by summing of  $\mathbf{n}$  and integrating over the frequencies of the dissociating pulse.

The key result of the method is that the probability  $P(q)$  is experimentally adjustable via the interference term, which is the signature of coherent control. Specifically, by altering the time-delay  $\tau$  between the two pulses or by varying the  $c_i$  coefficients (most conveniently done by shifting the  $\omega_x$  pulse center), one can alter the yield of a desired product.

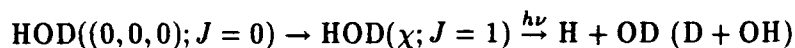
### 3. Results

Calculating the probability of controlling the  $q = \text{H+OD}$  channel vs. the  $q = \text{D+OH}$  channel requires, in accordance with Eq. (10), the bound-free  $\mu(q; v, j, m_j; i)$  matrix elements in both channels. The  $v, j, m_j$  quantum numbers denote, respectively, the vibration, the rotation, and the projection of the rotational angular momentum on a space-fixed  $z$  axis, of the OH or OD fragment. Our method of solution amounts to expanding the  $|E, \mathbf{n}, q^- \rangle$  wavefunction in the OH or OD vib-rotational basis. This leads to two sets of coupled-channels equations for the expansion coefficient, which are functions of either the H-OD(c.m.) separation or the D-OH(c.m.) separation. In principle, after obtaining the  $|E, \mathbf{n}, q^- \rangle$  wavefunctions for each arrangement, we have to overlap them with the product of  $\langle E_i |$  and  $\mu$ . This is however unnecessary, because we calculate the whole integral in one step using the *artificial channel method*.<sup>24</sup> This algorithm, which now incorporates a logarithmic-derivative propagator,<sup>25</sup> has therefore been used in all the present calculations.

The full details of the calculations, including the "natural" partial cross-sections to the various  $v, j$  channels in each  $q$  arrangement will be given elsewhere.<sup>26</sup> Some of the results concerning the "natural" D+OH vs. H+OD branching ratio have already been published.<sup>10</sup> Here we concentrate on the ability to coherently control the process.

Since our excitation pulse must excite two intermediate levels we have chosen two levels which are sufficiently close in energy to be excited by available laser sources. The (0,2,0) bend state and the (1,0,0) stretch state, where the first number applies to the OD stretch, the second number to the HOD bend and the third number to the OH stretch, are separated by  $43\text{cm}^{-1}$  from one another. Thus, a pulse of 0.2 psec in duration has a wide enough frequency spread to simultaneously excite these two states, yet its band-width is narrow enough to exclude other states.

In Figs. 1-4 we show the results of the H+OD yield in the



process, where  $J$  is the total angular momentum, as a function of  $\omega_x$  and  $\tau$  for three different dissociation pulse-widths. In all the computations the excitation pulse-width was fixed at  $50\text{cm}^{-1}$ . Results are reported as contour plots of the H+OD (percentage) yield as a function of the time delay  $\tau$  and of the detuning of the center of the excitation pulse ( $E_x = \hbar\omega_x$ ) from the energetic center [ $E_{av} = (E_1 + E_2)/2$ ] of the superposition state being excited.

Figures 1-3 demonstrate that the range of control is a strong function of the dissociation pulse-length: In Fig. 1 where a 50 fsec-long dissociation pulse (band-width of  $200\text{cm}^{-1}$ ) is used, a wide range (10%-90%) of control is demonstrated. It is worth noting that this type of control is achieved after a summation over all open channels (which at this

energy are only the OD and OH rotations) has been performed. Similar control is seen in Fig. 2 at a somewhat different dissociation pulse central frequency ( $72,100\text{cm}^{-1}$ ) and narrower bandwidth ( $100\text{cm}^{-1}$ ). However, when longer pulses are used the range of control diminishes considerably. Thus, in Fig. 3 for example, where the dissociation laser is 200 fsec long, the range of control is only 64.5% - 77.5%.

Two points are worthy of discussion. First, note that control depends more heavily upon the detuning [ $E_x - E_{av}$ ] than upon the time delay  $\tau$ . This is a reflection of the differing natural bias of the (0,2,0) and (1,0,0). That is, photodissociation from one favors production of H+OD, while the other favors production of D+OH. Second, control is improved for shorter dissociation pulses. This has already been explained in the context of the two-pulse control of IBr.<sup>13</sup> Basically, by broadening the pulse's band-width we diminish the importance of the uncontrollable "satellites" which arise from the excitation of  $|E, n, q^- \rangle$  states by the red edge or the blue edge of the dissociation pulse. These states are accessible from only *one* of the intermediate  $|E_i \rangle$  states. (The red-edge continuum states are only accessible from the  $|E_1 \rangle$  state and the blue-edge states - from only the  $|E_2 \rangle$  state). When this happens, we lose our control ability, which as shown in Eq. (10), comes from interference between the  $|E_1 \rangle$  and  $|E_2 \rangle$  routes. The broader the band-width of the pulse (i.e., the shorter the pulse) the less important are these satellites.

In Fig. 4 we show that the nature of the intermediate superposition state (and hence the exact nature of the mode structure of the molecule) is not important for coherent radiative control. We have used the ground (0,0,0) level and the second (0,2,0) bend states. As shown previously<sup>1</sup> excitation of the bending states *per se* does little to enhance isotopic selectivity in the B-continuum. However, in the context of CRC the (0,0,0)+(0,2,0) super-

position state is almost as efficient (control ranging from 44% to 96%) as the (0,2,0)+(1,0,0) state. Of course, because of the wide separation between the (0,0,0) and the (0,2,0) state, the creation of this superposition does require an extremely short excitation pulse (the results shown in Fig. 4 are generated with a 3 fsec excitation pulse).

In contrast to the "natural" process aided by the pre-excitation step, the degree of control is not expected to diminish even if we tune our dissociation laser to the center of the B-continuum. This is in fact shown in Figs 1 and 4 which involve dissociation frequencies differing by as much as  $4000\text{cm}^{-1}$ .

#### 4. Summary

We have shown that the pump-sump scenario of coherent radiative control of chemical reactions provides a means of controlling photochemical reactions which branch into products with different chemical arrangements. Sample 3D computations for the case of photodissociation HOD into HO + D and H + OD show that one can alter the yield substantially by manipulating the time delay between the laser and the central laser pump frequency. Applications to other chemical reactions are planned.

#### Acknowledgment

This research was supported by the Office of Naval Research of the U.S. under contract number N00014-90-J-1014.

## References

- [1] E. Segev and M. Shapiro, *J. Chem. Phys.* **77**, 5601 (1982).
- [2] G.C. Schatz, M.C. Colton, and J.L. Grant, *J. Phys. Chem.* **88**, 2971 (1984).
- [3] J. Zhang, D.G. Imre, *Chem. Phys. Lett.* **149**, 233 (1988).  
D.G. Imre, J. Zhang, *Chem. Phys.* **139**, 89 (1989).
- [4] V. Engel, R. Schinke, *J. Chem. Phys.* **88**, 6831 (1988)  
V. Engel, R. Schinke, V. Staemmler, *J. Chem. Phys.* **88**, 129 (1988)
- [5] P.I. Zittel, D.D. Little, *J. Chem. Phys.* **71**, 713 (1979).  
P.I. Zittel, V.I. Lange, *J. Photochem. Photobiol.* **149**, 56, (1991).
- [6] N. Shafer, S. Satyapal, and R. Bersohn, *J. Chem. Phys.* **90**, 6807 (1989).
- [7] F.F. Crim, *Ann. Rev. Phys. Chem.* **35**, 647 (1984).  
F.F. Crim, *Science* **249**, 1387 (1990);  
M.D. Likar, J.E. Baggott, A. Sinha, T.M. Ticich, R.L. Vander Wal, and F.F. Crim,  
*J. Chem. Soc. Faraday Trans. 2*, **84**, 1483 (1988);  
R.L. Vander Wal, J.L. Scott, and F.F. Crim, *J. Chem. Phys.* **92**, 803 (1990).
- [8] I. Bar, Y. Cohen, D. David, S. Rosenwaks, and J.J. Valentini,  
*J. Chem. Phys.* **93**, 2146 (1990); *ibid*, **95**, 3341 (1991).
- [9] M.J. Bronikowski, W.R. Simpson, B. Girard, and R.N. Zare, *J. Chem. Phys.* **95**, 8647  
(1991).

- [10] M. Shapiro "Mechanisms for Isotopic Enrichment in Photodissociation Reactions"  
ACS Symposium Series, ed. J.A. Kaye, Am. Chem. Soc., (Washington, 1992).
- [11] P. Brumer and M. Shapiro, Chem. Phys. Lett. **126**, 541 (1986)  
M. Shapiro, J.W. Hepburn, and P. Brumer, Chem. Phys. Lett. **149**, 451 (1988).  
P. Brumer and M. Shapiro, Acc. Chem. Res. **22**, 407 (1989), and references therein.
- [12] T. Seideman, M. Shapiro, and P. Brumer, J. Chem. Phys. **90**, 7132 (1989)
- [13] I. Levy, M. Shapiro, and P. Brumer, J. Chem. Phys. **93**, 2493 (1990).
- [14] M. Shapiro and P. Brumer, J. Chem. Phys. **95**, 8658 (1991).
- [15] M. Shapiro and P. Brumer, Annual Reviews of Physical Chemistry, (in press)
- [16] C. Chen, Y-Y. Yin, and D.S. Elliott, Phys. Rev. Lett. **64**, 507 (1990); *ibid*, **65**, 1737  
(1990).
- [17] S.M. Park, S-P. Lu, and R.J. Gordon, J. Chem. Phys. **94**, 8622 (1991).
- [18] B.A. Baranova, A.N. Chudinov, and B. Ya. Zel'dovitch, Opt. Comm., **79**, 116 (1990)
- [19] D.J. Tannor, and S.A. Rice, J. Chem. Phys. **83**, 5013 (1985).  
S.A. Rice, D.J. Tannor, and R. Kosloff, J. Chem. Soc. Faraday Trans. 2, **82**, 2423  
(1986).  
D.J. Tannor, R. Kosloff, and S.A. Rice, J. Chem. Phys. **85**, 5805 (1986).  
D.J. Tannor, and S.A. Rice, Adv. Chem. Phys. **70**, 441 (1988).  
R. Kosloff, S.A. Rice, P. Gaspard, S. Tersigni, and D.J. Tannor, Chem. Phys. **139**,  
201 (1989).

- [20] S. Shi, A. Woody, and H. Rabitz, *J. Chem. Phys.* **88**, 6870 (1988).  
S. Shi, and H. Rabitz, *Chem. Phys.* **139**, 185 (1989).  
S. Shi, and H. Rabitz, *J. Chem. Phys.* **92**, 364 (1990). R.S. Judson, K.K. Lehmann,  
H. Rabitz, and W.S. Warren, *J. Mol. Struct.*, **223**, 425 (1990).
- [21] See also, S. Chelkowski, A. Bandrauk, and P.B. Corkum, *Phys. Rev. Lett.* **65**, 2355  
(1990).
- [22] N.F. Scherer, A. J. Ruggiero, M. Du, and G.R. Fleming, *J. Chem. Phys.* **93**, 856  
(1990).  
N.F. Scherer, R.J. Carlson., A. Matro, M. Du, A. J. Ruggiero, V. Romero-Rochin,  
J.A. Cina, G.R. Fleming, and S.A. Rice, *J. Chem. Phys.* **95**, 1487 (1991).
- [23] P. Brumer and M. Shapiro, *Faraday Disc. Chem. Soc.* **82**, 177 (1987).
- [24] M. Shapiro , *J. Chem. Phys.* **56**, 2582 (1972).
- [25] B.R. Johnson, *J. Chem. Phys.* **67**, 4086 (1977)
- [26] M. Shapiro , to be published.

### Figure Captions

1. Percentage yield of the H+OD channel in the photodissociation of the DOH(0,2,0+1,0,0) superposition state. The excitation pulse band-width is  $50\text{cm}^{-1}$ , the dissociation pulse bandwidth is  $200\text{cm}^{-1}$  and the center frequency is  $71600\text{cm}^{-1}$ . Ordinate is the detuning of the excitation pulse  $\omega_x$  from the energy center of the (0,2,0) and (1,0,0) states.
2. The same as in Fig. 1 but for a  $100\text{cm}^{-1}$  dissociation pulse band-width and center frequency of  $72100\text{cm}^{-1}$ .
3. The same as in Fig. 1 but for a  $50\text{cm}^{-1}$  dissociation pulse band-width.
4. Percentage yield of the H+OD channel in the photodissociation of the DOH(0,2,0+0,0,0) superposition state. The excitation pulse band-width and that of the dissociation pulse is  $2800\text{cm}^{-1}$ . The center frequency of the dissociation pulse is  $74400\text{cm}^{-1}$ .

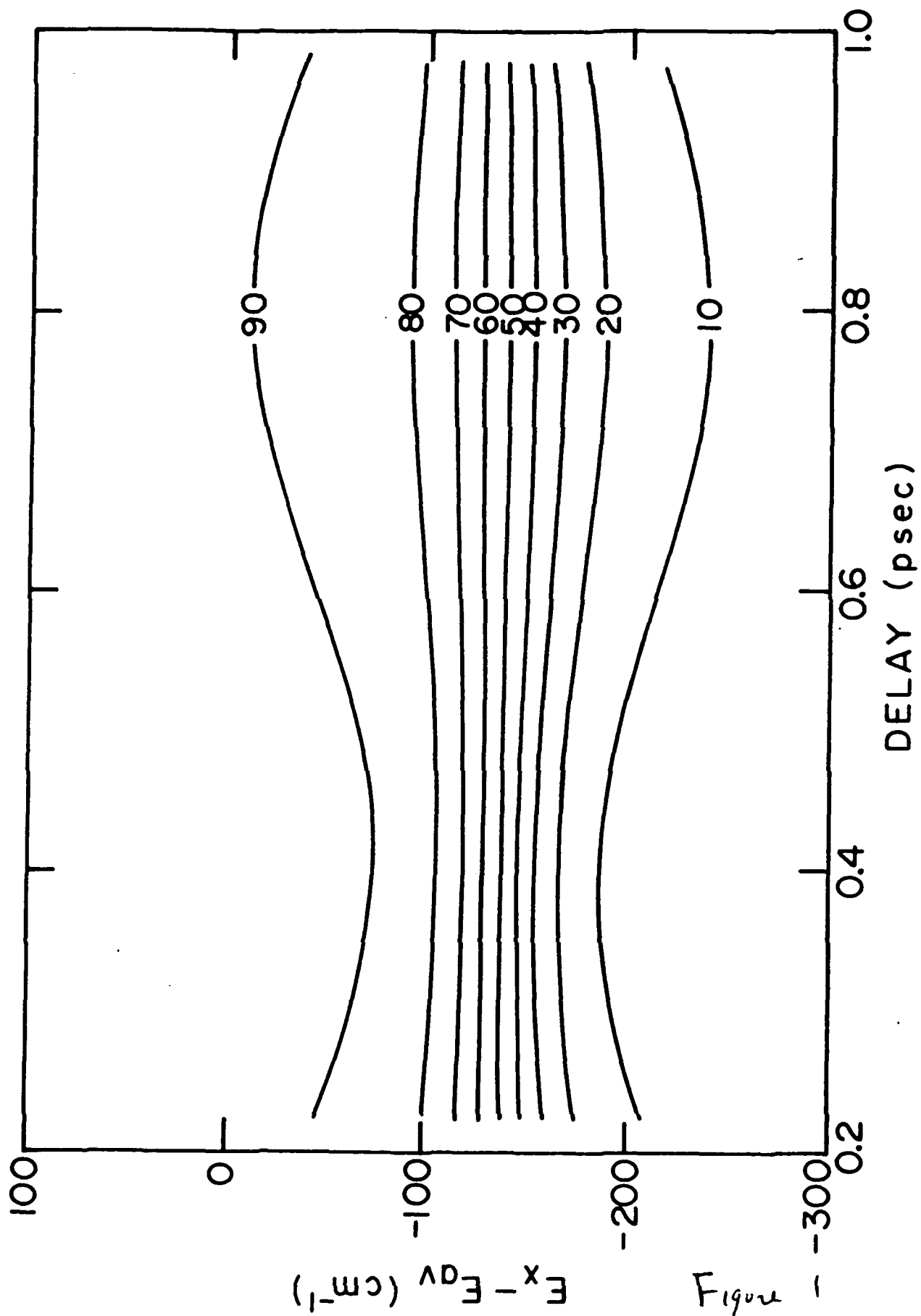


Figure 1

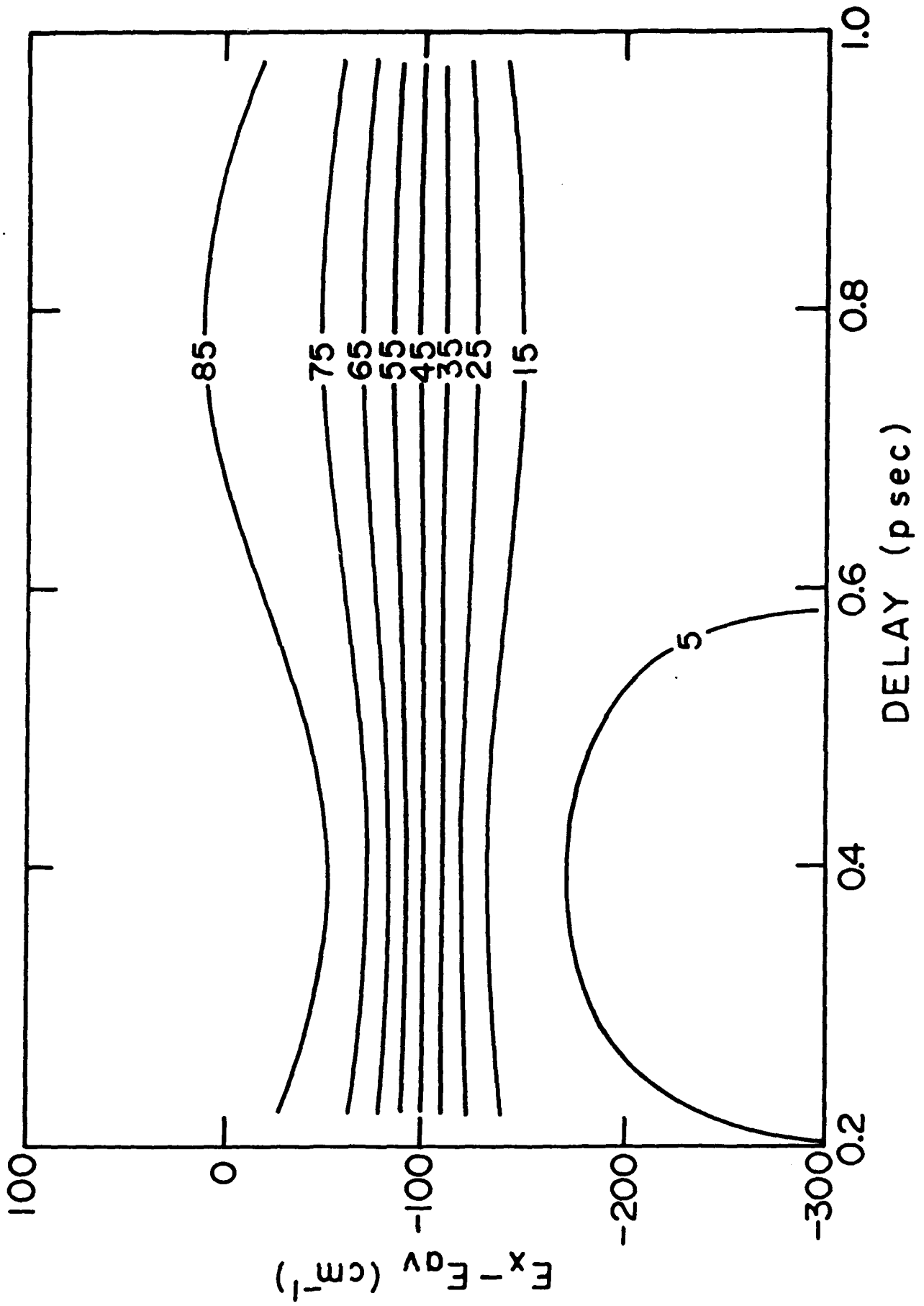


Figure 2

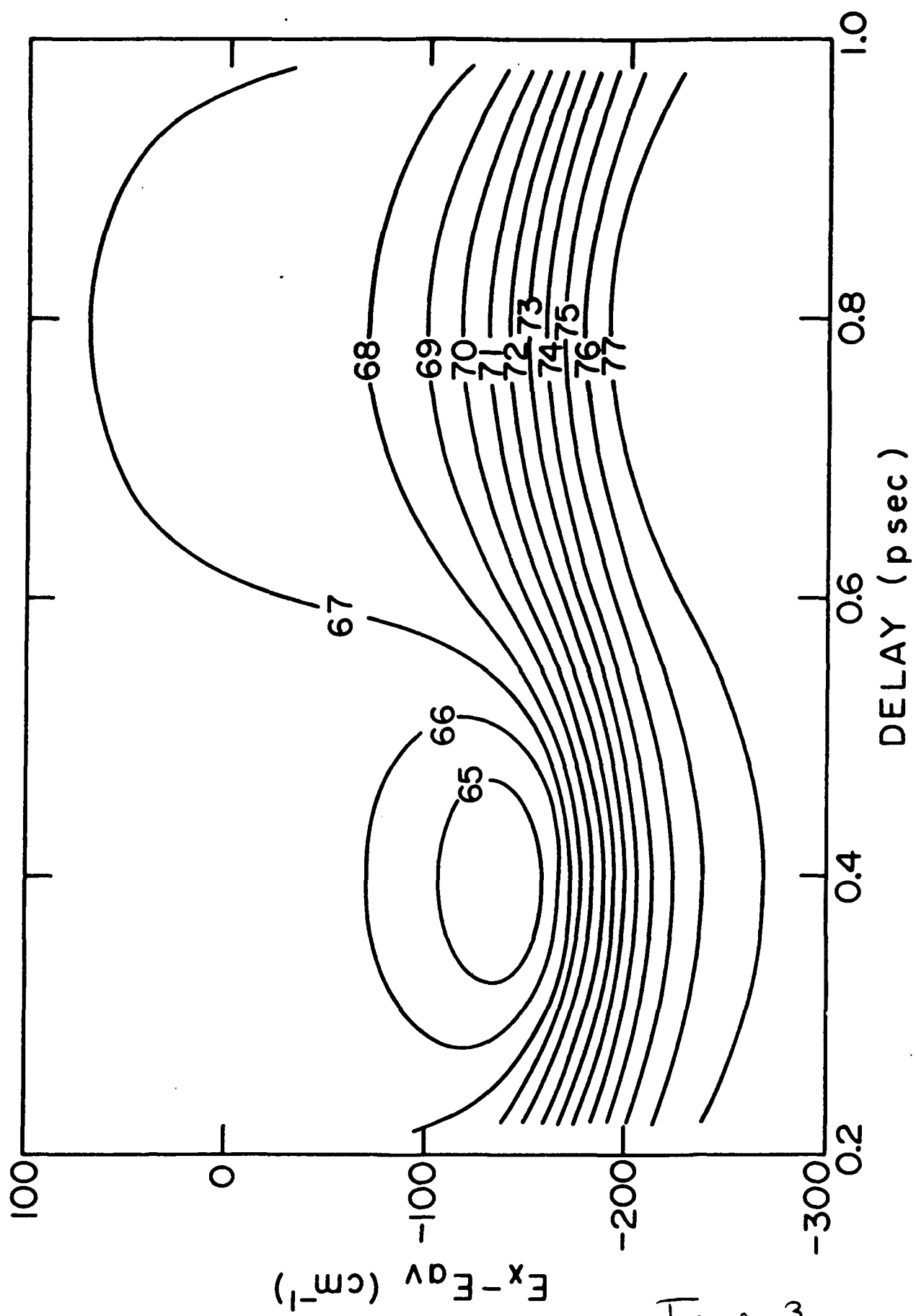


Figure 3

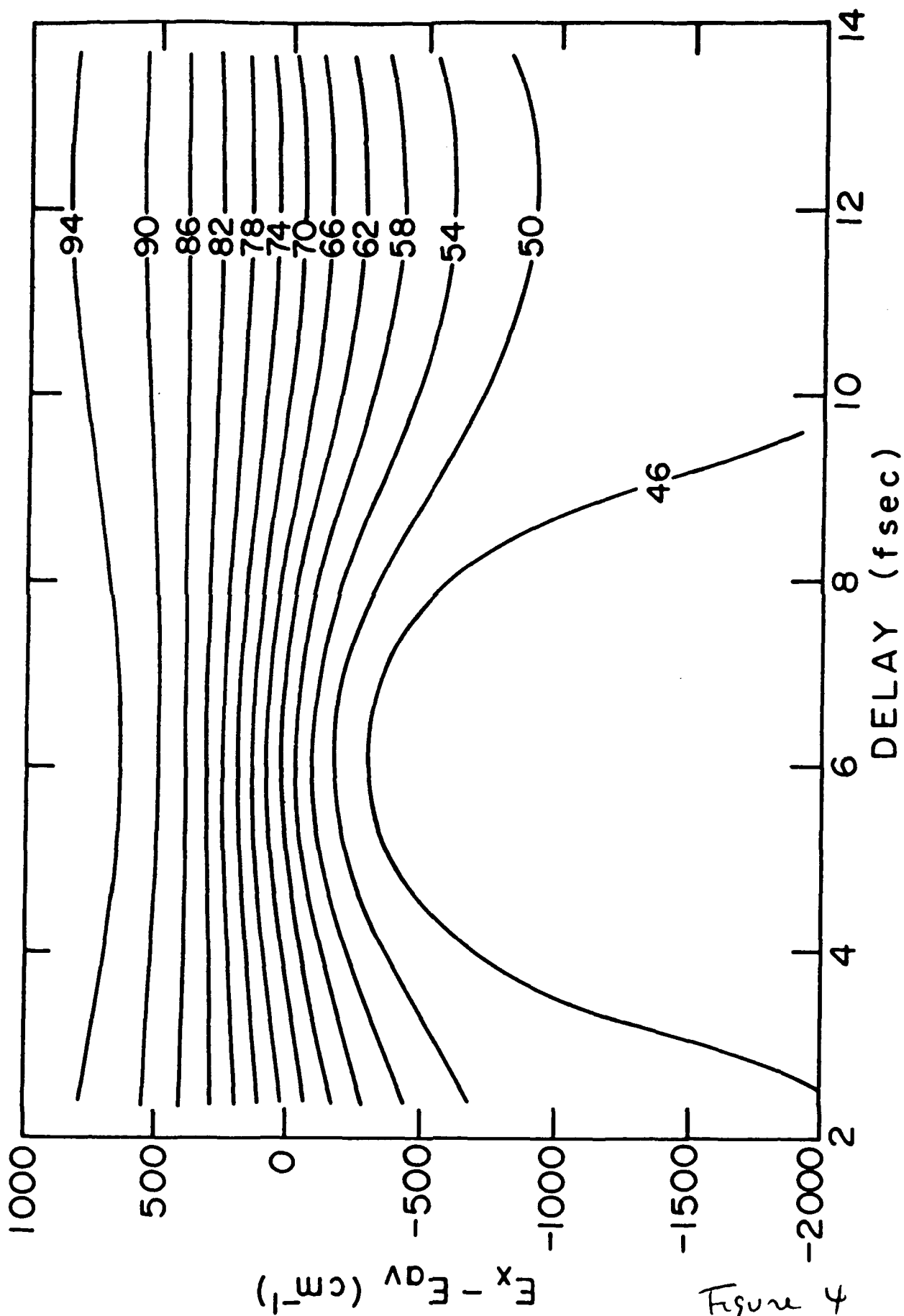


Figure 4

Multiproduct Coherent Control of Photodissociation via  
2-Photon vs. 2-Photon Interference

Zhidang Chen and Paul Brumer

Chemical Physics Theory Group,

Department of Chemistry

University of Toronto

Toronto M5S 1A1 Canada

and

Moshe Shapiro

Chemical Physics Department,

Weizmann Institute of Science,

Rehovot, Israel

## Abstract

We show that the branching ratios into two or three channel photodissociation products can be controlled by a resonant 2-photon vs. 2-photon coherent control scenario. The method allows for control even when the initial molecular system is in a mixed state, e.g. in thermal equilibrium. The resultant technique also allows cancellation of incoherences due to laser phase jumping as well as the reduction of uncontrolled background photodissociation contributions. The scenario is demonstrated computationally on  $\text{Na}_2$  photodissociation, where a wide range of control is achieved over branching into two product channels [ $\text{Na}(3s) + \text{Na}(4s)$  vs.  $\text{Na}(3s) + \text{Na}(3p)$ ] at lower energies and over three product channels at energies above the  $\text{Na}(3s) + \text{Na}(3d)$  threshold.

## 1 Introduction:

Utilizing and manipulating quantum interference phenomena has become an increasingly important area of atomic and molecular physics. Of particular interest is the possibility of controlling molecular processes via quantum interference, i.e. coherent radiative control of molecular processes<sup>1</sup>. In this approach<sup>2-7</sup> active control over product cross sections is achieved by driving an initially pure molecular state through two or more independent coherent optical excitation routes to the same final continuum state. If this continuum state can decay into a number of product arrangements then the probability of forming a particular product arrangement displays interference terms between the two routes, whose magnitude and sign depend upon laboratory parameters. Specifically, by manipulating laser parameters one can directly alter the quantum interference terms, and hence manipulate cross sections for various processes.

As in all interference phenomena the known system phase, both molecular and optical, plays a crucial role. Incoherence effects leading to a mixed initial matter-photon state, such as partial laser coherence or an initially mixed molecular state, degrade control in quantum interference based methods. As a consequence, all but one<sup>3</sup> of the previous coherent control scenarios were limited to isolated molecules in a pure state, e.g. molecular beam systems. Here we show that it is possible to maintain control in a molecular system in thermal equilibrium by interfering two distinct resonant two-photon routes to photodissociation. The resonant character of the excitations insure that only a selected state out of the molecular thermal distribution participates in the photodissociation. Hence coherence is re-established by the excitation out of a mixed state and maintained throughout the process. The proposed control scenario also provides a method for overcoming destructive interference loss due to phase jumps in the laser source. In addition, we show that this ap-

proach allows the reduction of contributions from uncontrolled ancillary photodissociation routes. Computational results support the feasibility and broad range of control afforded by this approach. Thus, this paper presents a coherent control scenario which eliminates three major incoherence effects and defines a method for controlling molecular reactions in natural environments. Further, this paper demonstrates, for the first time, the feasibility of controlling branching ratios into *three* reaction products in a realistic molecular system.

The paper is organized as follows: in the next section, we outline the relevant results of resonant two photon dissociation theory<sup>8</sup>, which serve as input to the coherent control scenario presented later below. The theory of multichannel product control is presented in Section 3. Numerical results are discussed in Section 4, where the wide range of control over the formation of two or three photodissociation products is shown.

## 2 Resonant Two Photon Dissociation

Although the control theory we propose is completely general, it is convenient to focus on the realistic case of two photon photodissociation in  $\text{Na}_2$ . Our recent analysis<sup>8</sup> of resonant two photon dissociation of a diatomic molecule yielded the following results, which serve as input to the coherent control scenario discussed later below. Consider a molecule in a state  $|E_i, J_i, M_i\rangle$  which is subjected to two laser fields  $(\omega_1 + \omega_2)$  and photodissociates to a number of different product channels labeled by  $q$ . Absorption of the first photon of frequency  $\omega_1$  lifts the system to a region close to an intermediate bound state  $|E_m, J_m, M_m\rangle$ , and a second photon of frequency  $\omega_2$  carries the system to the dissociating states  $|E, \hat{\mathbf{k}}q\rangle$ . These continuum states are of energy  $E$ , and correlate with the product in arrangement channel  $q$  in the direction specified by the scattering angles  $\hat{\mathbf{k}} = (\theta_k, \phi_k)$ . Here the  $J$ 's are the angular momentum,  $M$ 's are their projection along the z-axis, and the values of

bound state energy,  $E_i$  and  $E_m$ , include specification of the vibrational quantum numbers. Photon states of the incident lasers are described by the coherent states which contain phase information about the laser modes. Specifically, if we denote the phases of the coherent states of the laser modes by  $\phi_1$  and  $\phi_2$ , the wavevectors by  $\mathbf{k}_1$  and  $\mathbf{k}_2$  with overall phases

$$\theta_1 = \mathbf{k}_1 \cdot \mathbf{r} + \phi_1, \quad \theta_2 = \mathbf{k}_2 \cdot \mathbf{r} + \phi_2, \quad (1)$$

and the electric field amplitudes by  $\mathcal{E}_1$  and  $\mathcal{E}_2$ , then the probability amplitude for resonant two photon ( $\omega_1 + \omega_2$ ) photodissociation is given<sup>8</sup> by

$$\begin{aligned} & T_{\mathbf{k}q,i}(E, E_i J_i M_i, \omega_2, \omega_1) \\ &= \frac{1}{\delta E} \sum_{E_m, J_m} \frac{\langle E, \hat{\mathbf{k}}q^- | \mu_2 \mathcal{E}_2 | E_m J_m M_i \rangle \langle E_m J_m M_i | \mu_1 \mathcal{E}_1 | E_i J_i M_i \rangle \exp[i(\theta_1 + \theta_2)]}{\omega_1 - (E_m + \delta_m - E_i) + i\Gamma_m} \\ &= \frac{\sqrt{2\mu k_q}}{\delta E \hbar} \sum_{J,p,\lambda \geq 0} \sum_{E_m, J_m} \begin{pmatrix} J & 1 & J_m \\ -M_i & 0 & M_i \end{pmatrix} \begin{pmatrix} J_m & 1 & J_i \\ -M_i & 0 & M_i \end{pmatrix} \\ &\times \sqrt{2J+1} D_{\lambda, M_i}^{Jp}(\theta_k, \phi_k, 0) t(E, E_i J_i, \omega_2, \omega_1, q | Jp\lambda, E_m J_m) \exp[i(\theta_1 + \theta_2)] \quad (2) \end{aligned}$$

Here  $\mu_i$  is the component of the dipole moment along the electric-field vector of the  $i^{\text{th}}$  laser mode.  $E = E_i + (\omega_1 + \omega_2)$ ,  $\delta_m$  and  $\Gamma_m$  are respectively the radiative shift and width of the intermediate state,  $\mu$  is the reduced mass,  $\delta E$  is the (narrow) linewidth of the laser mode  $\omega_2$ , and  $k_q$  is the relative momentum of the dissociated product in  $q$ -channel. The  $D_{\lambda, M_i}^{Jp}$  is the parity adapted rotation matrix<sup>9</sup> with  $\lambda$  being the magnitude of the projection on the internuclear axis of the electronic angular momentum and  $(-1)^{Jp}$  the parity of the rotation matrix. We have set  $\hbar = 1$ , and assumed for simplicity that the lasers are linearly-polarized and that their electric-field vectors are parallel. The second step in Eq.(2) comes from the usual procedure of expanding the molecular wavefunctions in a partial wave resolution followed by the integration over rotational wavefunctions.

The essence of the photodissociation lies in the molecular two photon  $t$ -matrix element

whose structure has been analyzed in detail elsewhere<sup>8</sup>. It incorporates integrations over radial nuclear-vibrational wavefunctions of the bound and continuous states in the numerator and the energy offset  $\omega_1 - (E_m + \delta_m - E_i) + i\Gamma_m$  in the denominator [Eq.(2)], and thus contains the essential dynamics of the photodissociation process. Note that the  $T$ -matrix element in Eq.(2) is a complex quantity, whose phase is the sum of the laser phase  $\theta_1 + \theta_2$  and the molecular phase, i.e. the phase of  $\mathbf{t}$ . Below we compute the  $\mathbf{t}$ -matrix elements for  $\text{Na}_2$  exactly by the artificial channel method<sup>8, 10</sup>.

The square of  $T_{\mathbf{k}q,i}(E, E_i J_i M_i, \omega_2, \omega_1)$  gives the photodissociation probability per unit energy, and the overall dissociation probability of observing the product in channel  $q$  over all scattering angles and in the energy range  $(E - E + \delta E)$  is then of the form

$$\begin{aligned}
 P^{(q)}(E, E_i; \omega_2, \omega_1) &= \frac{\delta E}{2J_i + 1} \sum_{M_i} \int d\hat{\mathbf{k}} |T_{\mathbf{k}q,i}(E, E_i J_i M_i, \omega_2, \omega_1)|^2 \\
 &= \frac{8\pi\mu k_q}{\delta E h^2} \frac{1}{2J_i + 1} \sum_{M_i} \sum_{J,p,\lambda \geq 0} \left| \sum_{E_m, J_m} \begin{pmatrix} J & 1 & J_m \\ -M_i & 0 & M_i \end{pmatrix} \begin{pmatrix} J_m & 1 & J_i \\ -M_i & 0 & M_i \end{pmatrix} \right. \\
 &\quad \left. \times \mathbf{t}(E, E_i J_i, \omega_2, \omega_1, q | J p \lambda, E_m J_m) \right|^2. \tag{3}
 \end{aligned}$$

Since no  $M$ -selection prior to laser excitation is assumed we have averaged over the quantum number  $M_i$ . Because the  $\mathbf{t}$ -matrix element contains a factor of  $[\omega_1 - (E_m + \delta_m - E_i) + i\Gamma_m]^{-1}$  the probability is greatly enhanced by the approximate inverse square of the detuning  $\Delta = \omega_1 - (E_m + \delta_m - E_i)$  as long as the (laser induced) line width  $\Gamma_m$  is less than  $\Delta$ . Thus only the levels closest to the resonance  $\Delta = 0$  contribute significantly to the dissociation probability. This allows us to selectively photodissociate molecules from a thermal bath, reestablishing coherence necessary for quantum interference based control.

Two photon dissociation of  $\text{Na}_2$  from a bound state of the  $^1\Sigma_g^+$  state occurs<sup>8</sup> by initial excitation to an excited intermediate bound state  $|E_m J_m M_m\rangle$ . The latter is a superposition of states of the  $A^1\Sigma_u^+$  and  $b^3\Pi_u$  electronic curves, a consequence of spin-

orbit coupling. That is, the two photon photodissociation can be viewed<sup>8</sup> as occurring via intersystem crossing subsequent to absorption of the first photon. The continuum states reached in the excitation can be either of singlet or triplet character but, despite the multitude of electronic states involved in the computation, the predominant contributions to the products Na(3p), Na(4s) and Na(3d) are found to come from the  $^3\Pi_g$ ,  $^3\Sigma_g^+$  and  $^3\Pi_g$  states, respectively. Methods for computing the required photodissociation amplitude, which involve the fourteen electronic states shown in Figure 1, are discussed elsewhere<sup>8</sup>. Below we utilize these methods to compute the required amplitudes for coherent control in Na<sub>2</sub>.

The products of Na<sub>2</sub> photodissociation depend on the energy  $E = E_i + \omega_1 + \omega_2$  and we focus on the regime above the Na(4s) threshold. In the energy regime below the Na(3d) threshold dissociation is to two products Na(3s) + Na(3p) (denoted  $q = 3p$ ) and Na(3s) + Na(4s) (denoted  $q = 4s$ ). At higher photon energies, above the Na(3s) + Na(3d) ( $q = 3d$ ) threshold, we have a three product regime.

### 3 Coherent Control via Resonant 2-photon vs. 2-photon Interference

The essence of control lies in the simultaneous excitation of a molecule via two or more coherent paths, which introduces a controllable quantum interference term between them, and results in a control of products by varying laser intensities and relative phases between paths<sup>2</sup>. In the scenario described here, we have two excitation paths, each of which is composed of a resonant two photon dissociation process leading to the total energy  $E$ . These two coherent paths generally involve four different photon frequencies. That is,

path *a* consists of  $(\omega_1^{(a)} + \omega_2^{(a)})$  and path *b* of  $(\omega_1^{(b)} + \omega_2^{(b)})$  with  $\omega_1^{(a)} + \omega_2^{(a)} = \omega_1^{(b)} + \omega_2^{(b)}$ .

The photodissociation probability then displays the form

$$P^{(q)}(E, E_i | \omega_2^{(a)}, \omega_1^{(a)}; \omega_2^{(b)}, \omega_1^{(b)}) \\ \equiv \frac{\delta E}{2J_i + 1} \sum_{M_i} \int d\hat{\mathbf{k}} \left| T_{\hat{\mathbf{k}}q,i}^{(a)}(E, E_i; J_i M_i, \omega_2^{(a)}, \omega_1^{(a)}) + T_{\hat{\mathbf{k}}q,i}^{(b)}(E, E_i; J_i M_i, \omega_2^{(b)}, \omega_1^{(b)}) \right|^2 \quad (4)$$

where  $E = E_i + \omega_2^{(a)} + \omega_1^{(a)}$ . The right hand side is the sum of three terms: two independent photodissociation probabilities from each of the two paths, and interference between them. Below we consider both the four frequency scenario as well as the simpler three color case where  $\omega_1^{(a)} = \omega_2^{(a)} = \omega_0$ . In both cases we are careful to prescribe a specific means of obtaining these frequencies in the laboratory in order to minimize incoherence effects due to laser phase jumping.

### 3.1 Three Frequency Arrangement

Consider the case where a molecule is irradiated with three interrelated frequencies,  $\omega_0, \omega_+, \omega_-$ . That is,  $\omega_1^{(a)} = \omega_2^{(a)} = \omega_0$ ,  $\omega_1^{(b)} = \omega_+$  and  $\omega_2^{(b)} = \omega_-$ , and photodissociation occurs at  $E = E_i + 2\omega_0 = E_i + (\omega_+ + \omega_-)$ , where  $\omega_0$  and  $\omega_+$  are chosen resonant with intermediate bound state levels. Applying Eq.(4), we write the probability of photodissociation from pathway "a" ( $\omega_0 + \omega_0$ ) and pathway "b" ( $\omega_+ + \omega_-$ ) as

$$P^{(q)}(E, E_i; a, b) \equiv P^{(q)}(E, E_i | \omega_0, \omega_0; \omega_-, \omega_+) \\ = P^{(q)}(a) + P^{(q)}(b) + P^{(q)}(ab). \quad (5)$$

Here  $P^{(q)}(a)$  and  $P^{(q)}(b)$  are the independent photodissociation probabilities associated with routes *a* and *b*

$$P^{(q)}(a) \equiv P^{(q)}(E, E_i; \omega_0, \omega_0). \quad (6)$$

$$P^{(q)}(b) \equiv P^{(q)}(E, E_i; \omega_-, \omega_+). \quad (7)$$

with the right hand sides defined as in Eq.(3), and  $P^{(q)}(ab)$  is the interference term between them, discussed below. Note that the path  $a$  and  $b$  in Eq.(5) are associated with different lasers and as such contain different laser phases. Specifically, the overall phase of the three laser fields are

$$\theta_0 = \mathbf{k}_0 \cdot \mathbf{r} + \phi_0, \quad \theta_+ = \mathbf{k}_+ \cdot \mathbf{r} + \phi_+ \quad \text{and} \quad \theta_- = \mathbf{k}_- \cdot \mathbf{r} + \phi_-, \quad (8)$$

where  $\phi_0$ ,  $\phi_+$  and  $\phi_-$  are the photon phases, and  $\mathbf{k}_0$ ,  $\mathbf{k}_+$ , and  $\mathbf{k}_-$  are the wavevectors of the laser modes  $\omega_0$ ,  $\omega_+$  and  $\omega_-$ , whose electric field strengths are  $\mathcal{E}_0, \mathcal{E}_+, \mathcal{E}_-$  and intensities  $I_0, I_+, I_-$ .

The optical path-path interference term  $P^{(q)}(ab)$  is expressed by

$$P^{(q)}(ab) = 2|F^{(q)}(ab)| \cos(\alpha_a^q - \alpha_b^q) \quad (9)$$

with the relative phase between the two paths

$$\alpha_a^q - \alpha_b^q = \delta_a^q - \delta_b^q + \delta\theta, \quad \delta\theta = 2\theta_0 - \theta_+ - \theta_-. \quad (10)$$

where  $\delta_a^q - \delta_b^q$  and  $\delta\theta$  are the relative molecular and laser phase between the two paths, respectively. The amplitude  $|F^{(q)}(ab)|$  and the relative molecular phase are defined by

$$\begin{aligned} & |F^{(q)}(ab)| \exp[i(\delta_a^q - \delta_b^q)] \\ &= \frac{8\pi\mu k_q}{(2J_i + 1)\delta E h^2} \sum_{M_i} \sum_{J,p,\lambda \geq 0} \sum_{E_m, J_m} \sum_{E'_m, J'_m} \begin{pmatrix} J & 1 & J_m \\ -M_i & 0 & M_i \end{pmatrix} \begin{pmatrix} J_m & 1 & J_i \\ -M_i & 0 & M_i \end{pmatrix} \begin{pmatrix} J & 1 & J'_m \\ -M_i & 0 & M_i \end{pmatrix} \\ & \times \begin{pmatrix} J'_m & 1 & J_i \\ -M_i & 0 & M_i \end{pmatrix} \mathbf{t}(E, E_i, J_i, \omega_0, \omega_0, q|Jp\lambda, E_m J_m) \mathbf{t}^*(E, E_i, J_i, \omega_-, \omega_+, q|Jp\lambda, E'_m J'_m). \end{aligned} \quad (11)$$

Consider now the quantity of interest, the branching ratio of the product in  $q$ -channel to that in  $q'$ -channel, denoted by  $R_{qq'}$ . Note that the product in  $q$ -channel is the sum of  $P^{(q)}(E, E_i; a, b)$  at energy  $E = E_i + 2\omega_0$  [Eq.(5)] and  $B^{(q)}$  which, described below.

corresponds to background contributions of resonant photodissociation routes to energies other than  $E$  and hence<sup>11</sup> to terms which do not coherently interfere with the  $a$  and  $b$  pathways. In the weak field  $P^{(q)}(a)$  is proportional to  $\mathcal{E}_0^4$ ,  $P^{(q)}(b)$  to  $\mathcal{E}_+^2 \mathcal{E}_-^2$ , and  $P^{(q)}(ab)$  to  $\mathcal{E}_0^2 \mathcal{E}_+ \mathcal{E}_-$ , and we can write the branching ratio

$$\begin{aligned} R_{qq'} &\equiv \frac{P^{(q)}(E, E_i; a, b) + B^{(q)}}{P^{(q')}(E, E_i; a, b) + B^{(q')}} \\ &= \frac{\mathcal{E}_0^4 \mu_{aa}^{(q)} + \mathcal{E}_+^2 \mathcal{E}_-^2 \mu_{bb}^{(q)} + 2\mathcal{E}_0^2 \mathcal{E}_+ \mathcal{E}_- |\mu_{ab}^{(q)}| \cos(\alpha_a^q - \alpha_b^q) + B^{(q)}}{\mathcal{E}_0^4 \mu_{aa}^{(q')} + \mathcal{E}_+^2 \mathcal{E}_-^2 \mu_{bb}^{(q')} + 2\mathcal{E}_0^2 \mathcal{E}_+ \mathcal{E}_- |\mu_{ab}^{(q')}| \cos(\alpha_a^{q'} - \alpha_b^{q'}) + B^{(q')}} \end{aligned} \quad (12)$$

where  $\mu_{aa}^{(q)} = P^{(q)}(a)/\mathcal{E}_0^4$ ,  $\mu_{bb}^{(q)} = P^{(q)}(b)/(\mathcal{E}_+^2 \mathcal{E}_-^2)$  and  $|\mu_{ab}^{(q)}| = |F^{(q)}(ab)|/(\mathcal{E}_0^2 \mathcal{E}_+ \mathcal{E}_-)$ . The terms  $B^{(q)}$  and  $B^{(q')}$  are independent of the relative laser phase  $\delta\theta$ , and the minimization of these terms are discussed later below. Here we just emphasize that the product ratio in Eq. (12) depends upon both the laser intensities and the relative laser phase. Hence manipulating these laboratory parameters allows for control over the relative cross section between channels.

The proposed scenario, embodied in Eq. (12), also provides a means by which control can be improved by eliminating effects due to laser phase jumping. Specifically, the term  $2\phi_0 - \phi_+ - \phi_-$  contained in the relative phase  $\alpha_a^q - \alpha_b^q$  to any jumps in phase arising from laser instabilities. If such fluctuations are sufficiently large then the interference term in Eq.(12), and hence control, disappears<sup>12</sup>. The following experimentally desirable implementation of the above 2-photon plus 2-photon scenario readily compensates for laser incoherences which arise from jumps in phase. (Note, however, that other sources of laser incoherence must be treated differently). Specifically, consider generating  $\omega_+ = \omega_0 + \delta$  and  $\omega_- = \omega_0 - \delta$  in a parametric process by passing a beam of frequency  $2\omega_0$  through a nonlinear crystal. This latter beam is assumed generated by second harmonic generation from the laser  $\omega_0$  with the phase  $\phi_0$ . Then<sup>13</sup> the quantity  $2\phi_0 - \phi_+ - \phi_-$  in the phase

difference between the  $(\omega_0 + \omega_0)$  and  $(\omega_+ + \omega_-)$  routes is a constant. That is, in this particular scenario, fluctuations in  $\phi_0$  cancel and have no effect on the relative phase  $\alpha_a^q - \alpha_b^q$ . Thus the 2-photon plus 2-photon scenario is insensitive to the laser jitter of the incident laser fields.

We now show how this control scheme allows for the controlled reduction of the background contributions  $B^{(q)}$  and  $B^{(q')}$  [Eq. (12)] to improve the range of control over the branching ratio. These  $B$  terms include contributions from the resonant photodissociation processes due to absorption of  $(\omega_0 + \omega_-)$ ,  $(\omega_0 + \omega_+)$ ,  $(\omega_+ + \omega_0)$  or  $(\omega_+ + \omega_+)$  which lead to photodissociation at energies  $E_- = E_i + (\omega_0 + \omega_-)$ ,  $E_+ = E_i + (\omega_0 + \omega_+)$ ,  $E_{++} = E_i + (\omega_+ + \omega_+)$ , respectively. Possible non-resonant pathways are negligible by comparison. In the weak field limit we can write

$$B^{(q)} = \mathcal{E}_-^2 \mathcal{E}_0^2 \bar{\mu}_q(\omega_-, \omega_0) + \mathcal{E}_+^4 \bar{\mu}_q(\omega_+, \omega_+) + \mathcal{E}_+^2 \mathcal{E}_0^2 \bar{\mu}_q(\omega_+, \omega_0; \omega_0, \omega_+), \quad (13)$$

where

$$\bar{\mu}_q(\omega_-, \omega_0) = P^{(q)}(E_-, E_i, \omega_-, \omega_0) / (\mathcal{E}_-^2 \mathcal{E}_0^2) \quad (14)$$

$$\bar{\mu}_q(\omega_+, \omega_+) = P^{(q)}(E_{++}, E_i, \omega_+, \omega_+) / \mathcal{E}_+^4 \quad (15)$$

$$\bar{\mu}_q(\omega_+, \omega_0; \omega_0, \omega_+) = P^{(q)}(E_+, E_i | \omega_+, \omega_0; \omega_0, \omega_+) / (\mathcal{E}_+^2 \mathcal{E}_0^2), \quad (16)$$

and where  $P^{(q)}(E_+, E_i | \omega_+, \omega_0; \omega_0, \omega_+)$ , defined in Eq.(4), includes the interference term between the  $(\omega_+ + \omega_0)$  and  $(\omega_0 + \omega_+)$  photodissociation pathways. Note that the  $\bar{\mu}_q$ 's depend upon the photon energies chosen, and that in practice it may be difficult to minimize all terms simultaneously due to photon energy correlation  $2\omega_0 = \omega_+ + \omega_-$ . It is still possible, however, to reduce  $B^{(q)}$  and  $B^{(q')}$  by properly choosing the ratio of  $\mathcal{E}_+$  and  $\mathcal{E}_-$  because each of the terms in Eq.(13) is a function of  $\mathcal{E}_+$  or  $\mathcal{E}_-$ , while the products  $P^{(q)}(E, E_i; a, b)$  resulting from paths  $a$  and  $b$  depend on the product  $\mathcal{E}_+ \mathcal{E}_-$ . Thus, changing  $\mathcal{E}_+$  or  $\mathcal{E}_-$  while

keeping  $\mathcal{E}_+\mathcal{E}_-$  fixed will not affect the yield from the controllable paths  $a$  and  $b$ , but will affect  $B^{(q)}$ . To this end we introduce the ratio  $\eta$  of  $\mathcal{E}_-$  to  $\mathcal{E}_+$  through the parameters

$$\mathcal{E}_b^2 = \mathcal{E}_+\mathcal{E}_- \quad \text{with} \quad \mathcal{E}_-^2 = \eta\mathcal{E}_b^2, \quad \mathcal{E}_+^2 = \mathcal{E}_b^2/\eta, \quad (17)$$

and introduce the ratio of the laser intensity amplitudes

$$x = \frac{\mathcal{E}_+\mathcal{E}_-}{\mathcal{E}_0^2} = \frac{\mathcal{E}_b^2}{\mathcal{E}_0^2} = \frac{\sqrt{I_+I_-}}{I_0}. \quad (18)$$

The branching ratio in Eq.(12) becomes

$$R_{qq'} = \frac{\mu_{aa}^{(q)} + x^2\mu_{bb}^{(q)} + 2x|\mu_{ab}^{(q)}|\cos(\alpha_a^q - \alpha_b^q) + (B^{(q)}/\mathcal{E}_0^4)}{\mu_{aa}^{(q')} + x^2\mu_{bb}^{(q')} + 2x|\mu_{ab}^{(q')}|\cos(\alpha_a^{q'} - \alpha_b^{q'}) + (B^{(q')}/\mathcal{E}_0^4)} \quad (19)$$

where  $B^{(q)}/\mathcal{E}_0^4$  (or  $B^{(q')}/\mathcal{E}_0^4$ ) is given by

$$\frac{B^{(q)}}{\mathcal{E}_0^4} = x \left( \eta\bar{\mu}_q(\omega_-, \omega_0) + \frac{x\bar{\mu}_q(\omega_+, \omega_+)}{\eta^2} + \frac{\bar{\mu}_q(\omega_+, \omega_0; \omega_0, \omega_+)}{\eta} \right). \quad (20)$$

The terms  $B^{(q)}$  and  $B^{(q')}$  are the only terms dependent upon  $\eta$  and may be reduced by appropriate choice of this parameter. For instance, one can choose  $\eta < 1$  or  $\eta > 1$  depending on whether  $\bar{\mu}_q(\omega_-, \omega_0)$  is larger or smaller than other two  $\bar{\mu}_q$  values. Numerical examples are discussed in the next section.

### 3.2 Four Frequency Arrangement

Equation (19) is the primary result of the proposed control scenario using a three frequency arrangement. However, the approach is not limited to the specific frequency scheme discussed above. Essentially all that is required is that the two resonant photodissociation routes lift the molecule to the same energy and lead to interference, and that the cumulative laser phases of the two routes be independent of laser phase jumping. For example, the paths  $a$  and  $b$  can be composed of totally different photons,  $(\omega_+^{(a)} + \omega_-^{(a)})$  and  $(\omega_+^{(b)} + \omega_-^{(b)})$ , with  $\omega_+^{(a)} + \omega_-^{(a)} = \omega_+^{(b)} + \omega_-^{(b)}$  and with  $\omega_+^{(a)}$  and  $\omega_+^{(b)}$  in resonance with

intermediate states. Both these sets of frequencies can be generated, for example, by passing  $2\omega_0$  light through nonlinear crystals, hence yielding two pathways whose relative phase is independent of laser phase jumping in the initial  $2\omega_0$  source. Given these four frequencies we now have an additional degree of freedom in order to optimize control in terms of the reduction of the background terms.

The analysis of four frequency control is similar to that of the three color case, with additional care being taken to distinguish quantities of the path  $a$  from those of the path  $b$ . For instance, the overall phase of the four lasers are denoted now by  $\theta_+^{(a)}$ ,  $\theta_-^{(a)}$ ,  $\theta_+^{(b)}$  and  $\theta_-^{(b)}$ , whose electric field strengths are  $\mathcal{E}_+^{(a)}$ ,  $\mathcal{E}_-^{(a)}$ ,  $\mathcal{E}_+^{(b)}$  and  $\mathcal{E}_-^{(b)}$ . The relative phase between the two paths becomes

$$\alpha_a^q - \alpha_b^q = \delta_a^q - \delta_b^q + \delta\theta, \quad \delta\theta = \theta_+^{(a)} + \theta_-^{(a)} - \theta_+^{(b)} - \theta_-^{(b)}. \quad (21)$$

The  $\eta_a$  and  $\eta_b$ , the analogues of the  $\eta$ -parameter for the paths  $a$  and  $b$ , are defined by

$$\mathcal{E}_-^{(a)2} = \eta_a \mathcal{E}_a^2, \quad \mathcal{E}_+^{(a)2} = \frac{\mathcal{E}_a^2}{\eta_a} \quad (22)$$

$$\mathcal{E}_-^{(b)2} = \eta_b \mathcal{E}_b^2, \quad \mathcal{E}_+^{(b)2} = \frac{\mathcal{E}_b^2}{\eta_b} \quad (23)$$

and the ratio of the laser intensity amplitudes is  $x = \mathcal{E}_+^{(b)}\mathcal{E}_-^{(b)}/\mathcal{E}_+^{(a)}\mathcal{E}_-^{(a)} = \mathcal{E}_b^2/\mathcal{E}_a^2$ . The branching ratio for the four frequency case becomes

$$R_{qq'} = \frac{\mu_{aa}^{(q)} + x^2\mu_{bb}^{(q)} + 2x|\mu_{ab}^{(q)}| \cos(\alpha_a^q - \alpha_b^q) + (B^{(q)}/\mathcal{E}_a^4)}{\mu_{aa}^{(q')} + x^2\mu_{bb}^{(q')} + 2x|\mu_{ab}^{(q')}| \cos(\alpha_a^{q'} - \alpha_b^{q'}) + (B^{(q')}/\mathcal{E}_a^4)}. \quad (24)$$

Here  $\mu_{aa}^{(q)}$ ,  $\mu_{bb}^{(q)}$  and  $|\mu_{ab}^{(q)}|$  are defined similarly as in the three frequency case, and  $B^{(q)}/\mathcal{E}_a^4$  is given by

$$\begin{aligned} \frac{B^{(q)}}{\mathcal{E}_a^4} = & x \left[ \frac{\eta_b}{\eta_a} \bar{\mu}_q(\omega_-^{(b)}, \omega_+^{(a)}) + \frac{\eta_a}{\eta_b} \bar{\mu}_q(\omega_-^{(a)}, \omega_+^{(b)}) + \frac{x}{\eta_b^2} \bar{\mu}_q(\omega_+^{(b)}, \omega_+^{(b)}) \right. \\ & \left. + \frac{\bar{\mu}_q(\omega_+^{(b)}, \omega_+^{(a)}; \omega_+^{(a)}, \omega_+^{(b)})}{\eta_a \eta_b} \right] + \frac{\bar{\mu}_q(\omega_+^{(a)}, \omega_+^{(a)})}{\eta_a^2} \end{aligned} \quad (25)$$

with  $\bar{\mu}_q$ 's defined by analogy with Eqs.(14)-(16). There are now two parameters,  $\eta_a$  and  $\eta_b$ , through which the background terms can be reduced. This is, however, compensated by the larger number of terms in the right hand side of Eq.(25)

## 4 Control of Na<sub>2</sub> Photodissociation

The yield ratio  $R_{qq'}$  [Eq.(19) or (24)] depends on a number of laboratory control parameters including the relative laser intensity amplitudes  $x$ , relative laser phase  $\delta\theta$ , and the  $\eta$ -parameters. Experience teaches<sup>2</sup> that to enhance the effects of interference, the probability amplitudes arising from each of the paths  $a$  and  $b$  should be comparable. This can be achieved by modifying the detuning  $\Delta$  for each of the paths, as well as by choosing the intermediate levels and energies so that the Franck-Condon factors are as desired. In addition to these considerations, the photon energies can be chosen so that  $B^{(q)}$  and  $B^{(q')}$  with proper choice of the  $\eta$ -parameter(s), can be minimized to favor control. Below we discuss numerical results in which extensive control of two or three channel products is demonstrated.

### 4.1 Control of Two Channel Products

Cross sections for the photodissociation of Na<sub>2</sub> in the energy regime where the two products Na(3p) + Na(3s) and Na(4s) + Na(3s) are accessible have been discussed at length elsewhere<sup>8</sup>. Here we examine the range of control afforded amongst these products by both the three and four frequency scenarios. Since the resonant character of the two photon excitation allows us to select a single initial state from a thermal ensemble, we consider in this subsection, without loss of generality, the case of  $v_i = J_i = 0$  where  $v_i, J_i$  denote vibrational and rotational quantum numbers of the initial state. Below we discuss

the three and four frequency arrangements, in that order.

Typical control results of the three frequency arrangement are shown in Figures 2 and 3 which provide contour plots of the Na(3p) yield (i.e., the ratio of the probability of observing Na(3p) to the sum of the probabilities to form Na(3p) plus Na(4s)). The complementary Na(4s) yield is obtained by subtracting the Na(3p) yield from unity. The figure axes are the ratio of the laser amplitudes  $x$ , and the relative laser phase  $\delta\theta$ . Consider now Figure 2 resulting from excitation with  $\omega_0 = 623.367$  nm and  $\omega_+ = 603.491$  nm, which are in close resonance with the intermediate states  $v_m=13$  and 18,  $J_m=1$  of the  $^1\Sigma_u^+$  electronic state, respectively. The corresponding  $\omega_-$  is 644.596 nm, and  $E_i + \omega_0 + \omega_-$  is below the Na(4s) threshold so that the background  $\bar{\mu}_q(\omega_-, \omega_0)$  term is zero for the  $q = 4s$  channel. The yield of Na(3p) is seen to vary from 58% to 99% for  $\eta = 1$  (Figure 2), with the Na(3p) atom predominant in the products. Although this range is large, variation of the  $\eta$  parameter should allow for improved control by minimizing the background contributions. In fact, some improvement results by varying  $\eta$ . For example, control ranges from 48% to 97% Na(3p) for the case of  $\eta = 0.5$ . The improvement in this case is not substantial since reducing  $\eta$  decreases  $B^{(q)}$  contributions from the  $(\omega_0 + \omega_-)$  route but increases the contribution from the  $(\omega_0 + \omega_+)$  route. By comparison, the background can be effectively reduced for the frequencies shown in Figure 3, in which  $\omega_0 = 631.899$ ,  $\omega_+ = 562.833$  and  $\omega_- = 720.284$  nm. In this instance, the  $\bar{\mu}_q(\omega_+, \omega_0; \omega_0, \omega_+)$  term is primarily responsible for the large  $B^{(q)}$ . Choosing  $\eta = 5$  allows us to reduce this contribution and achieve a range of control (Figure 3) from 30% to 90% Na(3p) as  $\delta\theta$  and  $x$  are varied. This is a large improvement over the  $\eta = 1$  results (not shown) for this set of the frequencies which shows a range of control of 21% to 61%.

While the three frequency arrangement may be experimentally simpler than the four

frequency scenario, the latter provides an additional degree of freedom with which to reduce the background terms. Specifically, in the three frequency arrangement the choice of  $\eta$  is restricted because of competition between the term in Eq.(20) which is proportional to  $\eta$  and those which go as  $1/\eta$  and  $1/\eta^2$ . This makes minimization of  $B^{(q)}$  difficult unless these two terms are substantially different in size. By comparison, minimization of these competitive terms is easier in the four frequency arrangement since there is the possibility of improvement by varying an additional photon energy to change the relative size among the  $\bar{\mu}_q$  terms. A sample four frequency result is shown in Figure 4 where  $\omega_+^{(a)} = 599.728$ ,  $\omega_-^{(a)} = 652.956$ ,  $\omega_+^{(b)} = 562.833$  and  $\omega_-^{(b)} = 703.140$  nm. A preliminary study of control with this set of photon energies showed that  $\bar{\mu}_q(\omega_-^{(a)}, \omega_+^{(b)})$  dominates  $B^{(q)}$ , being two orders of magnitude larger than the other  $\bar{\mu}_q$  terms, and slightly smaller than  $\mu_{aa}^{(q)}$  and  $\mu_{bb}^{(q)}$ . Control with  $\eta_a = 1$ ,  $\eta_b = 1$  (not shown) ranges from 36% to 75% Na(3p). Substantial improvement results from choosing  $\eta_a = 1/2$  and  $\eta_b = 10$  (Figure 4) where control now ranges from 14 % to 95 %.

## 4.2 Control of Three Channel Products

### 4.2.1 Photodissociation to Three Products

With energy  $E$  higher than Na(3d) threshold, the three Na products, 3p, 4s and 3d, can be observed simultaneously. Control over these products requires that we first identify an energy regime where all three products appear in two photon dissociation. For Na<sub>2</sub>, we observed<sup>8</sup>, and readily explained in terms of Franck-Condon factors, that the first excitation step must lead to a high lying vibrational level in order to obtain a sizeable energy region where the three products appear. The photodissociation probability decreases, however, as high intermediate states are reached if excitation is carried out solely from

$r_i = 0$ . One can maintain, however, a substantial photodissociation probability in  $\text{Na}_2$  if the initial excitation is from higher  $v_i$  states, due to improved Franck-Condon factors in the first excitation step. Such states are, in fact, reasonably well populated in a typical  $\text{Na}_2$  (heat pipe) laboratory environment. For example, in a heat pipe at  $T = 600^\circ\text{K}$  the ratio of population  $n(v_i)$  in  $v_i = 5$  to that,  $n_0$ , in the ground vibrational state is 0.158, and, in  $v_i = 10$ , the ratio is 0.027. Thus selectively exciting from such higher vibrational levels is straightforward and advantageous. For example, the statistically weighted probability  $[n(v_i)/n_0]P^{(q)}(E, E_i, J_i, \omega_2, \omega_1)$  with frequencies  $\omega_1, \omega_2$  in the range 560 ~ 600 nm is a factor of  $10^3$  larger for  $v_i = 5$  or 10 than for  $v_i = 0$ .

Photodissociation cross sections into each of the three open channels were studied extensively. Typical results are plotted in Figures 5(a) and 5(b) which show  $[n(v_i)/n_0]P^{(q)}(E, E_i, \omega_2, \omega_1)$  ( $q = 3p, 4s$  and  $3d$ ) as a function of  $\omega_2$  for  $v_i = 5, J_i = 0, \omega_1 = 566.651$  nm [Figure 5(a)] and  $v_i = 10, J_i = 0, \omega_1 = 579.087$  nm [Figure 5(b)]. Here the photons  $\omega_1$  are resonant with the  $v_m=37$  and 41,  $J_m=1$  levels ( $\Delta \approx 0.003$   $\text{cm}^{-1}$  for both cases) of the  $^1\Sigma_u$  electronic state, respectively. These figures show oscillatory photodissociation probabilities, characteristic of high lying intermediate vibrational states, with the  $3p$  and  $4s$  product showing an overlap region with the  $3d$  product in the neighborhood of  $\omega_2 = 17,000$   $\text{cm}^{-1}$ . This region increases as the intermediate resonant state increases, as seen in a comparison of Figures 5(a) and 5(b). Nonetheless the region where all three products are populated is relatively small, with the  $3p$  and  $4s$  product rapidly disappearing after the opening of the  $3d$  threshold.

### 4.2.2 Control Results

Three product control using a three frequency arrangement, with substantial photodissociation probability, is shown in Figure 6, where the contour plots provide the Na(3*p*), Na(4*s*) and Na(3*d*) yields  $(\text{Na}(q)/(\sum_{q=3p,4s,3d} \text{Na}(q)))$  in Figures 6(a), 6(b) and 6(c). Here we consider an initial state consisting of  $v_i = 10, J_i = 0$  with path *a*, comprised of  $\omega_0 + \omega_0$ , with  $\omega_0 = 591.306$  nm, and path *b* consisting of  $\omega_+ = 582.057$  nm and  $\omega_- = 600.853$  nm. These consist of pathways which are resonant with the  $v_m = 37, J_m = 1$  and  $v_m = 40, J_m = 1$  states of the  $^1\Sigma_u^+$  electronic state, respectively. The figure axes are the relative laser phase  $\delta\theta$  and the parameter  $s$ , defined as  $x^2/(1+x^2)$ . The  $s$  varies from 0 to 1, corresponding to the change from complete shutoff of path *b* to complete shutoff of path *a*. The results (here with  $\eta = 0.4$ ) show reasonable control with the Na(3*p*) product controllable over a range of 11% to 42% [Figure 6(a)], the Na(4*s*) over a range of 2.4% to 57% [Figure 6(b)] and Na(3*d*) over the range 12% to 72% [Figure 6(c)]. Despite the similarity of the photodissociation probabilities for the  $q = 4s$  and  $q = 3p$  channels, the dependence of control on relative phase and amplitude is substantially different. The origin of this behavior, as well as the role of the background contributions in affecting control, is clear by comparing Figures 7 and 6. Here Figure 7 shows the hypothetical case, with the same laser energies and initial molecular state as in Figure 6 but the background terms  $B^{(q)}, B^{(q')}$  being arbitrarily set to zero. The background contribution is seen to reduce the range of control for all terms and to substantially alter the dependence of the yield on the control parameters. Note, nonetheless, that the range of control including the background is quite large, a consequence of minimization of the background contribution by choice of  $\eta$ .

A second example of three frequency, three product control is shown in Figure 8. In this instance the molecule is in  $v_i = 10, J_i = 0$ , and the path *a* now utilizes  $\omega_0 = 594.505$

nm, and the path b  $\omega_+ = 582.057$  nm and  $\omega_- = 607.498$  nm, in which  $\omega_0$  is resonant with  $v_m = 36, J_m = 1$  and  $\omega_+$  is with  $v_m = 40, J_m = 1$ . The results, obtained with  $\eta = 0.5$ , show substantial control over all three products, each in the range of 10% to 50%. Control over the  $q = 3p$  channel [Figure 8(a)] and  $q = 4s$  channel [Figure 8(b)] are similar in structure, but shifted by approximately  $\pi$  along the ordinate, a consequence of a phase difference of approximately  $\pi$  in the photodissociation amplitudes for the two pathways.

Finally, we show, in Figure 9 the effect of varying the control parameters on the three product yields for a four frequency arrangement. Here path *a* consists of  $\omega_+^{(a)} = 566.651$  and  $\omega_-^{(a)} = 592.965$ , and the path *b* of  $\omega_+^{(b)} = 555.421$  and  $\omega_-^{(b)} = 605.783$  nm. The paths *a* and *b* are in resonant with the transition lines between  $v_i = 5, J_i = 0$  of  $^1\Sigma_g$ , and  $v_m = 37$  and  $v_m = 41, J_m = 1$  of  $^1\Sigma_u$ , respectively. The photon frequencies  $\omega_-^{(a)}$  and  $\omega_-^{(b)}$  are so chosen that the possible background terms are as small as possible. A further reduction of the background is possible by proper choice of  $\eta_a$  and  $\eta_b$ , with the values 3 and 0.5, respectively. The  $3d$  product is shown in Figure 9(c) to have a wide range of control, from 15 % to 91 %, the Na( $4s$ ) yield changes from 5 % to 55 % [Figure 9(b)] and the Na( $3p$ ) over the range of 3 % to 29 % [Figure 9 (a)]. Further we note once again a distinct correlation between the behavior of the Na( $4s$ ) product and the Na( $3p$ ) product as a function of the control parameters. This is presumably a reflection of the similar behavior of these products in the direct photodissociation studies (see Figure 5) in conjunction with minimal differences in the background for these two products.

## 5 Summary

By using two two-photon pathways which are each resonant with a bound intermediate, one can overcome thermal population effects in coherent control. In addition, by using

nonlinear optics method for generating the required radiation one can overcome incoherence effects due to laser phase jitter. Finally, the availability of a number of control parameters, including the detuning to the bound states, the field strengths and the relative laser phases, allows one to substantially reduce other uncontrolled background terms. The result is an effective means of eliminating major incoherence effects in radiative control, allowing quantum interference effects to dominate and allowing for coherent control in a natural environment.

### **Acknowledgements**

This work was supported by the U.S. Office of Naval Research under contract number N00014-90-J-1014.

## References

- [1] P. Brumer and M. Shapiro, *Annual Reviews of Physical Chemistry*, **43**, (1992) (in press).
- [2] See, e.g., P. Brumer and M. Shapiro, *Chem. Phys. Lett.* **126**, 541 (1986); C. Asaro, P. Brumer and M. Shapiro, *Phys. Rev. Lett.* **60**, 1634 (1988); T. Seideman, P. Brumer, M. Shapiro, *J. Chem. Phys.* **90**, 7132 (1989); I. Levy, M. Shapiro and P. Brumer, *J. Chem. Phys.* **93**, 2493 (1990); C. K. Chan, P. Brumer and M. Shapiro, *J. Chem. Phys.* **94**, 4103 (1991); G. Kurizki, M. Shapiro, and P. Brumer, *Phys. Rev. B* **39**, 3435 (1989); M. Shapiro and P. Brumer, *J. Chem. Phys.*, **95**, 8658 (1991).
- [3] M. Shapiro and P. Brumer, *J. Chem. Phys.*, **90**, 6179 (1989). This limited method relies on a scheme where a saturating laser field constantly reestablishes coherence against collisional dephasing effects.
- [4] C. Chen, Y-Y. Yin, and D.S. Elliott, *Phys. Rev. Lett.*, **64**, 507 (1990); *Phys. Rev. Lett.*, **65**, 1737 (1990).
- [5] S.M. Park, S-P. Lu, and R.J. Gordon, *J. Chem. Phys.*, **94**, 8622 (1991); S-P. Lu, S.M. Park, Y. Xie, and R.J. Gordon, (to be published).
- [6] Baranova B.A., Chudinov A.N., and Zel'dovitch B. Ya., *Opt. Comm.*, **79** 116 (1990)
- [7] Tannor D.J., and Rice S.A., *Adv. Chem. Phys.*, **70**, 441 (1988); Kosloff R., Rice S.A., Gaspard P., Tersigni S., and Tannor D.J., *Chem. Phys.* **139**, 201 (1989); Tersigni S., Gaspard P. and Rice S.A., *J. Chem. Phys.*, **93**, 1670 (1990).
- [8] Z. Chen, M. Shapiro and P. Brumer, *J. Chem. Phys.* (submitted).

- [9] I. Levy and M. Shapiro, *J. Chem. Phys.*, **89**, 2900 (1988).
- [10] M. Shapiro, *J. Chem. Phys.*, **56** 2582 (1972); M. Shapiro. R. Bersohn, *Ann. Rev. Phys. Chem.*, **33** 409 (1982).
- [11] M. Shapiro and P. Brumer, *J. Chem. Phys.* **84**, 540 (1986).
- [12] X-P. Jiang, P. Brumer and M. Shapiro (to be submitted)
- [13] M. Schubert and B. Wilhelmi, "Nonlinear Optics and Quantum Electronics", (Wiley, New York, 1986).

## Figure Captions

Figure 1: Fourteen  $\text{Na}_2$  potential energy curves involved in the photodissociation computation. Arrows indicate typical conditions for the resonant 2-photon vs. 2-photon coherent control scenario.

Figure 2: Contours of equal  $\text{Na}(3p)$  yield. Ordinate is the relative laser phase and the abscissa is the field intensity ratio  $x$ . Here for  $\omega_0 = 623.367$ ,  $\omega_+ = 603.491$ ,  $\omega_- = 644.596$  nm and  $\eta = 1$ .

Figure 3: As in Figure 2 but for  $\omega_0 = 631.899$ ,  $\omega_+ = 562.833$ ,  $\omega_- = 720.284$  nm and  $\eta = 5$ .

Figure 4: As in Figures 2 but for four field case with  $\omega_+^{(a)} = 599.728$ ,  $\omega_-^{(a)} = 652.956$ ,  $\omega_+^{(b)} = 562.833$ ,  $\omega_-^{(b)} = 703.140$  nm,  $\eta_a = 1/2$  and  $\eta_b = 10$ .

Figure 5:  $[n(v_i)/n_0]P^{(q)}(E, E_i, \omega_2, \omega_1)$  ( $q = 3p, 4s$  and  $3d$ ) vs.  $\omega_2$  for two photon dissociation. Here (a)  $\omega_1 = 566.651$  nm,  $v_i = 5$ ,  $J_i = 0$ . and (b)  $\omega_1 = 579.087$  nm,  $v_i = 10$ ,  $J_i = 0$ . The  $\text{Na}(3p)$  product is shown as the solid curve, the  $\text{Na}(3d)$  by the short-dashed curve and the  $\text{Na}(4s)$  by the long dashes.

Figure 6: The contour plots of the three product yields ( $\text{Na}(q)/(\sum_{q=3p,4s,3d} \text{Na}(q))$ ) for  $\text{Na}(3p)$ ,  $\text{Na}(4s)$  and  $\text{Na}(3d)$  in Figures 6(a), 6(b) and 6(c), respectively. Each of the three products is generated in the coherently controlled photodissociation of  $\text{Na}_2$  ( $v_i = 10$ ) using the three frequency pathway described in the text. Ordinate is the relative laser phase and the abscissa is the parameter  $s = x^2/(1+x^2)$ . In this case the pathways are resonant with the  $J_m = 1$ ,  $v_m = 37$  and  $J_m = 1$ ,  $v_m = 40$  bound states of the  $^1\Sigma_u^+$  electronic state, respectively, and  $\eta = 0.4$  is chosen.

Figure 7: As in Figure 6 but without background  $B^{(q)}$ ,  $B^{(q')}$  terms.

Figure 8: As in Figure 6 but for  $\omega_0 = 594.505$ ,  $\omega_+ = 582.057$ ,  $\omega_- = 607.498$  nm and

$\eta = 0.5$ .

Figure 9: As in Figure 6, but for three product, four frequency scenario with frequencies as described in the text.

Fig 1

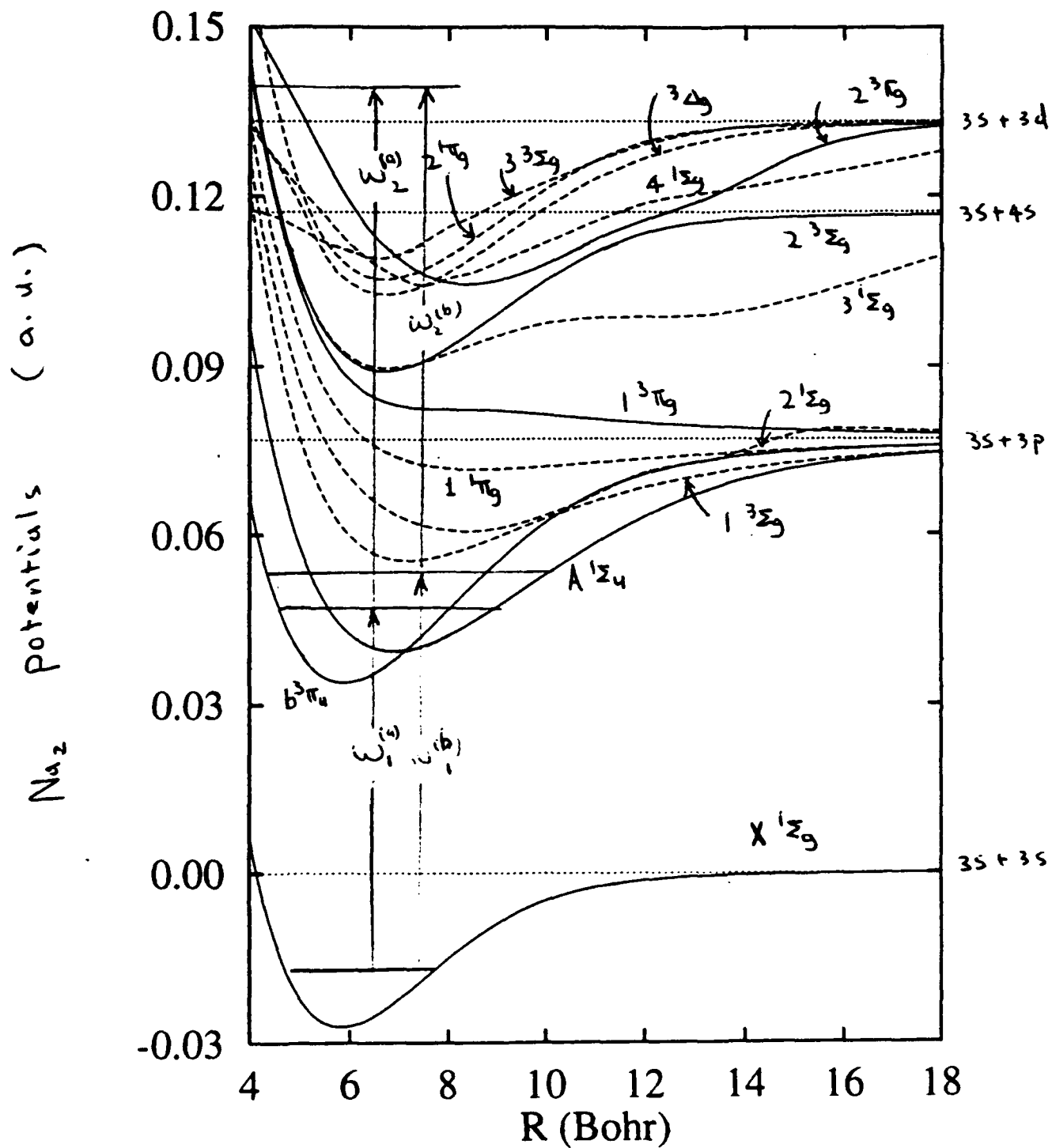


Fig 2

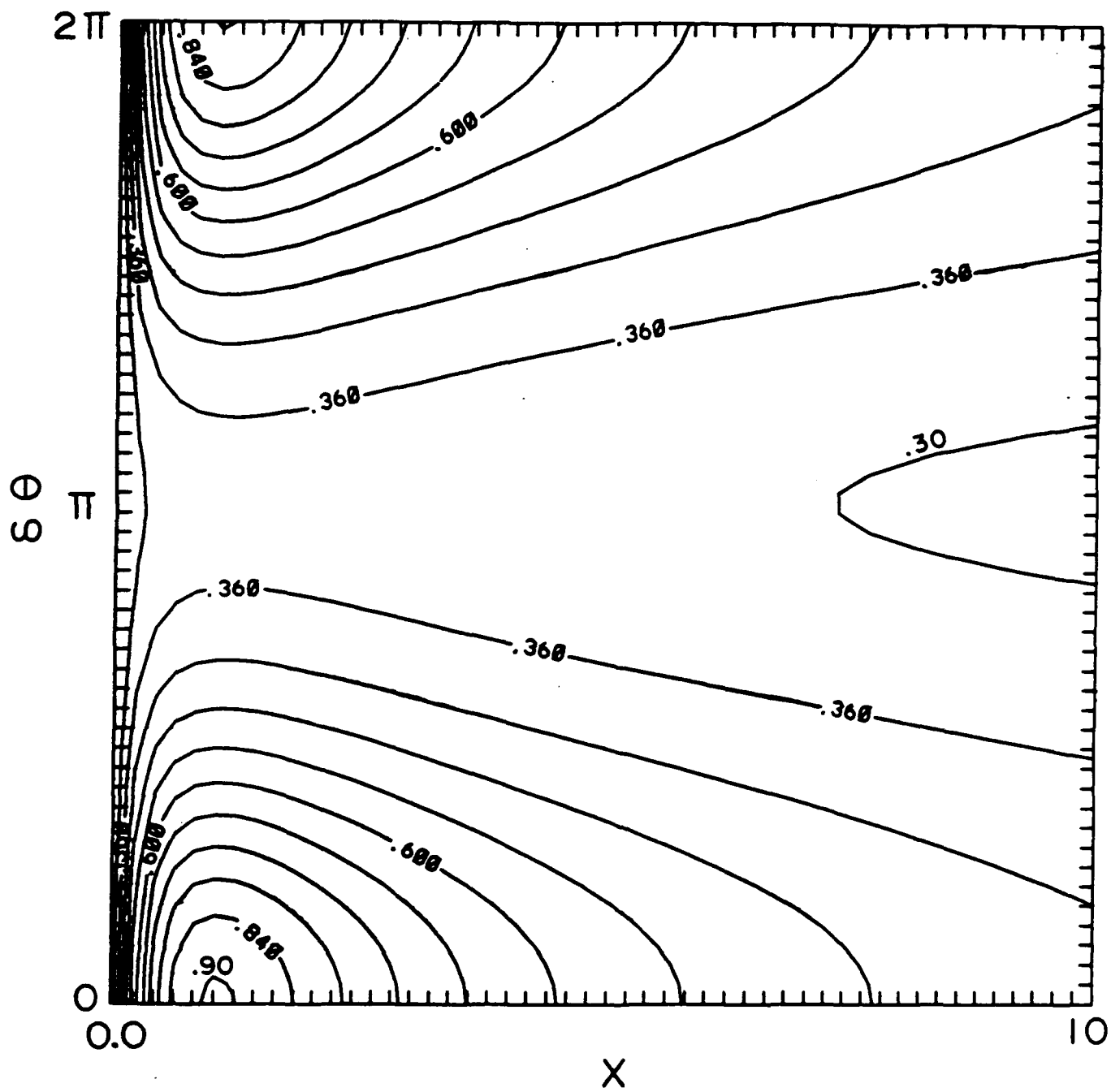


Fig 3

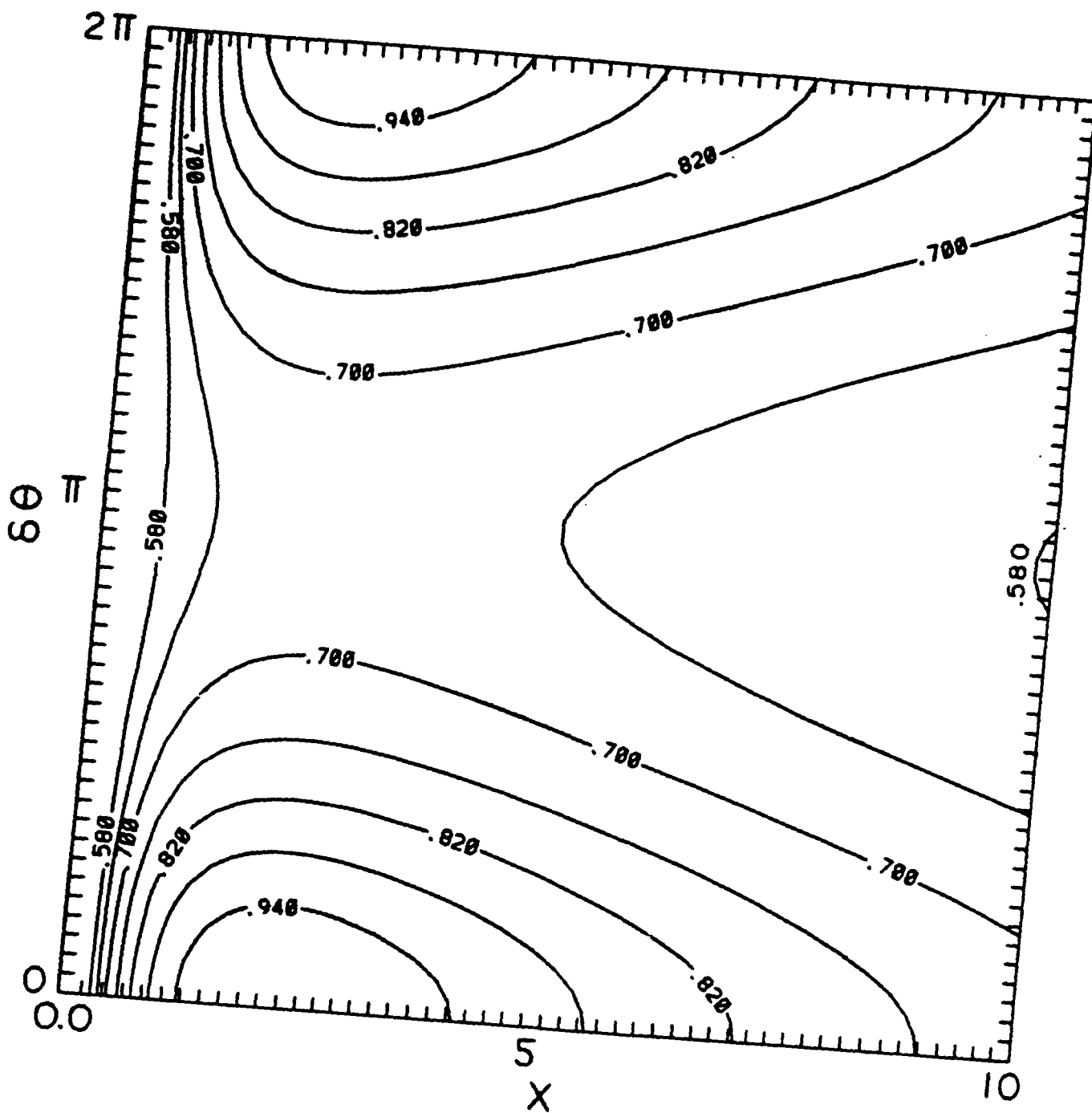


Fig 4

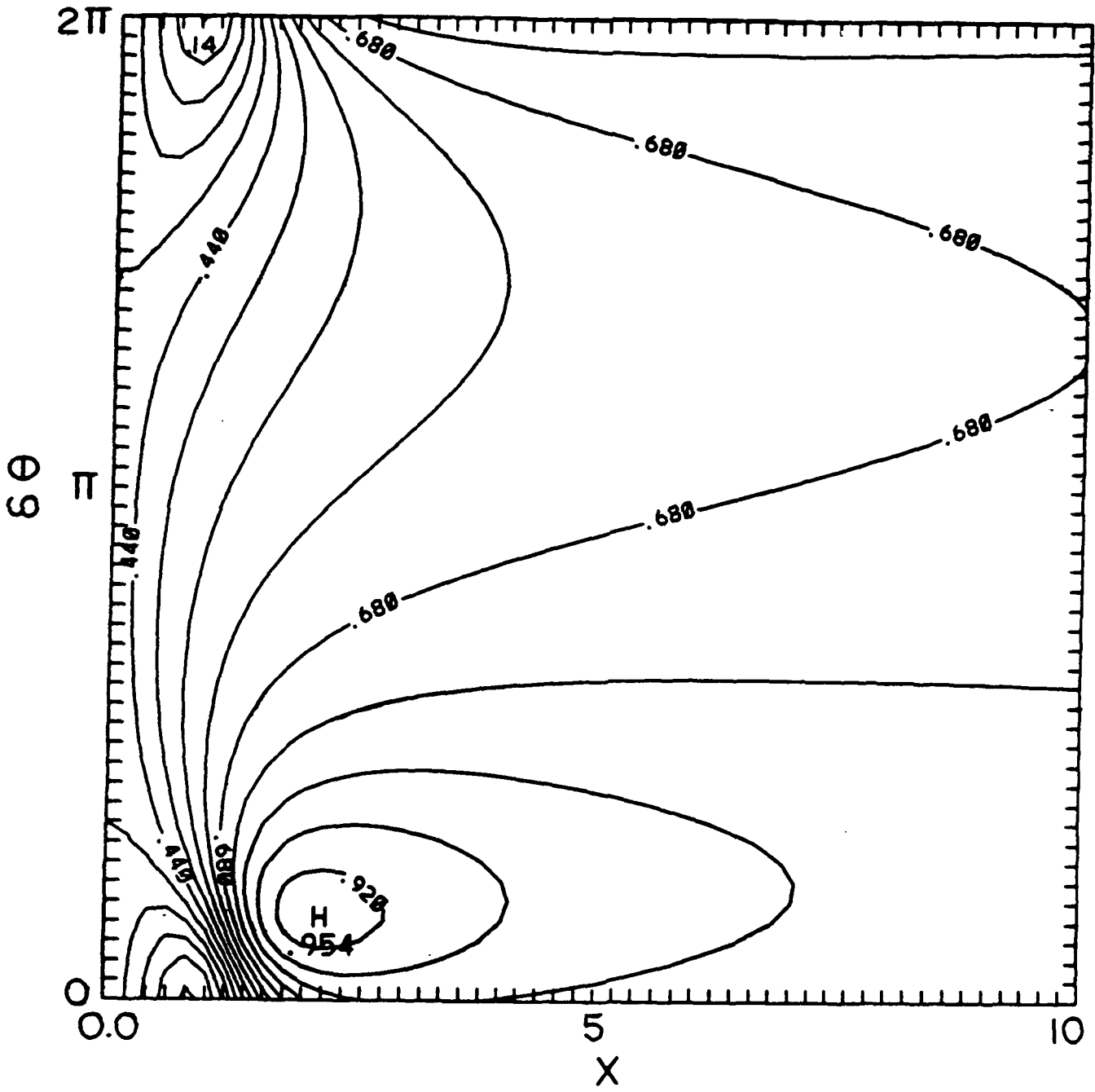


Fig 5(a)

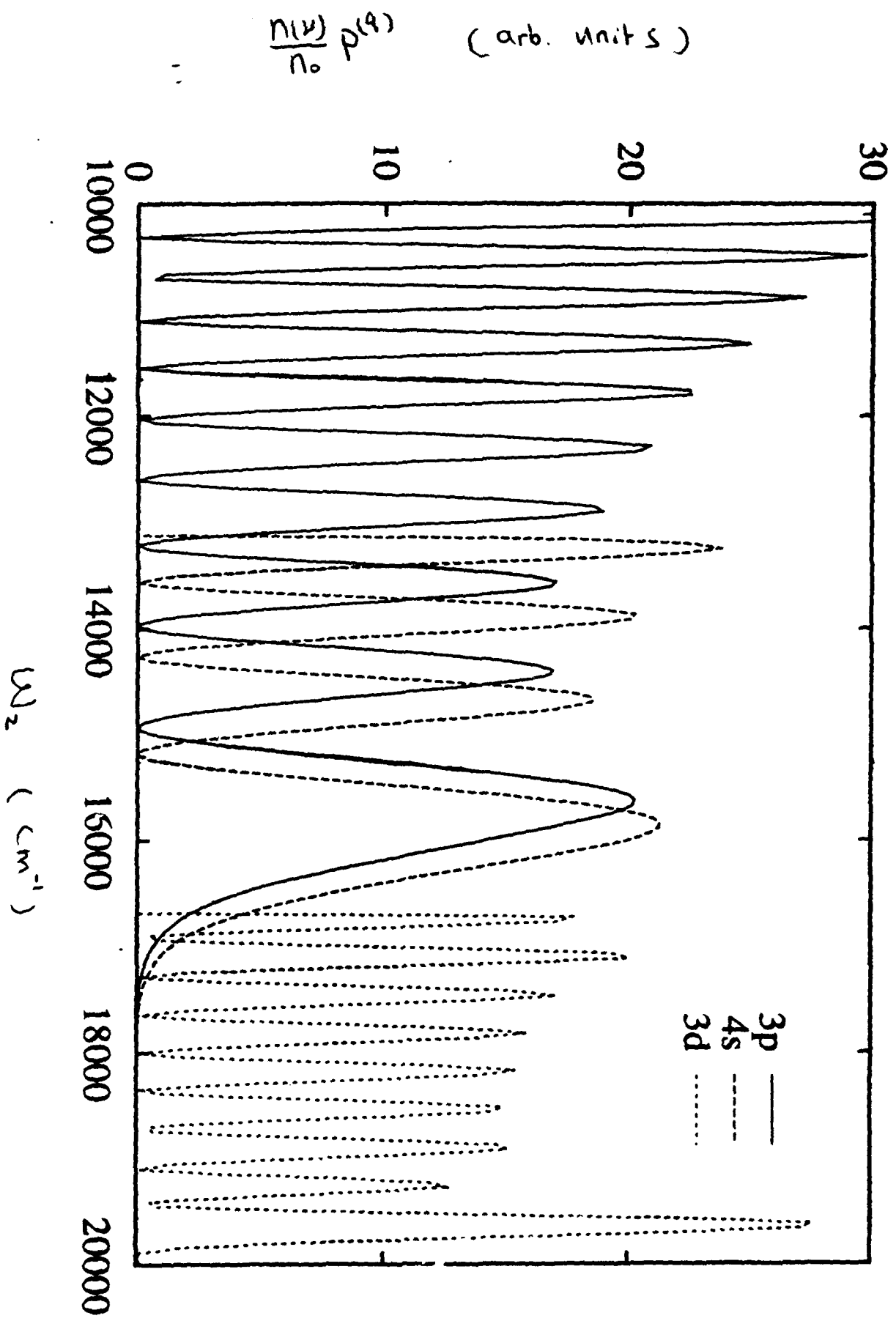


Fig 5(b)

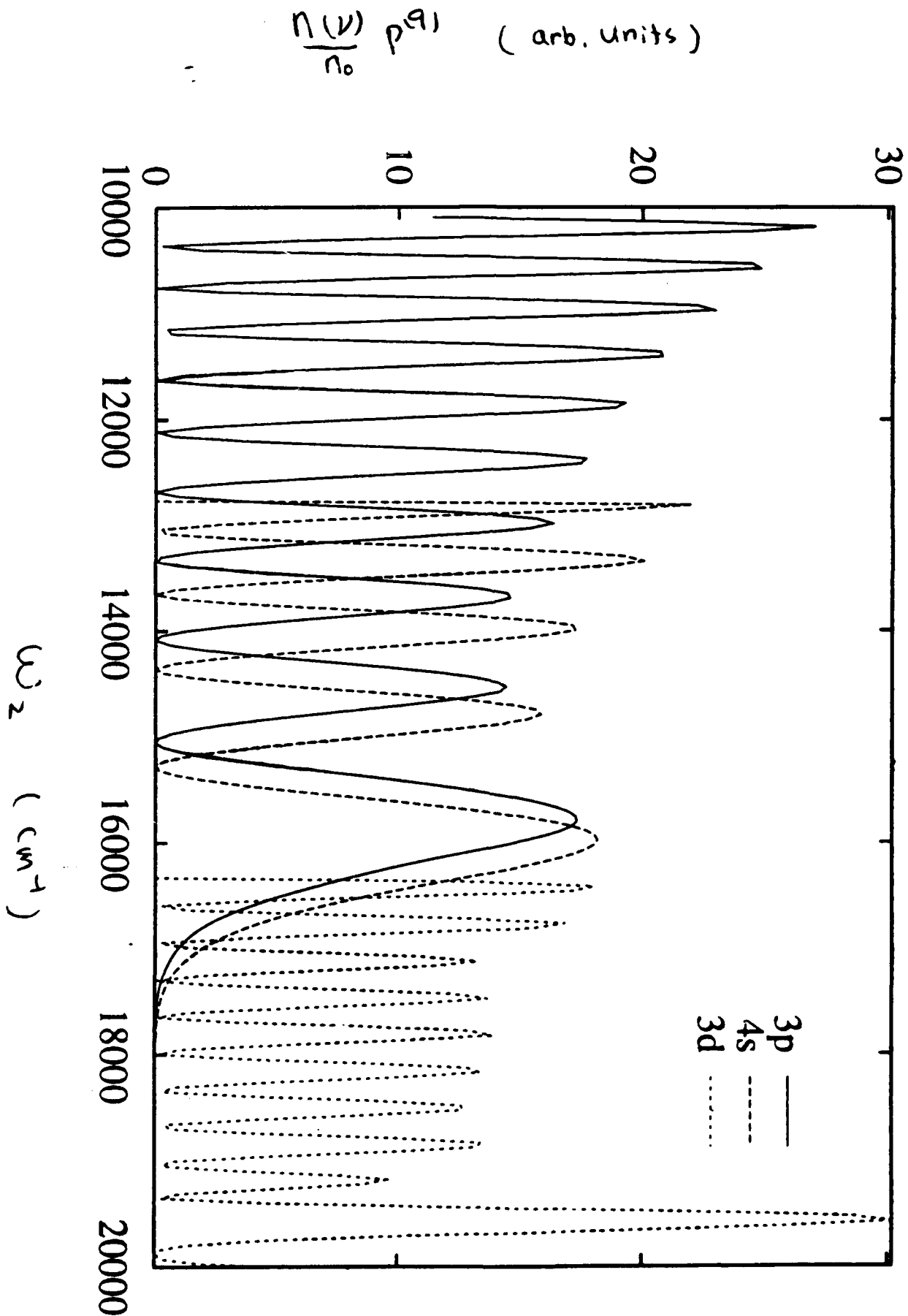


Fig 6 (a)

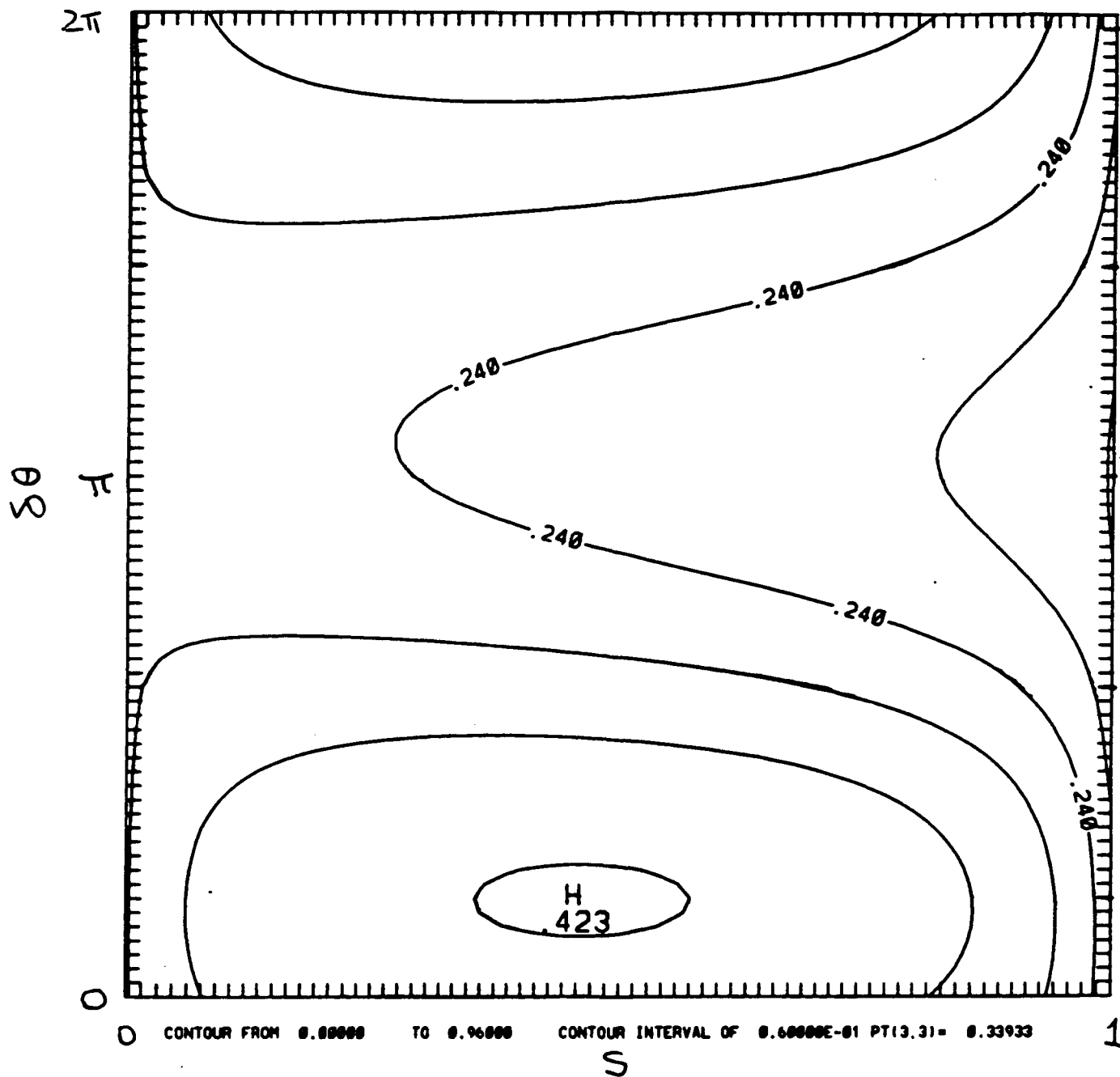


Fig 6(b)

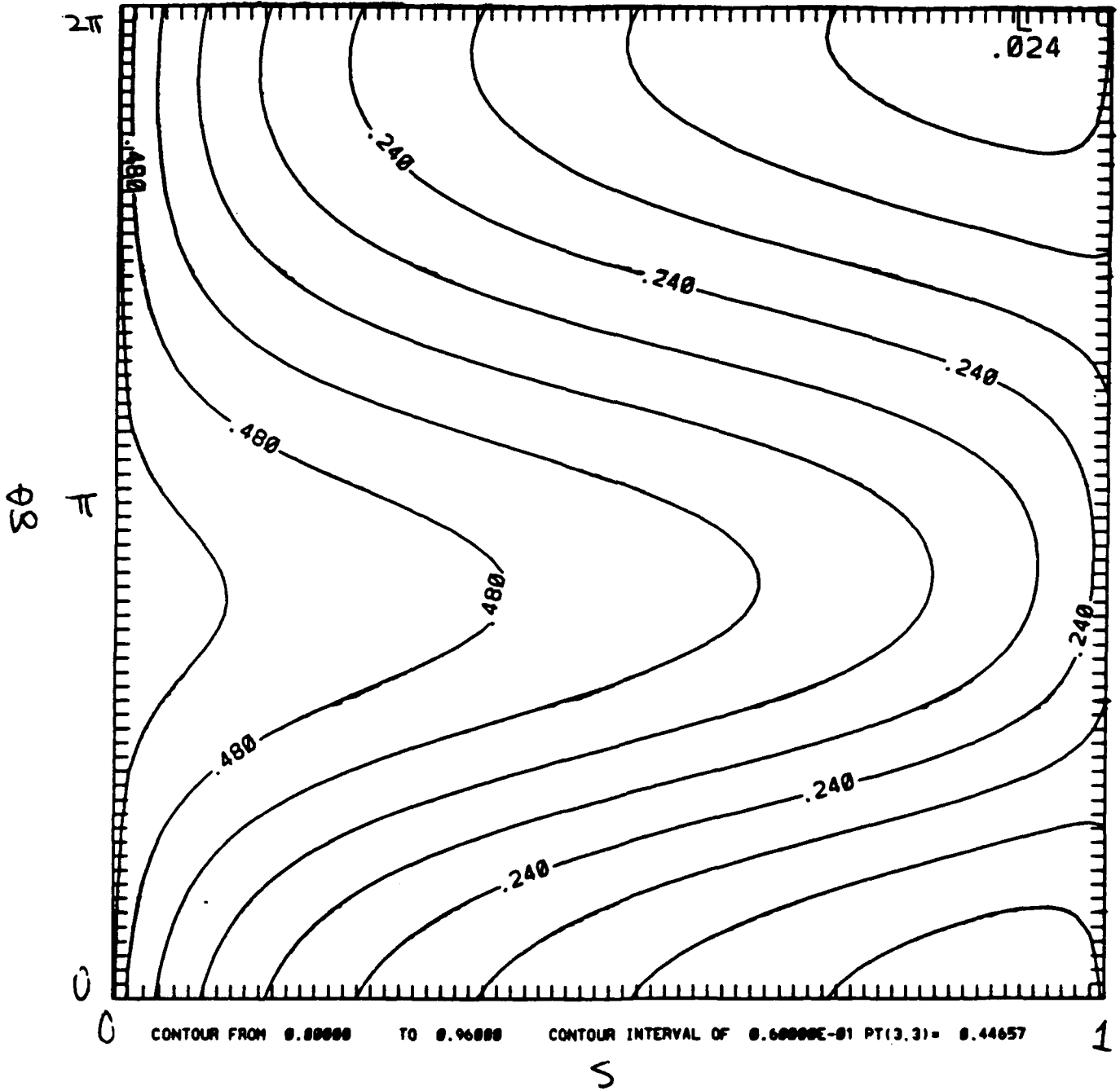


Fig 6(c)

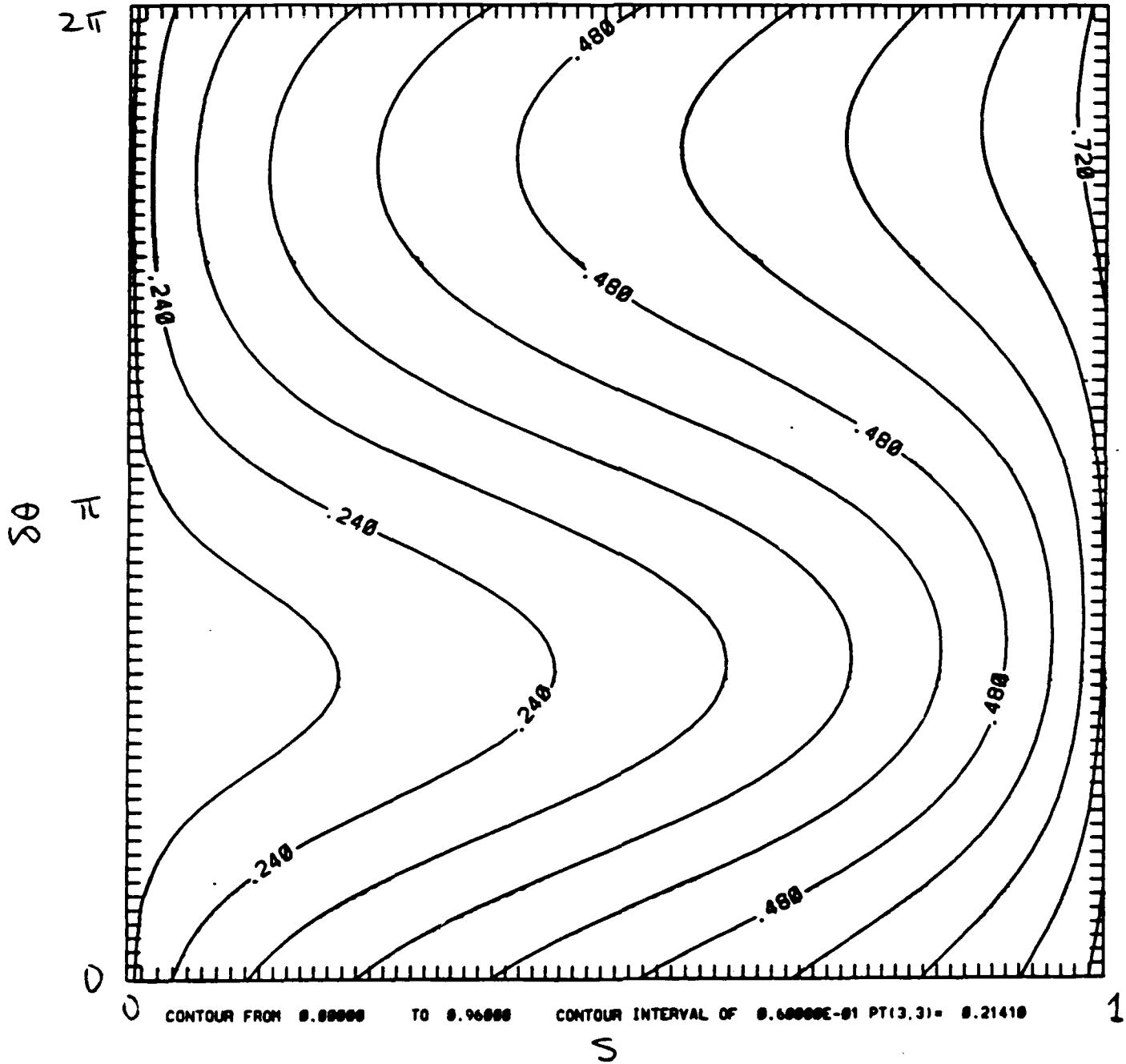
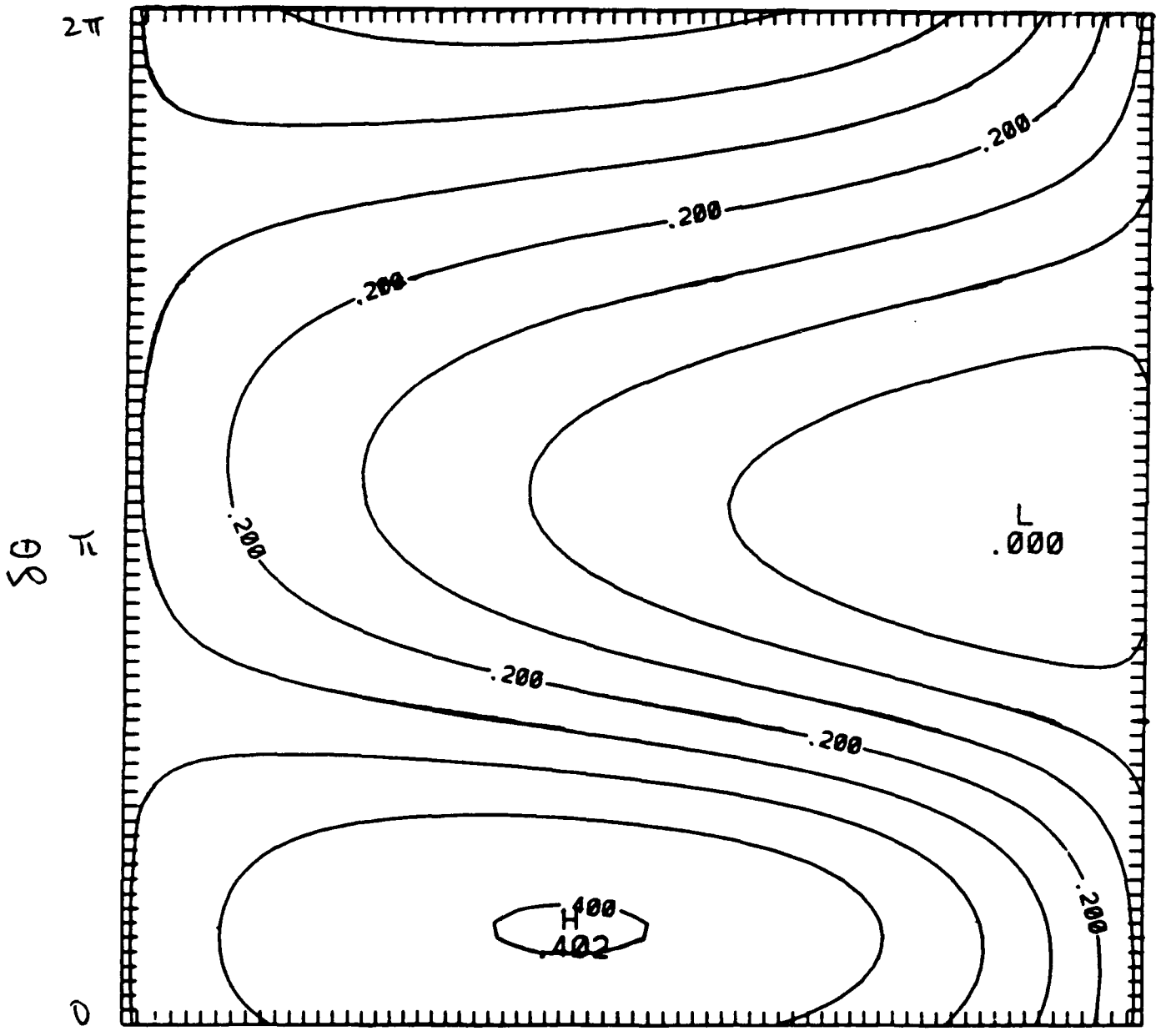


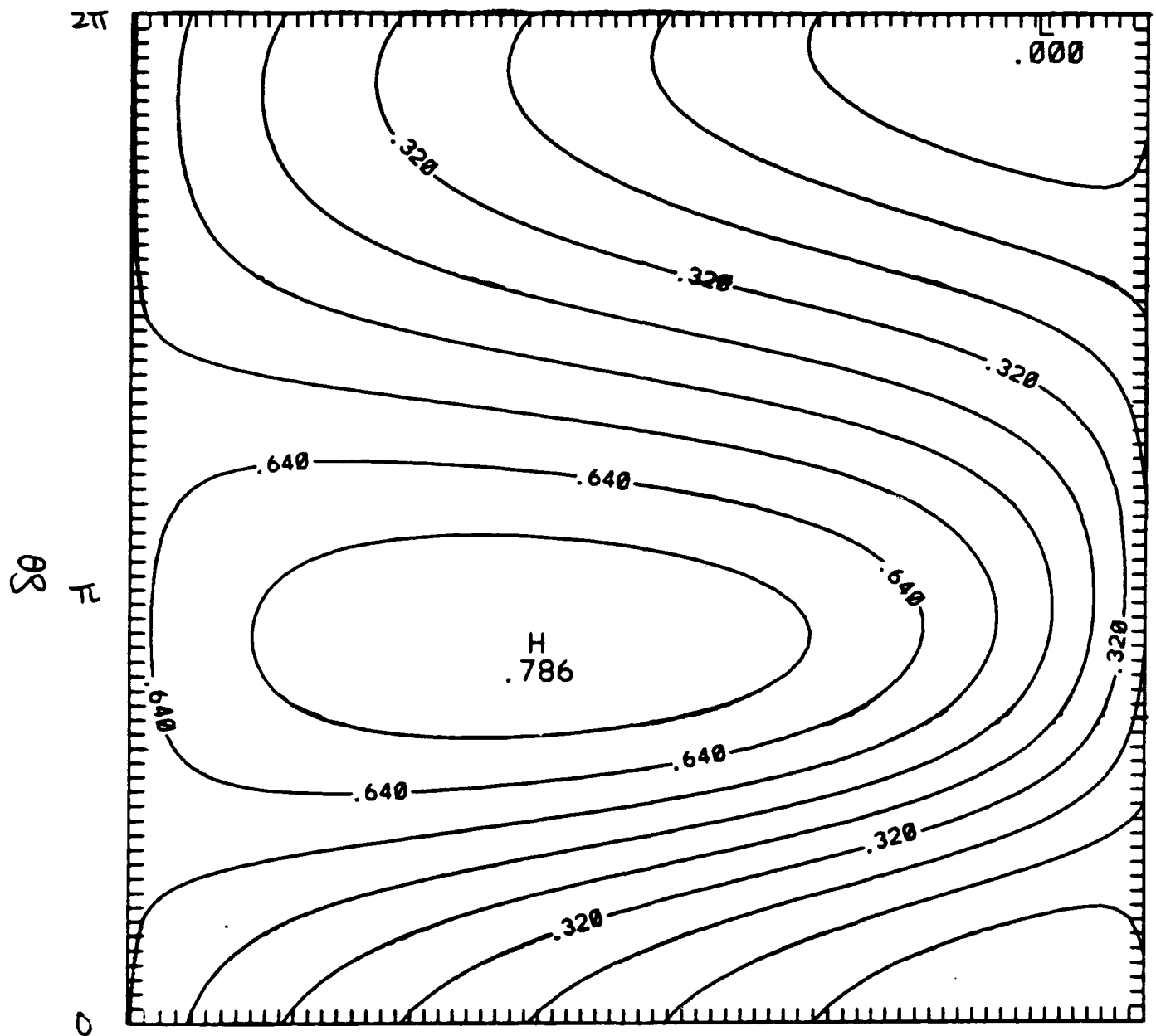
Fig 7(a)



0 CONTOUR FROM 0.00000 TO 0.95000 CONTOUR INTERVAL OF 0.50000E-01 PT(3,3)= 0.31921

S

Fig 1(b)



0 CONTOUR FROM 0.00000 TO 0.96000 CONTOUR INTERVAL OF 0.00000E-01 PT(3.3) = 0.51706 1

S

Fig T(c)

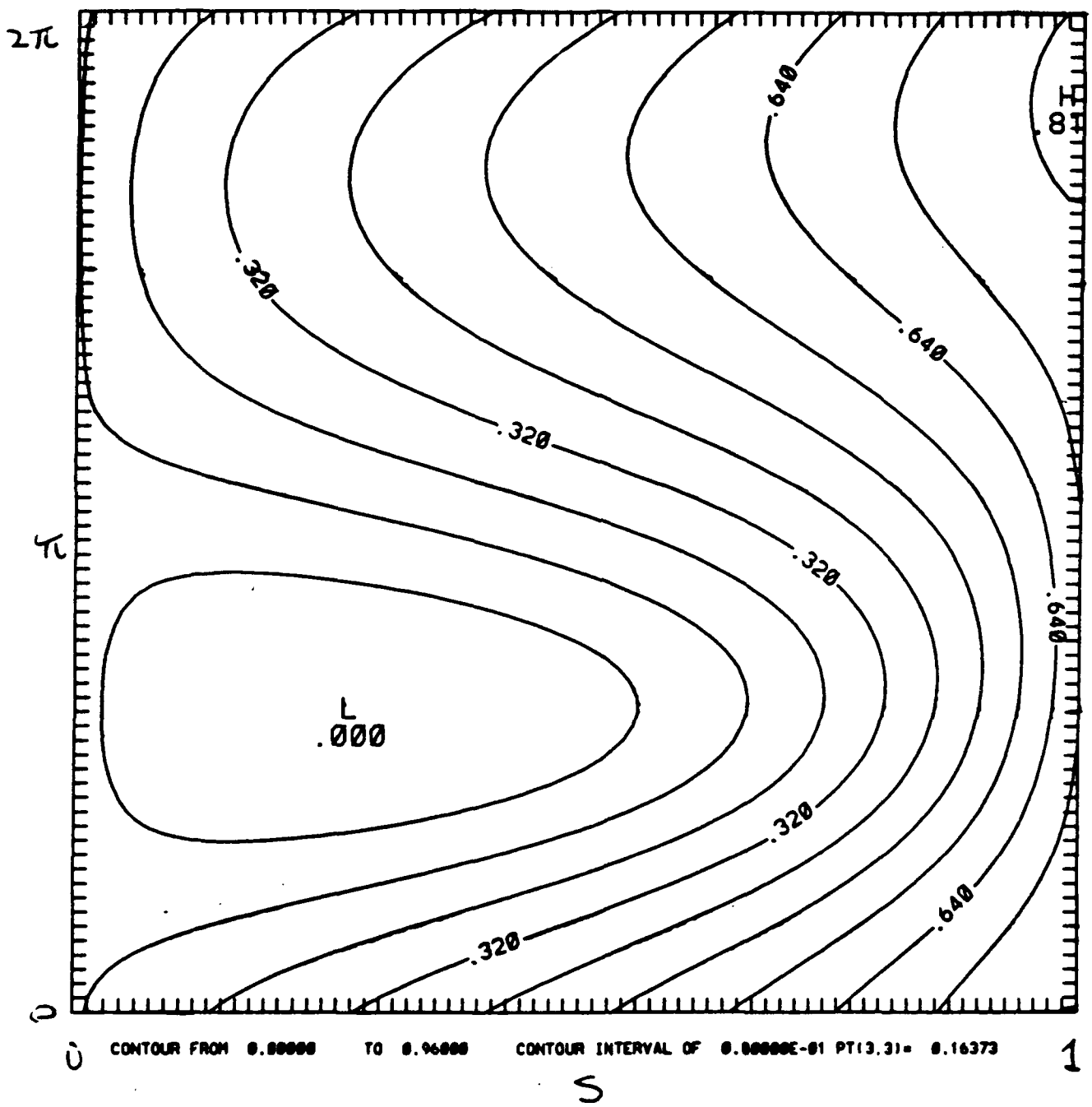


Fig 8 (a)

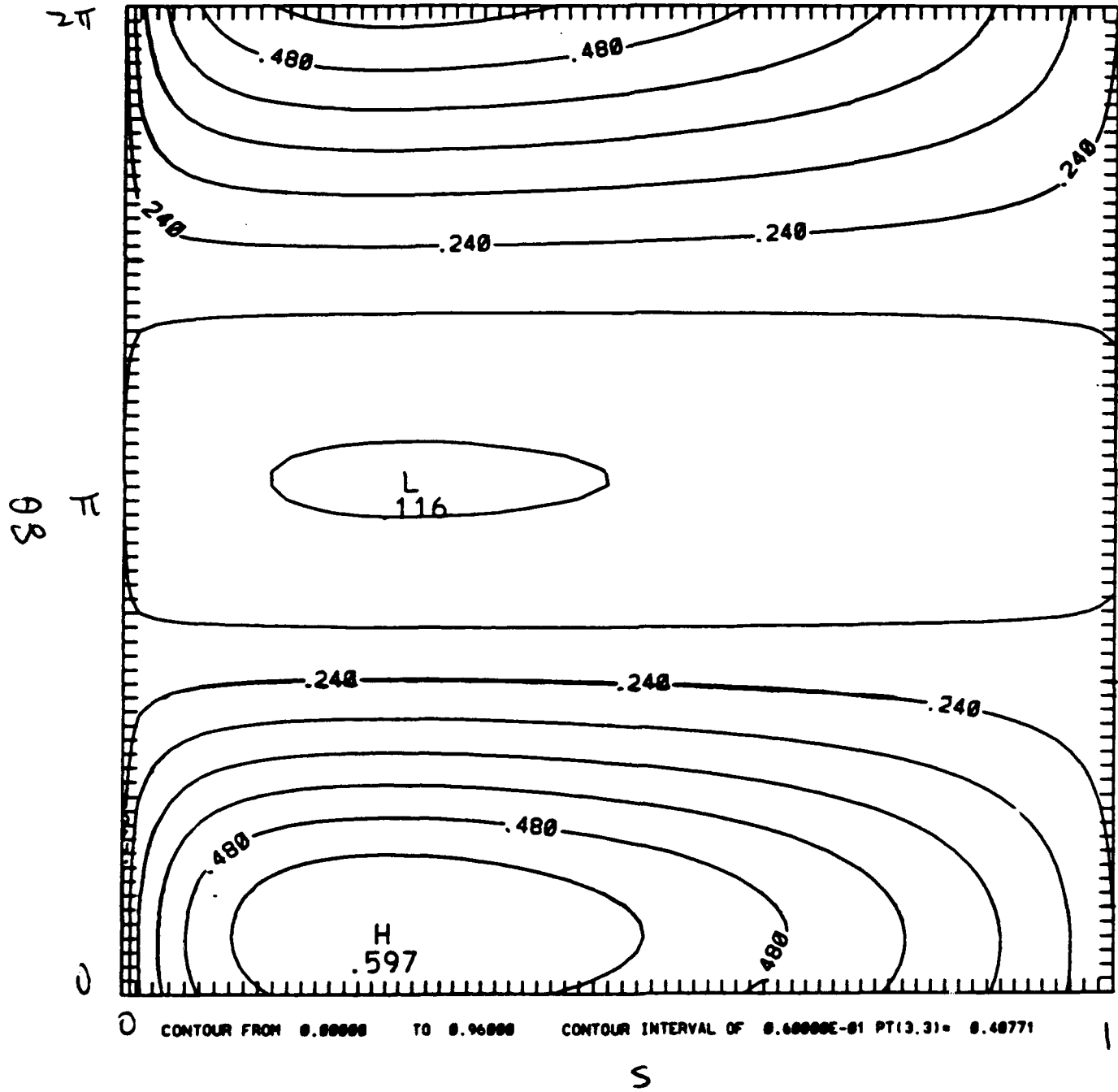


Fig 8(b)

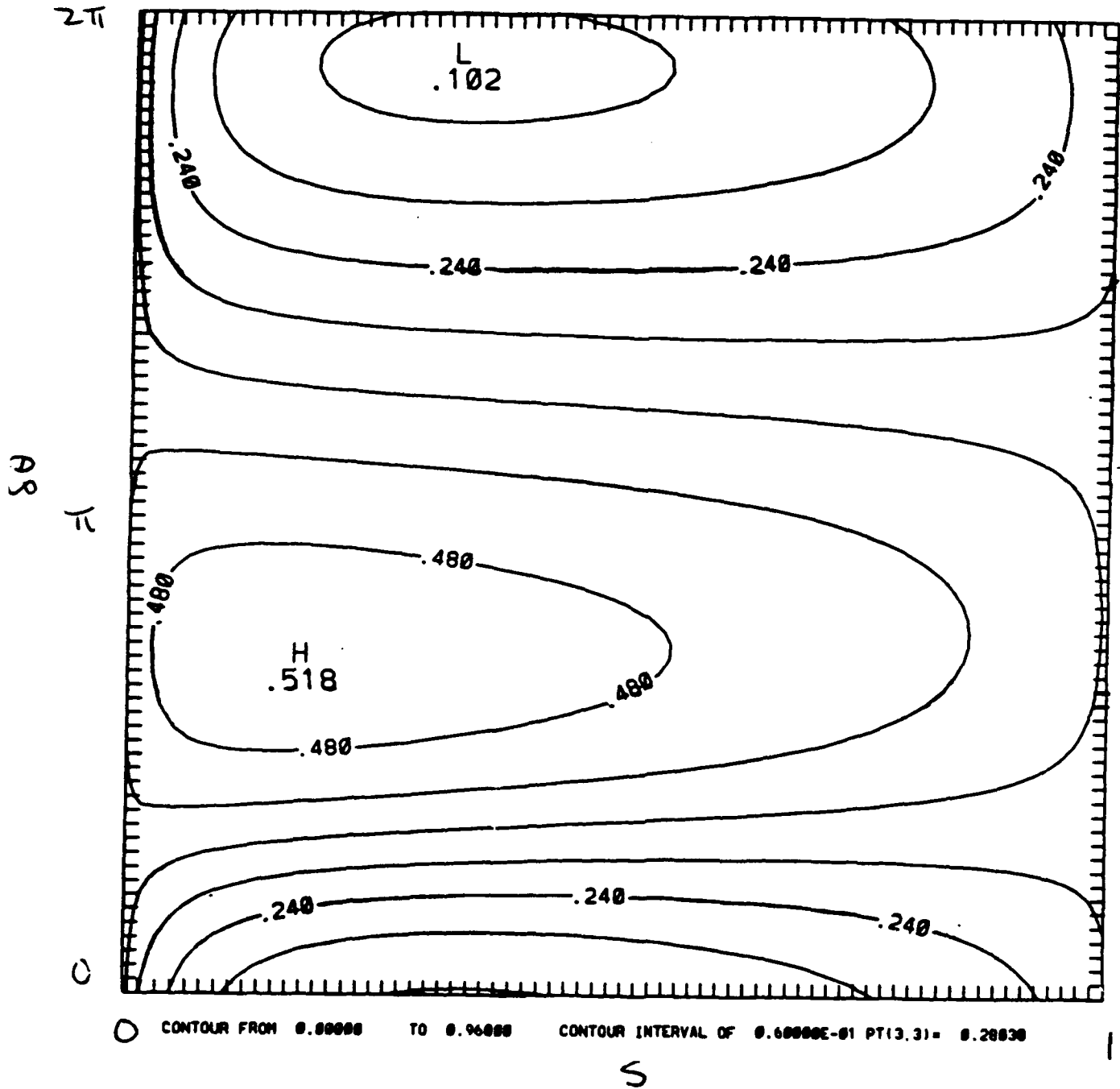


Fig 8(c)

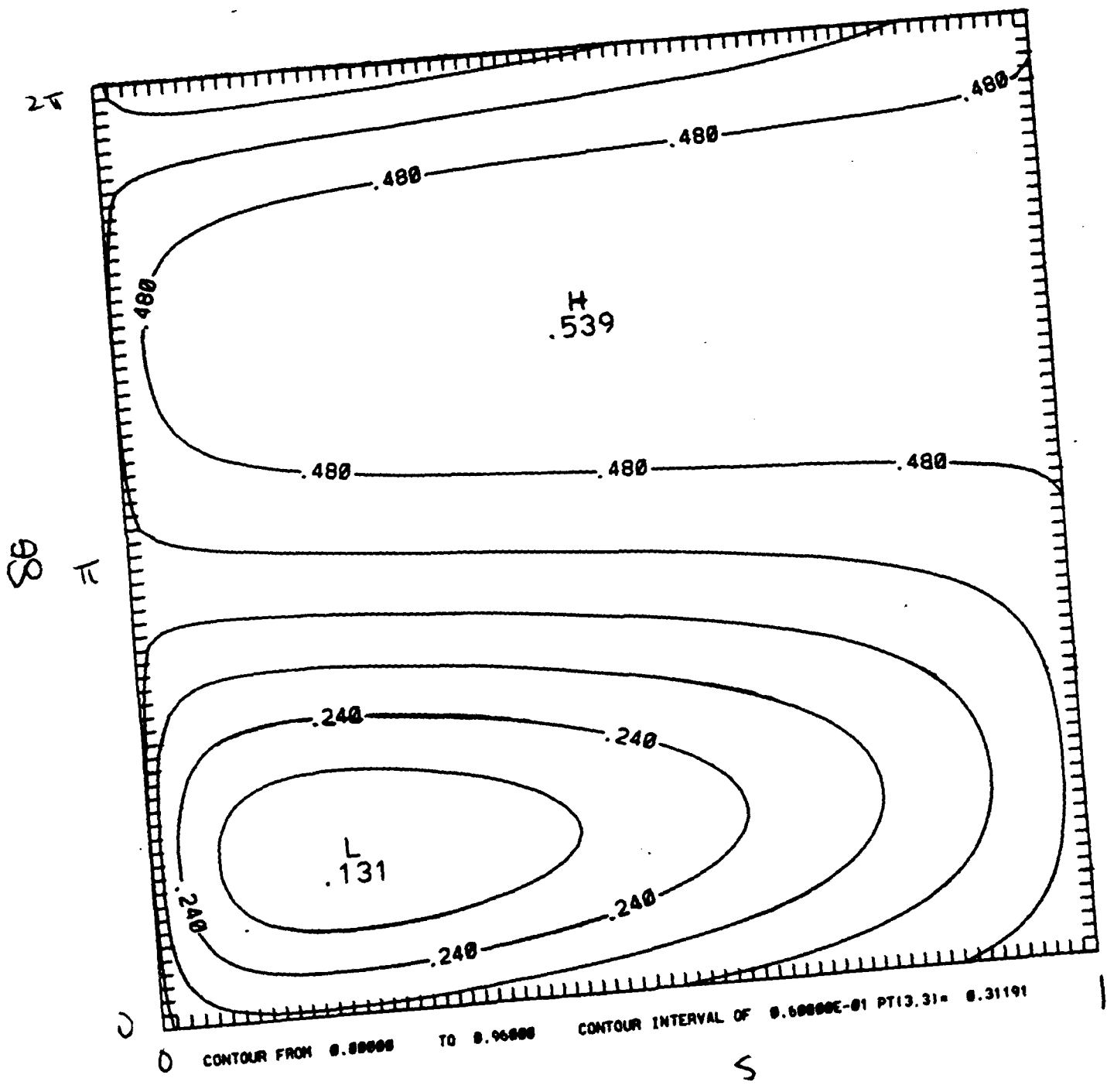


Fig 9 (a)

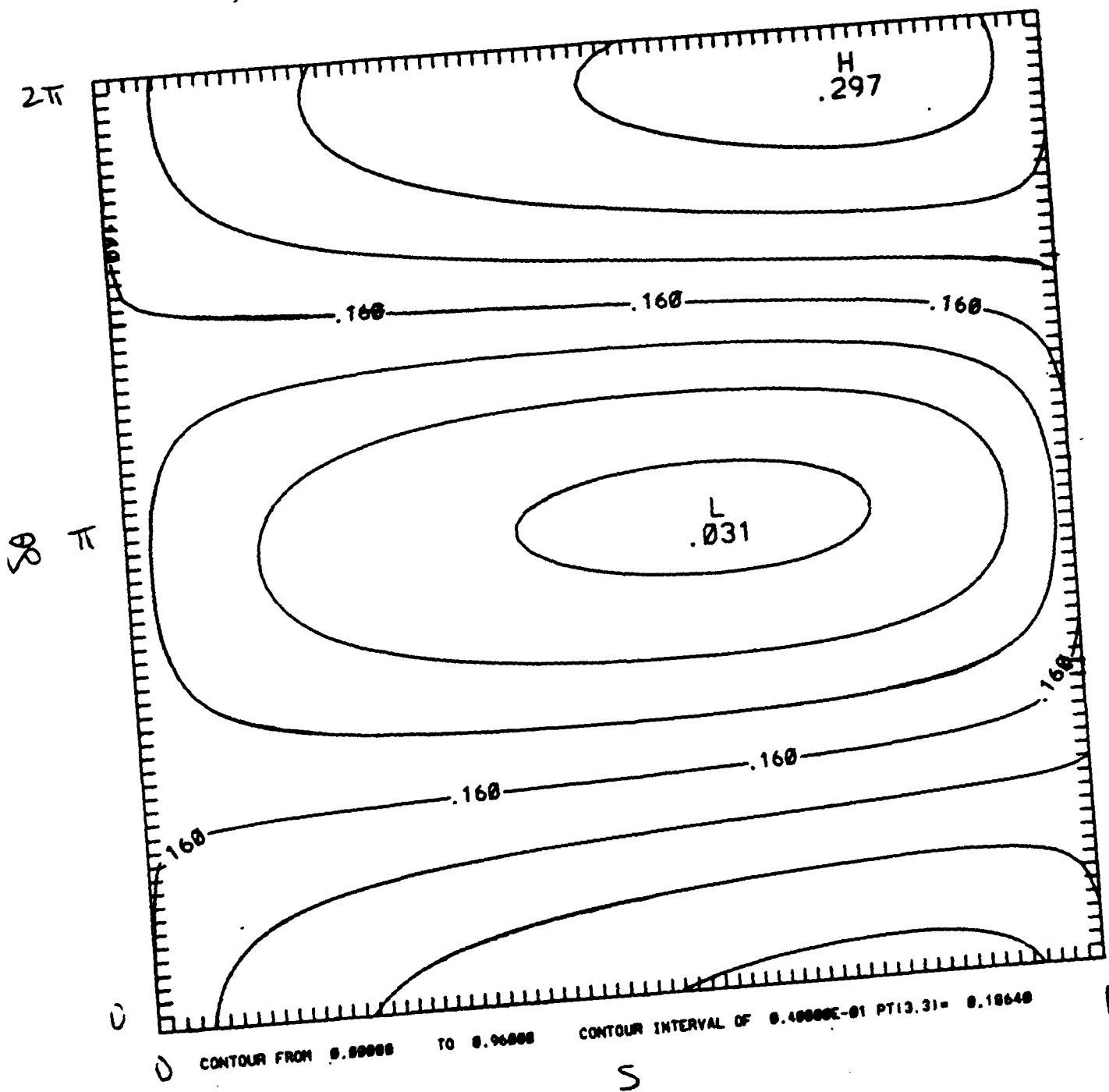


Fig 9 (b)

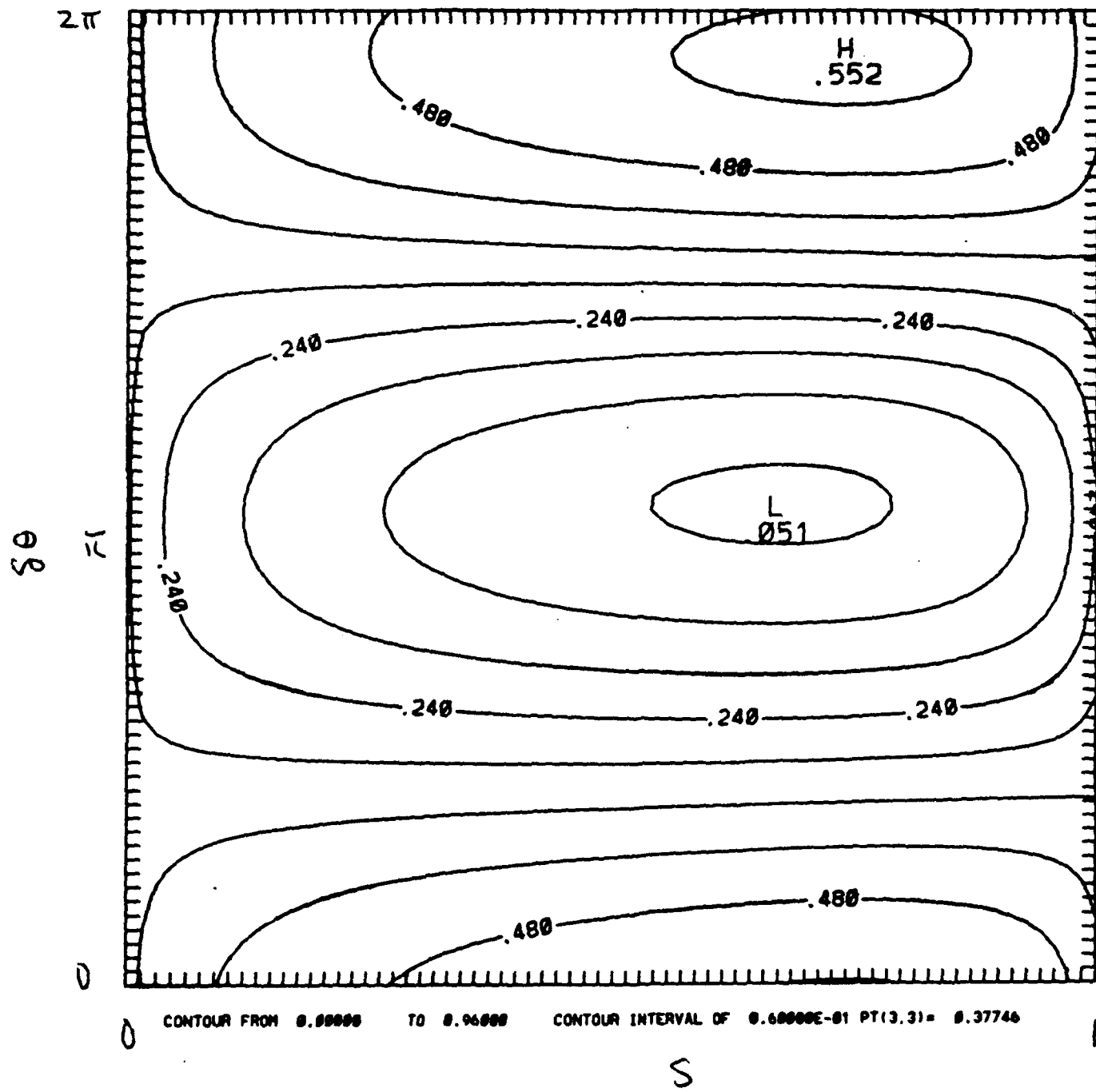
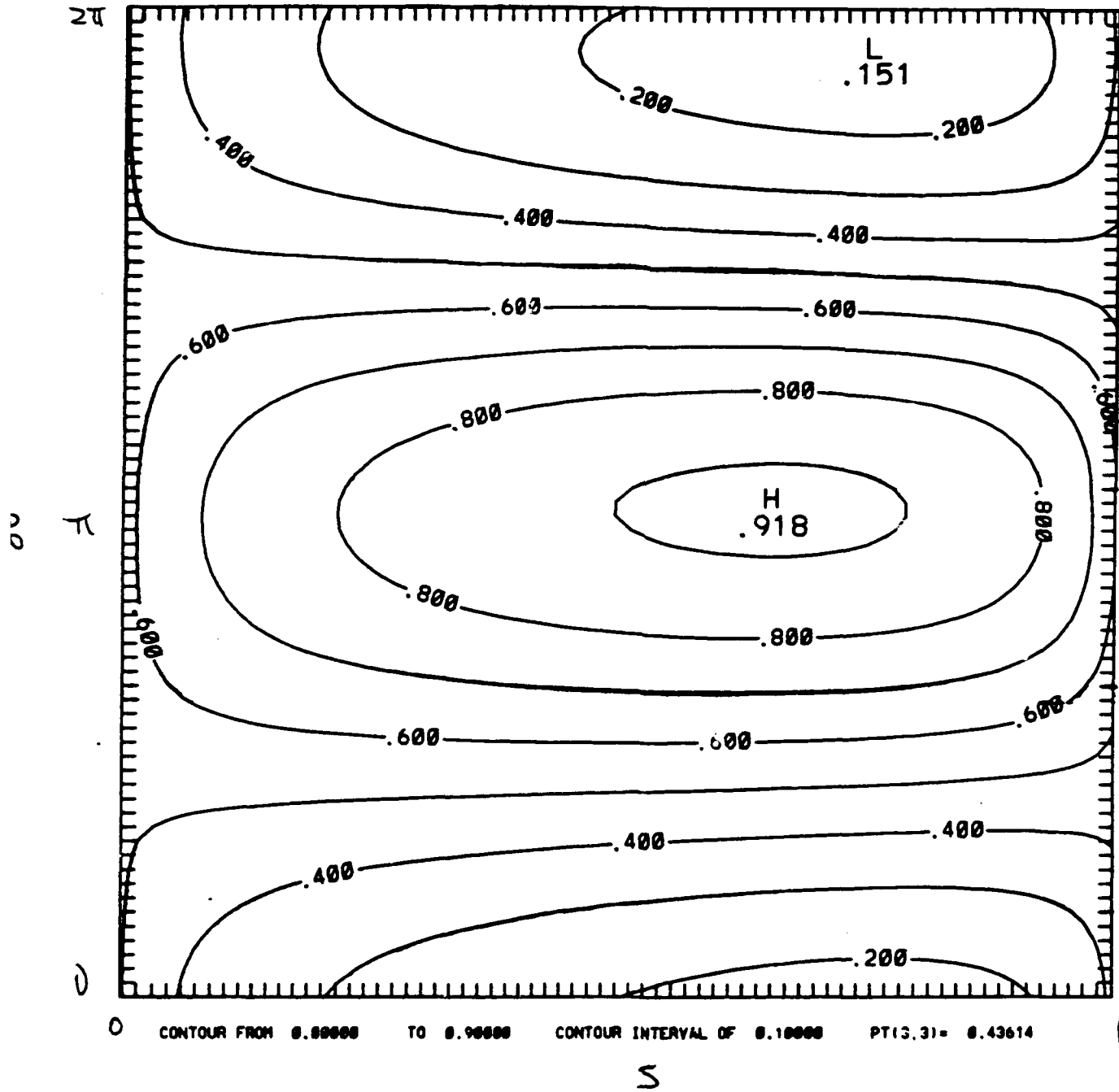


Fig 9(c)



# Total $N$ -Channel Control in the Weak Field Domain

Moshe Shapiro

Chemical Physics Department

Weizmann Institute of Science

Rehovot, Israel

and

Paul Brumer

Chemical Physics Theory Group

Department of Chemistry

University of Toronto

Toronto M5S 1A1 Canada

The goal of controlling chemical reactions with lasers has been advanced considerably with the introduction of the theories of Coherent Radiative Control (CRC)<sup>1-3</sup> and Optimal Control (OCT)<sup>4-9</sup>. The former deals with the use of quantum interference phenomena in the (weak field) control of chemical reactions and has been shown to work well both in the CW<sup>1</sup> and pulsed regimes.<sup>2</sup> By contrast, OCT searches for optimal (not necessarily weak) laser pulses in order to reach desired goals. Initial experimental verification of CRC has now been reported<sup>10</sup> and the importance of the relative phase between the pulses, common to both the CRC and OCT approaches, has been experimentally demonstrated.<sup>11</sup>

Recently, the important question of the theoretical limitations on complete control in the context of OCT has been addressed in a number papers.<sup>6-9</sup> Rice et al.<sup>9</sup> showed that the optimal solution is attainable under certain conditions, but in general, as shown by Yao et al.,<sup>7</sup> nonlinearities may give rise to multiple solutions, each producing exactly the same physical effect on the molecule. Here we demonstrate unique conditions under which *total* control of product yield distributions is possible in an  $N$ -interfering-path scenario for weak field coherent control of photodissociation.

Thus far, CRC theory has focused on the use of only *two* interfering paths to reaction. We have demonstrated, in studies on the dissociation of such molecules as CH<sub>3</sub>I<sup>1, 12</sup> and HOD,<sup>13</sup> and multiple products in Na<sub>2</sub>,<sup>14</sup> that in practice the degree of control achieved with two interfering paths can be extensive. Nonetheless, we have long known that the use of two paths poses theoretical limitations on the ability to control the photodissociation outcome when  $M$ , the number of open fragment channels, exceeds two. Specifically, we explored this issue in detail in Ref. [12] where we showed that the Schwarz inequality,

as applied to two general state-vectors, precludes the realization of *complete* control in that case.

In this communication we show that by extending the CRC treatment of controlled photodissociation to  $N$  paths we obtain an analytic solution for the laser fields which generate a desired target set of product chemical identities and internal state distribution of the photofragments. In doing so we show that the optimal light-amplitudes are obtained as the solution to a set of *linear* algebraic equations, avoiding the tedious non-linear search procedure required at high fields, yet guaranteeing a full solution. Further, we show that this complete control is achievable under the following conditions: that we use sufficiently-weak light sources so that perturbation theory is valid, that the continuum absorption spectrum is composed of a series of sufficiently-narrow resonances, and that the photodissociation process is a non-factorizable one, i.e., it cannot be broken up to an excitation process (of a "bright" state) and a dissociation process (to a set of "dark" states). The derivation follows below.

Consider the action of two pulses on a molecule. One pulse serves to excite a superposition of intermediate bound states  $\psi_i$  and the other to dissociate these states. We first treat the excitation process by representing the excitation pulse as,

$$\epsilon^{(1)}(t) = \int d\omega \{ \epsilon^{(1)}(\omega) \exp[-i\omega(t - z/c)] + c.c. \} = \int d\omega \{ \bar{\epsilon}^{(1)}(\omega) \exp[-i\omega t] + c.c. \}, \quad (1)$$

where  $\bar{\epsilon}(\omega) \equiv \epsilon(\omega) \exp(i\omega z/c)$  with  $z$  being the propagation direction and "c.c." denotes the complex conjugate of the preceding term.

The wavepacket formed at the end of the the action of this pulse on some initial state

$(\psi_g)$  is given, in first order perturbation theory,<sup>15, 16</sup> as,

$$\psi^{(1)}(t) = 2\pi \sum_i \bar{\epsilon}^{(1)}(\omega_{i,g}) \mu_{i,g} \psi_i \exp(-iE_i t/\hbar), \quad (2)$$

where

$$\omega_{i,g} \equiv (E_i - E_g)/\hbar, \quad \mu_{i,g} \equiv \langle \psi_i | \mu | \psi_g \rangle, \quad (3)$$

and  $\mu$  is the transition-dipole operator.

We now turn our attention to the dissociation process. After a delay time  $\tau$ , we subject the molecule to the action of a light source composed of a *discrete* number of modes,

$$\epsilon_i(t) = \epsilon_i \{ \exp[-i\omega_i(t - \tau - z/c)] + c.c. \} = \{ \bar{\epsilon}_i \exp[-i\omega_i(t - \tau)] + c.c. \}, \quad i = 1, \dots, N \quad (4)$$

where

$$\omega_i \equiv (E - E_i)/\hbar, \quad (5)$$

with  $E$  being some energy in the continuum spectrum of the molecule.

If each  $|E_i\rangle$  state only absorbed the right ( $\omega_i$ ) mode, the whole wavepacket would be converted to a wavepacket composed of continuum eigenstates with a single energy,  $E$ . However, there is no *a priori* reason why each state would not absorb other frequencies  $\omega_j \neq \omega_i$ , thus ending up in other continuum energies  $E_{i,j} \equiv E_i + \hbar\omega_j$ .

We consider first just the wavepacket of energy  $E$ . Its form in the long time limit is,

$$\psi^{(2)}(t) = 2\pi \sum_{v,q} \sum_{i=1}^N \bar{\epsilon}^{(1)}(\omega_{i,g}) \mu_{i,g} \bar{\epsilon}_i \mu_i^{(q,v)}(E) \psi_{q,v}^-(E) \exp[-i(Et + E_i\tau)/\hbar] \quad (6)$$

where  $q$  and  $v$  denote the chemical identity and the internal state of the photo-products, respectively. Here  $\psi_{q,v}^-(E)$  are the *incoming* scattering eigenstates of the field-free Hamiltonian, and

$$\mu_i^{(q,v)}(E) \equiv \langle \psi_{q,v}^-(E) | \mu | \psi_i \rangle. \quad (7)$$

are the transition-dipole matrix elements between the  $i$ 'th intermediate state and the scattering states.

The probability amplitude of observing a given channel  $q, v$  at infinite  $t$  is given, using the long-time properties of the incoming scattering states,<sup>17</sup> as,

$$A_v^{(q)}(E) = \sum_{i=1}^N \bar{\epsilon}^{(1)}(\omega_{i,g}) \mu_{i,g} \bar{\epsilon}_i \mu_i^{(q,v)}(E) \exp[-iE_i\tau/\hbar]. \quad (8)$$

with the associated probability  $P_v^{(q)}(E)$  then obtained as  $|A_v^{(q)}(E)|^2$ .

Defining a matrix  $d$  as

$$d_{qv,i} \equiv \bar{\epsilon}^{(1)}(\omega_{i,g}) \mu_{i,g} \mu_i^{(q,v)}(E) \exp(-iE_i\tau/\hbar) \quad (9)$$

and the vector of field amplitudes  $\epsilon$  with elements  $\epsilon_i = \bar{\epsilon}_i$  allows us to rewrite Eq.(8) as

$$\mathbf{A} = \mathbf{d} \cdot \boldsymbol{\epsilon} \quad (10)$$

where the elements of the complex  $M$  dimensional vector  $\mathbf{A}$  are  $A_v^{(q)}$ . If we now choose to replace  $\mathbf{A}$  with a set of desired target amplitudes

$$\mathbf{A}_{q,v} \equiv \mathbf{A}_{q,v}^0, \quad (11)$$

then Eq.(10) may be inverted to obtain the unknown field amplitudes as

$$\boldsymbol{\epsilon} = \mathbf{d}^{-1} \cdot \mathbf{A} \quad (12)$$

where a unique solution generally requires  $N = M$ .

Equation (12) needs to be supplemented by some conditions because, as noted above, in addition to creating continuum eigenstates at energy  $E$ , the set of  $\omega_i$  frequencies creates continuum eigenstates with other energies  $E_{i,j} = E_i + \hbar\omega_j$ . The probability amplitude of creating any of these "satellites" is given as,

$$B_v^{(q)}(E_{i,j}) = \bar{\epsilon}^{(1)}(\omega_{i,g})\mu_{i,g}\bar{\epsilon}_j\mu_i^{(q,v)}(E_{i,j}) \exp[-iE_i\tau/\hbar]. \quad (13)$$

These satellites are uncontrollable because each satellite is produced at a different energy and, as shown in the context of CRC,<sup>1, 3</sup> one of the prime conditions for control is interference between states of the *same* final energy. However, if the continuum spectrum is composed of a series of *resonances* whose widths  $\Gamma_n$  are narrower than the spacings between the intermediate  $E_i$  levels,

$$\Gamma_n \ll |E_i - E_{i+1}|, \quad (14)$$

and if the target energy  $E (= \hbar\omega_i + E_i)$  is in the center of one of these resonances, then (as illustrated in Fig. 1) the chances that  $E_{i,j}$  will not coincide with any of the other resonances are high. Under these conditions  $\mu_i^{(q,v)}(E_{i,j}) \approx 0$  and the probability of satellite production in accord with Eq. (13), is minimal.

Utilizing isolated resonances, while helping overcome the satellite problem, raises a different issue which might undermine our ability to control a process. Specifically, as shown in Ref. [12], if the transition dipole is factorizeable, e.g. if it may be written as,

$$\mu_i^{(q,v)}(E) = \mu_{n,i}F_n^{(q,v)}(E), \quad (15)$$

then the  $N$ -state interference of Eq. (8) does little to change the ratio between the yield to produce the various  $q, v$  channels. This follows because when Eq. (15) is substituted into Eq. (8) we obtain that,

$$A_v^{(q)}(E) = \left\{ \sum_i \bar{\epsilon}^{(1)}(\omega_{i,g})\mu_{i,g}\mu_{n,i}\bar{\epsilon}_i \exp[-iE_i\tau/\hbar] \right\} F_n^{(q,v)}(E). \quad (16)$$

The branching ratios to the various channels, given as  $R_{vq,v'q'} \equiv |A_v^{(q)}(E)/A_{v'}^{(q')}(E)|^2$ , therefore assume the form

$$R_{vq,v'q'} = |F_n^{(q,v)}(E)/F_n^{(q',v')}(E)|^2, \quad (17)$$

i.e., the coherent interference between the various paths has absolutely no effect on the branching ratios into the various final channels!

Thus, we need to assure that factorization of the type shown in Eq. (15) does not hold. Factorization occurs, for isolated resonances, whenever only *one* of the molecular modes is a "bright" mode, i.e., it carries oscillator strengths from the intermediate  $|E_i \rangle$  states. In order to see this we write the full continuum energy eigenstate as,<sup>17</sup>

$$|\psi_{q,v}^-(E) \rangle = \{I + [I + (E^- - PHP)^{-1}PH](E - E_n - i\Gamma_n/2)^{-1}|\phi_n \rangle \langle \phi_n|H\} P|\psi_{q,v}^{0-}(E) \rangle \quad (18)$$

where  $|\phi_n \rangle$  is an eigenstate of the "bright" mode Hamiltonian,  $I$  is the identity operator,  $P \equiv I - |\phi_n \rangle \langle \phi_n|$  is the projector onto all other states,  $H$  is the full Hamiltonian and  $P|\psi_{q,v}^{0-}(E) \rangle$  is an eigenstate of PHP,

$$\{E - PHP\}P|\psi_{q,v}^{0-}(E) \rangle = 0. \quad (19)$$

Factorization occurs if we assume that

$$P\mu|E_i \rangle = 0. \quad (20)$$

Under this condition it follows from Eq. (18) that,

$$\langle \psi_{q,v}^-(E) | \mu | E_i \rangle = \langle \psi_{q,v}^{0-}(E) | PH | \phi_n \rangle (E - E_n - i\Gamma_n/2)^{-1} \langle \phi_n | \mu | E_i \rangle \quad (21)$$

which is the factorized form of Eq. (15).

We therefore conclude that we can avoid factorization and maintain control whenever Eq. (20) is invalid. This is the case when strong mixing between molecular modes exists such that none of the modes retains its "purity", or that the resonance structure is due to slow predissociation from one bright state to another bright state. The signature of such predissociation is asymmetry of the lineshapes which arises from Fano-type interferences between the  $|\phi_n\rangle\langle\phi_n|$  and the P components.

In summary, we have presented a solution to the  $N$ -channel controllability problem in the weak field domain. We have shown that in a photodissociation process any desired distribution of  $N$  final fragment states can be generated using a series of  $N$  light frequencies. This is the case provided that the absorption spectrum is composed of a series of sufficiently narrow non-factorizable resonances and that the target distribution can arise within perturbation theory. An explicit expression [Eq.( 12)] for the complex field amplitudes needed to achieve this goal has been obtained.

The solution we have generated is remarkably simple. It is contained in an inverse of a matrix made up of readily measurable (or calculable) bound-bound and bound-free transition-dipole matrix-elements. Further work is currently ongoing to compute the electromagnetic fields required to achieve various target distributions in the dissociation of both diatomics and polyatomics.

### Acknowledgment

This research was supported by the Office of Naval Research of the U.S. under contract number N00014-90-J-1014.

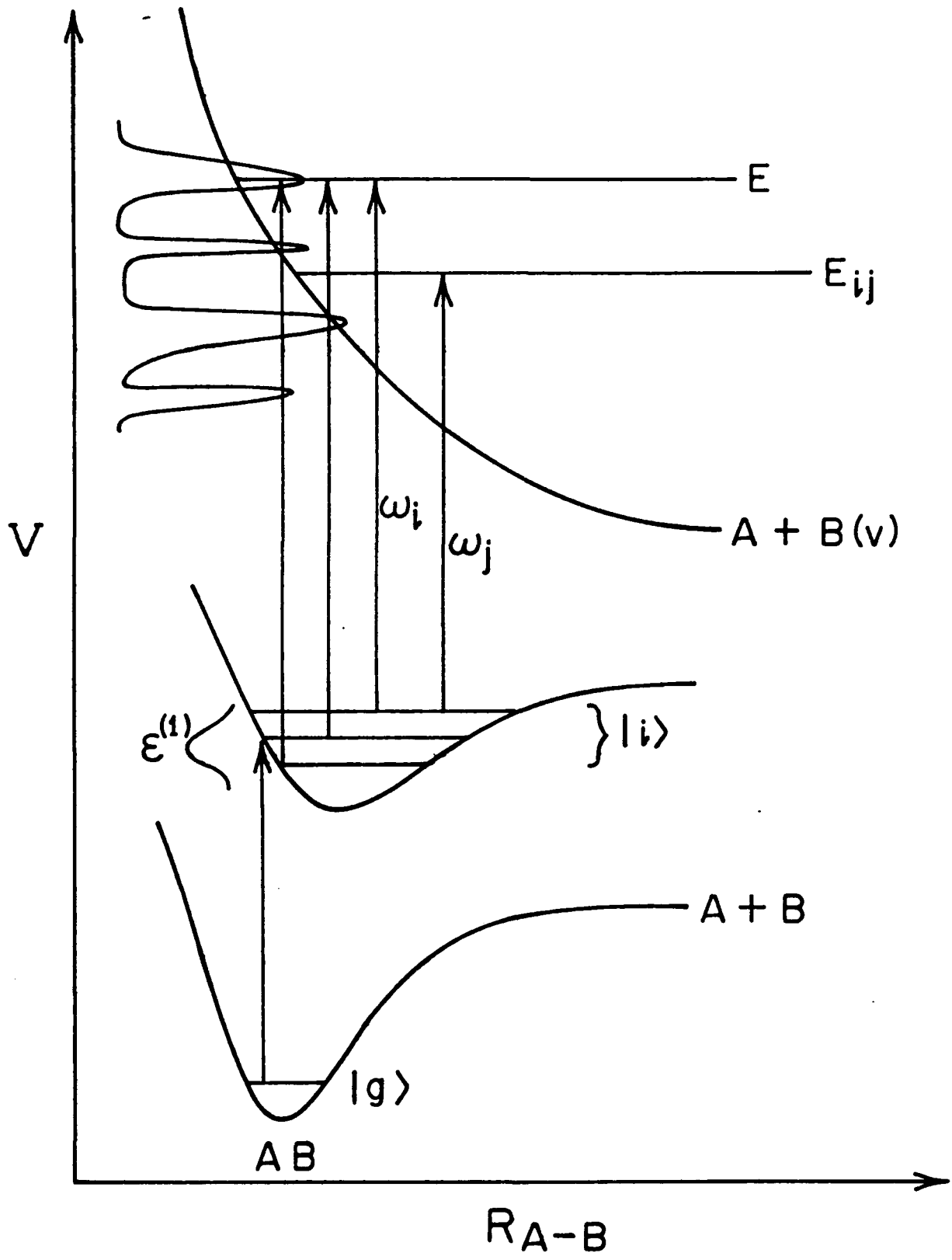
## References

- [1] P. Brumer and M. Shapiro, *Chem. Phys. Lett.* **126**, 541 (1986); M. Shapiro, J.W. Hepburn, and P. Brumer, *Chem. Phys. Lett.* **149**, 451 (1988); P. Brumer and M. Shapiro, *Acc. Chem. Res.*, **22**, 407 (1989), and references therein.
- [2] T. Seideman, M. Shapiro, and P. Brumer, *J. Chem. Phys.* **90**, 7132 (1989); I. Levy, M. Shapiro, and P. Brumer, *J. Chem. Phys.* **93**, 2493 (1990); M. Shapiro and P. Brumer, *J. Chem. Phys.* **95**, 8658 (1991).
- [3] M. Shapiro and P. Brumer, *Annual Reviews of Physical Chemistry*, (in press)
- [4] D.J. Tannor, and S.A. Rice, *J. Chem. Phys.* **83**, 5013 (1985); D.J. Tannor, and S.A. Rice, *Adv. Chem. Phys.* **70**, 441 (1988); R. Kosloff, S.A. Rice, P. Gaspard, S. Tersigni, and D.J. Tannor, *Chem. Phys.* **139**, 201 (1989).
- [5] See, e.g., S. Shi, A. Woody, and H. Rabitz, *J. Chem. Phys.* **88**, 6870 (1988); S. Shi, and H. Rabitz, *J. Chem. Phys.* **92**, 364 (1990); R.S. Judson, K.K. Lehmann, H. Rabitz, and W.S. Warren, *J. Mol. Struct.* **223**, 425 (1990).
- [6] A.P. Peirce, M. Dahleh, and H. Rabitz, *Phys. Rev. A* **37**, 4950 (1988).
- [7] K. Yao, S. Shi, and H. Rabitz, *Chem. Phys.* **150**, 373 (1990).
- [8] For the use of chirped optimized pulses, see, S. Chelkowski, A. Bandrauk, and P.B. Corkum, *Phys. Rev. Lett.* **65**, 2355 (1990).
- [9] M. Zhao and S.A. Rice, *J. Chem. Phys.* (submitted); S.A. Rice, in "Mode Selective Chemistry", J. Jortner R.D. Levine, and B. Pullman, Eds. (Kluwer, Dodrecht, 1991) p. 485.

- [10] C. Chen, Y-Y. Yin, and D.S. Elliott, *Phys. Rev. Lett.* **64**, 507 (1990); *ibid.* **65**, 1737 (1990); S.M. Park, S-P. Lu, and R.J. Gordon, *J. Chem. Phys.* **94**, 8622 (1991); B.A. Baranóva, A.N. Chudinov, and B. Ya. Zel'dovitch, *Opt. Comm.*, **79**, 116 (1990)
- [11] N.F. Scherer, A. J. Ruggiero, M. Du, and G.R. Fleming, *J. Chem. Phys.* **93**, 856 (1990); N.F. Scherer, R.J. Carlson., A. Matro, M. Du, A. J. Ruggiero, V. Romero-Rochin, J.A. Cina, G.R. Fleming, and S.A. Rice, *J. Chem. Phys.* **95**, 1487 (1991).
- [12] P. Brumer and M. Shapiro, *Faraday Disc. Chem. Soc.* **82**, 177 (1987).
- [13] M. Shapiro and P. Brumer *J. Chem. Phys.* (submitted)
- [14] Z. Chen, P. Brumer and M. Shapiro, *J. Chem. Phys.* (submitted).
- [15] M. Shapiro, "Theory of Continuum-Raman Spectroscopy with Pulses, and the Excitation Spectrum of  $\text{CH}_3\text{I}$ ", *J. Chem. Phys.* , submitted for publication.
- [16] R.D. Taylor and P. Brumer, *Disc. Faraday Soc.* **75**, 117 (1983); M. Shapiro, in *Mode-Selective Chemistry*, edited by J. Jortner, R.D. Levine and B. Pullman (Kluwer Academic, The Netherlands, 1991) p. 283.
- [17] R.D. Levine, "Quantum Mechanics of Molecular Rate Processes" (Oxford University Press, Oxford, 1969).

**Figure 1** : Schematic diagram depicting the photodissociation scenario discussed in the

text. Here  $|\psi_i\rangle$  is denoted  $|i\rangle$  and  $|\psi_g\rangle$  is denoted  $|g\rangle$ .



To Appear in  
"Coherence Phenomena in Atoms  
+ Molecules in Laser Fields"  
ed. A. Bandrauk

①

## COHERENCE IN THE CONTROL OF MOLECULAR PROCESSES

PAUL BRUMER

Chemical Physics Theory Group  
Department of Chemistry  
University of Toronto  
Toronto, Ontario M5S 1A1, Canada

and

MOSHE SHAPIRO

Chemical Physics Department  
Weizmann Institute of Science  
Rehovot, Israel

**ABSTRACT.** We describe the current status of coherent radiative control, a quantum-interference based approach to controlling molecular processes by the use of coherent radiation. In addition to providing an overview of proposed laboratory scenarios, ongoing experimental studies and recent theoretical developments, we call attention to recent theoretical results on symmetry breaking in achiral systems.

### 1. Introduction

This NATO workshop deals with the rapidly developing area of coherence phenomena in Chemistry and Physics. Of particular interest are the phase characteristics of molecular and optical states, and new phenomena which emerge when one can manipulate the quantum phase of material systems. In this paper we discuss a theory, based upon quantum interference effects, which predicts virtually total control over branching ratios in isolated molecular processes.

Control over the yield of chemical reactions is the *raison d'être* of practical chemistry and the ability to use lasers to achieve this goal is one primary thrust of modern Chemical Physics. The theory of coherent radiative control of chemical reactions, which we have developed over the last five years [1-16], affords a direct method for controlling reaction dynamics using coherence properties of weak lasers, with a large range of yield control expected in laboratory scenarios. In addition, the theory of coherent control provides deep insights into the essential features of reaction dynamics, and of quantum interference, which are necessary to achieve control over elementary chemical processes. Below we provide a schematic overview of coherent radiative control including an example which

emphasizes the general principles (Section 2), a survey of several experimental scenarios which implement the principles of coherent control (Section 3), an interesting application to symmetry breaking in achiral systems (Section 4) and a summary of the current status of theory and experiment. A qualitative introduction to coherent control is provided in reference [9]. An alternative approach, based upon the use of shaped light pulses has been advocated by Tannor and Rice [17] and Rabitz[18].

### 2. Interference and Control: An Example

Consider a chemical reaction which, at total energy  $E$  produces a number of distinct products. The total Hamiltonian is denoted  $H = H_q^0 + V_q$ , where  $H_q^0$  is the Hamiltonian of the separated products in the arrangement channel labeled by  $q$ , ( $q = 1, 2, \dots$ ) and  $V_q$  is the interaction between products in arrangement  $q$ . We denote eigenvalues of  $H_q^0$  by  $|E, n, q^0\rangle$ , where  $n$  denotes all quantum numbers other than  $E$ ; eigenfunctions of  $H$ , which correlate with  $|E, n, q^0\rangle$  at large product separation, are labeled  $|E, n, q^-\rangle$ . By definition of the minus states, a state prepared experimentally as a superposition  $|\Psi(t = 0)\rangle = \sum_{n,q} c_{n,q} |E, n, q^-\rangle$  has probability  $|c_{n,q}|^2$  of forming product in channel  $q$ , with quantum numbers  $n$ . As a consequence, control over the probability of forming a product in any asymptotic state is equal to the probability of initially forming the appropriate minus state which correlates with the desired product. The essence of control lies, therefore, in forming the desired linear combination at the time of preparation. The essential *modus operandi* of coherent radiative control is to utilize phase and intensity properties of laser excitation to alter the character of the prepared state so as to enhance production of the desired product.

Many of the proposed coherent control scenarios rely upon a simple way of achieving active control over the prepared state and product. Specifically, active control over products is achieved by driving an initially pure molecular state through two or more independent coherent optical excitation routes. The resultant product probability displays interference terms between these two routes, whose magnitude and sign depend upon laboratory parameters. As a consequence, product probabilities can be manipulated directly in the laboratory.

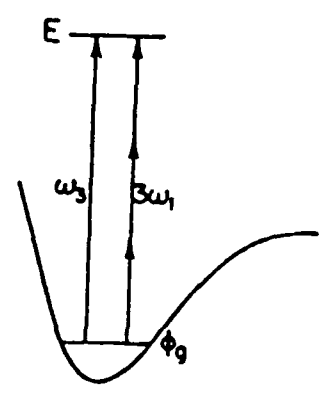


Figure 1: One-photon plus three-photon coherent control scenario.

The scheme outlined above has, as a well-known analogy, the interference between paths as a beam of either particles or of light passes through a double slit. In that instance source coherence leads to either constructive or destructive interference, manifest as patterns of enhanced or reduced probabilities on an observation screen. In the case of coherent control the overall coherence of a pure state plus laser source allows for the constructive or destructive manipulation of probabilities in product channels.

We note, as an aside, that practitioners of "mode-selective chemistry" often advocate the use of lasers to excite specific bonds or modes in the reactant molecule in order to drive a reaction in a desired direction. The brief remarks above, elaborated upon elsewhere[10], make clear that the proper modes to excite in order to produce product in arrangement  $q$  are the eigenfunctions  $|E, n, q^-\rangle$ , the system's "natural modes", if you will. Thus the extent to which excitation of some zeroth order state  $|\chi\rangle$  is successful in promoting reaction to the desired product  $q$  depends entirely on the extent to which  $|\chi\rangle$  overlaps  $|E, n, q^-\rangle$ .

Consider, as an example of coherent control, a specific scenario for unimolecular photoexcitation[5,13] (Figure 1) where a system, initially in pure state  $\phi_g$  (or  $|E_i\rangle$  below), is excited to energy  $E$ , by simultaneous application of two CW frequencies  $\omega_3$  and  $3\omega_1$  ( $\omega_3 = 3\omega_1$ ), providing two independent optically driven routes from  $\phi_g$  to  $|E, n, q^-\rangle$ .

Straightforward perturbation theory, valid for the weak fields under consideration, gives the probability  $P(E, q; E_i)$  of forming product at energy  $E$  in arrangement  $q$  as:

$$P(E, q; E_i) = P_3(E, q; E_i) + P_{13}(E, q; E_i) + P_1(E, q; E_i). \quad (1)$$

with terms defined as follows:

$$P_3(E, q; E_i) = \left(\frac{\pi}{\hbar}\right)^2 \epsilon_3^2 \sum_n |\langle E, n, q^- | (\hat{\epsilon}_3 \cdot \mu)_{e,g} | E_i \rangle|^2. \quad (2)$$

Here  $\mu$  is the electric dipole operator, and

$$(\hat{\epsilon}_3 \cdot \mu)_{e,g} = \langle e | \hat{\epsilon}_3 \cdot \mu | g \rangle, \quad (3)$$

where  $|g\rangle$  and  $|e\rangle$  are the ground and excited electronic state wavefunctions, respectively. The second and third terms in Eq. (1) are

$$P_1(E, q; E_i) = \left(\frac{\pi}{\hbar}\right)^2 \epsilon_1^2 \sum_n |\langle E, n, q^- | T | E_i \rangle|^2, \quad (4)$$

with

$$T = (\hat{\epsilon}_1 \cdot \mu)_{e,g} (E_i - H_g + 2\hbar\omega_1)^{-1} (\hat{\epsilon}_1 \cdot \mu)_{g,e} (E_i - H_e + \hbar\omega_1)^{-1} (\hat{\epsilon}_1 \cdot \mu)_{e,g}. \quad (5)$$

and

$$P_{13}(E, q; E_i) = -2 \left(\frac{\pi}{\hbar}\right)^2 \epsilon_3 \epsilon_1^2 \cos(\theta_3 - 3\theta_1 + \delta_{13}^{(q)}) |F_{13}^{(q)}| \quad (6)$$

with the amplitude  $|F_{13}^{(q)}|$  and phase  $\delta_{13}^{(q)}$  defined by

$$|F_{13}^{(q)}| \exp(i\delta_{13}^{(q)}) = \sum_n \langle E_i | T | E, n, q^- \rangle \langle E, n, q^- | (\hat{\epsilon}_3 \cdot \mu)_{e,g} | E_i \rangle. \quad (7)$$

The branching ratio  $R_{qq'}$  for channels  $q$  and  $q'$ , can then be written as

$$R_{qq'} = \frac{P(E, q; E_i)}{P(E, q'; E_i)} = \frac{\epsilon_3^2 F_3^{(q)} - 2\epsilon_3 \epsilon_1^2 \cos(\theta_3 - 3\theta_1 + \delta_{13}^{(q)}) |F_{13}^{(q)}| + \epsilon_1^6 F_1^{(q)}}{\epsilon_3^2 F_3^{(q')} - 2\epsilon_3 \epsilon_1^2 \cos(\theta_3 - 3\theta_1 + \delta_{13}^{(q')}) |F_{13}^{(q')}| + \epsilon_1^6 F_1^{(q')}}}, \quad (8)$$

where

$$\begin{aligned} F_3^{(q)} &= \left(\frac{\hbar}{\tau}\right)^2 \frac{P_3(E, q; E_i)}{\epsilon_3^2}, \\ F_1^{(q)} &= \left(\frac{\hbar}{\tau}\right)^2 \frac{P_1(E, q; E_i)}{\epsilon_1^2}, \end{aligned} \quad (9)$$

with  $F_3^{(q')}$  and  $F_1^{(q')}$  defined similarly.

The numerator and denominator of Eq. (8) each display what we regard as the canonical form for coherent control. That is, independent contributions from two routes, modulated by an interference term. Since the interference term is controllable through variation of laboratory parameters (here the relative intensity and relative phase of the two lasers), so too is the product ratio  $R$ .

This 3-photon + 1-photon scenario has now been experimentally implemented[19] in studies of HCl ionization through a resonant bound Rydberg state. Specifically, HCl is excited to a selected rotational state in the  $^3\Sigma^-(\Omega^+)$  manifold using  $\omega_1 = 336$  nm;  $\omega_3$  is obtained by third harmonic generation in a Krypton gas cell. The relative phase of the light fields was then varied by passing the beams through a second Krypton cell and varying the cell gas pressure. The population of the resultant Rydberg state was interrogated by ionizing to  $\text{HCl}^+$  with an additional photon. This REMPI type experiment showed that the  $\text{HCl}^+$  ion probability depended upon both the relative phase and intensity of the two exciting lasers, in accord with the theory described above. Note that in this case, control is achieved by simultaneous excitation to a nondegenerate bound state. As a consequence there is no sum over  $n$  in Eqs. (2), (4) and (7) and hence  $|F_3^{(q)} F_1^{(q)}| = |F_{13}^{(q)}|^2$ . Satisfaction of this Schwartz equality suffices to ensure that the probability of forming the HCl Rydberg state can be varied over the full range of zero to unity[1]. Specifically, setting  $\theta_3 - 3\theta_1 = -\delta_{13}^{(q)}$  and  $\epsilon_3^2/\epsilon_1^2 = F_1^{(q)}/F_3^{(q)}$  gives zero probability in channel  $q$ .

A similar phase control experiment has been performed on atoms[20], in the simultaneous 3-photon + 5-photon ionization of Hg. Although the effect of the relative laser intensity was not studied, the  $\text{Hg}^+$  ionization probability was shown to be a function of relative phase of the two lasers. Since in this case excitation is nonresonant, this experiment shows the feasibility of control over continuum channels via interfering optical excitation routes.

These experiments clearly show that coherent control of simple molecular processes through quantum interference of multiple optical excitation routes is both feasible and experimentally observable. Further experimental studies designed to show control over processes with more than one product channel are in progress by a number of experimental groups. Further, our recent computational results [13] on photodissociation of IBr, to produce  $\text{I} + \text{Br}$  and  $\text{I} + \text{Br}^*$  suggest that such experiments should show huge control over the product ratio. For example, 1-photon plus 3-photon photodissociation of the ground vibrotational state in the ground electronic state of IBr showed variations in the  $\text{Br}^*/\text{Br}$  ratio of 45% to 95% with variations of the relative laser intensity and phase. Similar results were obtained for higher  $J$ , including  $J = 42$  where extensive  $M_J$  averaging was required.

### 3. The Essential Principle and Assorted Coherent Control Scenarios

The 3-photon plus 1-photon case is but one example of a scenario which embodies the essential principle of coherent control, i.e. that *coherently driving a pure state through multiple optical excitation routes to the same final state allows for the possibility of control*. Given this general principle, numerous scenarios may be proposed to obtain control in the laboratory. Such proposals must, however, properly account for a number of factors which reduce or eliminate control. Amongst these are the need to (a) adhere to selection rule requirements, (b) minimize extraneous and parasitic uncontrolled satellites, (c) insure properly treated laser spatial dependence and phase jitter and (d) allow maintainance of coherence over time scale associated with any true relaxation processes, e.g. collisions. Briefly:

(a) control requires that the interference term (e.g.  $F_{13}^{(q)}$  above) arising between optical routes is nonzero. In general, this is the case only if the various optical excitation routes satisfy specific rules regarding conserved integrals of motion. For example[21], consider the 1-photon + 3-photon case discussed above. Here excitation from, e.g.  $J = 0$ , where  $J$  is the rotational angular momentum, yields  $J = 1$  for the 1-photon route and  $J = 1$  and  $J = 3$  for the three photon route. In this case selection rules are such that only final states with the same  $J$ , here  $J = 1$ , interfere;

(b) the  $J = 3$  state created by three photon absorption in this scenario is an example of a satellite state, i.e. an uncontrolled (and hence undesired) product state arising in the course of the photoexcitation. Effective scenarios must insure that such contributions are small compared to the controlled component;

(c) since the ability to accurately manipulate the laser relative phase is crucial to coherent control, one must account for all laboratory features which affect the phase. For example, scenarios must be designed so as to eliminate effects due to the  $k \cdot R$  spatial dependence of the laser phase. Not doing so would results in the diminition of control resulting from the variation of this term over the molecule beam-laser beam intersection volume.

(d) proposed scenarios must maintain phase coherence in the face of possibly dephasing effects (e.g. collisions or partial laser coherence ). Studies indicate[7,22] that control can survive moderate levels of such phase destructive processes.

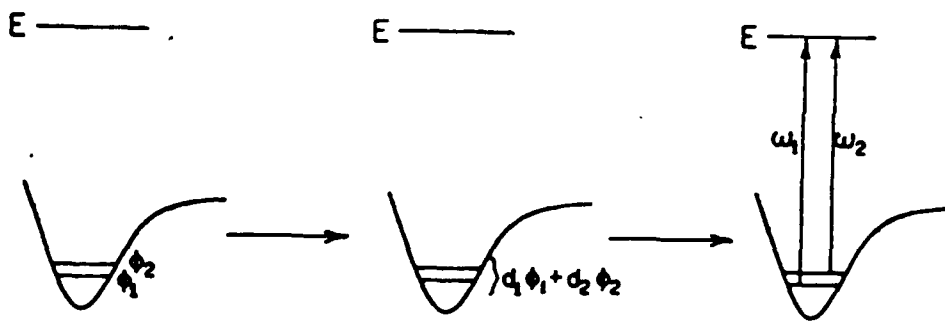


Figure 2: Basic control scenario.

We have, thus far, proposed a number of different scenarios for coherent control. Below we comment on some of them, with the intent of providing only the briefest of "roadmaps" for the proposed schemes. Detailed discussions are provided in the literature, along with extensive computations. The original coherent control scenario is shown in Figure 2 wherein a superposition of two bound states is subjected to two cw frequencies which lift the system to energy  $E$ . An analysis of this very basic scenario shows that the control parameters are the relative intensity and relative phase of the two indicated electromagnetic fields. This basic mechanism has been examined in the gas phase, both in the presence and in the absence of collisions and this scenario has been adapted to control currents in semiconductors. In all cases control was extensive.

Developments in pulsed laser technology may be used to good advantage in a straightforward modification of the above scenario. Specifically, the superposition state preparation and subsequent excitation with frequencies  $\omega_1, \omega_2$  may be both carried out using pulsed lasers in accord with Figure 3:

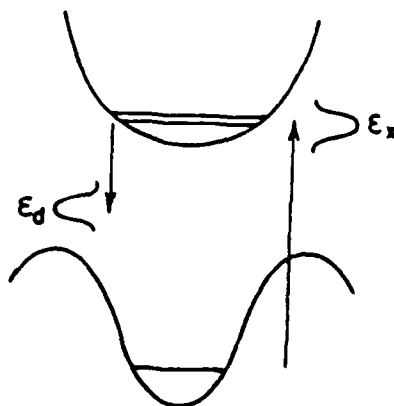


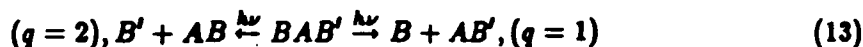
Figure 3: Pump-Pump scenario

In this instance the frequencies required to excite to energy  $E$  are contained within the second excitation pulse, which also creates product, and associated interference contributions over a wider energy range. Multiple excitation paths are contained within this overall pump-pump excitation scheme and serve to introduce the necessary interfering coherent paths. The straightforward analysis[8,11] of this scenario consists of a perturbation theory treatment of the molecule in the presence of two temporally separated, sequential pulses. The first pump step, in which the system is excited from ground state  $|E_g\rangle$ , yields a superposition state  $\sum_k c_k |E_k\rangle$  with  $c_k$  proportional to  $\langle E_k | \mu | E_g \rangle$ ; the subsequent pulse causes dissociation. Perturbation theory gives the probability,  $P(E, m_j, q)$ , required in the section below, of forming product in arrangement channel  $q$  at energy  $E$  with total fragment angular momentum projection  $m_j$  along a space fixed axis as,

$$\begin{aligned}
 P(E, m_j, q) &= \sum_n' |B(E, n, q|t = \infty)|^2 \\
 &= (2\pi/\hbar^2) \sum_n' \left| \sum_{k=1,2} c_k \langle E, n, q^- | \mu | E_k \rangle c_d(\omega E E_k) \right|^2
 \end{aligned}
 \tag{10}$$

#### 4. Symmetry Breaking and Chirality Control

The results above make clear that two arrangement channels, whose photodissociation amplitudes differ, can be controlled through manipulation of external laser fields. A particularly interesting example results from consideration of the photodissociation of a molecule schematically written as :



where  $q$  defines the product arrangement channel and  $BAB'$  denotes a molecule, or a molecular fragment, which is symmetric with respect to reflection  $\sigma$  across the plane which interchanges the enantiomers  $B$  and  $B'$  (e.g., Ref. 23). The existence of this plane implies that the point group of the reactant is at least  $C_s$ .

Consider then the molecule  $B'AB$  subjected to the two pulse scenario sketched above. The probability of forming product in arrangement channel  $q$  with products in the  $m_j$  state is given by Eq. (11). Active control over the products  $B - AB'$  vs.  $B' + AB$ , attained by manipulating the time delay or the pulse detuning will result as long as  $P(q = 1, m_j)$  and  $P(q = 2, m_j)$  have different functional dependences on laboratory parameters.

It is surprising that  $P(q = 1, m_j)$  and  $P(q = 2, m_j)$  differ in the  $B'AB$  case[24]. To see this consider the behavior of  $c_k$  and  $\mu_{i,k}^{(q)}$ , for  $|E_1\rangle$  and  $|E_2\rangle$  of different symmetry with respect to the reflection  $\sigma$ . For simplicity we restrict attention to  $BAB'$  belonging to point group  $C_s$ , the smallest group possessing the required symmetry plane. Further, we focus upon transitions between electronic potential energy surfaces of similar species, e.g.  $A'$  to  $A'$  or  $A''$  to  $A''$  and assume the ground vibronic state to be of species  $A'$ . Similar arguments apply for larger groups containing  $\sigma$ , to ground vibronic states of odd parity, and to transition between electronic states of different species.

**Excitation Coefficients  $c_k$ :** Components of  $\mu$  lying in the symmetry plane, denoted  $\mu_s$ , transform as  $A'$  and are symmetric with respect to reflection whereas the component perpendicular to the symmetry plane, denoted  $\mu_a$ , is antisymmetric ( $A''$ ). Hence  $\langle E_k | \mu | E_g \rangle = \langle E_k | \mu_s + \mu_a | E_g \rangle$ , and hence  $c_k$ , is nonzero for transitions between vibronic states of the same symmetry due to the  $\mu_s$  component, and nonzero for transitions between vibronic states of different symmetry due to the  $\mu_a$  component. The latter is common in IR spectroscopy. In electronic spectroscopy such transitions result from the non Franck-Condon Herzberg-Teller intensity borrowing[25] mechanism. Thus, the excitation pulse can create an  $|E_1\rangle, |E_2\rangle$  superposition consisting of two states of different reflection symmetry and hence a state which no longer displays the reflection symmetry of the Hamiltonian.

**Cumulative matrix elements  $\mu_{i,k}^{(q)}$ :** In contrast to the bound states, the continuum states of interest  $|E, n, q^-\rangle$  are neither symmetric nor antisymmetric. Rather,  $\sigma |E, n, q = 1^-\rangle = |E, n, q = 2^-\rangle$  and vice-versa. Such a choice is possible because of the exact degeneracies which exist in the continuum. To examine  $\mu_{i,k}^{(q)}$  we introduce symmetric and antisymmetric continuum eigenfunctions of  $\sigma$ ,  $|\psi^s\rangle = (|E, n, q = 1^-\rangle + |E, n, q = 2^-\rangle)/2$  and  $|\psi^a\rangle = (|E, n, q = 1^-\rangle - |E, n, q = 2^-\rangle)/2$ . Assuming  $|E_1\rangle$  is symmetric and  $|E_2\rangle$  antisymmetric, rewriting  $|E, n, q^-\rangle$  as a linear combination of  $|\psi^s\rangle$  and  $|\psi^a\rangle$ , and adopting the notation  $A_{s2} = \langle \psi^s | \mu_s | E_2 \rangle$ ,  $S_{s1} = \langle \psi^s | \mu_s | E_1 \rangle$ , etc. we have, after elimination of null

### Acknowledgements

We acknowledge support from the U.S. Office of Naval Research under contract numbers N00014-87-J-1204 and N00014-90-J-1014. Work carried out in conjunction with R.J. Gordon was supported by NSF PHY-8908161.

### References

1. P. Brumer and M. Shapiro, "Control of Unimolecular Reactions Using Coherent Light", *Chem. Phys. Lett.* **126**:541 (1986).
2. P. Brumer and M. Shapiro, "Coherent Radiative Control of Unimolecular Reactions: Three Dimensional Results", *Faraday Disc. Chem. Soc.* **82**:177 (1987).
3. M. Shapiro and P. Brumer, "Laser Control of Product Quantum State Populations in Unimolecular Reactions", *J. Chem. Phys.* **84**:4103 (1986).
4. C. Asaro, P. Brumer and M. Shapiro, "Polarization Control of Branching Ratios in Photodissociation", *Phys. Rev. Lett.* **60**:1634 (1988).
5. M. Shapiro, J.W. Hepburn and P. Brumer, "Simplified Laser Control of Unimolecular Reactions: Simultaneous ( $\omega_1, \omega_2$ ) Excitation", *Chem. Phys. Lett.* **149**:451 (1988).
6. G. Kurizki, M. Shapiro and P. Brumer, "Phase Coherent Control of Photocurrent Directionality in Semiconductors", *Phys. Rev.* **B39**:3435 (1989).
7. M. Shapiro and P. Brumer, "Laser Control of Unimolecular Decay Yields in the Presence of Collisions", *J. Chem. Phys.* **90**:6179 (1989).
8. T. Seideman, M. Shapiro and P. Brumer, "Coherent Radiative Control of Unimolecular Reactions: Selective Bond Breaking with Picosecond Pulses", *J. Chem. Phys.* **90**:7132 (1989).
9. For an introductory discussion see P. Brumer and M. Shapiro, "Coherence Chemistry: Controlling Chemical Reactions With Lasers", *Accounts Chem. Res.* **22**:407 (1989).
10. P. Brumer and M. Shapiro, "One Photon Mode Selective Control of Reactions by Rapid or Shaped Laser Pulses: An Emperor Without Clothes?", *Chem. Phys.* **139**:221 (1989).
11. I. Levy, M. Shapiro and P. Brumer, "Two-Pulse Coherent Control of Electronic States in the Photodissociation of IBr: Theory and Proposed Experiment", *J. Chem. Phys.* **93**:2493 (1990).
12. M. Shapiro and P. Brumer (to be published).
13. C.K. Chan, P. Brumer and M. Shapiro, "Coherent Radiative Control of IBr Photodissociation via Simultaneous ( $\omega_1, \omega_2$ ) Excitation", *J. Chem. Phys.* **94**: 2688 (1991).

14. J. Krause, M. Shapiro and P. Brumer, "Coherent Control of Bimolecular Reactions", *J. Chem. Phys.* **92**:1126 (1990).
15. M. Shapiro and P. Brumer (to be published).
16. P. Brumer, X-P. Jiang and M. Shapiro (to be published).
17. See, e.g., S.H. Tersegni, P. Gaspard and S.A. Rice, "On Using Shaped Laser Pulses to Control the Selectivity of Product Formation in a Chemical Reaction", *J. Chem. Phys.* **93**:1670 (1990) and references therein.
18. See, e.g., S. Shi and H. Rabitz, "Optimal Control of Selective Vibrational Excitation of Harmonic Molecules: Analytic Solution and Restricted Forms for the Optimal Field", *J. Chem. Phys.* **92**:2927 (1990) and references therein.
19. S.M. Park, S-P. Lu and R.J. Gordon, "Coherent Laser Control of the Resonant Enhanced Multiphoton Ionization of HCl", *J. Chem. Phys.* (in press)
20. C. Chen, Y-Y. Yin and D.S. Elliott, "Interference Between Optical Transitions", *Phys. Rev. Lett.* **64**:507 (1990).
21. As another interesting case consider the use of two components of laser polarization to excite a bound state  $|E_i\rangle$  to the continuum[4]. These two components will interfere constructively and destructively and allow control over product ratios in the differential cross section. However, the interference contribution to the *total* cross section vanishes since these two routes reach different values of  $M_j$ .
22. X-P. Jiang, P. Brumer, and M. Shapiro (to be published)
23. An example, although requiring a slight extension of the BAB' notation, is the Norrish type II reaction:  $D(CH_2)_3CO(CH_2)_3D'$  dissociating to  $DCHCH_2 + D'(CH_2)_3COCH_3$  and  $D'CHCH_2 + D(CH_2)_3COCH_3$  where D and D' are enantiomers.
24. M. Shapiro and P. Brumer, "Controlled Photon Induced Symmetry Breaking: Chiral Molecular Products from Achiral Precursors", *J. Chem. Phys.* (in press)
25. J.M. Hollas, "High Resolution Spectroscopy", (Butterworths, London, 1982)